THE EFFECT OF A VALINE TO PHENYLALANINE MUTATION IN THE PRECORE REGION OF HEPATITIS B VIRUS ON VIRUS REPLICATION, HBeAg MATURATION AND EXPRESSION

Chien-Yu Chen

Thesis submitted in compliance for the requirements for the degree of Doctor of Philosophy in the Faculty of Health Science at the University of Witwatersrand

Johannesburg 2010

DECLARATION

I, Chien-Yu Chen declare that this thesis is my own work. It is be being submitted for the degree of Doctor of Philosophy in the University of Witwatersrand, Johannesburg. It has not been submitted before for any degree or examination at this or any other University.

……

…… day of …… (month), 2010

DEDICATION

I dedicate this thesis to my dearest music teacher, the late Professor Walter A Mony. Thank you for teaching me endless wisdom beyond music, and bringing lots of joy to my life with the music. I will always remember you.

PRESENTATIONS

1. Conference: The XIth International Congress of Virology, Congresses of the International Union of Microbiological Societies (IUMS), Sydney, Australia (Aug 1999).

   Poster: The effect of the G to T mutation on Hepatitis B Virus HBeAg expression.

2. MRC review of the Molecular Hepatology Research Unit in Johannesburg, South Africa (27 June 2006).

   Presentation: A valine to phenylalanine mutation in the precore region of both Hepatitis B Virus and Woodchuck Hepatitis Virus induces endoplasmic reticulum stress and results in aggresome formation.

3. Symposium: Hepatitis B Virus Genotypes – from an academic question to the clinic, Johannesburg, South Africa (July 2008).

   Presentation: A valine to phenylalanine mutation in the precore region of Hepatitis B Virus casues intracellular retention and impaired secretion of HBe-antigen

PUBLICATION

1. Chen CY, Crowther C, Kew MC, Kramvis A (2008) A valine to phenylalanine mutation in the precore region of hepatitis B virus causes intracellular retention and impaired secretion of HBe-antigen. Hepatol Res. Jun; 38(6):580-92.

Hepatology Research 2008; **38**: 580–592 doi: 10.1111/j.1872-034X.2007.00315.x

Original Article

A valine to phenylalanine mutation in the precore region of hepatitis B virus causes intracellular retention and impaired secretion of HBe-antigen

Chien Yu Chen,[1] Carol Crowther,[2] Michael C. Kew[1] and Anna Kramvis[1]

[1]*MRC/University Molecular Hepatology Research Unit, Department of Medicine and* [2]*Hepatitis B Virus Research Unit, Department of Molecular Medicine and Haematology, University of the Witwatersrand, Johannesburg, South Africa*

Aim: Hepatitis B virus (HBV) e antigen (HBeAg) is translated from precore mRNA as a precore/core protein, which is post-translationally modified to give rise to the protein that is secreted into the serum. The G1862T mutation in HBV occurs in the bulge of the encapsidation signal within the pregenomic RNA. When the precore mRNA is translated, this mutation results in a valine to phenylalanine substitution at the –3 position to the signal peptide cleavage site at the amino end of the precursor protein. The aim of this study was to determine whether this mutation could affect HBV replication and/or HBeAg expression.

Methods: Following transfection of Huh 7 cells, HBV replication was followed using real time polymerase reaction (PCR) and expression of HBeAg expression was monitored using confocal microscopy.

Results: HBV replication was reduced when this mutation was introduced into genotype D but not into genotype A replication-competent constructs. Using mutant HBeAg-expressing plasmids, we demonstrated a 54% reduction in HBeAg secretion relative to the wild type. Confocal microscopy demonstrated that the mutant HBeAg accumulated in the endoplasmic reticulum, endoplasmic reticulum intermediate compartment and Golgi. These aggregates of mutant protein increased in size following treatment of the cells with a proteasome inhibitor, MG132, and had the hallmark features of aggresomes. They attracted ubiquitin, heat shock proteins and proteasomes and were isolated from the cytosol by the intermediate filaments, vimentin and cytokeratin.

Conclusion: The formation of aggresomes, as a result of the G1862T mutation, may play a contributory role in HBV-induced liver disease.

Key words: aggresomes, mutant, HBe-antigen, signal peptide cleavage

INTRODUCTION

HEPATITIS B VIRUS (HBV), a member of the family *Hepadnaviridae,* is endemic in the black population of southern Africa,[1] where genotype A is the dominant genotype[2–5] and subgenotype A1 is the dominant subgenotype.[3,5,6] A high rate of HBV e antigen (HBeAg) negativity is a feature of the chronic carriage of the virus in this population.[7] Distinctive sequence characteristics of subgenotype A1 have been identified that could account for the high HBeAg negativity rate.[8,9] At the transcriptional level, the core promoter mutations $1762^{T}1764^{A}$ can reduce HBeAg expression.[10–12] At the translational level, mutations at 1809–1812 that alter the Kozak sequence of the precore/core open reading frame are stable traits and affect HBeAg expression to an extent comparable to $1762^{T}1764^{A}$.[13] The co-existence of $1762^{T}1764^{A}$ and 1809–1812 mutations reduces HBeAg expression in an additive manner.[13] Approximately 25% of both southern African black asymptomatic carriers of the virus[14] and hepatocellular carcinoma patients[2] have been shown to have a G to T transversion at 1862 in the precore region. This mutation could affect HBeAg expression by interfering with signal peptide cleavage at the post-translational level.

HBeAg is expressed from the precore/core open reading frame (ORF) as a precore/core protein that is post-translationally modified to give rise to HBeAg, which is secreted into the serum and expressed on the

Correspondence: Professor Anna Kramvis, Department of Internal Medicine, University of the Witwatersrand, 7 York Road, Parktown, Johannesburg 2193, South Africa. Email: Anna.Kramvis@wits.ac.za
Received 5 September 2007; revision 24 October 2007; accepted 16 November 2007.

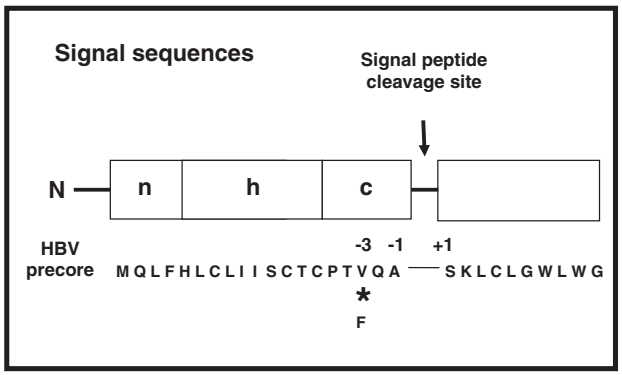

Figure 1 Schematic representation of signal peptide cleavage site in relation to the hepatitis B virus (HBV) precore/core protein. n is designated as the amino domain, h is the hydrophobic domain and c is the carboxyl domain of the signal sequences. The amino acids of each domain were defined using SignalP 3.0 software (Center for Biological Sequence Analysis, Technical University of Denmark: http://www.cbs.dtu.dk/services/signalP).

surface of hepatocytes. A hydrophobic signal sequence directs the precore/core protein to the endoplasmic reticulum (ER), where the 19 amino acid signal peptide is cleaved from the amino-terminal end by a signal peptidase and a variable number of amino acids are removed from the arginine-rich carboxy-terminal end to form HBeAg.[15,16] The G1862T mutation in the bulge of the RNA encapsidation signal (codon 17) changes the valine at the −3 position to the signal peptide cleavage site at position 19 to phenylalanine (Fig. 1). Phenylalanine, being aromatic, is a "forbidden" amino acid at this position (−3,−1 rule)[17–19] and may abrogate signal peptide cleavage,[14,20] as has been shown for *Escherichia coli* alkaline phosphatase.[21] Abrogation of signal peptide cleavage can lead to retention of the precursor protein in the ER and prevent the formation and secretion of HBeAg.[22]

The ER is the cell's quality control site for accurate folding of secretory and membrane proteins, including viral proteins.[23,24] Proteins that fail to achieve their native conformation are retained in the ER, in association with ER chaperones, and induce the unfolded protein response (UPR).[25] If this response fails to produce correct folding and assembly of the proteins, misfolded proteins are targeted for degradation by the ubiquitin–proteasome system. Accumulated misfolded proteins in the ER lumen are retrotranslocated to the cytoplasm, where they are ubiquinylated and degraded by the proteasome.[26,27] This process, called ER-associated degradation,[26] is also regulated by the UPR. Failure of this sequence of events to prevent accumulation of unfolded or misfolded proteins results in aggregation of the proteins and their sequestration into specialized "holding stations" called aggresomes.[28]

The purpose of this study was to determine the effect of the introduction of the G1862T mutation on HBV replication and on the secretory pathway of HBeAg.

METHODS

Site-directed mutagenesis

SITE-DIRECTED MUTAGENESIS using the QuickChange kit (Stratagene, La Jolla, CA, USA) according to the manufacturer's directions, together with the primers and amplification conditions shown in Table 1, were used for plasmid construction. The plasmid pCH9/3091-wt (Dr M. Nassal, University of Freiburg, Germany) was used to generate the HBeAg-expressing plasmids. pCH9/3091-wt encodes a wild-type, terminally redundant, replication-competent genotype D

Table 1 Oligonucleotides used for site directed polymerase chain reaction (PCR) mutagenesis

Primer	Change	Sequence‡	Annealing temperature
1836F† (+)	Genotype D to A	5′-TAATCATCTC**A**TGTACATGTCC**C**ACTGTTCAAGCCTCCAAGCTGT-3′	77.0°C
1880R† (−)	Genotype D to A	5′-ACAGCTTGGAGGCTTGAACAGT**G**GGACATGTACA**T**GAGATGATTA-3′	77.0°C
1839F† (+)	Val17Phe (G1862T)	5′-TCATCTCATGTACATGTCCCAC**TT**TTCAAGCCTCCA-3′	74.0°C
1874R† (−)	Val17Phe (G1862T)	5′-TGGAGGCTTGA**AA**AGTGGGACATGTACATGAGATGA-3′	74.0°C
1881F† (+)	Trp28* (G1896A)	5′-GCCTTGGGTGGCTTT**AG**GGCATGGAC-3′	72.5°C
1906R† (−)	Trp28* (G1896A)	5′-GTCCATGCCC**T**AAAGCCACCCAAGGC-3′	72.5°C

†Numbering of the nucleic acids is from *Eco*RI site according to genotype D HBV (AY233292). +, sense polarity; –, antisense polarity.
‡Mutated nucleotides are shown in bold face and mutated codons are underlined.

HBV genome and is transcribed using the cytomegalovirus (CMV) promoter.[29] The southern African HBV isolates in which the 1862T mutation was detected belong to genotype A. We therefore modified the original plasmid to the genotype A sequence in the precore region and generated mutants G1862T and G1896A from this template.

Amplification and cloning for HBeAg-expressing pCR3.1 plasmid constructs

The entire precore/core regions of the modified HBV constructs were amplified. Forward primer (1808*Xho*IF(+)): 5′-**C↓TCGAG**AGCCACCATGCAACTT TTTCA CCTCTG-3′; reverse primer (2458*Bam*HIR): 5′-**G↓GATCC**CTAACATTGAGA TTCCCGA-3′, yielded a 656 bp polymerase chain reaction (PCR) product. The PCR mixture, 100 μL in volume, contained 1.75 unit Expand high fidelity polymerase (Roche, Mannheim, Germany), 300 μM each of the dNTPs, 2 μM of each primer, 3 mM of magnesium chloride ($MgCl_2$), 1× high fidelity Expand PCR buffer, and 1.5 μL of plasmid DNA template. The PCR reaction was performed at 95°C for 45 s, 48°C for 60 s and 72°C for 80 s for 40 cycles in a programmable thermal cycler (Perkin Elmer, Boston, MA, USA). PCR products were polished with TaKaRa ExTaq polymerase (Takara Mirus Bio, Madison, WI, USA) at 2.5 U/100 μL for 10 min at 72°C before cloning into the pCR3.1 cloning vector with CMV promoter using the TA Eukaryotic cloning kit – bidirectional (Invitrogen, Carlsbad, CA USA). Clones with correct inserts were selected by restriction digestion and sequenced bidirectionally.

Cell culture and transfection

The Huh7 hepatocellular carcinoma cell line was obtained from Professor H. Nakabayashi of Hokkaido University, Japan.[30] The cell line was maintained in ISE-RPMI1640, 10% (v/v) fetal bovine serum (FBS) (Gibco-BRL, Paisley, Scotland, UK), with 5% CO_2 and sub-cultured every 2–3 days. Plasmid constructs were transfected into Huh7 cells using Lipofectamine 2000 (Invitrogen). Various inhibitors were used: MG132 (Z-Leu-Leu-Leu-CHO) (BIOMOL, Plymouth Meeting, PA, USA), a proteasome inhibitor, was used at 1 μM for 24 h incubation at 37°C before imaging the live cells transfected with precore/core constructs. Brefeldin A (BFA) (Sigma-Aldrich, St Louis, MO, USA) was used at 5 μg/mL, and incubated with the cells at 37°C for 30 min before fixing the cells.

Extraction of intracellular core particle-associated HBV-DNA

Media were collected at 72 h post-transfection and the cells were rinsed twice with phosphate-buffered saline (PBS). The cells were lyzed, the intracellular core particles were precipitated and resuspended according to the method of Parekh.[31] The intracellular core particle-associated HBV-DNA was extracted using QIAamp blood kit (Qiagen, Hilden, Germany), according to the manufacturer's directions. The DNA was finally eluted in 180 μL of elution buffer.

Real-time quantitative PCR amplification of HBV-DNA

Real-time quantitative PCR was performed in a LightCycler, Version 2 (Roche) with primer and hybridization probe (FRET) sets in the core and polymerase region of the HBV genome,[32] with modification of the probe sequences to match sequences of the plasmid DNA template (pCH-9/3091).

Preparation of biological standard

HBV-DNA was extracted from 200 μL of Eurohep standard serum containing 5×10^5 copies/mL genotype D HBV (kindly provided by Dr W. H. Gerlich, University of Giessen, Germany) using a QIAamp blood kit (Qiagen). The DNA was finally eluted in 180 μL of elution buffer.

Preparation of plasmid standard

The recombinant plasmid was purified with Qiagen endotoxin free plasmid Maxi kit (Qiagen). The concentration of the plasmid DNA was quantified using a high resolution spectrophotometer. Serial dilutions of the cloned plasmid DNA ranging from 5.54×10^2 – 5.54×10^9 copies/mL were used for the generation of the standard curve. The PCR was repeated three times in duplicate to generate the standard curve.

Hybridization probes and primers

Forward primer (BcP1): 5′-ACCACCAAA TGCCCCTAT-3′; reverse primer (BcP2): 5′-TTCTGCGACGCGGCGA -3′, yielded a 130 bp PCR product. The donor fluorescent probe (HBVcD: 5′-GAGTTCTTCTTCTAGGGGAC CTGC-FLUORESCEIN-3′) and acceptor probe (HBVcA: 5′-LightCycler Red 640TCGTCGTCTAACAACAGTA-GT CTCCG – PHOSPHATE -3′) were used as hybridization probes (Tib Molbiol, Berlin, Germany).

The amplification reaction mixture per capillary (20 μL) contained 4 μL extracted HBV-DNA template,

4 μL LightCycler FastStart DNA Master^{PLUS} Hybridization Probe kit (Roche), 1 mM each of PCR primer, 0.15 μM HBVcD (donor probe) and 0.15 μM HBVcA (acceptor probe). Thermal cycling conditions were as follows: initial activation of FastStart DNA polymerase at 95°C for 10 min followed by 40 cycles of amplification were performed at 95°C for 5 s, 60°C for 15 s and 72°C for 20 s. Fluorescent data were acquired at each cycle at the end of the annealing step with detection channel sets at F2/F1. Biological standard was included in every run of LightCycler PCR as an internal control. Four independent transfection experiments were performed and the HBV-DNA was extracted. Each construct was tested in triplicate for each transfection. The real-time quantification PCR was performed at least twice for each set of transfections.

Analysis of secreted HBeAg

The cell culture medium was collected at 48 h post-transfection and the HBeAg concentration determined using the Monolisa HBe kit (Bio-Rad, San Diego, CA, USA). Three independent transfection experiments were performed to test the HBeAg secreted into the culture media.

Statistical analysis

Viral replication and HBeAg data were analyzed using the ordinary one-way analysis of variance setting with the Bonferroni method for comparison between different mutations, using the GraphPad InStat statistical analysis software version 3.0 (GraphPad, San Diego, CA, USA). All data were expressed as means with standard deviations. Differences were considered significant when *P*-values were less than 0.05.

Antibodies

The following primary antibodies were used: monoclonal antiprotein disulfide-isomerase (PDI), 1:40 (Affinity BioReagents, Golden, CO, USA); monoclonal anti-ERGIC 53, 1:1000 (Professor H Hauri, University of Basel, Switzerland); monoclonal antigiantin, 1:1000 (Professor H Hauri); monoclonal antivimentin clone V9, 1:70 (Sigma-Aldrich); monoclonal antipan cytokeratin, 1:70 (Sigma-Aldrich); monoclonal antialpha (α) tubulin, 1:1000 (Sigma-Aldrich); monoclonal antigamma (γ) tubulin clone GTU-88, 1:1000 (Sigma-Aldrich); rabbit polyclonal antiHSP70, 1:100 (US Biological, SwampScott, MA, USA); rabbit polyclonal antiubiquitin, 1:100 (US Biological); rabbit polyclonal antihuman placental proteasome, 1:1000 (Professor B Dahlmann, Humboldt University, Berlin, Germany); monoclonal anti-HBeAg, 0.005 μg/μL. Secondary antibodies used were: AlexaFluor 488 chicken antirabbit IgG (H + L), 1:100 dilution; AlexaFluor 546 F(ab′)$_2$ fragment of goat antimouse IgG (H + L), 1:150; AlexaFluor 488 donkey antimouse IgG (H + L), 1:100; AlexaFluor 546 goat antirabbit IgG (H + L), 1:150 (Molecular Probe, Eugene, OR, USA).

Confocal fluorescence microscopy

At 72 h post-transfection, culture slides were rinsed and washed in PBS and cells were fixed in freshly prepared 4% (v/v) paraformaldehyde in PBS for 10 min at room temperature (RT). After fixation, the cells were washed three times for 10 min per wash in PBS, followed by a permeabilization step by incubating the slides in 0.01% (v/v) TX-100 in PBS for 10 min at RT. Cells were washed three times for 10 min per wash in PBS and incubated in blocking solution, 1% (w/v) bovine serum albumin (BSA) prepared in PBS, for 1 h at RT.

Cells were incubated with primary antibody overnight at 4°C, washed three times in PBS and incubated with fluorochrome conjugated secondary antibodies. The nuclei were counterstained with 4′, 6′-diamidino-2-phenylindole dihydrochloride (DAPI) (Molecular Probe), for 1 h at RT, protected from light. Cells were washed four times in PBS at RT. Slides were mounted under cover slips with antifade mounting medium, FluorSave (Calbiochem, San Diego, CA, USA), and sealed.

The cells were viewed using the Zeiss Axiovert 100 M microscope equipped with the CARV spinning disc confocal system (BD Bioscience, Sparks, MD, USA). Images were captured using the Hamamatsu CCD camera (Hamamatsu Cooperation, Hamamatsu, Shizuoka, Japan) and Axiovision 2.0 software (Carl Zeiss, Göttingen, Germany). Image analysis was performed with IMAGEJ software for windows V1.34 (http://rsb.info.nih.gov/ij).

RESULTS

Effects of HBV G1862T mutation on intracellular replication efficiency and HBeAg secretion

THE INTRACELLULAR LEVELS of HBV-DNA of wild-type and mutant replication-competent constructs were determined by real-time quantification of the encapsidated HBV. The G1862T mutant showed 31% reduction of replication efficiency relative to wild-type in the genotype D construct ($P < 0.05$), but did not affect viral replication in genotype A construct (Fig. 2).

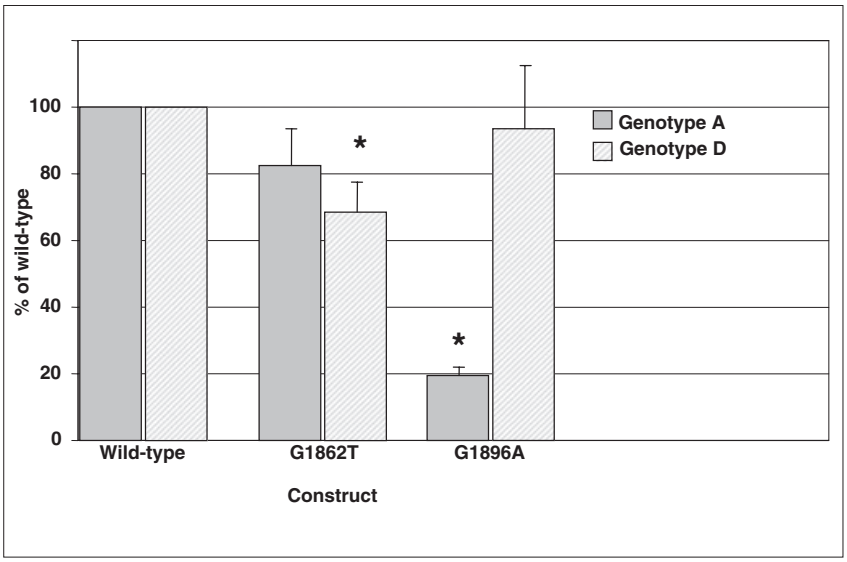

Figure 2 Quantification of intracellular viral particle-associated hepatitis B virus (HBV)-DNA. Mean values and standard deviations from three independent experiments are shown. Values are normalized to HBV copy number of the wild-type construct (100%). Statistically significant differences compared with wild type are indicated by an asterisk.

When introduced into the genotype D construct, the G1896A mutation displayed similar HBV-DNA levels to the wild-type, but a 80% reduction was obtained when the mutation was introduced into the genotype A construct ($P < 0.001$) (Fig. 2).

There was a 54% decrease in HBeAg concentration in the supernatant when Huh7 cells were transfected with HBeAg-expressing genotype A constructs with the G1862T mutation relative to the wild-type ($P < 0.001$, S.D ± 17.64). A similar reduction in HBeAg concentration was observed when the cells were transfected with the genotype D construct with the mutation. The G1896A mutation completely abolished the translation of HBeAg precursor when introduced in both genotype A and D constructs.

Intracellular localization of wild-type and mutant precore/core protein

The effects of expression of wild-type and mutant HBeAg were followed in Huh7 cells. Mock-transfected Huh7 cells, in which no fluorescence was detected when stained for anti-HBeAg, and cells transfected with a plasmid with the G1896A mutation, which results in the truncation of HBeAg at codon 28,[33] were used as negative controls. In subgenotype A1 HBV isolates, the G1862T mutant occurs frequently together with a G1888A silent mutation.[3] In order to preclude the possibility that G1888A could affect the phenotype of the G1862T mutant, constructs in which these two mutations occurred independently or in combination were used. The G1888A mutation either alone or in combination with G1862T did not affect the secretion or expression of HBeAg (data not shown).

When the Huh7 cells were transfected with wild-type HBeAg-expressing construct, the precore/core protein was evenly distributed throughout the cytoplasm, as demonstrated by the diffuse reticular and fine granular staining (Fig. 3: a1, b1, c1). The wild-type protein colocalized with protein disulfide isomerase (PDI), an ER resident chaperone (Fig. 3: a3), ERGIC-53 (a transmembrane lectin that cycles between ER, ERGIC and Golgi[34]) (Fig. 3: b3) and giantin (a Golgi membrane protein)[35] (Fig. 3: c3), indicating that the protein is moving along the ER to the Golgi via ERGIC, before being exported from the cell. The ER marker, PDI, showed a fine reticular staining pattern that extended throughout the cytoplasm (Fig. 3: a2). The staining pattern with the ERGIC-53 label was punctate and closer to the nucleus (Fig. 3: b2), and that with antigiantin staining gave a characteristic strong juxtanuclear label compatible with Golgi compartment labeling (Fig. 3: c2). There was no difference in the intensity of the staining of the markers for the different secretory pathway compartments. This steady state distribution was disrupted when the cells were treated with brefeldin A (BFA), an antibiotic that blocks the transport of proteins from the ER to the Golgi, by causing the disassembly[36] and protein redistribution[37] of the latter to the ER. This redistribution is evident by the change of staining for giantin from granular (Fig. 3: c2) to a finer, reticular pattern (Fig. 3: d2), similar to the staining for ER (Fig. 3: a2). In BFA-treated cells, in contrast to untreated cells (Fig. 3: c1), the wild-

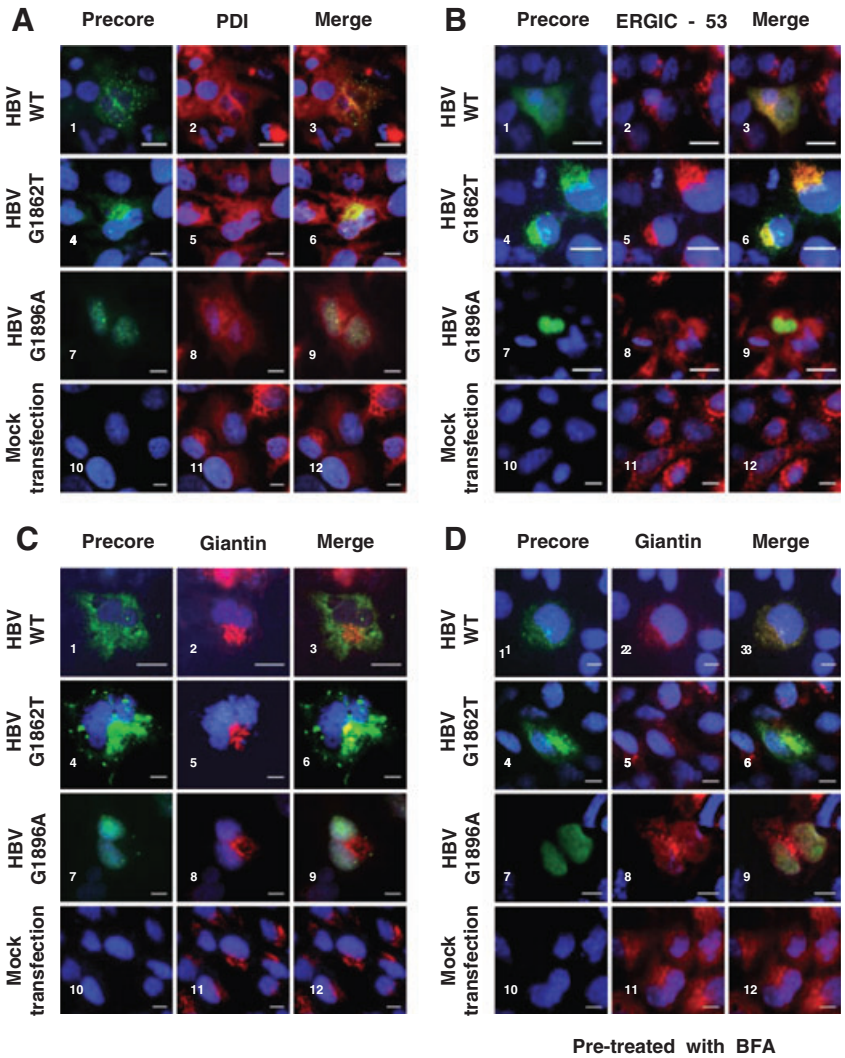

Figure 3 Intracellular localization of hepatitis B virus (HBV) precore/core protein in relation to the early secretory organelles. Huh7 cells were transfected with plasmid constructs, fixed and then subjected to indirect double immunofluorescence staining with antibodies against HBV precore/core protein, secondary antibody labeled with AlexaFluor 488, green and antibodies against endoplasmic reticulum (ER) marker, PDI (a), ERGIC marker, ERGIC-53 (b), Golgi apparatus marker, giantin (c) and treated with brefeldin A (BFA) prior to fixation, then stained with antigiantin antibody (d). All secretory organelles were detected with secondary antibodies labeled with AlexaFluor 546, red. Colocalization of precore/core protein and secretory organelles can be seen by the yellow color. Nuclei were counterstained with diamidino-2-phenylindole dihydrochloride (DAPI). Scale bar, 10 μm.

type protein accumulated in large, granular structures in the perinuclear region and little or no precore/core protein was seen on the periphery (Fig. 3: d1).

To follow the fate of the mutant HBV precore/core proteins, Huh7 cells were transfected with G1862T construct. In addition to the reticular pattern seen with the wild-type construct, the transfected cells showed punctate concentrations of precore/core protein that reacted with anti-PDI, indicating movement of the mutant protein through the ER (Fig. 3: a4–a6). The number of cells per field showing the punctate staining pattern was always higher in the cultures transfected with mutant constructs compared to those transfected with the wild-type. The intense costaining of precore protein with ERGIC-53 (Fig. 3: b4–b6) and to a lesser extent with anti giantin (Fig. 3: c4–c6) demonstrated that some of the

mutant HBV precore/core proteins moved from the ER. This demonstrates that the misfolded mutant protein is not confined to the ER but a proportion moves to ERGIC, where it appears to accumulate. A smaller fraction moves onto to the Golgi. Migration of the misfolded protein did not occur beyond the Golgi, and this was reflected by the 54% reduction of HBeAg expression relative to the wild-type in the supernatant medium. The truncated precore/core protein that results from the stop codon introduced by G1896A, localized to the nucleus (with faint staining only) and was not seen in other cellular organelles (Fig. 3: a7–a9, b7–b9, c7–c9). Moreover, there was no HBeAg secretion into the supernatant medium.

Association of mutant precore/core protein with chaperones, proteasomes and aggregate formation

To determine whether the quality control machinery within the ER is operative in Huh7 cells transfected with mutant HBV precore/core proteins, we stained cells with antibodies against precore/core protein and against Hsp70, ubiquitin and proteasomes. Small aggregates of precore/core protein were formed throughout the cell when the cells were transfected with the G1862T mutant construct (Fig. 4: a4, a7, b4, b7, c4, c7), whereas the distribution of the wild-type protein was more reticular and diffuse (Fig. 4: a1, b1, c1). There was a relative increase in the expression of Hsp70 in cells transfected with the HBV mutant protein when compared with the wild-type, as evidenced by the solid and bright staining (Fig. 4: a5, a8), as opposed to the finer and more diffuse reticular staining in cells transfected with the wild-type (Fig. 4: a2). The majority of Hsp70 in the cells transfected with the mutant construct colocalized with the precore/core protein (Fig. 4: a6, a9). Similarly, the expression of ubiquitin in the cytosol was markedly increased in cells transfected with the mutant strain (Fig. 4: b5, b8) compared to those transfected with the wild-type (Fig. 4: b2), with strong colocalization with the precore/core protein (Fig. 4: b6, b9). Staining for proteasomes was also increased when the cells were transfected with mutant construct (Fig. 4: c5, c8), as opposed to the wild-type (Fig. 4: c2). The mutant HBV colocalized with the proteasomes (Fig. 4: c6, c9).

Formation of aggresomes

The formation of aggregates was observed using immunofluorescence confocal microscopy of Huh7 cells transfected with mutant HBV construct, but not in cells transfected with wild-type construct. In addition to the wide distribution pattern seen in the cytoplasm (Fig. 4: a5, b5, c5), a more restricted staining pattern of Hsp70, ubiquitin and the proteasomes was observed. As shown in Fig. 4 (a8, b8, c8) Hsp70, ubiquitin and proteasomes were confined to the perinuclear region in aggregates that colocalized with the mutant precore/core protein (Fig. 4: a9, b9, c9), indicative of the formation of aggresomes. Between 15% and 20% of the cells transfected with mutant constructs developed aggresomes, which rarely occurred in cells transfected with the wild-type constructs.

A strong colocalization of γ-tubulin, a centrosome (centriole) marker[38,39] and aggresomes formed by mutant proteins was observed. Centrioles stained as a bright dot (Fig. 5: b5) that colocalized with the mutant HBV protein (Fig. 5: b6). When the cells were incubated with antibodies against α-tubulin (Fig. 5: a2, a5), the microtubule cytoskeleton had a normal morphology and was unaffected by aggresome formation in cells transfected with the mutant construct (Fig. 5: a6). However, a rearrangement of the intermediate filaments, which is characteristic of cells with aggresomes, was noted. The intermediate filament vimentin was shown to be re-arranged into condensed fibres forming a ring- or cage-like structure around the aggresomes in the cells transfected with mutant HBV construct (Fig. 5: c6). This rearrangement did not occur in cells transfected with wild-type construct (Fig. 5: c3). Furthermore, another intermediate filament protein, cytokeratin, was found to be rearranged in a similar fashion to vimentin, forming a halo around the aggresome in cells transfected with mutant construct (Fig. 5: d6) but not in cells transfected with the wild-type (Fig. 5: d3).

To distinguish clearly between Golgi apparatus and aggresomes formed by the mutant precore/core proteins, cells were treated with BFA prior to fixation. Unlike the Golgi apparatus, the aggresomes were not disrupted by the BFA treatment (Fig. 3: d6). Furthermore, the addition of the proteasome inhibitor, MG132, to the Huh7 cells transfected with the mutant construct enhanced aggresome formation, as demonstrated by an increase in the size of the aggresomes and a concomitant increased amount of Hsp70, ubiquitin and proteasomes that colocalized with the mutant precore/core protein (Fig. 6: a6, b6, c6). This effect was not observed when the cells were transfected with wild-type constructs and treated with MG132 (Fig. 6: a3, b3, c3).

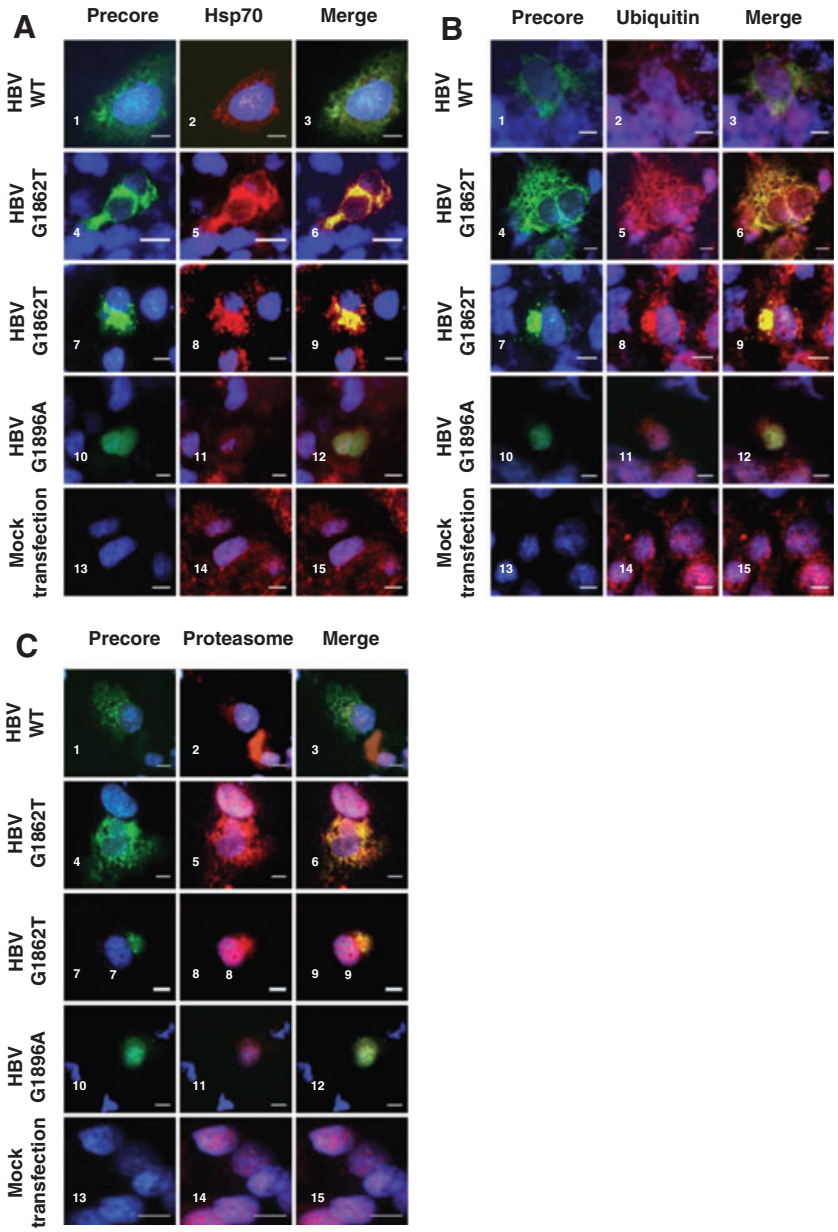

Figure 4 Colocalization of hepatitis B virus (HBV) precore/core wild-type and G1862T mutant proteins with molecular chaperone, ubiquitin and proteasomes. Huh7 cells were transfected, followed by double immunofluorescence staining with antibodies against HBV precore/core protein, shown in green. Hsp70 (a), ubiquitin (b) and proteasomes (c) are all shown in red. Nuclei were counterstained with diamidino-2-phenylindole dihydrochloride (DAPI). Note the recruitment of Hsp70, ubiquitin and proteasomes to the aggresomes. Scale bar, 10 μm.

DISCUSSION

THE G1862T MUTATION could conceivably have two functional consequences. First, it could interfere with, and hence reduce, HBV replication[40] because it occurs within the bulge of ε, which plays a pivotal role in the initiation of reverse transcription of pregenomic RNA (pgRNA).[41,42] Secondly, because the precore/core open reading frame on the precore mRNA, which encodes for the precursor of HBeAg, overlaps the region that codes for ε on the pgRNA, the 1862 missense mutation could affect HBeAg expression. We investigated both possibilities.

Using real-time PCR we showed that HBV-DNA levels were significantly reduced when the G1862T mutation was introduced into genotype D replication-competent constructs ($P < 0.05$) but were unaffected in the genotype D construct with genotype A precore region. This could explain why the G1862T mutation occurs more frequently in genotype A[43] than in any other geno-

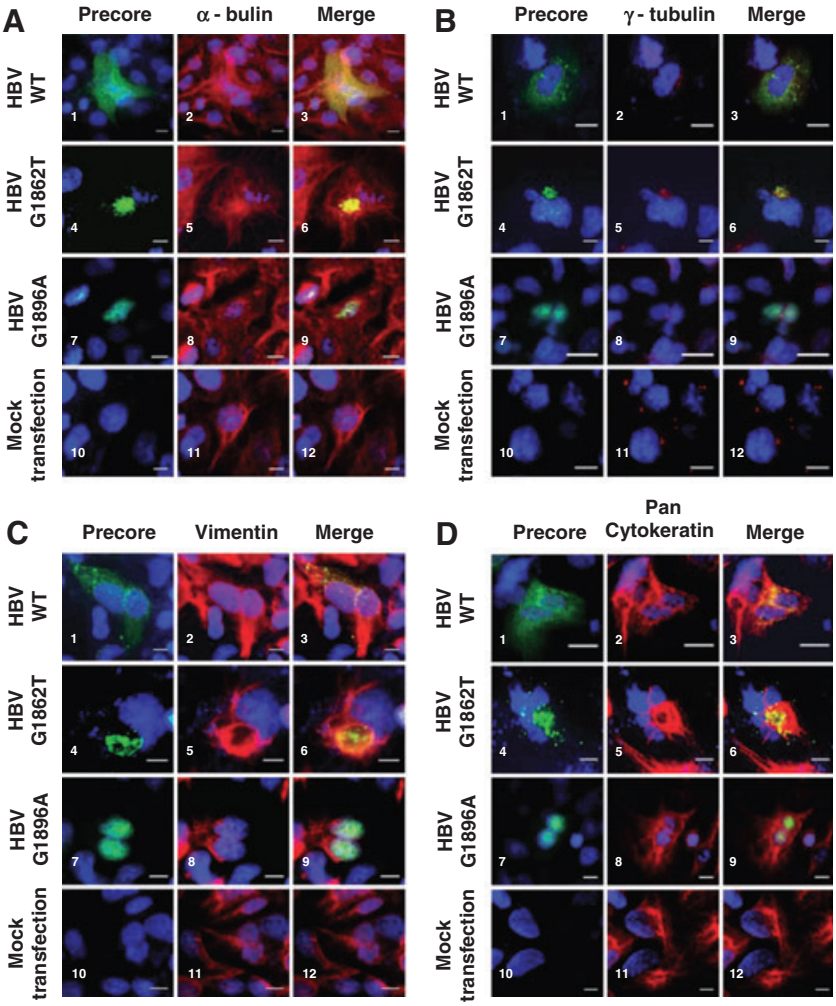

Figure 5 The large intracellular hepatitis B virus (HBV) precore/core mutant protein aggregates were localized to the microtubules organization center (MTOC) and did not distort the microtubule network. α-tubulin as marker for the microtubules (a), γ-tubulin as marker for MTOC (b), vimentin (c) or pan cytokeratin (d). HBV precore/core protein was labeled in green stain using a secondary antibody labeled with AlexaFluor 488; α- and γ-tubulins and intermediate filaments vimentin and cytokeratin were stained in red, using secondary antibody labeled with AlexaFluor 546. Nuclei were counterstained with diamidino-2-phenylindole dihydrochloride (DAPI). Scale bar, 10 μm.

types,[22,43] because in order to survive, viruses require a steady viral replication rate.[44] As expected and as previously demonstrated,[45–47] the G1896A mutation in genotype A constructs resulted in the reduction of HBV replication because it disrupts ε but did not affect the replication of genotype D constructs, where ε is stabilized. In genotype A, there would be destabilization of ε because the nucleotide at position 1858 is C and there is a stable G-C Watson-Crick base pair, which would be disrupted by a G to A mutation at 1896. On the other hand, in genotype D the nucleotide at 1858 is a T and the 1896 G to A mutation would convert the T-G wobble pair to a stable T-A Watson-Crick base pair.[14]

HBeAg-expressing constructs were used to follow the secretion and expression of both wild-type and mutant HBeAg. The wild-type HBV precore/core protein and HBeAg localized in sites of the secretory pathway necessary for the expression of HBeAg (Fig. 3),[23,24] and this distribution of the wild-type protein was not disturbed by the treatment of the cells with the proteasome inhibitor MG132 (Fig. 6). On the other hand, when cells were transfected with the mutant construct, a 54% reduction of HBeAg expression in the supernatant, relative to the wild-type, was observed. This is in agreement with the study of Hou and colleagues, which showed reduced HBeAg expression when the G1862T mutation was present,[22] but not with a more recent study that reported that HBeAg expression was not significantly affected by the introduction of the mutation.[48] The reasons for these discrepant results may be that we and Hou *et al.*[22] used HBeAg-expressing constructs as opposed to the replication-competent plasmids used by Guarnieri *et al.*[48] and the clones were derived from templates belonging to different genotypes/subgenotypes.

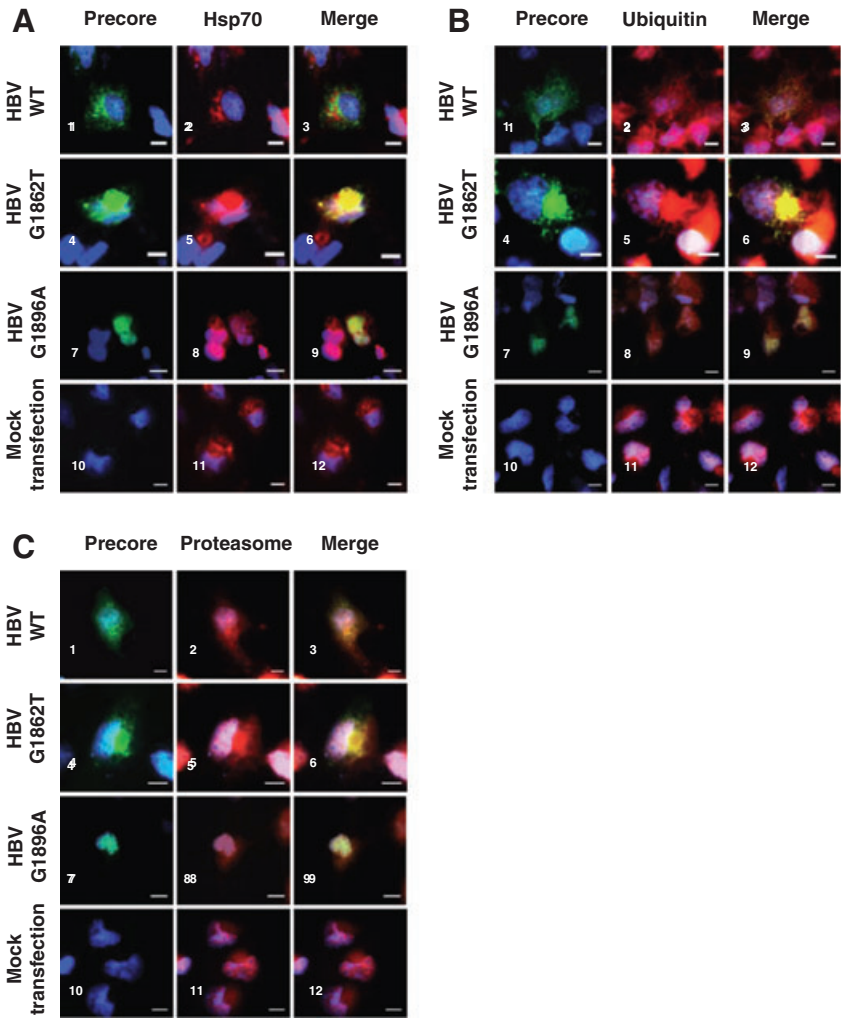

Figure 6 Proteasome inhibition promotes aggresome formation by the hepatitis B virus (HBV) precore/core mutant protein. Transfected Huh7 cells were treated with the proteasome inhibitor, MG132, followed by double immunofluorescence staining with antibodies against HBV precore/core protein, shown in green. Hsp70, ubiquitin and proteasomes are all shown in red. Hsp70 (a), ubiquitin (b), proteasomes (c). Nuclei were counterstained with diamidino-2-phenylindole dihydrochloride (DAPI). Scale bar, 10 μm.

The precursor protein produced by the G1862T mutant did not transfer to ERGIC and beyond and therefore accumulated in the ER, indicating that it failed to meet the ER quality control requirements (Fig. 3). This is the case with most incompletely or incorrectly folded proteins,[49,50] which are recycled to the ER for further folding.[49,50] Further evidence that mutant protein was misfolded was the increased expression of chaperones, such as Hsp70, involved in protein folding, translocation and degradation.[51] This finding was to be expected because misfolded but not wild-type proteins usually have their hydrophobic domains exposed, promoting chaperone binding.[52]

If chaperone binding does not result in correct folding and assembly of the proteins, the accumulated proteins are exported from the ER,[53] polyubiquitinated and then transferred to the proteasome for degradation.[26,27] The 26S proteasome complex is responsible for the majority of non-lysosomal protein degradation in eukaryotic cells.[54] Increased levels of both ubiquitin and proteasomes were detected in the cells infected with mutant constructs, but not in cells infected with the wild-type (Fig. 4). The misfolded precore/core protein accumulated along the microtubules in the cytosol, where they formed mini-aggregates (Fig. 5). This is further evidence that the mutant protein was not correctly folded, because *in vitro* studies have shown that misfolded proteins are prone to aggregation.[55] In fact, the precore signal sequence plays an important role not only in the secretion of HBeAg, but also in determining its structure and aggregational properties.[56,57] Therefore it is possible that the aggregation is the result of the misfolding caused by the interference of the mutation with post-translational modification of the precursor molecule.

From this observation, it can be intimated, as previously predicted by us[2] and others[20] and shown for *Escherichia coli* alkaline phosphatase[21], that the −3, −1 rule[18,19] holds true for the post-translational modification of the HBeAg precursor. The phenylalanine, expressed as a result of the G1862T mutation, is a "forbidden" amino acid at position −3 because its aromatic ring sterically hinders the activity of the signal peptidase, leading to the failure of signal peptide cleavage at the amino end of the precore/core fusion protein.

The mini-aggregates formed increased in size over time and were transported, presumably by the protein dynein, along microtubules to the microtubules organization center (MTOC) in the region of the centrosome, which colocalizes with γ-tubulin, in a perinuclear position.[51,58–60] Using antibodies against α-tubulin, an intact microtubule network was shown to be associated with the retrograde transport of the smaller aggregates along the microtubules and their deposition at the MTOC.[28,59] At this site, indigestible aggregates were spontaneously sequestered into aggresomes,[28,59,60] even in the absence of proteasome inhibitor. In agreement with Johnston *et al.*[60] our observations show that the aggregation of the precursor of HBeAg occurred when the expression of the misfolded protein exceeded the degradation capacity of the proteasome. The accumulation of HBV protein was greatly enhanced when proteasome activity was exceeded. The fact that aggresomes did not form in cells transfected with wild-type constructs indicates that the accumulation of the mutant protein is the result of its overexpression rather than the ubiquitin–proteasome machinery not functioning in Huh7 cells.[61] A high accumulation of mutant precore/core protein but not wild-type protein was observed when the cells were treated with MG132, a proteasome inhibitor.

The aggregates of the unprocessed HBeAg precursor demonstrated the hallmarks of aggresomes. They were ubiquitin-rich aggregates in the region of the MTOC that recruited Hsp70 and proteasomes[39,60] and were surrounded by a vimentin sheath[58,60,62] (Fig. 5). Although some of the misfolded protein did reach the Golgi apparatus before aggregating (Fig. 3), aggresome formation did not require an intact Golgi apparatus, because these structures were undisturbed by BFA treatment that has been shown to cause disassembly[36] and protein redistribution[37] of the Golgi to the ER (Fig. 3). This observation is consistent with similar findings for other proteins and other cellular systems.[28] Moreover, the ability of aggresomes to concentrate proteins and attract chaperones may make them suitable viral assembly sites.[52] An increasing number of publications have described the formation of aggresomes at various stages of the life cycle of a number of viruses.[52,63–66]

As far as we know, ours is the first demonstration of aggresome formation as a result of the accumulation of abnormal hepadnaviral proteins. Aggresome formation may have a role to play in hepadnaviral-induced liver disease. ER storage (conformational) disease is the result of the toxic effects of aggregates of abnormal proteins.[67] Additionally, the cells' reaction to chronic or acute ER stress may include activation of signaling pathways that ultimately lead to cell death via activation of ER-dependent apoptotic pathways and/or autophagy.[24]

ACKNOWLEDGMENTS

THIS WORK WAS supported by grants from the National Research Foundation (NRF) (#GUN2037093) and the Poliomyelitis Research Foundation (PRF 97/6). Ms Chien Yu Chen received scholarships from the NRF, PRF and the University of the Witwatersrand. The Zeiss CARV confocal microscope with micromanipulation attachments was purchased with a grant awarded by The Wellcome Trust (#057672/Z/99). We thank all of our colleagues, listed in the "Methods" section, who generously provided plasmids, antibodies and cell lines used in the study. We thank Professor Costas Koumenis of the Department of Radiation Oncology, University of Pennsylvania School of Medicine, Philadelphia, USA, for critically reading the manuscript and for his useful advice.

REFERENCES

1 Mphahlele MJ, Francois G, Kew M, Van Damme P, Hoosen A, Meheus A. Epidemiology and control of hepatitis B: implications for eastern and southern Africa. *SA J Epidemiol Infect* 2002; **17:** 12–17.
2 Kramvis A, Kew MC, Bukofzer S. Hepatitis B virus precore mutants in serum and liver of Southern African Blacks with hepatocellular carcinoma. *J Hepatol* 1998; **28:** 132–41.
3 Kimbi GC, Kramvis A, Kew MC. Distinctive sequence characteristics of subgenotype A1 isolates of hepatitis B virus from South Africa. *J Gen Virol* 2004; **85:** 1211–20.
4 Hardie DR, Williamson C. Analysis of the preS1 gene of hepatitis B virus (HBV) to define epidemiologically linked and un-linked infections in South Africa. *Arch Virol* 1997; **142:** 1829–41.
5 Bowyer SM, van Staden L, Kew MC, Sim JG. A unique segment of the hepatitis B virus group A genotype identified in isolates from South Africa. *J Gen Virol* 1997; **78:** 1719–29.

6 Kramvis A, Weitzmann L, Owiredu WK, Kew MC. Analysis of the complete genome of subgroup A hepatitis B virus isolates from South Africa. *J Gen Virol* 2002; **83:** 835–9.
7 Song E, Dusheiko GM, Bowyer S, Kew MC. Hepatitis B virus replication in southern Africa blacks with HBsAg-positive hepatocellular carcinoma. *Hepatology* 1984; **4:** 608–10.
8 Tanaka Y, Hasegawa I, Kato T *et al.* A case-control study for differences among hepatitis B virus infections of genotypes A (subtypes Aa and Ae) and D. *Hepatology* 2004; **40:** 747–55.
9 Kramvis A, Kew MC. Molecular characterization of subgenotype A1 (subgroup Aa) of hepatitis B virus. *Hepatol Res* 2007; **37** (Suppl 1)**:** S27–32.
10 Takahashi K, Aoyama K, Ohno N *et al.* The precore/core promoter mutant (T1762A1764) of hepatitis B virus: clinical significance and an easy method for detection. *J Gen Virol* 1995; **76:** 3159–64.
11 Kurosaki M, Enomoto N, Asahina Y *et al.* Mutations in the core promoter region of hepatitis B virus in patients with chronic hepatitis B. *J Med Virol* 1996; **49:** 115–23.
12 Baptista M, Kramvis A, Kew MC. High prevalence of 1762(T) 1764(A) mutations in the basic core promoter of hepatitis B virus isolated from black Africans with hepatocellular carcinoma compared with asymptomatic carriers. *Hepatology* 1999; **29:** 946–53.
13 Ahn S, Kramvis A, Kawai S *et al.* Sequence variation upstream of the precore AUG start codon of hepatitis B virus reduces HBe-antigen production. *Gastroenterology* 2003; **125:** 1370–8.
14 Kramvis A, Bukofzer S, Kew MC, Song E. Nucleic acid sequence analysis of the precore region of hepatitis B virus from sera of southern African black adult carriers of the virus. *Hepatology* 1997; **25:** 235–40.
15 Ou JH, Laub O, Rutter WJ. Hepatitis B virus gene function: the precore region targets the core antigen to cellular membranes and causes the secretion of the e antigen. *Proc Natl Acad Sci USA* 1986; **83:** 1578–82.
16 Jean-Jean O, Levrero M, Will H, Perricaudet M, Rossignol JM. Expression mechanism of the hepatitis B virus (HBV) C gene and biosynthesis of HBe antigen. *Virology* 1989; **170:** 99–106.
17 Bruss V, Gerlich WH. Formation of transmembraneous hepatitis B e-antigen by cotranslational in vitro processing of the viral precore protein. *Virology* 1988; **163:** 268–75.
18 von Heijne G. Patterns of amino acids near signal-sequence cleavage sites. *Eur J Biochem* 1983; **133:** 17–21.
19 von Heijne G. How signal sequences maintain cleavage specificity. *J Mol Biol* 1984; **173:** 243–51.
20 Valliammai T, Thyagarajan SP, Zuckerman AJ, Harrison TJ. Precore and core mutations in HBV from individuals in India with chronic infection. *J Med Virol* 1995; **45:** 321–5.
21 Karamyshev AL, Karamysheva ZN, Kajava AV, Ksenzenko VN, Nesmeyanova MA. Processing of Escherichia coli alkaline phosphatase: role of the primary structure of the signal peptide cleavage region. *J Mol Biol* 1998; **277:** 859–70.
22 Hou J, Lin Y, Waters J *et al.* Detection and significance of a G1862T variant of hepatitis B virus in Chinese patients with fulminant hepatitis. *J Gen Virol* 2002; **83:** 2291–8.
23 Rutishauser J, Spiess M. Endoplasmic reticulum storage diseases. *Swiss Med Wkly* 2002; **132:** 211–22.
24 Ellgaard L, Helenuius A. Quality control in the endoplasmic reticulum. *Nat Rev Mol Cell Biol* 2003; **4** (3): 181–91.
25 Kaufman RJ. Orchestrating the unfolded protein response in health and disease. *J Clin Invest* 2002; **110:** 1389–98.
26 Hampton RY. ER-associated degradation in protein quality control and cellular regulation. *Curr Opin Cell Biol* 2002; **14:** 476–82.
27 Kostova Z, Wolf DH. For whom the bell tolls: protein quality control of the endoplasmic reticulum and the ubiquitin–proteasome connection. *EMBO J* 2003; **22:** 2309–17.
28 Garcia-Mata R, Gao YS, Sztul E. Hassles with taking out the garbage: aggravating aggresomes. *Traffic* 2002; **3:** 388–96.
29 Junker M, Galle P, Schaller H. Expression and replication of the hepatitis B virus genome under foreign promoter control. *Nucleic Acids Res* 1987; **15:** 10117–32.
30 Nakabayashi H, Taketa K, Miyano K, Yamane T, Sato J. Growth of human hepatoma cells lines with differentiated functions in chemically defined medium. *Cancer Res* 1982; **42:** 3858–63.
31 Parekh S, Zoulim F, Ahn SH *et al.* Genome replication, virion secretion, and e antigen expression of naturally occurring hepatitis B virus core promoter mutants. *J Virol* 2003; **77:** 6601–12.
32 Ho SK, Yam WC, Leung ET *et al.* Rapid quantification of hepatitis B virus DNA by real-time PCR using fluorescent hybridization probes. *J Med Microbiol* 2003; **52:** 397–402.
33 Carman WF, Jacyna MR, Hadziyannis S *et al.* Mutation preventing formation of hepatitis B e antigen in patients with chronic hepatitis B infection. *Lancet* 1989; **2:** 588–91.
34 Hauri HP, Kappeler F, Andersson H, Appenzeller C. ERGIC-53 and traffic in the secretory pathway. *J Cell Sci* 2000; **113:** 587–96.
35 Linstedt AD, Hauri HP. Giantin, a novel conserved Golgi membrane protein containing a cytoplasmic domain of at least 350 kDa. *Mol Biol Cell* 1993; **4:** 679–93.
36 Fujiwara T, Oda K, Yokota S, Takatsuki A, Ikehara Y. Brefeldin A causes disassembly of the Golgi complex and accumulation of secretory proteins in the endoplasmic reticulum. *J Biol Chem* 1988; **263:** 18545–52.
37 Doms R, Russ G, Yewdell J. Brefeldin A redistributes resident and itinerant Golgi proteins to the endoplasmic reticulum. *J Cell Biol* 1989; **109:** 61–72.
38 Dictenberg JB, Zimmerman W, Sparks CA *et al.* Pericentrin and gamma-tubulin form a protein complex and are organized into a novel lattice at the centrosome. *J Cell Biol* 1998; **141:** 163–74.

39 Wigley WC, Fabunmi RP, Lee MG *et al.* Dynamic association of proteasomal machinery with the centrosome. *J Cell Biol* 1999; **145:** 481–90.
40 Fallows DA, Goff SP. Mutations in the epsilon sequences of human hepatitis B virus affect both RNA encapsidation and reverse transcription. *J Virol* 1995; **69:** 3067–73.
41 Knaus T, Nassal M. The encapsidation signal on the hepatitis B virus RNA pregenome forms a stem-loop structure that is critical for its function. *Nucleic Acids Res* 1993; **21:** 3967–75.
42 Pollack JR, Ganem D. An RNA stem-loop structure directs hepatitis B virus genomic RNA encapsidation. *J Virol* 1993; **67:** 3254–63.
43 Kramvis A, Arakawa K, Yu MC, Nogueira R, Stram DO, Kew MC. Relationship of serological subtype, basic core promoter and precore mutations to genotypes/subgenotypes of hepatitis B virus. *J Med Virol* 2008; **80**(1): 27–46.
44 Sallie R. Replicative homeostasis: a fundamental mechanism mediating selective viral replication and escape mutation. *Virol J* 2005; **2:** 10.
45 Li JS, Tong SP, Wen YM, Vitvitski L, Zhang Q, Trepo C. Hepatitis B virus genotype A rarely circulates as an HBe-minus mutant: possible contribution of a single nucleotide in the precore region. *J Virol* 1993; **67:** 5402–10.
46 Lok AS, Akarca U, Greene S. Mutations in the pre-core region of hepatitis B virus serve to enhance the stability of the secondary structure of the pre-genome encapsidation signal. *Proc Natl Acad Sci USA* 1994; **91:** 4077–81.
47 Tong SP, Li JS, Vitvitski L, Trepo C. Replication capacities of natural and artificial precore stop codon mutants of hepatitis B virus: relevance of pregenome encapsidation signal. *Virology* 1992; **191:** 237–45.
48 Guarnieri M, Kim KH, Bang G *et al.* Point mutations upstream of hepatitis B virus core gene affect DNA replication at the step of core protein expression. *J Virol* 2006; **80:** 587–95.
49 Hammond C, Helenius A. Quality control in the secretory pathway: retention of a misfolded viral membrane glycoprotein involves cycling between the ER, intermediate compartment, and Golgi apparatus. *J Cell Biol* 1994; **126:** 41–52.
50 Taxis C, Vogel F, Wolf DH. ER-golgi traffic is a prerequisite for efficient ER degradation. *Mol Biol Cell* 2002; **13:** 1806–18.
51 Hartl FU. Molecular chaperones in cellular protein folding. *Nature* 1996; **381:** 571–9.
52 Heath CM, Windsor M, Wileman T. Aggresomes resemble sites specialized for virus assembly. *J Cell Biol* 2001; **153:** 449–55.
53 Pilon M, Schekman R, Romisch K. Sec61p mediates export of a misfolded secretory protein from the endoplasmic reticulum to the cytosol for degradation. *EMBO J* 1997; **16:** 4540–8.
54 Hochstrasser M. Ubiquitin-dependent protein degradation. *Annu Rev Genet* 1996; **30:** 405–39.
55 Ellgaard L, Molinari M, Helenius A. Setting the standards: quality control in the secretory pathway. *Science* 1999; **286:** 1882–8.
56 Schlicht HJ, Wasenauer G. The quaternary structure, antigenicity, and aggregational behavior of the secretory core protein of human hepatitis B virus are determined by its signal sequence. *J Virol* 1991; **65:** 6817–25.
57 Wasenauer G, Kock J, Schlicht HJ. A cysteine and a hydrophobic sequence in the noncleaved portion of the pre-C leader peptide determine the biophysical properties of the secretory core protein (HBe protein) of human hepatitis B virus. *J Virol* 1992; **66:** 5338–46.
58 Harada M, Sakisaka S, Terada K *et al.* A mutation of the Wilson disease protein, ATP7B, is degraded in the proteasomes and forms protein aggregates. *Gastroenterology* 2001; **120:** 967–74.
59 Kopito RR, Sitia R. Aggresomes and Russell bodies. Symptoms of cellular indigestion? *EMBO Rep* 2000; **1:** 225–31.
60 Johnston JA, Ward CL, Kopito RR. Aggresomes: a cellular response to misfolded proteins. *J Cell Biol* 1998; **143:** 1883–98.
61 Gu WJ, Corti O, Araujo F *et al.* The C289G and C418R missense mutations cause rapid sequestration of human Parkin into insoluble aggregates. *Neurobiol Dis* 2003; **14:** 357–64.
62 Saliba RS, Munro PM, Luthert PJ, Cheetham ME. The cellular fate of mutant rhodopsin: quality control, degradation and aggresome formation. *J Cell Sci* 2002; **115:** 2907–18.
63 Liu Y, Shevchenko A, Berk AJ. Adenovirus exploits the cellular aggresome response to accelerate inactivation of the MRN complex. *J Virol* 2005; **79:** 14004–16.
64 Araujo FD, Stracker TH, Carson CT, Lee DV, Weitzman MD. Adenovirus type 5, E4orf3 protein targets the Mre11 complex to cytoplasmic aggresomes. *J Virol* 2005; **79:** 11382–91.
65 Spiropoulou CF, Goldsmith CS, Shoemaker TR, Peters CJ, Compans RW. Sin Nombre virus glycoprotein trafficking. *Virology* 2003; **308:** 48–63.
66 Laszlo L, Tuckwell J, Self T *et al.* The latent membrane protein-1 in Epstein–Barr virus-transformed lymphoblastoid cells is found with ubiquitin-protein conjugates and heat-shock protein 70 in lysosomes oriented around the microtubule organizing centre. *J Pathol* 1991; **164:** 203–14.
67 Kim PS, Arvan P. Endocrinopathies in the family of endoplasmic reticulum (ER) storage diseases: disorders of protein trafficking and the role of ER molecular chaperones. *Endocr Rev* 1998; **19:** 173–202.

ABSTRACT

Hepatitis B virus (HBV) infection is endemic in South Africa. A unique feature of HBV carriers in this geographical region is that majority of the carriers are HBV e antigen (HBeAg) negative before they reach adulthood. Up to a few years ago the reason for this early loss of HBeAg was unknown. HBeAg is translated from the precore mRNA whose transcription is controlled by the basic core promoter. The dominant subgenotype of HBV in South Africa is subgenotype A1. This subgenotype is characterized by various variations/mutations in the basic core promoter and precore region of HBV that can affect HBeAg expression. Within the basic core promoter, A1762T/G1764A mutations can affect the expression of HBeAg at the transcriptional level. These mutations interfere with transcription factor binding to the basic core promoter and suppress the transcription of precore mRNA that is translated into HBeAg, hence reducing HBeAg expression. Mutations at nucleotides 1809-1812, also within the basic core promoter, reduce HBeAg expression at the translational level by creating a "sub-optimal" Kozak sequence upstream from the precore start codon at position 1814 from the *EcoR*I site. Following translation of the precore/core fusion protein, this precursor molecule of HBeAg is post-translationally modified by signal peptide cleavage at a fixed site on the amino end and at variable sites on the carboxyl end. The precore/core open reading frame on the precore mRNA that codes for the precursor of HBeAg, overlaps the region that codes for the encapsidation signal (ε) on the pregenomic RNA (pgRNA). pgRNA plays a pivotal role in the initiation of reverse transcription and is translated into the capsid protein and the polymerase enzyme.

In previous studies, a guanine (G) to thymine (T) mutation at nucleotide 1862 within the precore region was identified in subgenotype A1 isolates from asymptomatic carriers of the virus and from hepatocellular carcinoma patients from South Africa. This mutation could conceivably have two functional consequences. Firstly, the G1862T mutation could change the secondary structure of ε and could interfere with and hence affect HBV replication. Secondly, the phenotypic change from valine to phenylalanine introduced by the G1862T mutation at codon 17 (-3 position to the signal peptidase recognition motif) is close to the signal peptide cleavage site at position 19 (-1 position to the signal peptidase recognition motif), and may therefore abrogate signal peptide cleavage. Therefore the objective of this study was to functionally characterize the HBV G1862T mutation and its equivalent G1982T found in woodchuck hepatitis virus (WHV). This was done by determining the effect of this mutation on viral replication and eAg expression of plasmid constructs *in vitro*.

Replication competent clones were constructed by mutating the wild-type of HBV and the mutant of WHV. The G1862T and T1982G mutation were introduced into the precore region of replication competent HBV and WHV plasmids, respectively, by site-directed mutagenesis. HBeAg-expression and WHeAg-expression plasmids were constructed using the replication competent clones as templates. For HBV, the templates used belonged to genotype D or to genotype D in which the precore region was mutated into a genotype A context, genotype 'A'. Huh 7 hepatoma cells were transfected with the respective replication competent clones and HBV replication was followed using Southern hybridization and real time polymerase chain reaction (PCR). The secretion and expression of HBeAg were monitored using enzyme-linked immunosorbent assay (ELISA), immunocytochemistry and

confocal microscopy, following transfection with the eAg expressing plasmids. The secretion and expression of WHeAg were monitored using pulsed radioactive-label, immunoprecipitation, sodium dodecyl sulfate-polyacrylamide gel electrophoresis (SDS-PAGE) and immunocytochemistry and confocal microscopy.

HBV replication was significantly reduced when the G1862T was introduced into genotype D but not into genotype 'A' HBV replication competent constructs. Following transfection with mutated HBeAg-expression plasmids, a reduction of 38 % for genotype D, and 54 % for genotype 'A' in HBeAg secretion relative to the wild-type were observed. Using the WHV constructs, reduced processing of the mutant relative to the wild-type protein was demonstrated using pulse-radioactive labelling. Using confocal microscopy it was demonstrated that both the mutant HBeAg and mutant WHeAg accumulated in the endoplasmic reticulum, endoplasmic reticulum Golgi intermediate compartment and Golgi. This accumulation is because the introduction of a phenylalanine at position -3 of the signal peptide cleavage site interfered with the post-translational modification of the HBeAg precursor protein. The aggregates of mutant HBV protein increased in size following treatment of cells with a proteasome inhibitor, MG132, and had the hallmark features of aggresomes. They attracted ubiquitin, heat shock proteins and proteasomes, and were isolated from the cytosol by the intermediate filaments, vimentin and cytokeratin. Aggresomes formed by the HBV mutant precore protein resembled Mallory-Denk bodies which are histological and potential markers of progressive liver diseases.

ACKNOWLEDGEMENTS

I would like to thank both of my supervisors, Professor Anna Kramvis and Professor M.C. Kew, for all their help, encouragement and advice on this project, as well as for their endless support when it was needed most.

To Professor Trefor Jenkins, thank you for the never-ending hours of mentoring sessions. You made this "finishing product" possible.

To my sister, thank you for going through the tough time with me. Ah Zah!!

To my dear friends, Dr Raquel Duarte, Dr Kurt Lightfoot, Mrs Jeanne Strong, and Mrs G Ngoi, thank you for your encouragement and support in every possible way.

To my friends from the Molecular Hepatology Research Unit, Dr Michelle Skelton, Dr Gerald Kimbi and Dr George Asare, thank you for everything, especially the words of encouragement when they were most needed. I would like to give special thanks to Mrs Roshni Desai for always ordering reagents and kits so promptly.

Lastly, I would like to acknowledge the financial assistance provided to me by the University of the Witwatersrand, the National Research Foundation, and the Poliomyelitis Research Foundation

TABLE OF CONTENTS

CHAPTER 1

LIST OF FIGURES

LIST OF TABLES

LIST OF ABBREVIATIONS

3'r	3' terminally redundant
5'r	5' terminally redundant
aa	amino acid
ASCs	asymptomatic carriers
ATG	protein translation start codon
ATP	adenosine 5'-triphosphate
ATP7B	copper-transporting ATPase
ATPase	enzyme catalyse the hydrolysis of ATP
Au	Australian antigen
BCP	basic core promoter
BFA	brefeldin A
bp	base pair
cccDNA	covalently close circular DNA
CMV	cytomegalovirus
COPI	coatomer protein complex I
COPII	coatomer protein complex II
CSV	constitutive secretory vesicles
CTFR	cystic fibrosis transmembrane regulator
DNA	deoxy nucleic acid
DAPI	4',6-diamidino-2-phenylinodole, dihydrochloride
DL	duplex linear
DR	direct repeat
EBV	Epstein-Barr virus
EDTA	ethylene diamine tetra-acetic acid di-sodium salt

EE	early endosomes
ELISA	enzyme-linked immunosorbent assay
EN1	enhancer 1
EN2	enhancer 2
eGFP	enhanced green fluorescent protein
epsilon (ε)	encapsidation signal
ER	endoplasmic reticulum
ERAD	endoplasmic reticulum-associated degradation
ERGIC	endoplasmic reticulum Golgi intermedia compartment
FBS	foetal bovine serum
FITC	fluorescein isothiocyanate
FRET	fluorescence resonance energy transfer
GTP	guanosine triphosphate
HBV	hepatitis B virus
HBcAg	hepatitis B core antigen
HBeAg	hepatitis B virus e antigen
HBsAg	hepatitis B surface antigen
HBx	hepatitis B x protein
HCC	hepatocellular carcinoma
Hsp	heat shock protein
ISG	immature secretory granules
kb	kilobase(s)
kDa	kilodalton(s)
LB	Luria-Bertini broth
LE	late endosomes

LHBs	large surface protein
MHBs	middle surface protein
MHC	major histocompatibility complex
Mr	relative molecular weight/mass
mRNA	messenger RNA
MHC	major histocompatibility complex
MSG	matured secretory granules
MTOC	microtubule organization center
nt	nucleotide
ORF	open reading frame
PBS	phosphate buffered saline
PCR	polymerase chain reaction
PDI	proline disulphide isomerase
PEG	polyethylene glycol
PGCs	post Golgi carriers
pgRNA	pregenomic RNA
RC	relaxed circular
RER	rough endoplasmic reticulum
RNA	ribonucleic acid
RNC	ribosome nascent protein complex
rpm	revolutions per minute
RPMI	Roswell Park Memorial Institute
SDS-PAGE	Sodium dodecyl sulphate polyacrylamide gel electrophoresis
SER	smooth endoplasmic reticulum
SH	serum hepatitis

SHBs	small surface protein
SRP	signal recognition particle
ss	single stranded
TLM	translocation motif
TAP	Transporter associated with antigen processing
TGN	trans-Golgi network
TRITC	tetramethylrhodamine-5-isothiocyanate
UPR	unfolded protein response
UPS	ubiquitin-proteasome system
VSV	vesicular stomatitis virus
WHV	woodchuck hepatitis virus
WHeAg	woodchuck hepatitis virus e antigen
YMDD	tyrosine-methionine-aspartate-aspartate

Note: The IUPAC-IUBMB nucleotide codes and three letter codes for amino acids are used in this study.

CHAPTER 1

1.0 INTRODUCTION

1.1 HEPATITIS B VIRUS

1.1.1 Historical perspective

Hepatitis B virus (HBV) is the most common hepatitis virus that causes chronic infections of the liver in humans and poses a global public health problem. In 1855, Lurman first documented a form of hepatitis that was transmitted by direct inoculation of blood during a smallpox immunization campaign (Lurman, 1855). In the early and mid 20th century, outbreaks of "long-incubation" hepatitis were described in a variety of groups or populations at risk (Neefe, 1946; Mahoney, 1999). Studies of human volunteers in the 1930s and 1940s provided further convincing evidence of a viral cause, with at least two etiologic agents described (Havens, 1946; MacCallum, 1947). The nomenclature of hepatitis A for infectious hepatitis and hepatitis B for "homologous serum" hepatitis was proposed by MacCallum and Bauer in 1947 (MacCallum, 1947).

The groundbreaking study of Krugman and co-workers in 1967 confirmed the existence of two distinct types of hepatitis, referred to as hepatitis A and hepatitis B (Krugman, 1967). In the same year, Blumberg and co-workers discovered a protein in the blood of an Australian aborigine that was named the Australian antigen (Au) (Blumberg, 1967). In an independent study, Prince and co-workers confirmed the presence of the serum hepatitis (SH) antigen in the serum of a hepatitis B infected patient (Prince, 1968). Further research established that the Au and SH antigens were identical, and the antigen was later named the hepatitis B surface antigen (HBsAg).

The viral etiology of hepatitis B was firmly established by electron microscopy and the detection of viral particles (also known as Dane particles) that reacted with antisera to HBsAg (Dane *et al*, 1970). With the discovery of HBsAg and viral particles, and the subsequent rapid advances in research technology, more information was obtained about the physical properties and epidemiology of the virus, as well as the course and consequences of the viral infection.

1.1.2 Epidemiology

Two billion people worldwide have been infected with HBV. Of these, approximately 350 million are currently chronically infected with the virus and at risk for HBV related chronic liver diseases. Ten million new carriers of the virus are identified each year (WHO, 2008). HBV-related deaths number between 500000 and 1.2 million per year (Lavanchy, 2004).

The prevalence of HBV infections and patterns of transmission vary greatly in different population subgroups (Figure 1.1) (WHO, 2008). The incidence of HBV infections is highest in developing countries, including most of sub-Saharan Africa, Asia, Oceania and some parts of South America (Lavanchy, 2005; Shepard *et al*, 2006). Approximately 45 % of the world's population live in highly endemic areas with a lifetime risk to HBV infection of greater than 60 % (Mast & Alter, 1993). Highly endemic countries also have markedly higher rates of hepatocellular carcinoma (HCC) (Chuang *et al*, 1992; Bosch *et al*, 2005; McGlynn & London, 2005; Nguyen *et al*, 2009). The infection is predominately acquired as an infant or a very young child, either by perinatal or horizontal transmission, the latter from young siblings or playmates (Chiaramonte *et al*, 1991; Ahn, 1996; Kew, 1996; Mahoney, 1999; Maddrey, 2001).

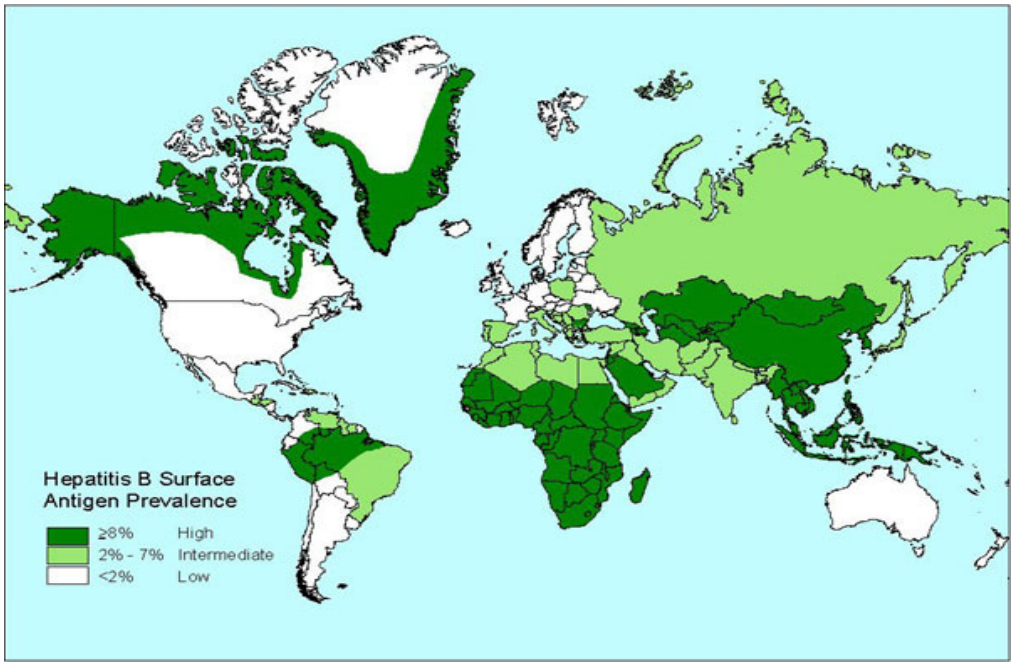

Figure 1.1 Geographical distribution of chronic hepatitis B virus infection. http://www.who.int/csr/disease/hepatitis/whocdscsrlyo20022/en/index1.html.

HBV infections are found with an intermediate incidence in North Africa, some parts of the Middle East, the southern parts of Eastern and Central Europe, the USSR, the Indian subcontinent and parts of Brazil (Lavanchy, 2004; Lavanchy, 2005; Shepard *et al*, 2006). Forty three percent of world's population lives in areas with an intermediate incidence, with a lifetime risk of the HBV infection ranging between 20 to 60 % (Mast & Alter, 1993). HBV infection occurs at all age groups, and the mode of transmission is mixed, including perinatal, horizontal, sexual, needle sharing and occupational/health care-related routes (Mahoney, 1999).

In contrast to HBV infections found in developing countries, chronic HBV infection is rare in developed countries of Western Europe, North America and Australia (Lavanchy, 2004; Lavanchy, 2005; Shepard *et al*, 2006). Only 12 % of the global

population live in areas of low incidence of HBV infection and where the lifetime risk of HBV infection is less than 20 % (Mast & Alter, 1993). The infection is predominantly acquired in the late teenage years or adulthood through sexual contact, needle sharing between illicit drug users, or occupational/health care-related sources (Mahoney, 1999).

Africa is one of the most severely affected continents, with about 65 million of the population chronically infected with HBV (Kiire, 1996; Kramvis & Kew, 2007a). It also has a very high mortality rate from hepatitis B virus infection, with 250 000 deaths out of a global annual mortality rate of 1 million per year. The carrier rate in Africa ranges from 6.5 % in Tunisia, North Africa to 19 % in Niger, West Africa and 20.6 % in Democratic Republic of the Congo, with an average of 10.4 % throughout the continent (Kew, 1996). In sub-Saharan Africa, the virus is hyperendemic, with a carrier rate of > 8 % (Kramvis & Kew, 2007a). South Africa is a country with intermediate HBV endemicity with regions of high endemicity occurring in rural areas (Dusheiko *et al*, 1989a; Dusheiko *et al*, 1989b). There is a marked difference in prevalence rate of chronic carriers between rural and urban populations in South Africa (Kew, 1996; Burnett *et al*, 2005): 5-15 % carrier rate in rural areas of South Africa and less than 5 % in urban areas of South Africa (Dusheiko *et al*, 1989a; Dusheiko *et al*, 1989b). In South Africa, the different racial groups have different prevalence rates of chronic carriage of the virus. Black South Africans have the highest carrier rate of more than 10 %. In contrast, Caucasian and Indian South Africans have a 0.2 % carrier rate, those of mixed descent (European-Africans) a rate between 0.4 - 3 %, and South African Chinese a rate of 5.3 % (Kew *et al*, 1976; Kew, 1996).

1.1.3 Clinical outcome of HBV infection

The incubation period of HBV infection ranges between 1 and 6 months (Seeger & Mason, 2000), with different clinical consequences. Most adults infected with HBV recover from the infection, but in approximately 5-10 % of adult patients and up to 90 % of neonates and young children infections progress to chronic infection (Stevens *et al*, 1975; Liang, 2009). Acute HBV infections can lead to a number of clinical consequences depending of the age, sex, and the immunological defense system of the individual (Feitelson, 1994), and the symptoms can range in severity from mild to fulminant hepatitis, the latter occurring in 1-2 % of infected persons and having a case-fatality ratio of 63 to 93 % (Mahoney, 1999).

Chronic HBV infection, defined as the persistence HBV infection for more than 6 months (Mahoney, 1999), can be either asymptomatic or symptomatic. Individuals with chronic HBV infection are at substantially increased risk of developing chronic liver diseases, including cirrhosis and HCC (Beasley, 1988; Liaw *et al*, 1988; Feitelson, 1994; Kew, 1996).

1.2 The family *Hepadnaviridae*

The members of the family *Hepadnaviridae* are highly cell type specific and have a very narrow host range, restricted to their natural host and a few closely related species (Seeger & Mason, 2000). This family is classified into two genera, the *Orthohepadnaviruses* and the *Avihepadnaviruses,* infecting mammals and avian hosts, respectively (Schaefer, 2007).

1.2.1 Genotypes of HBV

A genotype is defined as the genetic constitution of an organism (Brown, 1999). In the case of viruses, the term genotypes applies to the forms of the genomic sequences that have stabilized after a prolong period of time (Francois *et al*, 2001). HBV genotypes are currently classified into 8 genotypes (from A to H) (Miyakawa & Mizokami, 2003; Kramvis *et al*, 2005; Schaefer, 2007). This classification system is based on an intergroup divergence of more than 8 % in the complete genome sequence (Okamoto *et al*, 1988; Norder *et al*, 1992a) and more than 4 % at the level of the S gene (Norder *et al*, 1992b). Two additional genotypes I (Tran *et al*, 2008) and J (Tatematsu *et al*, 2009) have recently been proposed.

The HBV genotypes have distinct patterns of geographical distribution (Figure 1.2) (Norder *et al*, 1993; Lindh *et al*, 1997; Norder *et al*, 2004; Kramvis *et al*, 2005). HBV genotype A is mainly found in Northwestern Europe, North America, and sub-Saharan Africa (Norder *et al*, 1993; Bowyer *et al*, 1997; Lindh *et al*, 1997). Genotype B and C predominate in the indigenous population of Asia and Oceania (Okamoto *et al*, 1988; Kidd-Ljunggren *et al*, 1995; Lindh *et al*, 1997; Theamboonlers *et al*, 1999). Genotype D has a worldwide distribution but predominates in the Mediterranean area, and genotype E is found in South-West and Central Africa (Norder *et al*, 1994; Lindh *et al*, 1997; Odemuyiwa *et al*, 2001; Hubschen *et al*, 2008). Genotype F is the most divergent of the genotypes and is prevalent in South and Central American (Norder *et al*, 1993; Arauz-Ruiz *et al*, 1997). It is unique among the Amerindians and is indigenous to the native population of the New World (Nakano *et al*, 2001).

The exact distribution of genotype G has not been ascertained because of the small number of genomes sequenced from this group. From the available data, this genotype is found in Europe and North America (Stuyver *et al*, 2000; Kato *et al*, 2002; Vieth *et al*, 2002; Westland *et al*, 2003). All known genomic sequences of genotype G are closely related to each other, which suggests either an epidemiological link between the isolates or high genetic stability of this viral genotype (Gunther, 2006). Genotype H is confined to the Amerindian populations of North and Central American (Arauz-Ruiz *et al*, 1997; Arauz-Ruiz *et al*, 2002). Genotype H is more closely related to genotype F than the other genotypes. It is most likely to have split off from genotype F within the New World (Arauz-Ruiz *et al*, 2002).

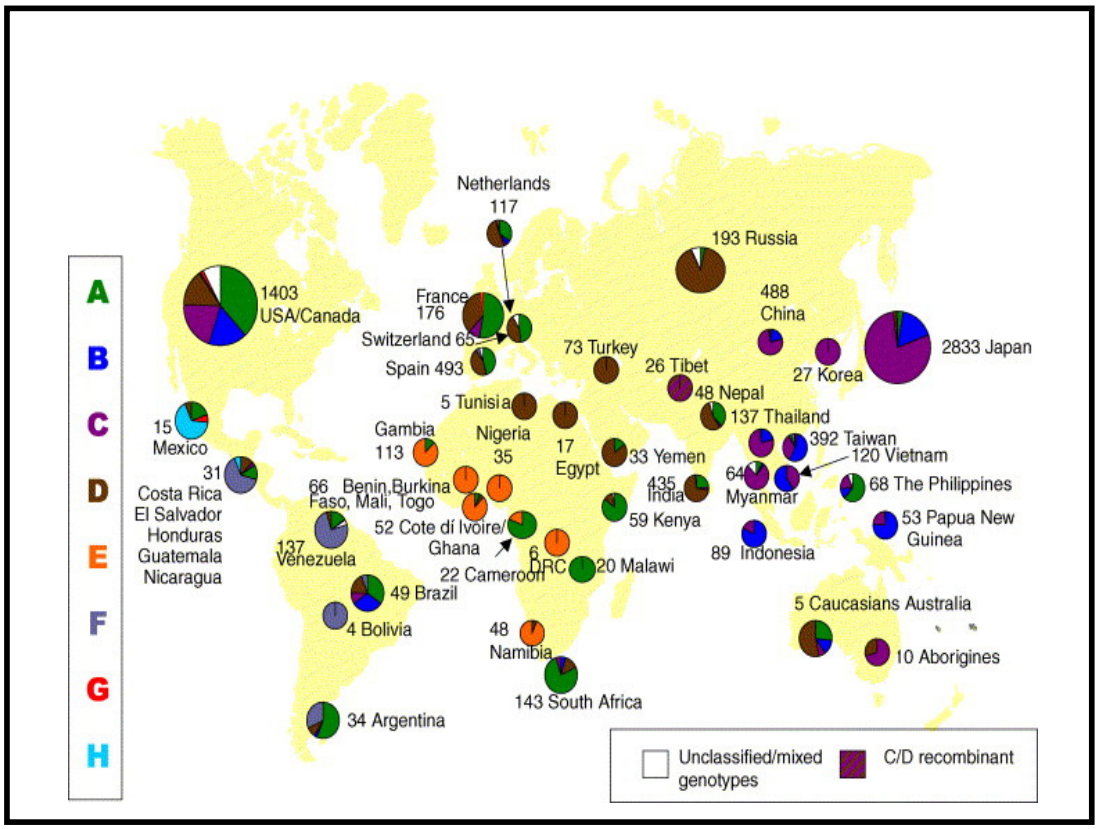

Figure 1.2 Global distributions of the eight genotypes of hepatitis B virus (Kramvis *et al*, 2005). The numbers next to the pie charts are the number of isolates genotyped and the ratio of the respective genotypes.

1.2.2 Subgenotypes of HBV

The HBV genotypes A, B, C, D and F are further sub-divided into subgenotypes with between 4 % to 8 % intergroup nucleotide difference across the complete genome, and the subgenotypes are divided into clades, showing less than 4 % nucleotide difference (Norder *et al*, 2004; Kramvis *et al*, 2005).

Subgenotype A1 is of African/Asian origin, whereas subgenotype A2 is mainly found in Europe and America (Bowyer *et al*, 1997; Sugauchi *et al*, 2004a), and more recently subgenotype A2 is found in Kenya (Mwangi *et al*, 2008). Subgenotype A3 was originally described in patients of Gambian origin (Hannoun *et al*, 2005) and later also found in the Cameroon (Kurbanov *et al*, 2005) and Gabon (Makuwa *et al*, 2006). Subgenotypes A4 and A5 are of west-African origin (Olinger *et al*, 2006), and most recently subgenotype A6 was identified in Belgium patients of African descent (Pourkarim *et al*, 2009). HBV subgenotype B1 is prevalent in Japan (Sugauchi *et al*, 2004b) and subgenotype B2 is found in mainland Asia. Subgenotype B3 is confined to Indonesia (Norder *et al*, 2004), B4 to Vietnam (Norder *et al*, 2004), and B5 to the Philippines (Nagasaki *et al*, 2006; Sakamoto *et al*, 2006). B6 is found in the indigenous populations living in the Arctic region (Sakamoto *et al*, 2007), and B7 and B8 are found in Indonesia (Nurainy *et al*, 2008; Mulyanto *et al*, 2009).

Subgenotype C1 is mainly found in Vietnam, Myanmar, and Thailand, whereas subgenotype C2 is prevalent in Japan, Korea and China (Huy & Abe, 2004; Kramvis *et al*, 2005). C3 is found in the Oceania (Norder *et al*, 2004), C4 in Aborigines from Australia (Sugauchi *et al*, 2001), C5 (Sakamoto *et al*, 2006) and C6 in the Philippines (Cavinta *et al*, 2009) and Indonesia (Lusida *et al*, 2008), and

C7 in the Indonesia (Mulyanto *et al*, 2009). Subgenotypes D1 to D4 are widely spread in Europe, Africa and Asia, with D4 predominating in the Oceania (Norder *et al*, 2004). D5 was found in India (Banerjee *et al*, 2006; Chandra *et al*, 2009) and D6 in Indonesia (Lusida *et al*, 2008). Subgenotypes F1 to F4 were found exclusively in Central and South America (Huy *et al*, 2006; Devesa & Pujol, 2007; Devesa *et al*, 2008).

More specifically, the genotypes found within southern Africa include A, B, C and D, with subgenotypes A1 and D3 predominating (Kramvis *et al*, 2005; Kramvis & Kew, 2007a; Kramvis & Kew, 2007b; Selabe *et al*, 2009). Genotype B and C were probably introduced into the country by immigrants from South East Asia.

1.3 Virion structure

1.3.1 Ultra structure and physical properties

The infectious HBV virion, or Dane particle, is the complete packaged, spherical-shaped viral particle that has a diameter of 42 nm (Figure 1.3 A). The viral envelope encloses the icosahedral core particle that contains the viral nucleic acid and DNA polymerase (Dane *et al*, 1970). Three related envelope glycoproteins found in the outer envelope are essential for the formation of Dane particle (Ueda *et al*, 1991). They are the large (LHBs), middle (MHBs), and small (SHBs) surface proteins (Tiollais *et al*, 1985; Ueda *et al*, 1991). In the Dane particle, the LHBs and MHBs together constitute 30 % of the total envelope protein content in equal proportion, and the remaining 70 % is made up of SHBs (Heermann *et al*, 1984; Heermann *et al*, 1987).

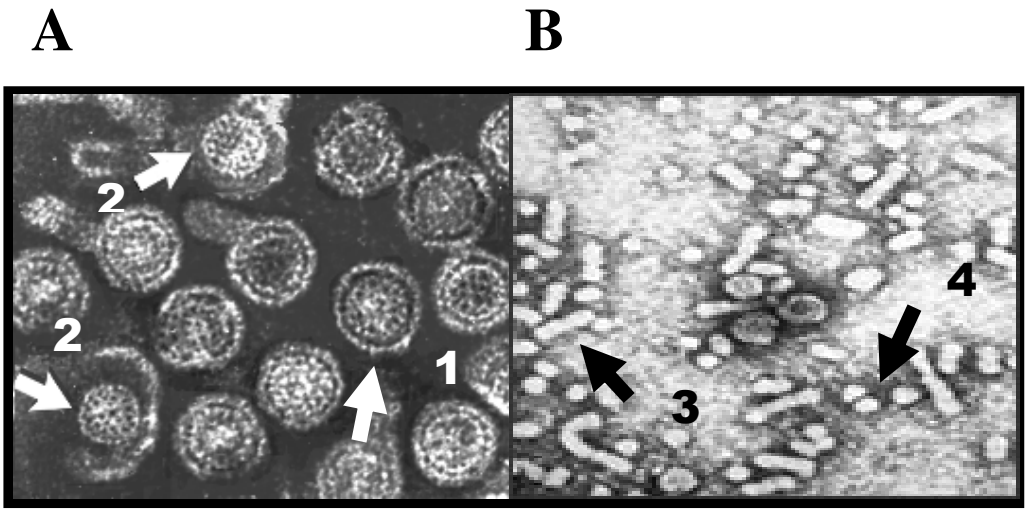

Figure 1.3 Electron micrographs of HBV virions and sub-viral particles. (A) HBV virions (Dane particles) [1] and exposed core particles [2]. http://web.uct.ac.za /depts/mmi/stannard/hepb.htm. (B) Non-infectious filamentous [3] and spherical particles [4]. http://www.cdc.gov/vaccines/vpd-vac/hepb/photos.htm

In addition to the Dane particles, two distinct types of non-infectious defective sub-viral particles are also found in the serum of infected individuals: filamentous and small spherical particles (Figure 1.3B) (Gerin *et al*, 1975; Alberti *et al*, 1978; Yamada *et al*, 1980; Sakamoto *et al*, 1983). Both types of particles have a diameter of 22 nm and do not contain viral nucleic acids. The spherical sub-viral particle is composed of the small and middle surface protein, whereas the filamentous particle also includes a small proportion of the large surface protein and is variable in length (Dane *et al*, 1970). These sub-viral particles contain only envelope glycoproteins and host-derived lipids, and typically outnumber Dane particles by 1000:1 to 10 000:1 in serum (Ganem & Prince, 2004). High levels of these non-infectious particles can be found during the acute phase of infection. Non-infectious sub-viral particles present the same antigenic sites as the Dane particles, therefore allowing

the infectious Dane particles to remain in the bloodstream undetected by neutralizing anti-surface antibodies during the progression of the infection (Fields *et al*, 1977; Gerber & Thung, 1985; Ganem & Varmus, 1987; Thomas *et al*, 1988).

The viral envelope encircles the 27 nm in diameter inner icosahedral nucleocapsid formed by HBV core protein (Figure 1.4) (Stannard & Hodgkiss, 1979). Nucleocapsid assembly starts with the formation of homodimers (Zhou & Standring, 1992) as a result of disulfide bridge formation between the Cys residues of the core protein (Nassal *et al*, 1992; Zheng *et al*, 1992). Homodimeric units are held together by weak interdimeric interactions (Ceres & Zlotnick, 2002).

Two types of nucleocapsids based on size difference are recognized (Crowther *et al*, 1994), and both are found in the liver of HBV infected patients (Kenney *et al*, 1995). Type 1 has a diameter of 30 nm and consists of 90 homodimers arranged according to an icosahedral T = 3 symmetry (T is the triangulation number). Type 2 is slightly larger with a diameter of 34 nm and is made up of 120 homodimers, which are arranged into T = 4 dimer clustered packings (Crowther *et al*, 1994; Beterams *et al*, 2000; Roseman *et al*, 2005). The partially double stranded, circular HBV genome and covalently bound DNA dependent polymerase are enclosed within the nucleocapsid (Figure 1.4) (Delius *et al*, 1983; Gerber & Thung, 1985; Ganem & Varmus, 1987).

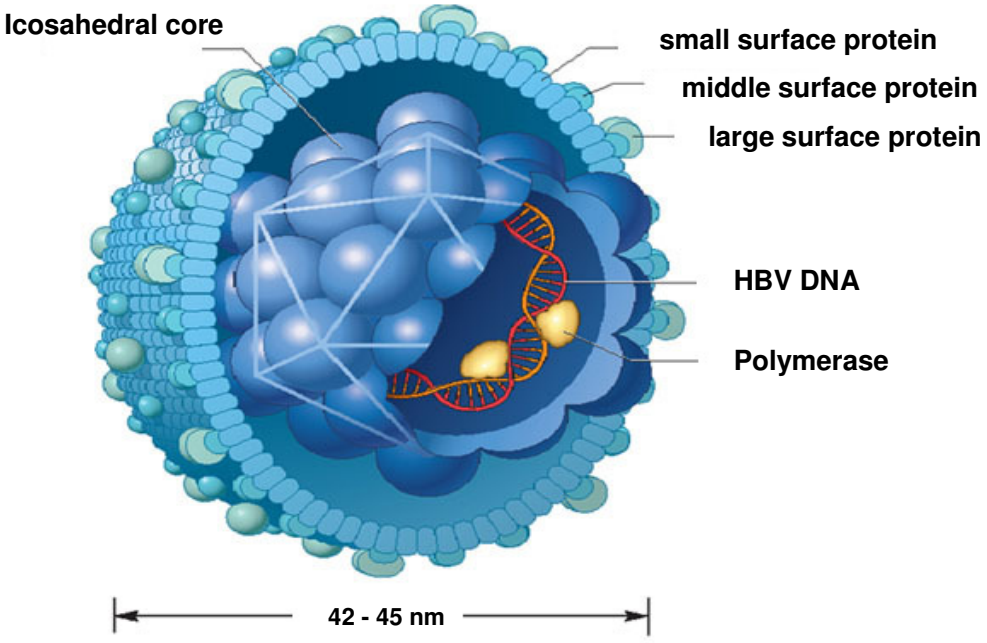

Figure 1.4 Schematic representation of the structure and components of HBV particles. The large, middle and small surface proteins are the enbeded in the viral envelope. The nucleocapsid contains the partially double stranded DNA, covalently attached via its minus strand to the polymerase. http://www.dbs-decipher.com/pic/61144207238154034HBV.

1.3.2 Viral genome

HBV has the smallest genome of all viruses known to be capable of independent infection of man. The viral genome consists of a circular partially double stranded DNA molecule with a complete minus strand DNA having a fixed length of 3200 bases, and an incomplete plus strand DNA that has a length that varies between 1700 and 2800 bases (Figure 1.5) (Summers *et al*, 1975; Hruska *et al*, 1977; Landers *et al*, 1977; Galibert *et al*, 1979). The circular nature of the viral DNA is maintained by base pairing at the 5' ends of both strands (the cohesive overlap region) (Tiollais *et al*, 1985).

HBV polymerase is attached to the 5' end of the minus strand DNA (Gerlich & Robinson, 1980; Seeger *et al*, 1986), and a capped oligonucleotide is covalently linked to the 5' end of the plus strand DNA. The function of the 5' cap is to prevent/block the phosphorylation of the plus strand (Gerlich & Robinson, 1980; Delius *et al*, 1983; Seeger *et al*, 1986).

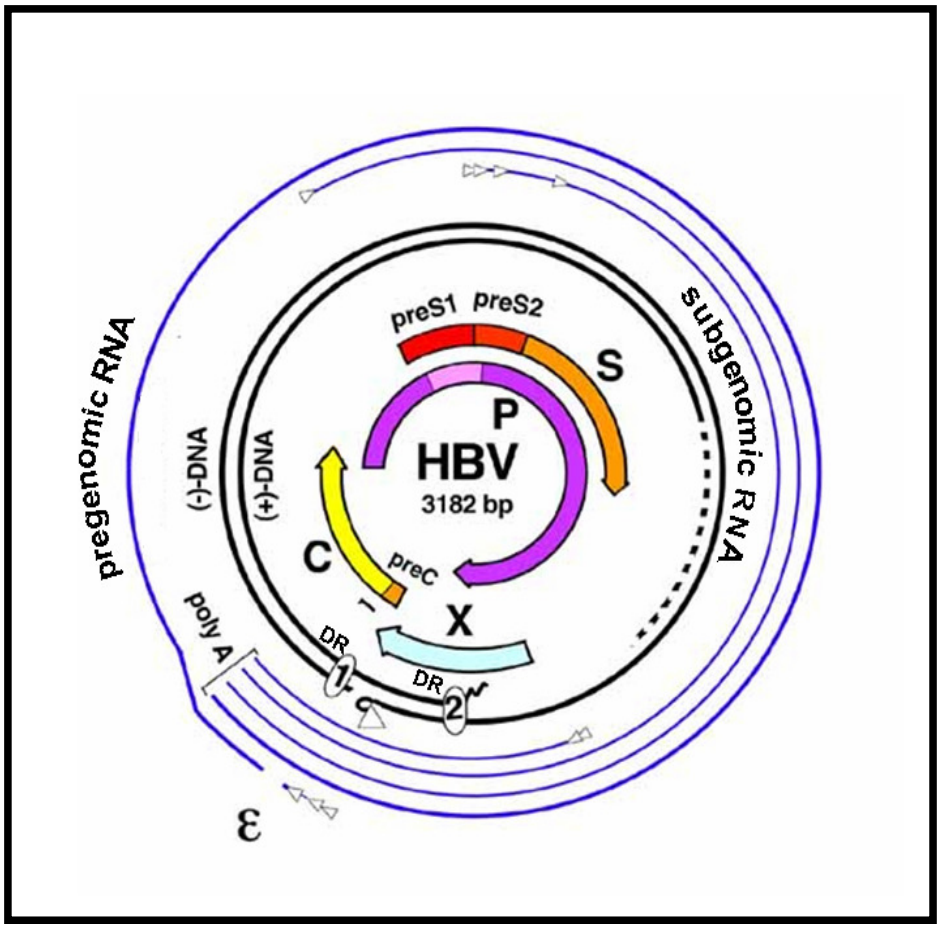

Figure 1.5 Genome organization of HBV. The outer lines represent the different HBV transcript, the bold inner circles the DNA genome as present in the virion. The four major open reading frames (pre-C/C, pre-S1/pre-S2/S, P and X) are indicated in the center. http://www.med.uni-heidelberg.de/\hyg/hyg5 /EN/FRAMESET-res-hbv.HTM

HBV has four open reading frames (ORFs), which are partially overlapping with each other and cover the entire genome (Gerber & Thung, 1985; Tiollais *et al*, 1985; Miller *et al*, 1989). These ORFs encode the precore/core protein, core protein, polymerase, three surface proteins (the SHBs, MHBs and LHBs), and X protein, respectively (Figure 1.5).

1.3.3 HBV transcripts

Hepadnaviruses replicate their genome by reverse transcription of the RNA intermediate, the pregenomic RNA (pgRNA). HBV transcription is uni-directional. All HBV transcripts are transcribed from viral covalently closed circular (ccc) DNA by cellular RNA polymerase II (Rall *et al*, 1983). Transcription generates six viral transcripts, namely the pgRNA, precore, pre-S1, pre-S2, S, and X messenger RNA (mRNA). All transcripts are modified with the addition of a 5' cap and a common polyadenylation signal at the 3' end (Ganem & Varmus, 1987). Therefore, the 5' end of the transcripts is variable, and is determined by the location of the promoters. The single polyadenylation signal terminates transcription at the common 3' end, approximately 20 bases from the 3' end of the minus strand (Schaller & Fischer, 1991).

The 3.5 kilobases (kb) pgRNA is the most abundant transcript. It has two functions: (1) serving as template for core protein and polymerase translation; (2) acting as a template for viral reverse transcription (Summers & Mason, 1982; Cattaneo *et al*, 1984; Will *et al*, 1987; Yaginuma & Koike, 1989). The precore transcript is slightly longer than the pgRNA, and it serves as template for the translation of the precore/core protein, which is the precursor of HBeAg. LHBs is translated from the

2.4 kb pre-S1 mRNA. MHBs is translated from the 2.1 kb pre-S2 mRNA (Cattaneo *et al*, 1983; Malpiece *et al*, 1983; Standring *et al*, 1984; Siddiqui *et al*, 1986). SHBs is translated from the 2.1 kb S mRNA. Hepatitis B x protein (HBx) is translated from the 0.7 kb X mRNA (Siddiqui *et al*, 1987; Treinin & Laub, 1987; Zheng *et al*, 1994).

HBV transcription is initiated and regulated by the four *cis* regulators, namely the precore/core, S1, S2 and X promoters (Tiollais *et al*, 1985; Ganem & Varmus, 1987). In addition, two regions in the HBV genome have been shown to act as transcriptional enhancers, namely the enhancer 1 (EN1) and enhancer 2 (EN2) (Su & Yee, 1992).

1.3.4 HBV life cycle

1.3.4.1 Attachment, fusion and entry of virus

The early part of virus infection involves the following three stages: (1) attachment; (2) fusion; (3) entry (Figure 1.6) (Lu & Block, 2004). The pre-S1 domain of LHBs plays a major role in mediating virus attachment and infection (Neurath *et al*, 1986a; Pontisso *et al*, 1989; De Meyer *et al*, 1997; Le Seyec *et al*, 1999; Blanchet & Sureau, 2007). The 21-47 amino acid (aa) epitope of pre-S1 domain of the LHBs was shown to mediate binding the virion to the cell surface of HepG2 cells (Neurath *et al*, 1986b). Furthermore, an 'Gln-Leu-Asp-Pro-Ala-Phe' epitope situated within the 21-47 aa region was mapped to be the key receptor-binding determinant that mediates viral attachment (Paran *et al*, 2001). HBV attachment is multivalent and synergistically involves SHBs with the 'Gln-Leu-Asp-Pro-Ala-Phe' epitope (Paran *et al*, 2001). The abundance of SHBs on the HBV envelope forms multiple contacts with the cell membrane, and as the consequence it increases the virus attachment

rate by facilitating the specific interactions of the pre-S1 domain with its receptor. SHBs is also found to be able to bind plasma membrane of human hepatocytes (de Bruin *et al*, 1995). A site situated within the small S domain was postulated to be involved in viral attachment synergistically with the 'Gln-Leu-Asp-Pro-Ala-Phe' epitope, by assisting the internalization of the gold labelled sub-viral particles (Paran *et al*, 2001).

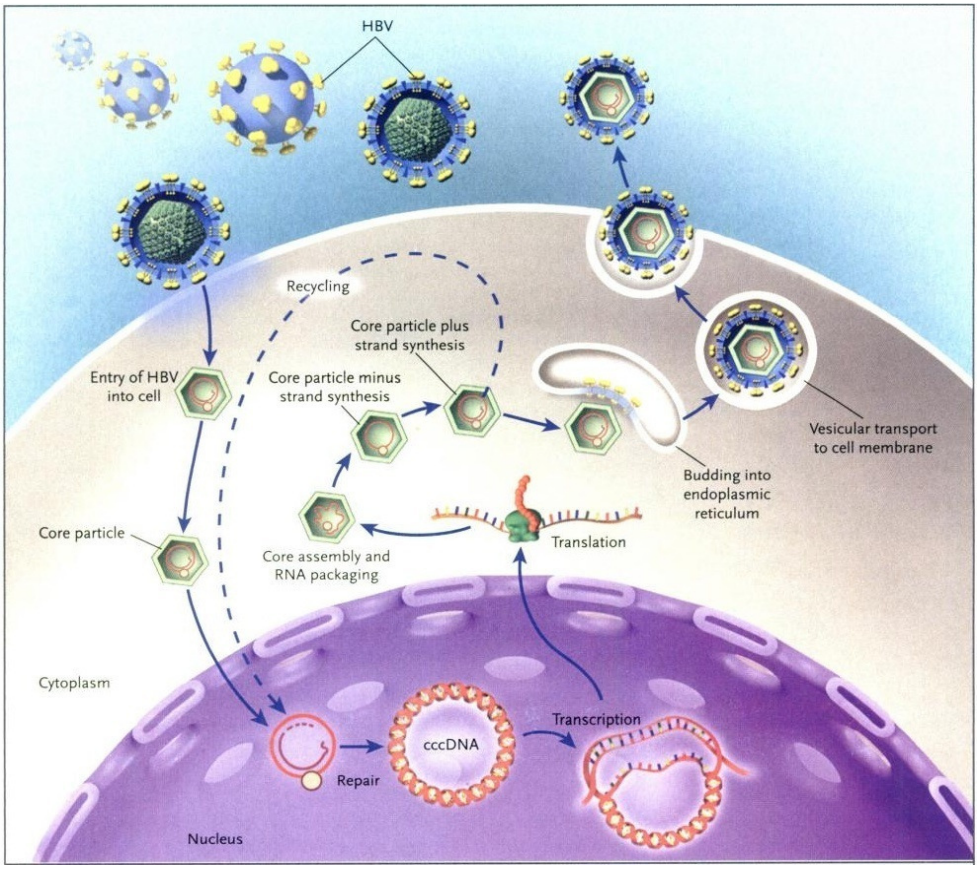

Figure 1.6 The overview of HBV life cycle (Ganem & Prince, 2004). HBV virions bind to surface receptors and are internalized. Viral core particles migrate to the hepatocyte nucleus, where their genomes are repaired to form a covalently closed circular DNA (cccDNA) that is the template for viral messenger RNA (mRNA) transcription. The viral mRNA that results is translated in the cytoplasm to produce the viral surface, core, polymerase, and X proteins. There, progeny viral capsids assemble, incorporating genomic viral RNA (RNA packaging). This RNA is reverse-transcribed into viral DNA. The resulting cores can either bud into the endoplasmic reticulum to be enveloped and exported from the cell or recycle their genomes into the nucleus for conversion to cccDNA. The small, peach-colored sphere inside the core particle is the viral DNA polymerase.

HBV has a region in the N-terminus of its pre-S2 domain that contains a hydrophobic sequence of 13 aa (Gerlich *et al*, 1993), which is conserved among all hepadnaviruses (Lu *et al*, 1996; Lu *et al*, 2001). It has all the characteristics of a fusion motif mediating virus-cell fusion (Lu *et al*, 1996). The pre-S2-translocation motif (TLM), which is cell permeable, was subsequently identified within the above mentioned fusion motif (Oess & Hildt, 2000). TLM is a 12 aa, amphipathic α-

helical structure within the region of 41-52 aa of the pre-S2 domain (Oess & Hildt, 2000). This unique amphipathic motif was found to be conserved between different HBV subtypes. Stoeckl *et al* proposed that this TLM motif mediates the energy-independent process of internalization of HBV viral particles by receptor mediated endocytosis across the endosomal membrane into the cytosol (Stoeckl *et al*, 2006), and this putative TLM motif was later proven to be indispensable for HBV infectivity (Lepere *et al*, 2007).

Fusion of viral protein and cell membrane allows the release of viral DNA into cytosol. Viral envelope protein is proteolytically processed in the endosome by a specific protease (Lu *et al*, 1996). Viral particles escape from the endosomes, and the reducing environment in the cytoplasm destroys the disulfide bridges in the S-domain and destabilizes the interaction between the surface protein and nucleocapsid, allowing the removal of envelope from the nucleocapsid. Capsids are retrograde transported along the microtubule network towards the microtubule organization centre (MTOC) located at the perinuclear region of the host cells (Kann *et al*, 2007). The carboxyl terminus of hepatitis B core antigen (HBcAg) contains a signal for nuclear localization that is responsible for the targeting of the nucleocapsid to the nucleus of host cell (Yeh *et al*, 1990; Eckhardt *et al*, 1991). Nuclear transport receptors of the importin β superfamily facilitate the docking of the capsid to the nuclear basket and translocation through the nuclear pore. The capsid interacts with nuclear basket, before releasing the viral DNA into the nucleus (Kann *et al*, 2007).

1.3.4.2 HBV replication

HBV replication can be divided into several phases (1) cccDNA formation; (2) transcription of all viral mRNA; (3) packaging transcripts (encapsidation) and viral capsid assembly; (4) reverse transcription (Nassal, 2008).

Following viral entry into the nucleus of hepatocytes, the partially double stranded relaxed circular viral DNA is released from viral nucleocapsid, and is subsequently converted into episomal cccDNA (Ruiz-Opazo *et al*, 1982b; Ruiz-Opazo *et al*, 1982a; Weiser *et al*, 1983; Beck & Nassal, 2007). The phosphodiester bond between the Tyr63 of polymerase and the 5′ phosphoryl group of minus strand DNA is cleaved, and the covalently linked polymerase and the RNA primer at the 5' end of plus strand DNA are removed (Guo *et al*, 2007; Nassal, 2008). Gaps in the plus strand DNA are filled, and the ends of both strands of viral DNA are covalently ligated to produce closed circles (Nassal, 2008). HBV cccDNA serves as the template for the transcription of pgRNA and all subgenomic mRNAs. The pgRNA is the key transcript that involves in the translation of core protein and polymerase, and is thus crucial for viral replication. All HBV transcripts are transcribed by cellular RNA polymerase II, using the cccDNA as the template.

The pgRNA and polymerase are encapsidated (packaged) into the newly assembled capsid by the binding of encapsidation signal, epsilon (ε), a structured 5'-proximal stem-loop element of the pgRNA to the polymerase (Bartenschlager *et al*, 1990; Hirsch *et al*, 1990; Bartenschlager & Schaller, 1992; Pollack & Ganem, 1994).

ε is a *cis*-acting sequence of 85-nucleotides (nt) in length that is folded into a stable secondary stem-loop structure, and located at the 5' end of the pgRNA (Figure 1.7)

(Nassal *et al*, 1990). ε has a bipartite stem-loop structure with a 6 nt apical loop, upper stem, a single unpaired U residue in the upper stem, a 6 nt bulge, and lower stem (Figure 1.7) (Bartenschlager *et al*, 1990; Junker-Niepmann *et al*, 1990; Knaus & Nassal, 1993; Pollack & Ganem, 1993). ε is the origin of HBV replication (Nassal & Rieger, 1996). The 3' half of the ε bulge serves as template for the DNA primer synthesis, and the 5' proximal nucleotides mediate encapsidation by its association with polymerase (Rieger & Nassal, 1995; Rieger & Nassal, 1996).

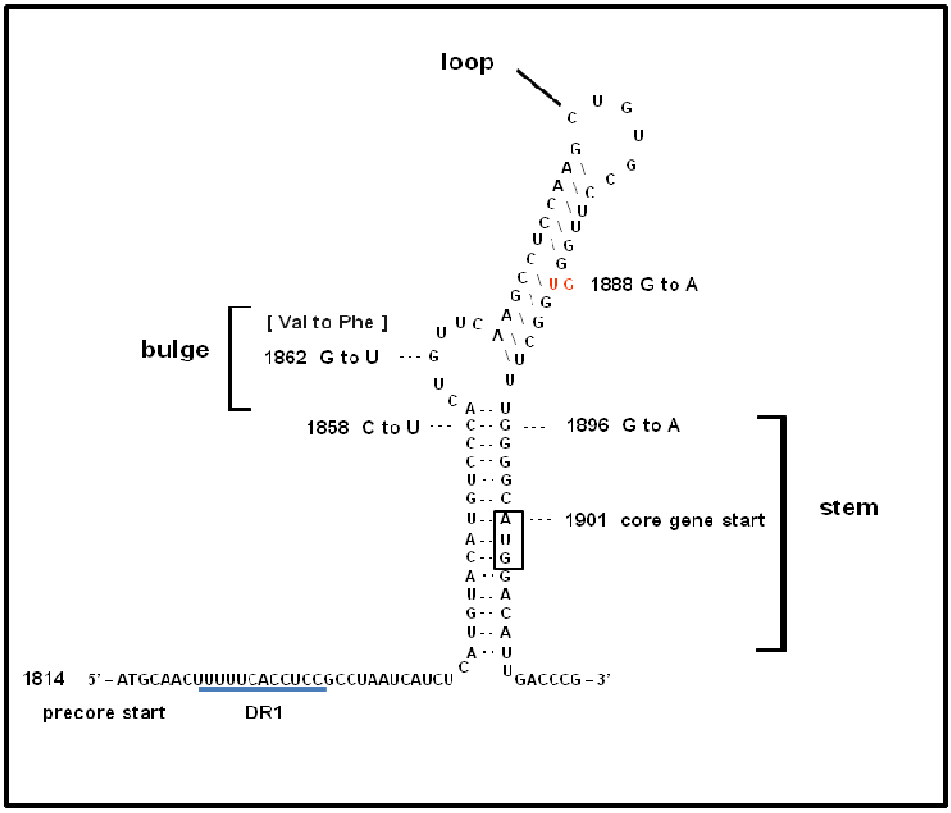

Figure 1.7 Secondary structure of HBV encapsidation signal (ε). Figure is obtained with permission from Prof A.Kramvis.

Reverse transcription of hepadnaviruses is a complex multi-step process that takes place inside nucleocapsid in infected cells (Yu & Summers, 1991; Nassal *et al*, 1992; Beck & Nassal, 1997). Reverse transcription is triggered/initiated by the interaction of the polymerase with ε (Bartenschlager *et al*, 1990; Hirsch *et al*, 1990; Bartenschlager & Schaller, 1992; Pollack & Ganem, 1994; Wang *et al*, 1994).

In addition to other functions, the polymerase as protein primer and a reverse transcriptase for the initiation of minus strand DNA synthesis using nucleotides within the ε as the template (Wang & Seeger, 1992; Wang & Seeger, 1993; Pollack & Ganem, 1994; Tavis *et al*, 1994). The molecular chaperone, heat shock protein (Hsp)70 is responsible for the adenosine 5'-triphosphate (ATP) energy-driven activation of the polymerase from an inactive to a meta-stable, active state (Mayer & Bukau, 2005; Beck & Nassal, 2007). The activated polymerase is able to bind to the ε. A second dynamic, energy driven, multi-component chaperone complex consisting of Hsp90, p23 and potentially additional co-factors act together to maintain the polymerase in the optimal and specific conformation required for pgRNA packaging and priming of viral DNA synthesis (Hu *et al*, 1997; Wang *et al*, 2003; Hu *et al*, 2004).

HBV DNA synthesis starts with the priming of polymerase (Wang & Seeger, 1992; Wang *et al*, 1994; Lanford *et al*, 1997). The first nucleotide of the short oligomer is covalently linked to the Tyr63 residue of the terminal protein domain of HBV polymerase (Weber *et al*, 1994; Zoulim & Seeger, 1994), and uses the 5'-ε as its template. The 2'-OH group of Tyr63 residue is responsible for the initiation site selection and programmed primer synthesis arrest (Schaaf *et al*, 1999).

After synthesis of three or four nucleotides, the short nascent DNA oligomer pauses synthesis and switches templates (translocated) to a complementary UUCA (motif) sequences at direct repeat (DR) 1 (DR1, nt2872-2882), near the 3' end of the pgRNA (Figure 1.8). This transfer of the short oligomer is called the first template switch (Wang & Seeger, 1993; Tavis *et al*, 1994; Rieger & Nassal, 1996). Φ (or β5) is a *cis*-acting element of 27 or 28 nt, located between DR2 and the 3' of DR1 (Tang & McLachlan, 2002; Shin *et al*, 2004). It acts as mediator to facilitate the first template switch by bringing the acceptor site into close proximity with the donor site via base pairing with the 5' half of ε, or by interacting with protein factors involved in this process (Shin *et al*, 2004; Abraham & Loeb, 2006). Another *cis*-acting element, ω, is located downstream of the acceptor site of the short oligomer. ω overlaps with the 3' end of DR1, and is base paired with the left part of the upper ε stem (Abraham & Loeb, 2007). ε, ω, Φ, and a small 6 nt region located upstream of short oligomer acceptor site interact with each other, and facilitate the first template switch (Abraham & Loeb, 2007).

Minus strand DNA synthesis resumes at DR1 and elongation proceeds toward the 3' end of the pgRNA template (Rieger & Nassal, 1996). The RNase H activity of the polymerase degrades the pgRNA template that has been copied concurrently with the elongation process (Summers & Mason, 1982; Radziwill *et al*, 1990). This synthesis results in the formation of full-length (complete) minus strand DNA with the polymerase covalently linked to its 5' end (Seeger *et al*, 1986; Lien *et al*, 1987; Will *et al*, 1987). A short RNA fragment of 17 to 18 nucleotides, a remnant of the pgRNA, is cleaved by the RNase H, and functions as a conventional nucleic acid primer for the initiation of plus strand DNA synthesis (Lien *et al*, 1986; Will *et al*, 1987; Loeb *et al*, 1991).

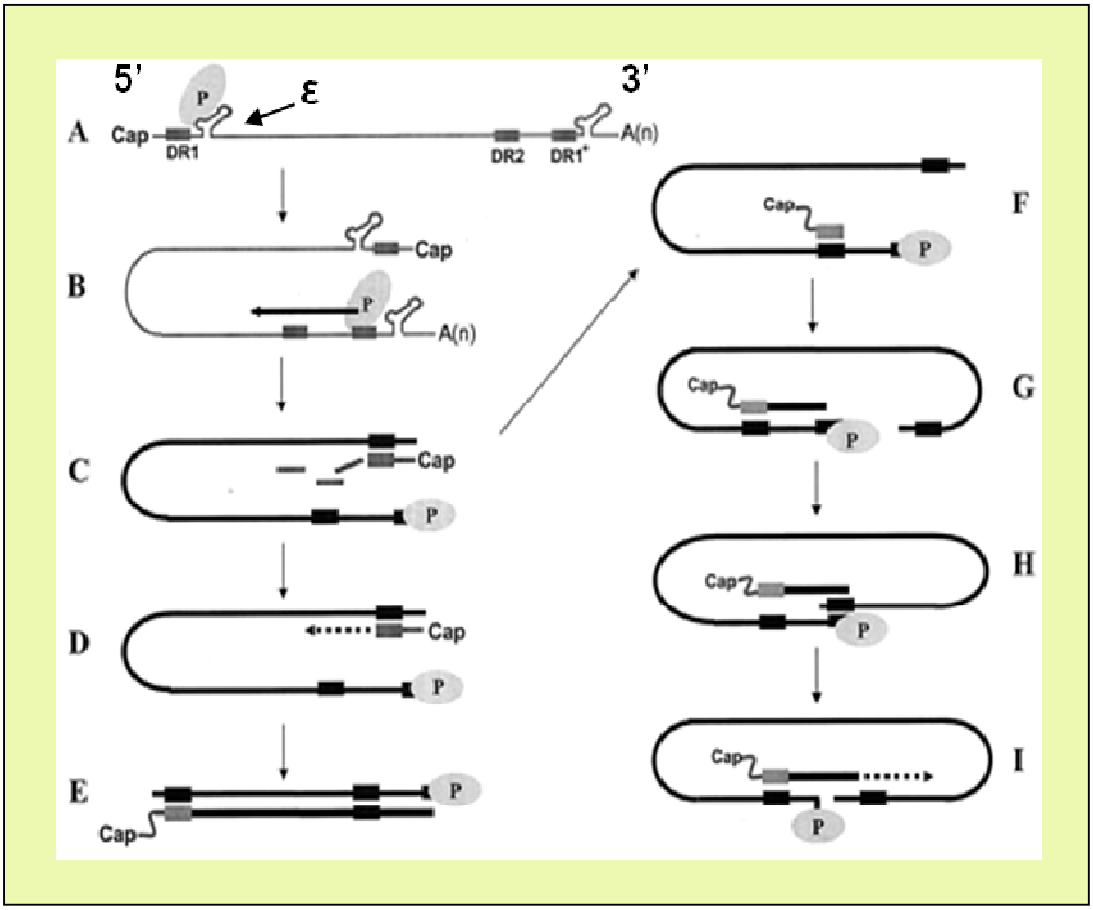

Figure 1.8 Model for hepadnavirus reverse transcription. (A) Initiation of minus strand DNA synthesis. The thin line represents the pgRNA. The direct repeats, DR1 and DR2, are indicated by boxes. Minus strand DNA synthesis is templated by the UUCA sequence within the bulge region of the 5' ε. The oval circle represents the P protein. (B) Minus strand template switch. The 4-nt-linked viral P protein translocates to an acceptor site, the UUCA sequence, overlapping the 3' copy of DR1 via 4-bp homology. (C) Elongation and completion of minus strand DNA synthesis. Following the minus strand transfer, the minus strand synthesis resumes, with concomitant degradation of the pgRNA by RNase H activity encoded by the P protein. (D) In situ priming from DR1. Some of the plus strand primers do not translocate but are used to initiate plus-strand synthesis from DR1 to generate a DL DNA. (E) Generation of a DL genome. (F) Plus strand primer translocation to DR2. The RNA primer contains a DR1 sequence complementary to DR2. This complementarity is required for subsequent translocation to DR2. To generate the circular duplex genome, the RNA primer translocates from DR1 to an acceptor site, DR2. (G) Initiation of plus strand DNA synthesis following translocation. After translocation to DR2, plus strand DNA synthesis is initiated at DR2. (H) Template switches to circularize the viral genome. The growing point of plus strand DNA synthesis switches templates from the 5' end to the 3' end of minus strand DNA. (I) Generation of an RC DNA genome (Lee *et al*, 2004).

The second template switch takes place by translocation of the short RNA primer that contains the DR1 sequences, to an acceptor site (DR2) near the 5' end of the minus strand DNA template (Figure 1.8). The RNA primer anneals to the 5' end of minus strand DNA template, initiates the synthesis of plus strand DNA from DR2, and proceeds toward the 5' end of minus strand DNA (Staprans *et al*, 1991). The second template switch occurs in approximately 90 to 95 % of the template, which comprises the major pathway of plus strand DNA synthesis for HBV.

A secondary minor pathway of plus strand synthesis also exists and does not involve the template DR2. It initiates the synthesis of plus strand DNA from DR1 on the minus strand *in situ*, resulting in the formation of a duplex linear (DL) DNA genome (Staprans *et al*, 1991). This type of synthesis of plus strand of DL DNA is called *in situ priming*.

The nascent plus strand DNA undergoes third template switch (Lien *et al*, 1986). The minus strand DNA is terminally redundant for 9 or 10 nt at 5' and 3' end (named 5'r and 3'r) (Lien *et al*, 1987). Nascent plus strand DNA copies the 5' r sequence from the minus strand. The growing plus strand DNA transfers and anneals to the the new location at 3' r of minus strand DNA, enabling the further elongation of the plus strand DNA, and ultimately generating the relaxed circular (RC) form of HBV DNA (Nassal, 2008).

1.3.5 Viral proteins

(A) Polymerase

The polymerase ORF is the largest ORF, and it overlaps with all the other three ORFs of HBV. The polymerase is translated from the ATG within the polymerase ORF of the pgRNA (Ganem & Varmus, 1987; Schlicht *et al*, 1989; Chang *et al*, 1990a; Ou *et al*, 1990) by a ribosomal shunting mechanism (Sen *et al*, 2004), and it produces the 95 kilodalton (kDa) polymerase protein. The polymerase ORF lacks its own promoter, and the translation of polymerase is therefore regulated at translational level (Hwang & Su, 1998).

The polymerase protein is made up of four domains (Radziwill *et al*, 1990). They are arranged in the following order, starting from the amino terminus (Figure 1.9): (1) the terminal protein; (2) spacer; (3) reverse transcriptase/DNA polymerase; (4) RNase H. The terminal protein plays a vital role in the priming of the minus strand to initiate reverse transcription, and the packaging of pgRNA (Wang & Seeger, 1993; Seeger & Mason, 2000). The spacer domain is not a functional domain and is therefore prone to mutations (Radziwill *et al*, 1990). The reverse transcriptase domain contains the classical tyrosine-methionine-aspartate-aspartate (YMDD) consensus motif that is involved in the nucleotide binding at the catalytic (active) site of polymerase (Poch *et al*, 1989). RNase H is the last domain of polymerase and is situated at the carboxyl end of the polymerase protein. The function of RNase H is to stabilize the terminal protein-reverse transcriptase complex during interaction with the template and to degrade the RNA in RNA-DNA hybrids during the minus strand DNA synthesis (Chang *et al*, 1990b; Radziwill *et al*, 1990; Preisler-Adams *et al*, 1993).

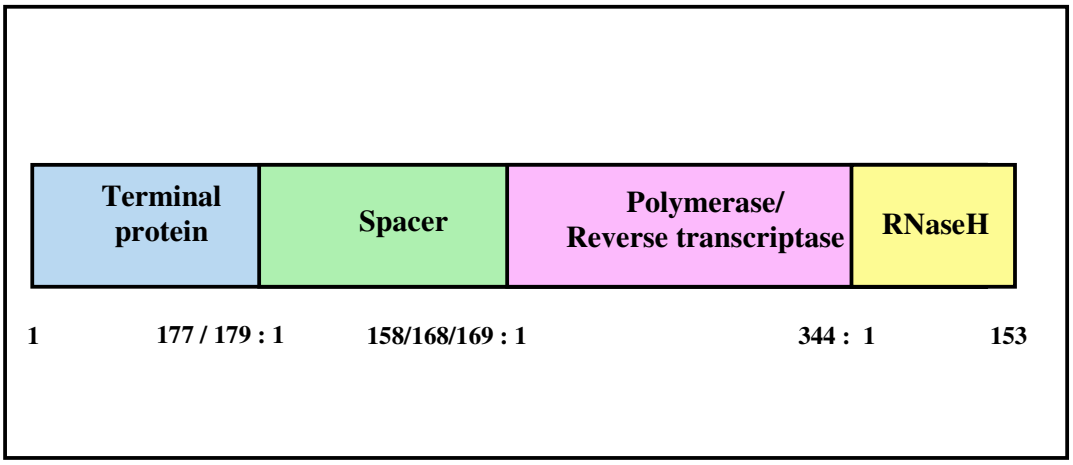

Figure 1.9 Schematic representation of the HBV polymerase gene. Amino acids are numbered at beginning of each domain, using the standardized numbering system proposed by Stuyver et al (Stuyver *et al*, 2001).

(B) Surface proteins

The surface ORF encodes three surface proteins, namely the SHBs, MHBs and LHBs. This ORF has three in-frame translation start codons and one common termination codon. The three types of surface protein share the common S-domain (Ganem & Varmus, 1987; Feitelson, 1994) (Figure 1.10). These surface proteins are transmembrane proteins that are co-translationally translocated across the endoplasmic reticulum (ER), and post-translationally modified with N-linked oligosaccharides in the ER. The N-linked glycosylation is an important process because it is necessary for the secretion of the Dane particles (Lu *et al*, 1995). Furthermore, the surface proteins interact with viral nucleocapsids to form virus particles during the maturation process by budding into the lumen of a pre-Golgi compartment and are then secreted into the serum via the constitutive secretory

pathway of the host cell (Bruss & Ganem, 1991; Ueda *et al*, 1991; Huovila *et al*, 1992).

SHBs is 226 aa long. It is produced in excess, and is the major constituent of the envelope of Dane and sub-viral particles. HBV has a common immunodominant and immunoprotective determinant, the 'a' determinant. It is located between 124 - 147 aa of the SHBs (Chen *et al*, 1996).

MHBs is 281 aa long. It is composed of SHBs with the additional 55 aa upstream encoded by the pre-S2 region. Like the SHBs, MHBs is also present in the Dane particle and sub-viral particles. The pre-S2 domain is not essential for HBV infectivity or viral particle morphogenesis, but it may contribute to virus-host cell/hepatocyte attachment as a secondary mechanism (Fernholz *et al*, 1993; Bruss, 2007).

LHBs is the largest of the three surface proteins. It contains the pre-S1, pre-S2 and S domains. The total length of LHBs is 389 or 400 aa. In the pre-S1 domain of LHBs, it becomes myristylated at the N-terminus in order to anchor the N-terminus to the membrane. Although myristylation is not essential for efficient virion assembly, it is required for infectivity (Gripon *et al*, 1995; Bruss *et al*, 1996; Chouteau *et al*, 2001).

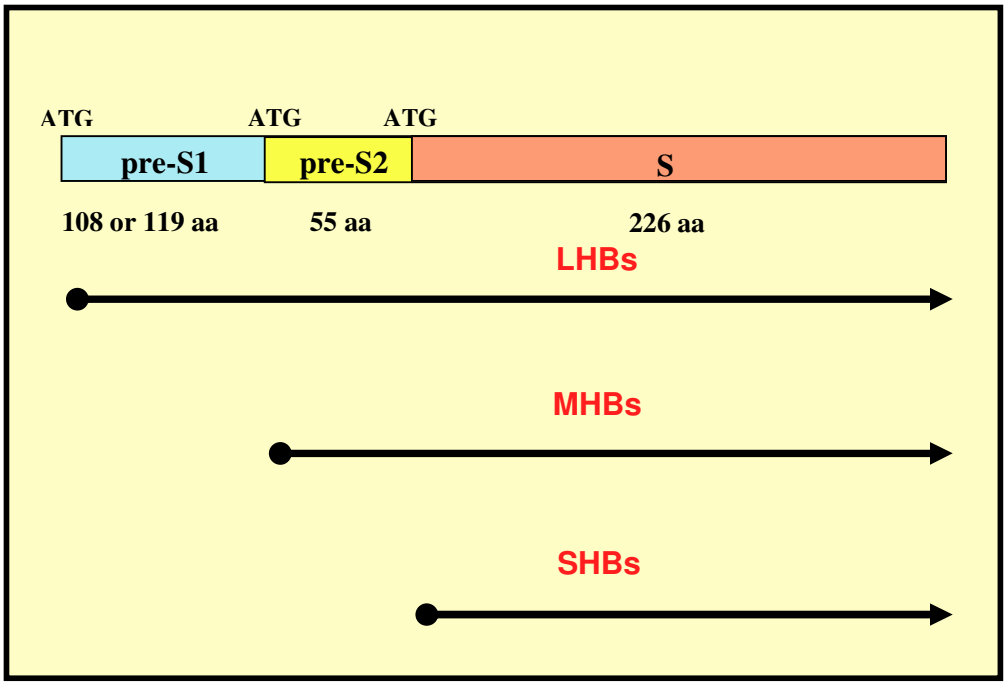

Figure 1.10 Organization of the HBV surface ORF. The large, middle and small surface proteins are encoded by a single ORF. The gene is divided into the pre-S1, pre-S2 and S domains. Length of each domain is specified at the top.

(C) Core protein

Although there are two in-frame translation initiation codons in the precore/core mRNA that encode the precore protein (precursor of hepatitis B e antigen) and core protein (HBcAg), respectively, the two proteins have different biosynthetic mechanisms (Ou *et al*, 1986; Junker *et al*, 1987; McLachlan *et al*, 1987; Schlicht *et al*, 1987; Garcia *et al*, 1988). The core protein is translated from the pgRNA. Depending on the genotype of the virus, the 21 kDa core protein consists of 183, 185 or 195 aa (Locarnini *et al*, 2003). Translation of core protein from the pgRNA starts at the ATG codon at position 1901 (from *Eco*RI site). Core protein is the major component of the viral nucleocapsid. It has intrinsic ability to self-assemble to form the nucleocapsid, and this self-assembly mechanism is essential for the

packaging of viral pgRNA and reverse transciptase (polymerase) (Birnbaum & Nassal, 1990; Nassal, 1992; Bruss, 2007). The first 149 aa on the amino terminus comprise the assembly domain, and are required to direct the self-assembly of the capsids (Conway *et al*, 1997). The protamine domain is within the region of 150-180 aa, and is obligatory for the packaging of pgRNA (Pasek *et al*, 1979; Nassal, 1992; Conway *et al*, 1997).

HBcAg can elicit both T-cell-independent and T-cell-dependent antibody responses (Schodel *et al*, 1996). HBcAg elicits a rapid and strong humoral immune response in all infected individuals (Magnius & Espmark, 1972b; Hoofnagle *et al*, 1981).

(D) X protein

The HBx protein contains 154 amino acids, and has a molecular mass of 17 kDa. HBx has been reported to be localized to the cytoplasm, nucleus and perinuclear region of hepatocytes of infected livers (Su *et al*, 1998; Nomura *et al*, 1999; Sirma *et al*, 1999). In the woodchuck hepatitis virus model, X protein is essential for viral replication *in vivo* (Chen *et al*, 1993; Zoulim *et al*, 1994). Using the transgenic mice model it has been suggested that HBx is a co-factor in hepatocarcinogenesis (Terradillos *et al*, 1997). HBx has been shown to activate transcription of host cellular genes and viral genes (Spandau & Lee, 1988; Colgrove *et al*, 1989; Arbuthnot *et al*, 2000) and also induces apoptosis mediated by an endogenous cellular pathway, both *in vitro* and *in vivo* (Terradillos *et al*, 1998). HBx is not a DNA binding protein and therefore it is not classified as a typical transactivator.

(E) Non-structural protein: HBeAg

In addition to the structural proteins described above, HBV synthesizes a non-particulate protein, hepatitis B e antigen (HBeAg) (see section 1.5 for the expression of HBeAg), which is not required for viral infection, replication or assembly (Chang *et al*, 1987; Schlicht *et al*, 1987; Chen *et al*, 1992). HBeAg and HBcAg share most of their amino acid sequences but exhibit fundamentally different biophysical and antigenic properties (Imai *et al*, 1982). Both act as distinct antigens during HBV infection (Milich, 1988). HBeAg induces a weaker and delayed response that frequently correlates with virus elimination (Magnius & Espmark, 1972b; Hoofnagle *et al*, 1981). Using the murine experimental model, it was suggested that HBeAg may have an immunoregulatory role (Milich, 1997; Milich *et al*, 1998), functioning as a T cell tolerogen and regulating the immune response to HBcAg (Chen *et al*, 2004). Therefore, HBeAg is vital in biasing the virus-host interaction toward chronicity by down regulating the host T-cell response to HBcAg via a variety of tolerance-inducing mechanisms (Chen *et al*, 2005). Furthermore, HBeAg can down-regulate the toll-like receptor 2, resulting in downstream inhibition of the cytokine production, thus regulating the host innate immune response to HBV infection (Visvanathan *et al*, 2007).

Until mutations affecting HBeAg expression were described (see section 1.5.1-1.5.3), HBeAg was widely used as the classical marker for HBV infection (Trepo *et al*, 1976). Seroconversion of HBeAg to corresponding antibody (anti-HBe) is generally associated with normalization of liver function (Hoofnagle *et al*, 1981), and regarded by physicians as end point goal for chronic hepatitis B patients undergoing anti-viral therapy (Liaw, 2009). Patients who undergo HBeAg seroconversion are more likely to experience better long-term outcomes, including

disease remission, reduced progression to cirrhosis and HCC, increased survival rate, and the possibility of HBsAg loss or seroconversion (Hsu *et al*, 2002; van Zonneveld *et al*, 2004; Lin *et al*, 2007; Liaw, 2009). A meta-analysis study showed that HBeAg negativity is associated with higher grades of fibrosis in a subset of paitents in whom HBV replicative markers were measured (Thompson *et al*, 2010).

1.4 HBV and the secretory pathway

Viruses are obligate intracellular parasites that totally depend on the host cell functions for their morphogenesis and propagation (Weiss, 2002; Freed, 2004). HBV utilizes the protein synthesis machinery and secretory pathway in the hepatocyte, for the production and maturation of viral proteins, as well as the assembly of viral particles (Patzer *et al*, 1986; Huovila *et al*, 1992). Mature, newly produced nucleocapsids can follow two different intracellular pathways (Bruss, 2004):

(1) *maturation of virion in the constitutive secretory pathway* HBV utilizes host cell machinery to synthesise the nucleocapsid, envelope and precore/core proteins using viral mRNA in the cytoplasm. Viral nucleocapsids are assembled and reach the ER, where they associate with the envelope protein. The viral particles complete their maturation during their movement from ER through Golgi apparatus, and are secreted/exported out of the cell (Huovila *et al*, 1992);

(2) *the genome amplification pathway* The nucleocapsid can be recycled back to the nucleus providing more viral genomic material for the amplification of intra-nuclear pool of cccDNA (Tuttleman *et al*, 1986).

1.4.1 Overview of secretory pathway

The secretory pathway is comprised of structurally distinct cellular organelles including the ER, tubular-vesicular transport intermediates that mediate intracellular membrane transport between ER to the Golgi Apparatus, Golgi Apparatus, and post-Golgi carriers (PGCs) that are responsible for the transportation of cargo molecules from Golgi to the plasma membrane (Lippincott-Schwartz *et al*, 2000; Lippincott-Schwartz, 2001) (Figure 1.11).

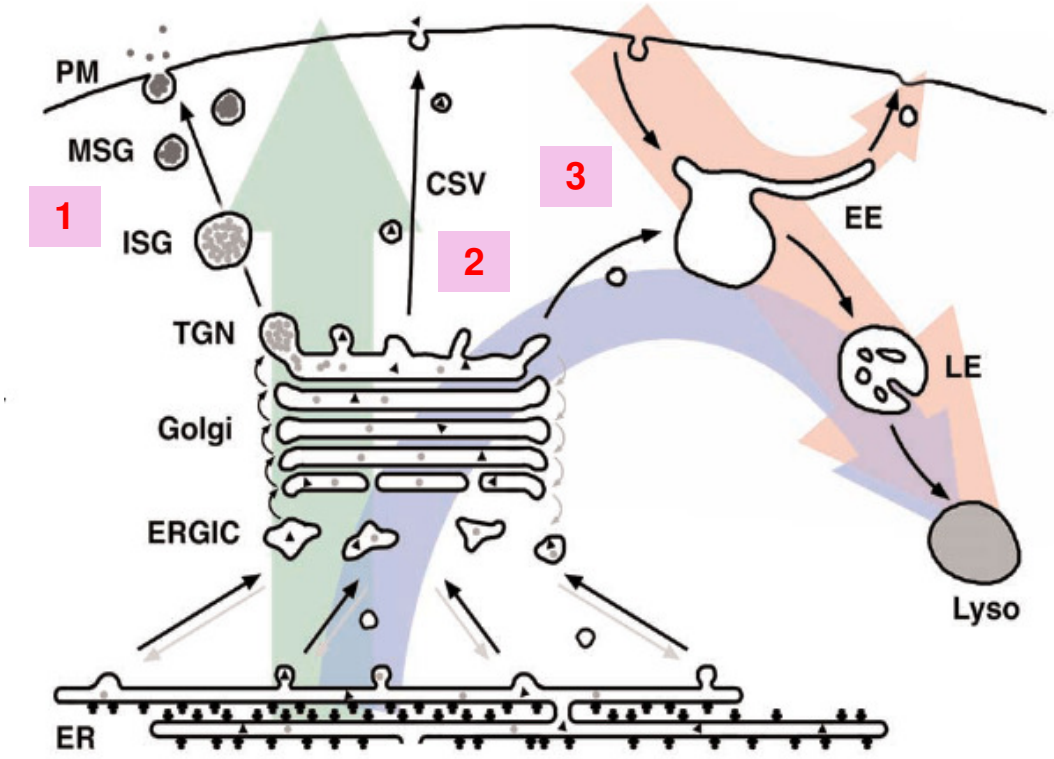

Figure 1.11 Secretory and endocytotic pathway of eukaryotic cells. ER-endosplasmic reticulum; ERGIC-endoplasmic reticulum Golgi intermediate compartment; TGN-trans-Golgi network; ISG-immature secretory granules; MSG-mature secretory granules; CSV-constitutive secretory vesicles; EE-early endosomes; LE-late endsomes; lyso-lysomes. (1) secretory granules of the regulated secretory pathway; (2) constitutive secretory vesicles to the cell surface; (3) endosome-lysosome directed carrier system (Rutishauser & Spiess, 2002).

A) Endoplasmic Reticulum

The ER is the starting point of the secretory pathway. Peripheral ER is a dynamic network, and is the largest intracellular compartment (Lippincott-Schwartz *et al*, 2000). The ER is made up of an extensive array of interconnecting, continuous linear membrane tubules, cisternal sheets, polygonal reticulum and three-way junctions (Voeltz *et al*, 2002). The domains of the ER consist of the nuclear envelope, rough ER (RER) and smooth ER (SER) (Dayel *et al*, 1999; Lippincott-Schwartz *et al*, 2000; Voeltz *et al*, 2002). ER membranes are differentiated into rough and smooth, depending on their association with ribosomes at their cytoplasmic surfaces. RER is the site of translocation and processing of newly synthesized secretory or membrane proteins, and SER is an overflow site to house up-regulated enzymes (Lippincott-Schwartz *et al*, 2000).

The ER has multiple functions, including the translocation of secretory and membrane proteins across the ER membrane, folding and post-translational modification of secretory and membrane proteins in the ER lumen (Rutishauser & Spiess, 2002; Ellgaard & Helenius, 2003), oxidative protein folding, and protein processing (Csala *et al*, 2006).

The ER is involved with the translocation of antigenic peptides. Antigenic polypeptides are firstly degraded in the cytosol by the ubiquitin-proteasome system (UPS) into smaller peptides of 3-22 aa in length, and translocated across ER lumen by the transporter associated with antigen processing (TAP). This process provides antigenic epitopes to be loaded onto major histocompatibility complex (MHC) class 1 molecule, and presented to the cytotoxic T lymphocytes (Koch & Tampe, 2006). Finally, the ER is an active metabolic compartment, where calcium ion regulation,

carbohydrate metabolism, second-phase reaction of biotransformation of glucuronosyl group, antioxidant metabolism, phospholipids and steroids metabolism occur (Csala *et al*, 2006).

Protein translation, translocation and processing

Protein translation and translocation in the ER serves as the entry point for directing secretory and membrane protein precursors into the exocytic and protein sorting pathway of the cell (Nicchitta *et al*, 2005). Most secretory and membrane proteins produced in eukaryotic cells are targeted to, and co-translationally translocated across the ER membrane by signal peptides (Walter *et al*, 1984; von Heijne, 1986; Walter & Johnson, 1994; Martoglio & Dobberstein, 1998). Signal peptides are usually 15-50 aa in length, and situated in the amino terminal extension of the precursor protein. Signal peptides are characterized by three structurally distinct domains:

(1) A hydrophilic amino terminal domain designated as the *n* region, which contains a net positive charge. This is the most variable in terms of overall length.

(2) A central hydrophobic core domain designated as the *h* region. It usually contains 6-15 aa residues. Mutational analysis demonstrated that this region is the most essential part of the signal peptide and is required for targeting and membrane insertion (von Heijne, 1985).

(3) A polar carboxyl terminal domain of 4-6 residues designated as the *c* region that contains helix-breaking Pro and Gly residues (Perlman & Halvorson, 1983; von Heijne, 1985).

Small, uncharged residues are usually found in positions -3 and -1 upstream of the signal peptide cleavage site (von Heijne, 1990). Their small uncharged side chains

fit into the active site of signal peptidase with ease, and this is crucial for the signal peptidase to cleave the precursor protein efficiently (Karamyshev *et al*, 1998).

Nascent, newly synthesized preproteins or precursor proteins carry the signal sequences on their amino terminal end. The newly emerged signal sequences from the ribosome tunnel mediate the interaction between the conserved cytoplasmic ribosome nascent protein complex (RNC) and the signal recognition particle (SRP) (Walter *et al*, 1981; Luirink & Sinning, 2004), resulting in the formation of the ribosome nascent protein complex-RNC (SRP-RNC) (Figure 1.12). In eukaryotes, the complete complex formation retards/arrests the peptide elongation process.

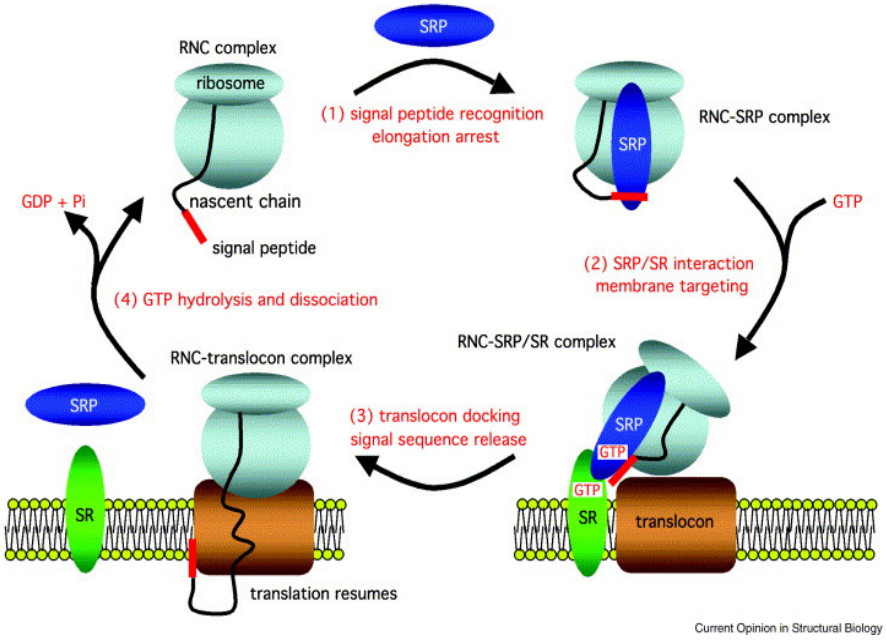

Figure 1.12 The SRP-mediated co-translational protein targeting cycle. (1) A nascent polypeptide with a signal peptide emerges from the ribosome and is recognized by the SRP, causing elongation arrest. (2) The RNC–SRP complex is then targeted to the membrane through guanosine triphosphate (GTP)-dependent interactions between the SRP and its SR. (3) At the membrane, after the ribosome docking to the translocon, the signal sequence is released from the SRP by co-translational cleavage by the membrane-bound signal peptide peptidase (Blobel & Dobberstein, 1975). This is followed by the elongation and transportation of remaining part of the nascent polypeptide chain into the lumen of the ER. (4) Following GTP hydrolysis, the SRP–SR targeting complex dissociates and is recycled (Egea *et al*, 2005).

The SRP-RNC complex is targeted to the ER membrane by interaction with the SRP receptor in the ER membrane, followed by binding of the SRP-RNC complex to the SRP receptor site of ER membrane (Gilmore *et al*, 1982; Meyer *et al*, 1982). After docking to the ER membrane, the RNC is transferred to the translocon, a protein-conducting channel that is formed by the heterotrimeric Sec61 complex (Keenan *et al*, 2001; Koch *et al*, 2003). SRP and SRP receptor are dissociated from the SRP-RNC-SRP receptor complex with the aid of energy generated from hydrolysis of GTP. The binding of the RNC to the translocon leads to its gating, as a result of the interaction with the signal sequences. Unfolded, nascent polypeptide chain is inserted into the channel and translocated while protein synthesis resumes (Keenan *et al*, 2001; Doudna & Batey, 2004; Halic & Beckmann, 2005). The leader signal sequence is now co-translationally cleaved by membrane-bound signal peptide peptidase (Blobel & Dobberstein, 1975), and followed with the elongation and transportation of remaining part of the nascent polypeptide chain into the lumen of the ER.

(B) ER to Golgi transport

Newly synthesized polypeptide chain is folded to native conformation, oligomerized in the ER, and is transported to the transitional ER (ER exit sites) before exiting the ER. The transitional ER is biochemically, functionally and morphologically distinct from RER. It is situated adjacent to the pre-Golgi intermediate compartment, and scattered over the surface of the ER (Lippincott-Schwartz *et al*, 2000). Secretory protein exited/exported from the transitional ER (Mezzacasa & Helenius, 2002) is carried by the coatomer protein complex II (COP II-coated vesicles) to Golgi via the pre-Golgi intermediate compartment (Gorelick & Shugrue, 2001).

The pre-Golgi or ER-Golgi intermediate compartment (ERGIC) is made up of tubulo-vesicular membrane clusters (Saraste & Kuismanen, 1992; Bannykh *et al*, 1996; Hauri *et al*, 2000), and is situated in the vicinity of ER exit site (Hammond & Helenius, 1994; Hammond & Glick, 2000; Stephens *et al*, 2000). ERGIC is structurally distinct from ER or Golgi, and ERGIC membranes are enriched with ERGIC-53 (a marker protein of ERGIC) (Schweizer *et al*, 1991). ERGIC-53 is a mannose-lectin that functions as a secretory cargo receptor (Hauri *et al*, 2000). The ERGIC is the first anterograde (ER to Golgi) and retrograde (Golgi to ER) sorting station in the secretory pathway (Klumperman *et al*, 1998; Appenzeller *et al*, 1999; Appenzeller-Herzog & Hauri, 2006). Newly synthesized secretory proteins concentrate and accumulate at ERGIC prior to their delivery to the *cis*-side of the Golgi apparatus.

(C) Golgi Apparatus

The Golgi apparatus is a highly dynamic organelle that receives, modifies, and sorts newly synthesized proteins transported from the ERGIC. It is composed of biochemically distinct *cis*-, *medial*-, and *trans-Golgi* sub-compartments, with the *cis*-Golgi located closest to the ER. The three sub-compartments (stacks) are connected by the tubulo-vesicular domains. Transport intermediates, COP II vesicles, carry cargo and deliver their content from ERGIC to the *cis*- side of the elaborate tubular network of the Golgi (Cooper *et al*, 1990; Lippincott-Schwartz *et al*, 2000). Secretory and membrane proteins continue their outbound journey in the Golgi complex, by moving through polarized stacks of flattened cisternae.

The secretory cargo can further undergo post-translational modification such as phosphoglycosylation and glycosylation in the Golgi apparatus (Spiro, 2002).

Phosphorylation occurs during the movement of protein through the *cis*-side of the Golgi, and glycosylation of protein takes place while the protein is moving through the *medial*-side of the Golgi. Proteins that are destined to exit from the Golgi arrive at the *trans*-side of the Golgi where they can be sorted and packaged into different PGCs. The Golgi apparatus serves as a quality control check-point to segregate/separate proteins and lipids to be retained in the ER/Golgi system from those to be delivered to the plasma membrane (Lippincott-Schwartz *et al*, 2000).

(D) Golgi to plasma membrane transport

The enriched protein is packaged into post-Golgi, membrane-bound, PGCs/transport carriers destined for the plasma membrane (Lippincott-Schwartz *et al*, 2000; Luini *et al*, 2008). Microtubule motor-dynein is able to drive the PGCs to their desired destination (Tai *et al*, 1999). Three different and distinct pathways are involved with the transport of mature protein out of the cells: (1) secretory granules of the regulated secretory pathway; (2) constitutive secretory vesicles to the cell surface; (3) endosome-lysosome directed carrier system (Rutishauser & Spiess, 2002). These PGCs are able to fully fuse and integrate all their membranes with the plasma membrane, and release the cargo proteins to the extracellular environment (Schmoranzer *et al*, 2000; Toomre *et al*, 2000).

(E) Quality control in the secretory pathway

All polypeptides translocated across the secretory are mandatorily subjected to quality control (Hurtley *et al*, 1989; Ellgaard *et al*, 1999; Ellgaard & Helenius, 2003; Sitia & Braakman, 2003).

The ER is the first checkpoint for protein quality control: it monitors the fidelity of protein structure/folding and assembly, hence prevents the further transport of immature or faulty proteins along the secretory pathway (Sayeed & Ng, 2005). The ER compartment is enriched with a broad-range of chaperones and folding enzymes, which assist in correct protein folding, the maintainance of the protein in its native state, and the prevention of the intermediates forming protein aggregates (Marquardt *et al*, 1993). Molecular chaperones such as protein disulphide isomerase (PDI) in the lumen of ER play a central role in the protein quality control, being involved in the first line of defense. Selective recognition of the non-native protein is the first step towards its elimination. Molecular chaperones have the ability to interact with non-native folding intermediates, and retain them in the ER. Once the faulty proteins have being identified, the cell responds in three different ways. Firstly, cellular factors may attempt to rescue the misfolded proteins by refolding them to a functional native state. Secondly, the cell can sequester misfolded proteins in an attempt to prevent toxic interactions. Finally, those proteins that cannot be refolded are eliminated by co-operation of the unfolded protein response (UPR) pathway (McClellan *et al*, 2005; Zhang & Kaufman, 2006) with the ER-associated degradation (ERAD) pathway (Sommer & Wolf, 1997; Brodsky & McCracken, 1999; McCracken & Brodsky, 2000; Travers *et al*, 2000).

Following retrotranslocation from the ER to cytosol, nearly all misfolded proteins are polyubiquitinated by a cascade of ubiquitin ligase enzymatic reactions that lead to ubiquitination of lysine residues of the substrate, prior to proteolytic degradation by 26S proteasome (Thrower *et al*, 2000; Hampton, 2002; Kostova & Wolf, 2003). The entrance to the proteasome complex is relatively small, and proteins must be unfolded before they can enter (Gillece *et al*, 1999; Jarosch *et al*,

2002; Wolf & Hilt, 2004). If unfolded proteins do not gain access they cannot be degraded (Kisselev *et al*, 2002).

In some severe cases, the defective proteins are not degraded and aggregate, either transiently or permanently in the ER compartment. This occurs when correct protein folding is difficult or impossible to achieve, and the degradation process is not initiated swiftly. Unfolded proteins or partially folded proteins expose their hydrophobic domains, leading to the non-productive associations of protein and protein aggregation (Wetzel, 1994; Speed *et al*, 1996; Wickner *et al*, 1999; Garcia-Mata *et al*, 2002). Protein aggregates are defined as covalently cross-linked oligomeric complexes of misfolded or unfolded proteins. They are insoluble and stable under physiological conditions (Johnston *et al*, 1998). These cross-linked protein aggregates have been referred to as "protein aggregates", "aggresomes", "inclusion bodies" or "plaques" (Kopito, 2000).

Not all proteins that fail ER quality control are retro-translocated into the cytosol, and degraded by the classical ubiquitin-proteasome system. Some proteins with minor conformational defects may escape quality control in the ER, and undergo anterograde transport to the Golgi. These defective proteins can be detected by the quality control system as they transit through the Golgi and retrograde transported back to the ER, and re-targeted to the ERAD pathway. Alternatively, these proteins can be diverted to lysosomes/endosomes for degradation by the vacuolar/lysosomal proteases (Minami *et al*, 1987; Arvan *et al*, 2002). LHBs and MHBs are diverted to lysosomes for degradation when treated with glucosidase inhibitors (Lu *et al*, 1997).

Oxidative stress in the ER or cytosol is also another main contributing factor to protein aggregation by inducing oxidative modification to the protein, and promoting protein aggregation (Grune *et al*, 2004). Protein aggregates can be further chemically modified by various cellular metabolites, including aldehydic lipid peroxidation products, and bi-functional aldehydes (Friguet *et al*, 1994; Grune *et al*, 1997; Grune *et al*, 2004). The rate of protein aggregate formation is totally dependent on time, protein concentration, and intracellular conditions (Grune *et al*, 2004). Intracellular protein aggregates are able to inhibit proteasome activity (Friguet *et al*, 1994; Sitte *et al*, 2000). The inhibition of proteasome activity can further delay the degradation of aggregates, regulatory protein and transcription factors. Thus may lead to the initiation of the apoptosis pathway.

1.5 Expression of HBeAg

The precore/core protein is translated from precore mRNA, whereas the core protein is translated from the pgRNA. Precore/core protein translation initiates at the first in-frame ATG at the 5' end in the precore/core ORF of precore mRNA. Translation produces the precore/core protein-precursor of HBeAg of 25 kDa (p25). The p25 protein has 212 aa in length, and consists of the precore domain of 29 aa followed by a core polypeptide chain (Figure 1.13).

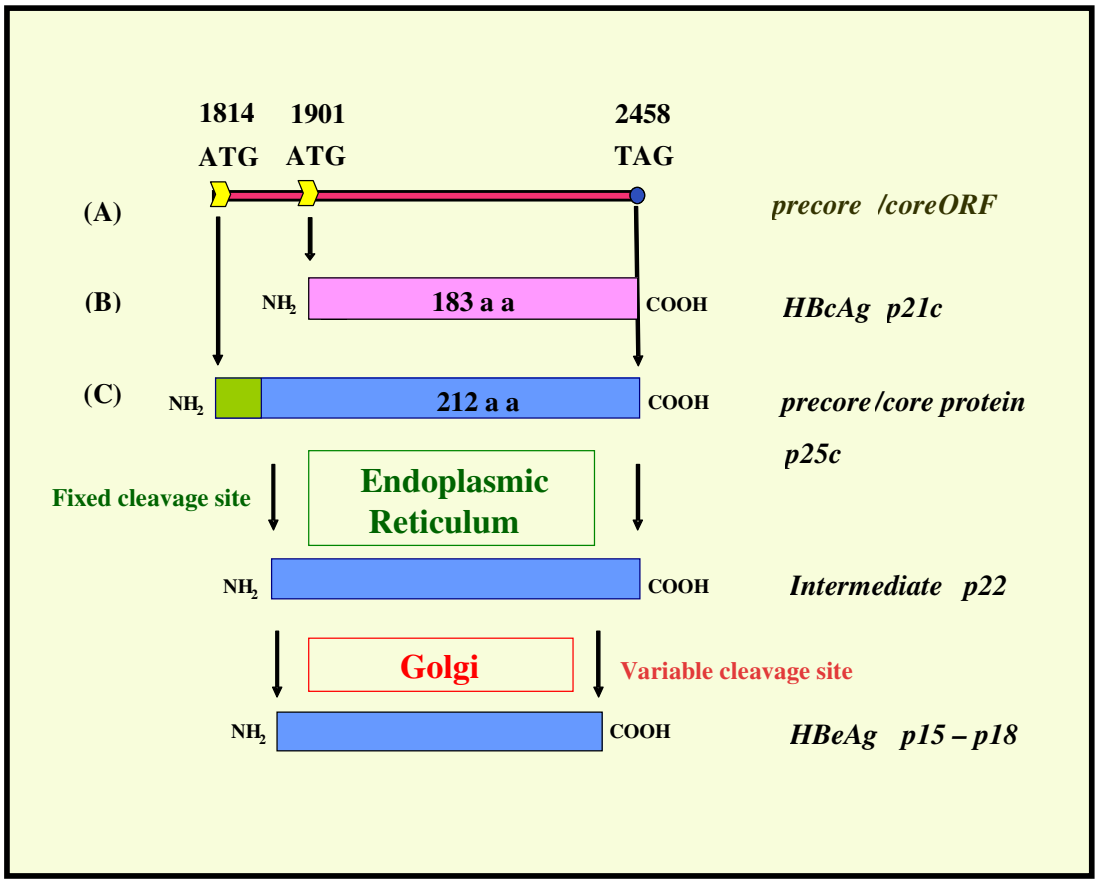

Figure 1.13 Schematic representations of the translation of HBcAg and precore/core protein, and the processing of HBeAg. Please note translation of HBcAg occurs from the pgRNA, whereas translation of the precore/core protein occurs from the precore mRNA.

The first 29 aa in the amino-terminus of precore protein are highly evolutionarily conserved among the orthohepadnaviruses (Revill *et al*, 2010), suggesting their functional importance (Ou *et al*, 1986). The sequence of the first 19 aa of the precore region resembles that of signal sequences and can direct and translocate the precore/core protein into the lumen of the ER (Watson, 1984; Ou *et al*, 1986; Standring *et al*, 1988). The signal peptide of p25 is co-translationally cleaved by host cell signal peptidase during translocation of the p25 protein into ER lumen (Junker *et al*, 1987; Garcia *et al*, 1988). Processing of the first 19 aa generates a 22 kDa intermediate protein (p22) of 193 aa in length (Ou *et al*, 1986; Junker *et al*,

1987; Bruss & Gerlich, 1988; Garcia *et al*, 1988; Standring *et al*, 1988). The remaining p22 has 10 extra amino acids at its amino terminus followed by the core polypeptide chain (Standring *et al*, 1988). The p22 protein is transported out of ER, and delivered to the Golgi complex. The second endoproteolytic cleavages take place at the carboxyl terminus of the p22 in the Golgi (Wang *et al*, 1991) by furin or furin-like proprotein convertase (Gil-Torregrosa *et al*, 1998; Messageot *et al*, 2003; Ito *et al*, 2009). Furin, a transmembrane proprotein convertase, is localized in the trans-Golgi network (TGN) (Molloy *et al*, 1999; Remacle *et al*, 2008). The trimming of p22 carboxyl terminus by furin in the TGN provides antigen presentation to the cytotoxic T lymphocytes (Gil-Torregrosa *et al*, 1998).

The exact location of carboxyl terminus cleavage has been the subject of debate. Takahashi *et al* initially identified cleavage site at Val149 (Takahashi *et al*, 1983). However, the study of Messageot *et al* showed that the maturation of HBeAg from p22 can be in one step or two steps (Messageot *et al*, 2003). The first cleavage site is at Arg167, and this cleavage gives rise to a 20 kDa intermediate, approximately 177 aa in length. The second cleavage site is at Arg154 and the cleavage generates the 17 kDa mature HBeAg of 164 aa in length (Messageot *et al*, 2003). The study of Ito *et al* demonstrated that the cleavage site at the carboxyl terminus is genotype specific (Tong, 2007; Ito *et al*, 2009). The non-A genotype cleavage site was identified to be the Arg154 (Messageot *et al*, 2003; Tong, 2007; Ito *et al*, 2009), whereas in genotype A, the cleavage site of the majority of HBeAg was mapped to Arg159 (Ito *et al*, 2009). In addition to the Arg159 site, two other alternative cleavage sites, Arg154 and Arg169 have also been recognized in genotype A (Ito *et al*, 2009). This produces a heterogenous final mature HBeAg of 15-18 kDa. The intra-molecular disulfide bond formed between Cys7 (counting from the first amino

acid of core region) and Cys61, is important to prevent dimerization of monomeric HBeAg, and is critical in maintaining the tertiary structure of HBeAg and the antigenicity of HBeAg (Wasenauer *et al*, 1992; Nassal & Rieger, 1993; Bang *et al*, 2005). In fact, HBeAg was identified by Magnius and Espmark, in the plasma of a chronic carrier of HBV, as a distinct antigen-antibody complex using an immunodiffusion method (Magnius & Espmark, 1972a). Mature HBeAg is transported out of the hepatocytes, and secreted into the blood in a monomeric form (Wasenauer *et al*, 1992). HBeAg is also found to be expressed on the surface of infected hepatocytes (Mushahwar & Overby, 1981).

HBV DNA negative Dane particles were documented to exist in serum (Gerin *et al*, 1975; Alberti *et al*, 1978; Takahashi *et al*, 1980; Sakamoto *et al*, 1983). Kimura *et al* reported the existence of DNA negative Dane particles, which are rich in 22 kDa precore protein (p22cr), without viral DNA and core capsid (Kimura *et al*, 2005). This p22cr protein has uncleaved signal peptides on the amino end and is cleaved on the carboxyl terminus in the arginine-rich domain (Kimura *et al*, 2005). The functions of the p22cr are largely unknown, but it has been suggested that it may play a role in persistence of HBV infection (Gerin *et al*, 1975; Takahashi *et al*, 1980; Sakamoto *et al*, 1983), and may disturb the host immune response (Kimura *et al*, 2005). Kimura *et al* postulated that p22cr may possibly also play a role in the inhibition of HBV replication during natural infection (Kimura *et al*, 2005) because overexpression of precore protein has been shown to inhibit viral replication in cell culture (Scaglioni *et al*, 1997b) and the transgenic mice system (Guidotti *et al*, 1996).

Various mutations in the basic core promoter (BCP) and precore region of HBV may affect the expression of HBeAg at three levels, namely the transcriptional, translational and post-translational levels.

1.5.1 The transcriptional level: A1762T/G1764A mutants

The BCP (nt1742-1849) controls the transcription of the precore mRNA and pgRNA (Yaginuma & Koike, 1989; Yuh & Ting, 1990). The most common BCP mutations A1762T/G1764A were first discovered by Okamoto *et al* (Okamoto *et al*, 1994). The combination of A1762T/G1764A synergistically reduce the basic core promoter activity and suppress the transcription of precore mRNA (Buckwold *et al*, 1996; Moriyama *et al*, 1996; Sterneck *et al*, 1998), thus resulting in reduced expression of HBeAg (Moriyama *et al*, 1996; Moriyama, 1997; Scaglioni *et al*, 1997a; Parekh *et al*, 2003). The mutations also increase transcription of pgRNA (Moriyama *et al*, 1996; Moriyama, 1997), leading to moderately increased viral replication (Buckwold *et al*, 1996; Moriyama *et al*, 1996; Scaglioni *et al*, 1997a; Parekh *et al*, 2003; Tong *et al*, 2005; Jammeh *et al*, 2008).

1.5.2 The translational level: 1896 and 1809-1812 mutants

1896 mutant

The classical G1896A mutation, which results in the generation of translational stop codon by converting the TGG codon for Trp to the stop codon TAG (Carman *et al*, 1989; Tong *et al*, 1990). This is the predominant mutation in the precore region (Revill *et al*, 2010) and has been implicated in resulting in HBeAg-negativity as a consequence of the premature termination of the synthesis of the precore precursor protein (Carman *et al*, 1989; Tong *et al*, 1990).

G1896A mutation occurs at the lower stem of the ε in the pgRNA, and is base paired with T1858 in the opposite position of the lower stem. Base pairing of G1896A with 1858T stabilizes the encapsidation signal, improves viral genome stability, encapsidation of pgRNA, and initiation of DNA synthesis (Lok *et al*, 1994; Rodriguez-Frias *et al*, 1995). This mutation is frequently observed in HBV from Asian and Mediterranean patients, but rarely in Western Europe and North America (Kramvis *et al*, 1997; Nagasaka *et al*, 1998; Grandjacques *et al*, 2000). The reason for this is that the G1896A is genotype-specific (Li *et al*, 1993; Lok *et al*, 1994). This mutation is rarely identified in genotypes A (Li *et al*, 1993; Lok *et al*, 1994; Kramvis *et al*, 2008), genotype F (Arauz-Ruiz *et al*, 1997; Lindh, 1997; Norder *et al*, 2003) or in certain strains of HBV genotype C (Lindh, 1997) because position 1858 in these genotypes is a C instead of a T. The stable Watson-Crick base pairing between 1858C and 1896G would be disrupted by G1896A, destabilizing the lower stem of ε (Li *et al*, 1993; Lok *et al*, 1994). In contrast, genotypes B, D and some strains of genotype C, the wobble base pair is formed between 1858T and 1896G (Li *et al*, 1993; Lok *et al*, 1994). In these genotypes, the G1896A mutation is more favorable because it converts the wobble base pair into a stable Watson-Crick base pair contributing to the enhancement of ε stability (Lok *et al*, 1994).

1809-1812 mutants

In 1999, Baptista *et al* reported the missense mutations that are unique to subgenotype A1 at nt1809, 1811 and 1812 (Baptista *et al*, 1999; Owiredu *et al*, 2001; Kramvis *et al*, 2002; Kimbi *et al*, 2004). The 1809, 1811 and 1812 mutations corresponding to the -5, -3 and -2 position to the precore translation initiation codon (Ahn *et al*, 2003). The sequence around precore initiation codon (nt1808-1817) is

well conserved among genotypes A to H (Arauz-Ruiz *et al*, 1997), and is regarded as the "optimal" Kozak sequence for the translational initiation of the precore precursor protein (Kozak, 1987; Kozak, 1999). The combination of the triple mutations creates a "sub-optimal" translational initiation context, which reduces precore/core protein translation by a leaky scanning mechanism (Ahn *et al*, 2003). The "sub-optimal" context of the precore AUG region caused by the triple mutation results in small ribosomal subunit (40S) missing this AUG codon, and re-initiating translation at the next downstream in-frame initiation codon, leading to core protein translation from the precore mRNA (Ahn *et al*, 2003). The reduction of HBeAg expression as a result of the 1809-1812 mutations in the Kozak sequence is comparable to that resulting from the effect of A1762T/G1764A mutants on transcription. Moreover, the presence of both the BCP A1762T/G1764A mutants together with the 1809-1812 mutations results in an additive reduction of HBeAg expression (Ahn *et al*, 2003).

In addition to the mutations described above sequencing of HBV isolates from southern African Blacks lead to the identification of a G1862T mutation in the precore region that could conceivably affect the expression of HBeAg.

1.5.3 Can the G1862T mutation affect HBeAg expression at the post-translational level?

The guanine (G) to thymine (T) transversion at nt 1862 (numbering from the *EcoR*1 cleavage site) within the bulge of the RNA encapsidation signal (ε) of the HBV was initially reported in occasional patients with various forms of acute or chronic HBV-induced liver disease (Carman *et al*., 1995; Clementi *et al*., 1993; Horikita *et al*., 1994; Laskus *et al*., 1993; Laskus *et al*., 1994; Li *et al*., 1993; Loriot *et al*., 1995;

Santantonio *et al*., 1991; Tran *et al*., 1991; Valliammai *et al*., 1995; Zhang *et al*., 1996). Subsequently, the mutation was detected in 24 % southern African Black asymptomatic carriers of the virus (Kramvis *et al*, 1997), and in 26 % of southern African Black patients with HBV-induced HCC (Kramvis *et al*, 1998). This mutation occurs together with the G1888A silent mutation commonly found in subgenotype A1 (Kimbi *et al*, 2004). The G1862T mutation was present in 35 % of the tumor tissues but was absent in non-tumorous hepatic tissue (Kramvis *et al*, 1998), 74 % of patients with various forms of liver disease who were infected with subgenotype A1 of the virus (but in none of similar patients infected with subgenotype A2 or genotype D) (Tanaka *et al*, 2004b), and 14 % of Chinese patients with fulminant hepatitis B (Hou *et al*, 2002).

Woodchuck hepatitis virus (WHV) is naturally found in the Eastern North American woodchuck (*Marmota monax*). WHV shares approximately 65 % nucleotide sequence identity with HBV (Galibert *et al*, 1982). The WHV genomic organization, replication strategies and biological properties are similar to those of HBV and other mammalian hepadnaviruses (Kodama *et al*, 1985). WHV produces acute and/or chronic infections similar to the HBV infections in human. In addition, WHV chronically infected woodchucks develop HCC within a relative short period of time (2-3 years) (Popper *et al*, 1987; Gerin *et al*, 1989). Therefore, the WHV infected woodchuck is an ideal animal model to study the course of viral infection, antiviral therapy and hepadnavirus-induced HCC (Menne & Cote, 2007). A greater than 90 % sequence homology exists between HBV and WHV in the ε region (Figure 1.14) (Kramvis & Kew, 1998).

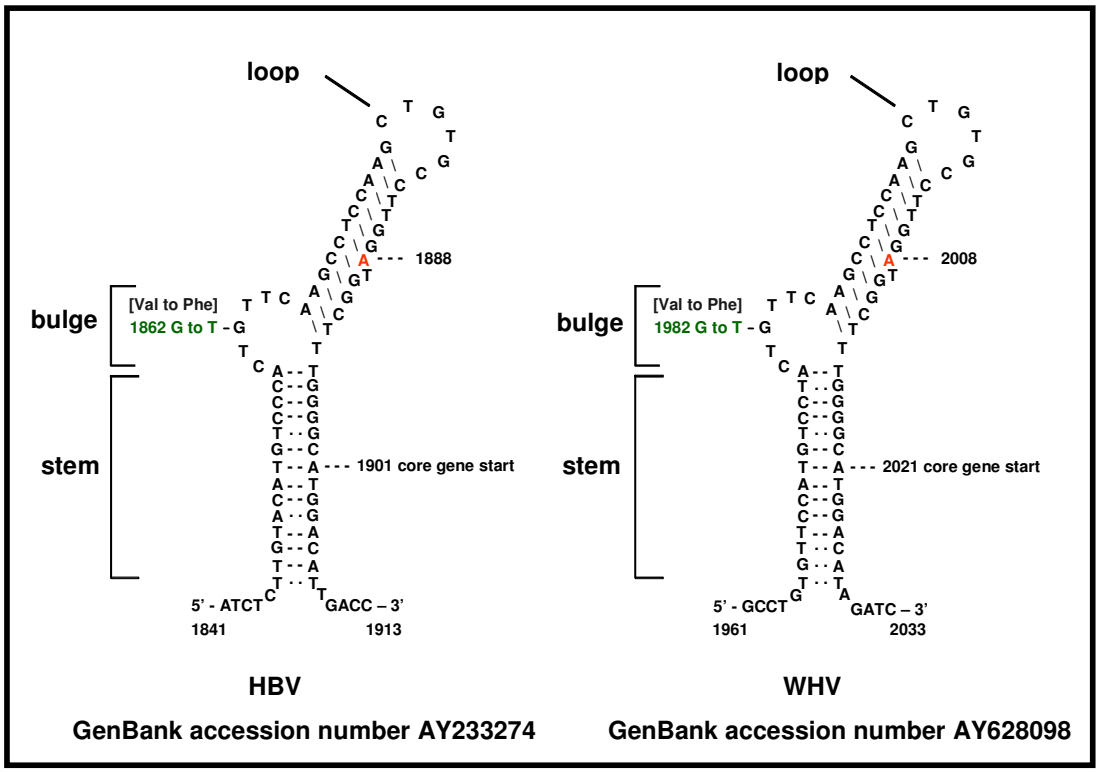

Figure 1.14 The nucleotide sequences and predicted secondary structure of the encapsidation signal of HBV genotype A and WHV (Junker-Niepmann *et al*, 1990). The DNA sequences are shown for ease of interpretation.

The earliest evidence for the presence of a woodchuck hepatitis virus e antigen (WHeAg)/anti-WHeAg system was from the indirect immunoassay performed using blood from the WHV-infected Eastern woodchucks (Hantz *et al*, 1984). Documented proof for the existence of WHeAg, however, was not reported until 1994. The maturation pathway of WHeAg is similar to that of HBeAg, via the signal peptidase cleavage of the amino end as it passes through ER lumen, and cleavage of the arginine-rich carboxyl terminus in the Golgi by furin (Carlier *et al*, 1994). The difference between completely processed WHeAg and HBeAg is that WHeAg is N-glycosylated with a molecular weight (M_r) of 24 kDa (Carlier *et al*, 1994) and HBeAg is not glycosylated and has a M_r of 17kDa (Messageot *et al*, 2003) .

WHV G1982T mutation (equivalent to G1862T in HBV) is found in approximately 33.3 % of complete WHV sequences deposited in GenBank. The prevalence of WHV G1982T was found to be 88.6 % in the study of Li *et al* where a total of 53 WHV isolates were sequenced in their study (Li *et al*, 1996). For the sake of clarity, the WHV 1982G will be referred as wild-type in this thesis although it is difficult to conclude whether this is strictly speaking correct.

The phenotypic change from Val to Phe introduced by the G1862T (G1982T in WHV) mutation at codon 17 of the precore core precursor protein (-3 position to the signal peptidase recognition motif) is close to the signal peptide cleavage site at position 19 (-1 position to the signal peptidase recognition motif) (Figure 1.15), and may therefore interfere and abrogate signal peptide cleavage (Valliammai *et al*, 1995; Kramvis *et al*, 1997). Phe has a bulky, aromatic side chain and is regarded as a "forbidden" amino acid at -3 position to the signal peptidase recognition motif (von Heijne, 1985; von Heijne, 1990). In both prokaryotic and eukaryotic organisms, signal peptidase exhibits similar substrate requirements. Type 1 signal peptidase recognizes substrate with small amino acid residues at the -1 position or small uncharged residues at -3 position of the signal peptide relative to the cleavage site (Dierstein & Wickner, 1986; Fikes *et al*, 1990; Shen *et al*, 1991; Karamyshev *et al*, 1998). The complete abrogation of signal peptide cleavage as a result of amino acid substitution to Phe at -3 position was observed in the *Escherichia coli* alkaline phosphatase model (Karamyshev *et al*, 1998).

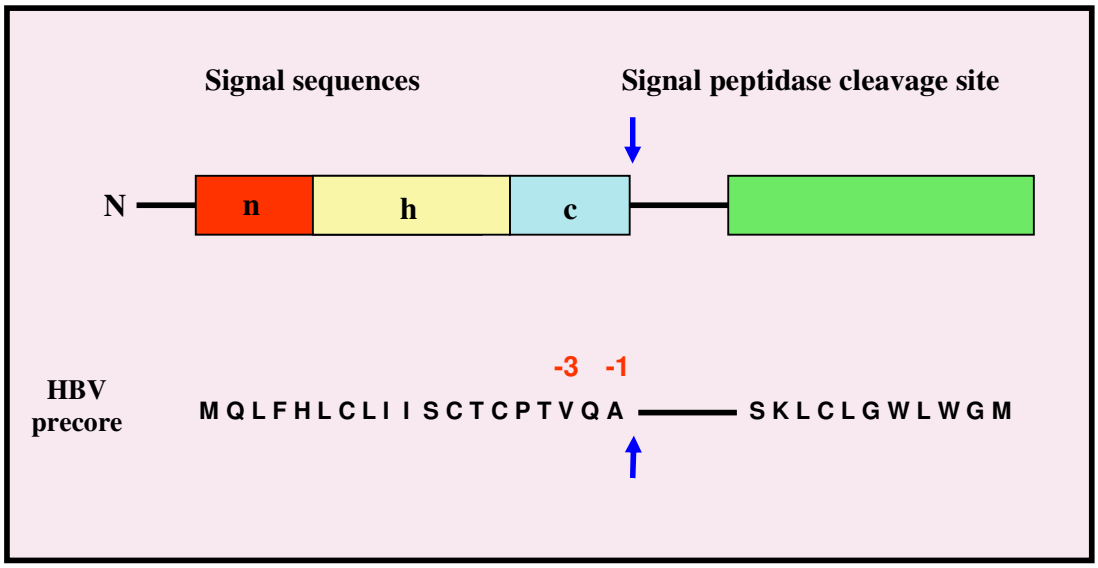

Figure 1.15 Structure of signal peptide with relation to HBV precore sequences. The amino acids of each domain were defined using SignalP 3.0 software, available at http://www.cbs.dtu.dk/services/SignalP.

1.6 Rationale and aims of this study

HBV is endemic in the Black population of southern Africa. A high rate of HBeAg-negativity is a unique feature of chronic carriage of the virus in this population, with HBeAg expression being lost relative early during the course of the infection (Song *et al*, 1984). Approximately 5 % of carriers are HBeAg-positive when they reach adulthood (Dusheiko *et al*, 1985), as opposed to a rate of 40 % or higher found in other hyperendemic areas of the world (Stevens *et al*, 1980). In this population subgenotype A1 of genotype A is the dominant strain circulating (Bowyer *et al*, 1997; Hardie & Williamson, 1997; Kramvis *et al*, 1998; Kramvis *et al*, 2002; Kimbi *et al*, 2004; Kramvis & Kew, 2007b). Subgenotype A1 carriers have been shown to have a significantly lower frequency of HBeAg-positivity than subgenotype A2 or D, and this lower frequency is statistically significant in carriers younger than 30 years (Tanaka *et al*, 2004b). Distinctive sequence characteristics of subgenotype

A1 have been identified that could account for the high HBeAg negativity rate (Tanaka *et al*, 2004b; Kramvis & Kew, 2007b). At the transcriptional level, the core promoter mutations A1762T/G1764A can reduce HBeAg expression (Takahashi *et al*, 1995; Kurosaki *et al*, 1996; Baptista *et al*, 1999). At the translational level, mutations at 1809-1812 that alter the Kozak sequence of the precore/core open reading frame are stable traits and affect HBeAg expression to an extent comparable to A1762T/G1764A (Ahn *et al*, 2003). The co-existence of A1762T/G1764A and 1809-1812 mutations reduces HBeAg expression in an additive manner (Ahn *et al*, 2003).

Approximately 25% of both southern African black asymptomatic carriers of the virus (Kramvis *et al*, 1997) and HCC patients (Kramvis *et al*, 1998) have been shown to have a G to T transversion at 1862 in the precore region. This mutation could conceivably have two functional consequences. Firstly, the bulge of ε plays a pivotal role in the initiation of reverse transcription of pgRNA (Knaus & Nassal, 1993; Pollack & Ganem, 1993). The G1862T mutation could change the secondary structure of ε and could interfere with and hence affect HBV replication (Fallows & Goff, 1995). Secondly, the precore/core ORF from the precore mRNA, which codes for the precursor of HBeAg overlaps the region that codes for ε on the pgRNA. The phenotypic change from Val to Phe introduced by the G1862T mutation at codon 17 (-3 position to the signal peptidase recognition motif) is close to the signal peptide cleavage site at position 19 (-1 position to the signal peptidase recognition motif), and may therefore abrogate signal peptide cleavage (Valliammai *et al*, 1995; Kramvis *et al*, 1997).

The objective of the present study was to functionally characterize the HBV G1862T mutation and its equivalent G1982T found in WHV. This was achieved by attaining the following aims:

- The introduction of the G1862T mutation into the precore region of replication competent HBV plasmid by site-directed mutagenesis with or without the presence of the 1888A mutation.
- The introduction of the T1982G mutations into the precore region of replication competent WHV plasmid by site-directed mutagenesis.
- The construction of HBeAg-expression plasmids from the wild-type and mutant replication competent HBV plasmids.
- The construction of WHeAg-expression plasmids from the wild-type and mutant replication competent WHV plasmids.
- The comparison of HBV replication of wild-type and mutant constructs in transfected Huh7 cells.
- The monitoring of secretion and expression of HBeAg in Huh7 cells transfected with wild-type or mutant HBeAg-expression plasmids.
- The monitoring of secretion and expression of WHeAg in Huh7 cells transfected with wild-type or mutant WHeAg-expression plasmids.

CHAPTER 2

2.0 MATERIALS AND METHODS

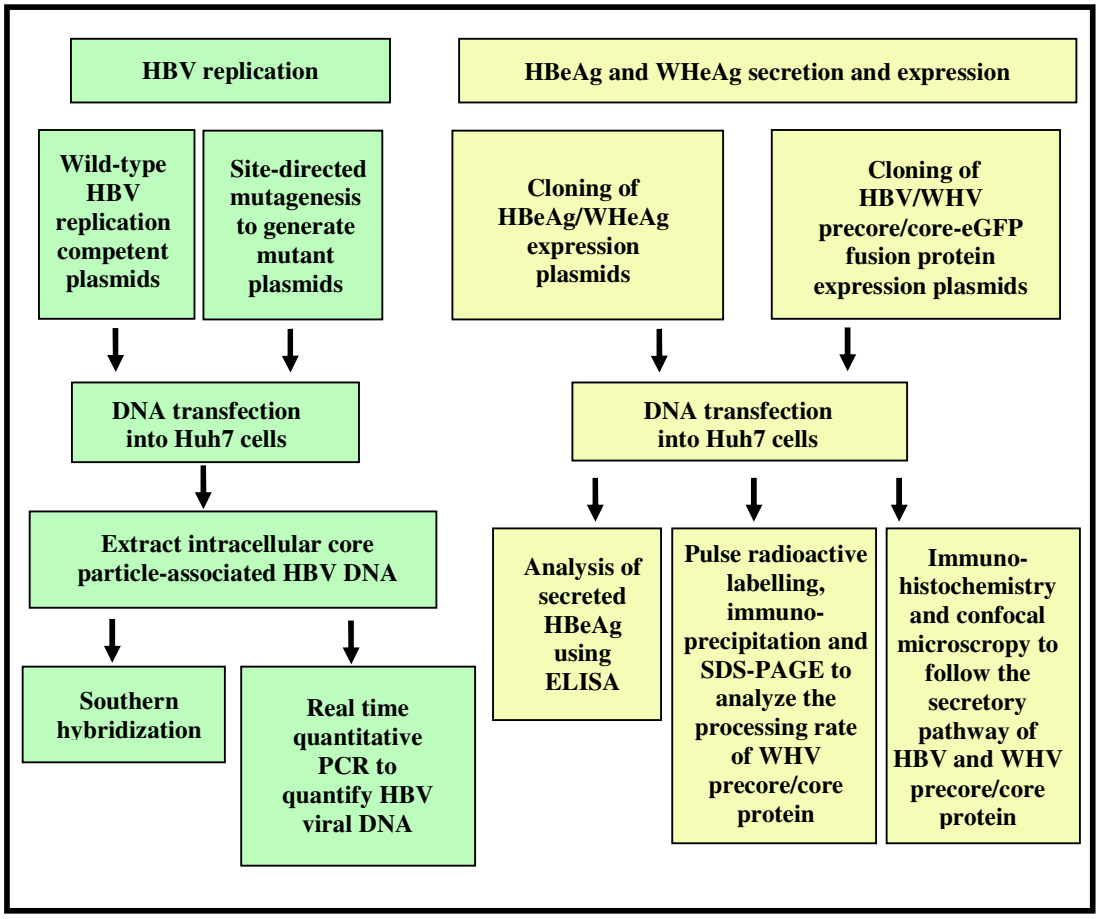

Figure 2.1 Overview of experimental design and methodologies.

2.1 Plasmid construction

2.1.1 Hepatitis B virus plasmids

The HBV plasmid pCH-9/3091-wt encoding a wild-type, terminally redundant, 1.3X unit over-length, replication competent genotype D HBV genome was the generous gift from Dr M. Nassal, University of Freiburg, Germany (Nassal, 1992). pCH-9/3091 is a pgRNA expression plasmid, from which a wild-type pgRNA is transcribed from a cytomegalovirus (CMV) IE promoter (Junker *et al*, 1987). The southern African HBV isolates in which the G1862T mutation was detected, belong to genotype A. Therefore, the original replication competent genotype D plasmid was modified to genotype A context in the precore region and mutant constructs were generated from this template. Genotype 'A' refers to the genotype D construct mutated to genotype A in the precore region.

2.1.2 Woodchuck hepatitis virus (WHV) plasmids

The WHV replication competent plasmid pCWT-9/3235 has native 1982T (expressing Phe and equivalent to mutant G1862T in HBV), and it was a gift from Dr M. Nassal. pCWT-9/3235 contains a complete WHV-2 genome (Kodama *et al*, 1985) under control of the CMV promoter. The pCWT-9/3235 plasmid was used as the template for the generation of WHV plasmids expressing Val, 1982G, the quivalent to wild-type in HBV.

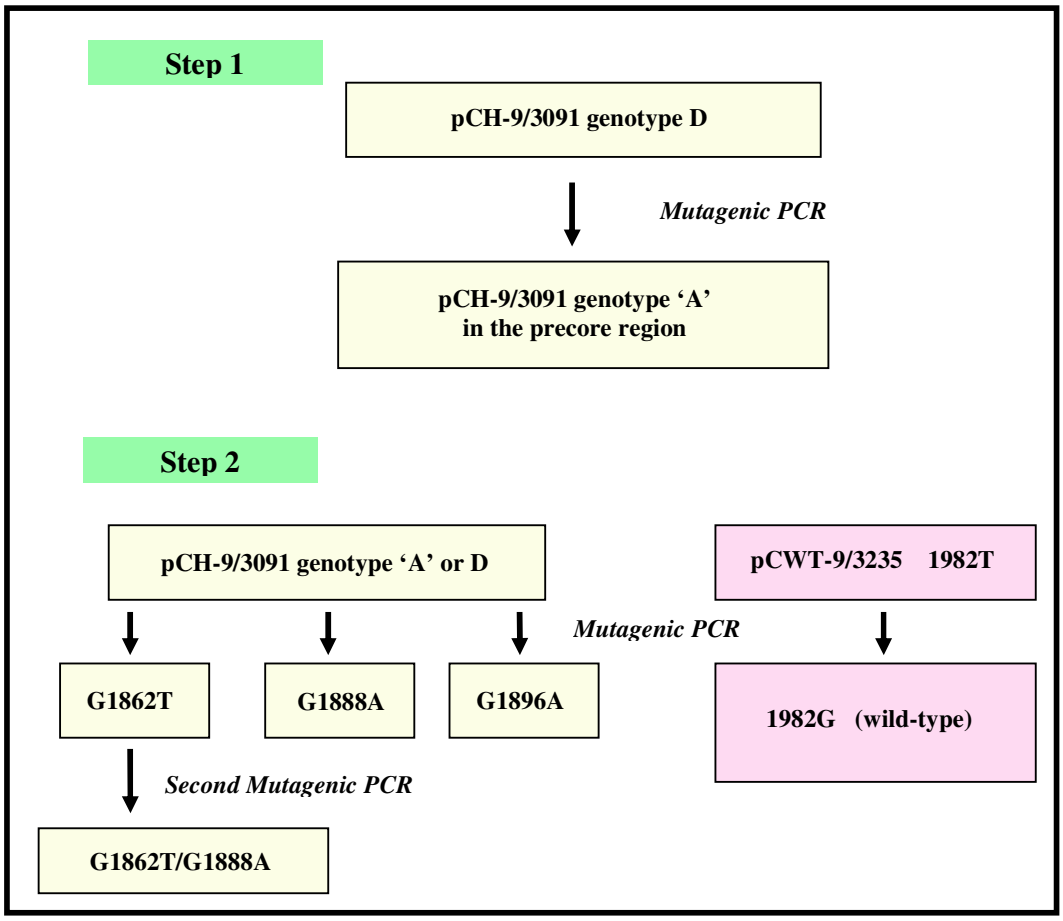

Figure 2.2 Flow chart showing the generation of mutant HBV and WHV replication competent plasmids. Genotype 'A' refers to the genotype D construct mutated to genotype A in the precore region.

2.1.3 Site-directed mutagenesis

Using the pCH-9/3091-wt plasmid as the template, in conjunction with the QuickChange kit (Stratagene, La Jolla, CA, USA) and appropriately designed mutagenic primer pairs and polymerase chain reaction (PCR) conditions (Table 2.1), the precore region was firstly mutated from genotype D to A. Subsequently, G1862T, G1888A, G1862T/ G1888A and G1896A mutants were generated from the wild-type genotype 'A' and D plasmids. The G1862T/G1888A double mutation was generated using the G1862T mutant plasmid as template together with the G1888A mutagenic primer pair in a second mutagenic PCR. The PCR mix was composed of 5 µl of 10 X reaction buffer, 2 µl of template plasmid DNA (5-50 ng), 125 ng of forward mutagenic primer, 125 ng of reverse complimentary mutagenic primer, 1 µl of dNTP mix provided by the mutagenesis kit, 1 µl of *Pfu* Turbo DNA polymerase at 2.5 U/µl, and made up to a final volume of 51 µl with best quality water. PCR were carried out using the GeneAmp PCR system 9600 thermal cycler (Applied Biosystems, Foster City, CA, USA) or Eppendorf Mastercycler Gradient (Eppendorf, Hamburg, Germany). PCR amplification conditions were as follows: initial denaturation at 95 °C for 30 sec, followed by 12 cycles of 95 °C for 30 sec, variable temperature °C for 1 min (note: please see Table 2.1 for detailed annealing temperature for each primer set) and 68 °C for 7 min (1 kb = 1 min). After PCR cycling, PCR tubes were placed on ice for 2 min to cool down the reaction mix before proceeding with the enzyme digestion. Each PCR product was digested with 10 U of restriction enzyme, *Dpn* I (10 U/ µl) for 1 hour at 37 °C. This digestion allows the methylated parental supercoiled template DNA to be degraded.

An aliquot (1 µl) of *Dpn* I digested PCR product was gently mixed with 50 µl of supercompetent XL1-Blue *E.coli* cells (provided by the QuickChange kit). The

wild-type and mutated daughter plasmid was transformed individually into XL1-Blue cells using the heat shock method according to the manufacturer's directions. The transformed bacteria were plated onto ampicillin (50 µg/ml) enriched LB agar plates (Appendix A1). The plates were incubated at 37 °C overnight, after which colonies were selected and inoculated in LB broth supplemented with ampicillin at 50µg/ml (Appendix A2, A3). Bacterial cultures were grown overnight at 37 °C in the Orbital Shaker Incubator LM-510 (YIH DER, Germany) with constant shaking at 150 revolutions per minute (rpm). Bacteria were harvested by centrifugation for 20 min at 6000 x g at 4 °C. Plasmids were purified from the harvested bacteria using QIAprep Spin Miniprep kit (Qiagen, Hilden, Germany), according to manufacturer's instructions.

The WHV replication competent plasmid, pCWT-9/3235 bearing the 1982G (equivalent to the HBV wild-type) was generated using the same mutagenic method described above for HBV replication competent plasmid mutagenesis. Details of WHV mutagenic primer sequences and annealing temperature for the PCR used can be found in Table 2.1.

The plasmids were sequenced directionally using the sequencing primer, 3091 CMVIE promoter: 5'-CATTGACGCAAATGGGCGGTA-3'.

Table 2.1: Oligonucleotide primers used for site-directed PCR mutagenesis

Virus	Primer	Change	Sequence[c]	Annealing temp
HBV	1836F[a] (+)	Genotype D to 'A'	5' –TAATCATCTC**A**TGTACATGTCC**C**ACTGTTCAAGCCTCCAAGCTGT–3'	77.0 °C
	1880R[a] (-)	Genotype D to 'A'	5' –ACAGCTTGGAGGCTTGAACAGT**G**GGACATGTACA**T**GAGATGATTA–3'	77.0 °C
	1839FA[a] (+)	Val17Phe (G1862T) Genotype 'A'	5' –TCATCTCATGTACATGTCCCAC**TT**TTCAAGCCTCCA–3'	74.0 °C
	1874RA[a](-)	Val17Phe (G1862T) Genotype 'A'	5' –TGGAGGCTTGA**AA**AGTGGGACATGTACATGAGATGA–3'	74.0 ° C
	1850FD[a] (+)	Val17Phe (G1862T) Genotype D	5' –TCATGTCCTACT**T**TTCAAGCCTCCA–3'	63.5 °C
	1874RD[a](-)	Val17Phe (G1862T) Genotype D	5' – TGGAGGCTTGAA**A**AGTAGGACATGA–3'	63.5 °C

	1878R[a](+)	G1888A	5’ – TGTGCCTTGG**A**TGGCTTTGGGGCAT -3’	74.2 °C
	1902R[a](-)	G1888A	5’ – ATGCCCCAAAGCCA**T**CCAAGGCACA -3’	74.2 °C
	1881F[a] (+)	Trp28* (G1896A)	5’ –GCCTTGGGTGGCTT**TAG**GGCATGGAC–3’	72.5 °C
	1906R[a] (-)	Trp28* (G1896A)	5’ –GTCCATGCC**CTA**AAGCCACCCAAGGC–3’	72.5 °C
WHV	1970F[b](+)	Phe17Val (T1982G)	5’ –CCATGTCCTAC**TGT**TCAAGCCTCCAAGC–3’	53.0 °C
	1997[b](-)	Phe17Val (T1982G)	5’–GCTTGGAGGCTTGAA**CA**GTAGGACATGG–3’	53.0 °C

[a]: numbering of nucleic acids from *EcoR* I site according to genotype D HBV(AY233292) +:sense polarity; -: antisense polarity

[b]: numbering of nucleic acids according to WHV genome (AY628098) +: sense polarity; -: antisense polarity

[c]:Mutated nucleotides are shown in boldface and mutated codons are underline

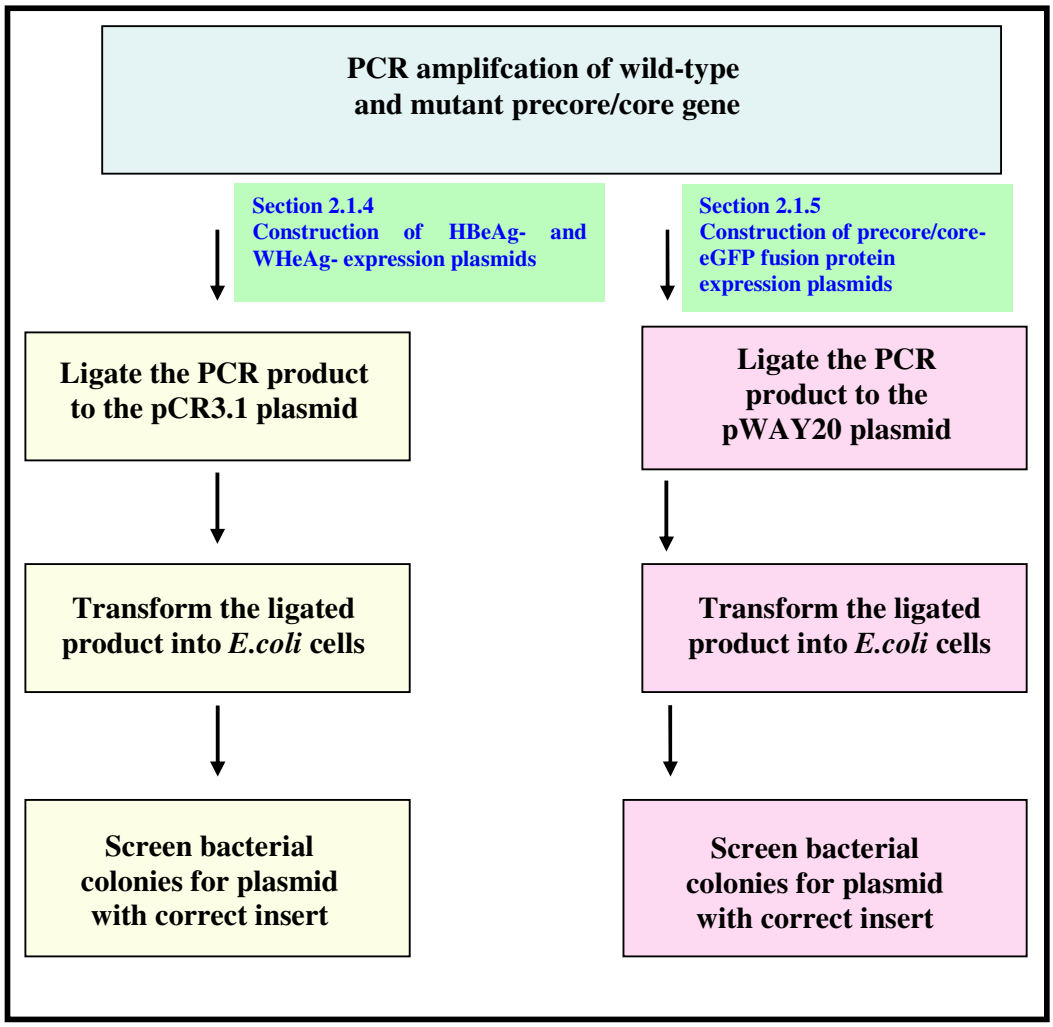

Figure 2.3 Flow chart summarizing the construction of HBeAg- and WHeAg-expression plasmids, and also the precore/core-eGFP fusion protein expression plasmids.

2.1.4 Construction of HBeAg- and WHeAg-expression plasmids

2.1.4.1 HBV HBeAg-expression pCR3.1 plasmids

The entire precore/core regions of the wild-type or modified mutant pCH-9/3091 plasmids were amplified using primer set shown in Table 2.2. The total PCR mixture was 100 µl containing 1.75 U Expand high fidelity polymerase (Roche, Mannheim, Germany), 300 µM each of the dNTPs, 2 µM of each primer, 3 mM of magnesium chloride, 1 X Expand high-fidelity PCR buffer and 1.5 µl of plasmid DNA template. PCR amplification condition was as follows: initial denaturation at 94 °C for 2 min, followed by 40 cycles of 94 °C for 45 sec, 48 °C for 1 min, 72 °C for 1 min 20 sec, and one cycle of 10 min at 72 °C for final extension. PCR reactions were carried out using the GeneAmp PCR system 9600 thermal cycler (Applied Biosystems, Foster City, CA, USA) or Eppendorf Mastercycler Gradient (Eppendorf, Hamburg, Germany). An aliquot of PCR product was analyzed by electrophoresis on 1 % (w/v) agarose gel (Appendix A4-A5) in 1 X TBE buffer (Appendix A6). Expand high-fidelity polymerase is a blend of Taq polymerase and proofreading polymerase, therefore the PCR product generated using this enzyme will have a mixture of blunt and sticky ends. When using PCR product generated using this polymerase blend, it is necessary to take an additional step by treating with Taq polymerase, to generate PCR product with A overhang. PCR products were incubated with TaKaRa ExTaq^{TM} polymerase (Takara Mirus Bio, Madison, WI, USA) at 2.5 U/100 µl for 10 min at 72 °C before proceeding with the cloning procedure.

The PCR product was subsequently cloned into the pCR3.1 cloning vector using the TA Eukaryotic cloning kit-bidirectional (Invitrogen, Carlsbad, CA, USA) according to manufacturer's instructions. Ligated vector was transformed into supercompetent

TOP10 *E coli* cells, provided with the kit. Transformed bacteria were plated onto kanamycin (50 µg/ml) supplemented LB agar plates (Appendix A7). These agar plates were incubated at 37 °C overnight, after which colonies were selected and inoculated in LB broth supplemented with kanamycin (50 µg/ml) (Appendix A2, A8). Bacterial cultures were grown overnight at 37 °C in the Orbital Shaker Incubator LM-510 (YIH DER, Germany) with constant shaking at 150 rpm. Bacteria were harvested by centrifugation for 20 min at 6000 x g at 4 °C. Plasmids were purified from the harvested bacteria using QIAprep Spin Miniprep kit. Plasmids with the correct insert were selected by restriction digestion, and sequenced bi-directionally using sequencing primers provided by the cloning kit.

2.1.4.2 WHV WHeAg-expression pCR3.1 plasmids

The same approach as described in section 2.1.4.1 was used to generate the WHeAg-expression pCR3.1 plasmids. The entire WHV precore/core region bearing either the G1982T nucleotide (equivalent of HBV mutant at position 1862) or the 1982G (equivalent of HBV wild-type) was amplified from pCWT-9/3235 G1982T or 1982G (wild-type) plasmids using primer set shown in Table 2.2. The total PCR mixture was 100 µl containing 1.75 U Expand high fidelity polymerase, 300 µM each of the dNTPs, 2 µM of each primer, 2.5 mM of magnesium chloride, 1 X Expand high fidelity PCR buffer and 1.5 µl of plasmid DNA template. The PCR reactions were performed as follows: initial denaturation at 94 °C for 2 min, followed by 30 cycles of 94 °C for 40 sec, 55.5 °C for 1 min, 72 °C for 1 min, and one cycle of 7 min at 72 °C for final extension. PCR were carried out using the GeneAmp PCR system 9600 thermal cycler (Applied Biosystems, Foster City, CA, USA) or Eppendorf Mastercycler Gradient (Eppendorf, Hamburg, Germany).

Table 2.2: Oligonucleotide primers used for the PCR to amplify the HBV and WHV precore/core genes for the construction of the HBeAg- and WHeAg- expression pCR3.1 plasmids

Amplicon	Primer	Sequence[c]	Size[d]
HBV precore/core pCR3.1	1808*Xho*IF(+)[a] 2458*Bam*HIR(-)[a]	5'– **C↓TCGAG***AGCCACCATGCAACTTTTTCACCTCTG*–3' 5'– **G↓GATCC***CTAACATTGAGATTCCCGA*–3'	656
WHV precore/core pCR3.1	1928F(+)[b] 2587R(-)[b]	5'–TCTAGGAGCC*ACCATGTATCTTTTTCACCTGTGCC*–3' 5'–*GTACCTCCGCCACCACTACCTCCGCCACCGCAGTTG GCAGATGGAGATTGA*–3'	669

[a]: numbering of nucleic acids from *EcoR*I site according to genotype D HBV(AY233292) +:sense polarity; -: antisense polarity

[b]: numbering of nucleic acids according to WHV genome (AY628098) +: sense polarity; -: antisense polarity

[c]: viral sequences are shown in *italics;* restriction sites in **boldface** and <u>underlined</u>

[d]: Size of the amplicons in base pairs.

2.1.5 Construction of the precore/core-eGFP fusion protein expression plasmids

The enhanced green fluorescent protein (eGFP) can be use as a fusion tag in *vivo* or *in vitro* to localize proteins, follow their movement, or to study the dynamics of protein targeting to the secretory pathway. In order to monitor the dynamic movement of wild-type or mutant HBV or WHV precore/core protein in their secretory pathway, we designed and generated the HBV or WHV precore/core protein-eGFP fusion protein expression plasmids with a flexible poly-linker between the upstream precore/core gene and the downstream eGFP gene.

2.1.5.1 Construction of the HBV precore/core-eGFP fusion protein expression plasmids

The entire precore/core region of HBV was amplified using the pCH-9/3091 as template and primer set shown in Table 2.3. Briefly, the total PCR mixture was 100 µl containing 1.75 U Expand high fidelity polymerase, 300 µM each of the dNTPs, 1 µM of each primer, 2.5 mM of magnesium chloride, 1 X Expand high fidelity PCR buffer and 2 µl of plasmid DNA template. PCRs were performed as follows: initial denaturation at 94 °C for 2 min, followed by 40 cycles of 94 °C for 35 sec, 63 °C for 1 min, 72 °C for 1 min 10 sec, and final extension cycle of 10 min at 72 °C. The PCR product was cloned into the *Sma* I site of the eGFP fusion vector-pWay20 (generous gift from Dr T. Hughes, Molecular Motion Lab, Montana State University, USA), using ligase and the reaction buffer from the pCR-Script Amp cloning kit (Stratagene, La Jolla, CA, USA). The ligated plasmid was transformed into supercompetent TOP10 *E. coli* cells (Invitrogen, Carlsbad, CA, USA). Transformed bacteria were plated onto kanamycin (50µg/ml) enriched LB agar plates. These agar plates were incubated at 37 °C overnight, after which colonies

selected and inoculated in LB broth with kanamycin supplemented at 50µg/ml. Bacterial cultures were grown overnight at 37 °C in the Orbital Shaker Incubator LM-510 (YIH DER, Germany) with constant shaking at 150 rpm. Bacteria were harvested by centrifugation for 20 min at 6000 x g at 4 °C. Plasmids were purified from the harvested bacteria using QIAprep Spin Miniprep kit. Plasmids with the correct insert were identified by restriction digestion, and sequenced directionally using pWay20-eGFP primer, 5'-TCCAGTGTG GTGGAATTCGGCTTG-3'.

2.1.5.2 Construction of the WHV precore/core-eGFP fusion protein expression plasmids

The entire precore/core region of WHV was amplified using the primer set shown in Table 2.3. PCR mixture preparation was identical to the HBV precore/core gene amplification PCR for the cloning of HBV precore/core-eGFP fusion protein expression plasmid (see section 2.1.5.1) except the magnesium chloride concentration was optimized to 3 mM. PCR were performed as follows: initial denaturation at 94 °C for 2 min, followed by 40 cycles of 94 °C for 35 sec, 63 °C for 1 min, 72 °C for 1 min 10 sec, and final extension cycle of 10 min at 72 °C. PCR were carried out using the GeneAmp PCR system 9600 thermal cycler (Applied Biosystems, Foster City, CA, USA) or Eppendorf Mastercycler Gradient (Eppendorf, Hamburg, Germany). The PCR product was cloned into the eGFP fusion vector-pWay20 using the same method used for the construction of HBV precore/core-eGFP fusion protein expression plasmid mentioned in section 2.1.5.1. Plasmids with the correct insert were selected by restriction digestion, and sequenced directionally using pWay20-eGFP primer, 5'-TCCAGTGTGGTGGAA TTCGGCTTG-3'.

Table 2.3: Oligonucleotide primers used for the PCR to amplify HBV and WHV precore/core genes for the construction of precore/core-eGFP fusion protein expression plasmids

Amplicon	Primer	Sequence[c]	Size[d]
HBV precore/core-eGFP	1808*Xho*IF(+)[a] 2432R(-)[a]	5'– **C↓TCGAG***AGCCACCATGCAACTTTTTCACCTCTG*–3' 5'– **AGTACCTCCGCCACCACTACCTCCGCCA***CCACA TTGAGATCCCGAGA*–3'	664
WHV precore/core-eGFP	1928F(+)[b] 2587R(-)[b]	5' –TCTAGGAGCC*ACCATGTATCTTTTTCACCTGTGCC*– 3' 5' –**AGTACCTCCGCCACCACTACCTCCG***CCACCGCA GTTGGCAGATGGAGATTGA*– 3'	698

[a]: numbering of nucleic acids from *EcoR*I site according to genotype D HBV(AY233292) +:sense polarity; -: antisense polarity

[b]: numbering of nucleic acids according to WHV genome (AY628098) +: sense polarity; -: antisense polarity

[c]: viral sequences are shown in *italics;* restriction sites in **boldface** and underlined; sequence coding for linkers are shown in **bold**; abolished stop codons of core ORF are underlined.

[d]: Size of the amplicons in base pairs.

2.1.5.3 Plasmids extraction and purification

All recombinant plasmids were extracted and purified from the overnight bacterial culture using the QIAprep Spin Miniprep kit for small scale plasmid extraction and Qiagen Endofree Plasmid Maxi kit for transfection experiments (Qiagen, Hilden, Germany). The concentrations of all plasmid DNA were quantified for transfection purposes, by measuring absorbance at 260 nm using a high-resolution spectrophotometer, GeneQuant (Amersham Bioscience, Buckinghamshire, UK).

2.1.6 Automated sequencing

Mutations and plasmids with correct inserts were confirmed by sequencing using the BigDye Terminator V3.0 Cycle Sequencing Ready Reaction Kit (Applied Biosystems, Foster City, CA, USA) according to the manufacturer's instructions and subjected to cycle sequencing on a GeneAmp PCR system 9600 thermal cycler (Applied Biosystems, Foster City, CA, USA). Unincorporated dye terminators were removed using DyeEx 2.0 Spin Kit (Qiagen, Hilden, Germany). The sequencing reactions were loaded and analyzed on the Applied Biosystem 377 automated sequencer (Applied Biosystems, Foster City, CA, USA).

2.2 Cell culture

The Huh7, a human hepatoma cell line was a generous gift from Prof H. Nakabayashi, Department of Biochemistry, Graduate School of Medicine, Hokkaido University, Japan (Nakabayashi *et al*, 1982). The cell line was maintained and sub-cultured every 2 to 3 days in chemically defined medium, ISE- Roswell Park Memorial Institute (RPMI) 1640 + L-Glutamine (Gibco-BRL, Paisley, Scotland, UK) (Appendix A9), supplemented with 10 % (v/v) foetal bovine serum (FBS) (Gibco-BRL, Paisley, Scotland, UK). The culture medium was prepared according to the formulations in Appendix A9. The spent culture medium (conditioned medium) was removed from the culture vessel and filtered through a 0.2 μm MiniSart filter (Sartorius, Göttingen, Germany) to remove any cellular debris. Cells were first rinsed once with phosphate buffered saline (PBS) (Gibco-BRL, Paisley, Scotland, UK). A volume of 0.01 % (w/v) ethylene diamine tetra-acetic acid di-sodium salt (EDTA) / PBS (Appendix A10) was added to the cells, and further incubated at 37 °C for 10 min to allow the cells to detach from the culturing vessel. The detached cells in 0.01 % EDTA/ PBS solution were centrifuged for 2 min at 300 rpm in the Minor centrifuge (MSE, London, UK). The supernatant was discarded and the cell pellet was re-suspended in fresh medium supplemented with 10 % (v/v) FBS before adding to the culturing vessel. The filtered conditioned medium was also added at 20-25 % of the total final volume of medium. The growth factors in the conditioned medium will enhance the growth of Huh 7 cells. Cells were grown at 37 °C incubator in a humidified atmosphere containing 5 % CO_2.

MG132 (Z-Leu-Leu-Leu-CHO) (BIOMOL, Plymouth Meeting, PA, USA), a potent and selective reversible proteasome inhibitor was added to the Huh7 cells

at 1 µM. Cells were further incubated for 24 hours at 37 °C after the addition of MG132. The fungal metabolite, brefeldin A (BFA) (Sigma-Aldrich, St Louis, MO, USA), induces the disassembly of the Golgi complex and cause rapid redistribution of Golgi proteins to the ER in mammalian cells. Huh7 cells were incubated with BFA at 5 µg/ml for 30 min at 37 °C before fixing the cells.

2.3 Transfection

Huh7 cells were seeded 24 hours prior to transfection into 100 mm dishes (Corning, Corning, NY, USA) for the HBV replication and metabolic labelling experiments, 6 well plate for HBeAg analysis (Corning, Corning, NY, USA) or 8-well LAB-TEK® II chamber slides and 4-well LAB-TEK®II chamber coverglass (Nalge Nunc International, Rochester, NY, USA) for confocal microscopy. When the cells had reached approximately 70-80 % confluency, transfection by the cationic lipid-mediated method using lipofectamine™2000 (Invitrogen, Carlsbad, CA, USA) was performed according to manufacturer's directions (Table 2.4). Briefly, the appropriate volume of plasmid DNA was added to the Opti-MEM1 reduced serum medium (Gibco-BRL, Paisley, Scotland, UK). In a separate tube, lipofectamine™2000 was added to the second aliquot of Opti-MEM1 reduced serum medium and incubated at room temperature for 5 min. The diluted DNA was combined with the diluted lipofectamine™2000 with gentle mixing, and incubated at room temperature for 20 min to allow the cationic lipid-DNA complexes to form. The complexes were added to the cells followed by gently rocking to evenly distribute the complexes. The culture vessels were further incubated at 37 °C for 48 to 72 hours, allowing the gene of interest to be expressed.

Table 2.4: Transfection reaction volumes used for the different types of culture vessels

Culture Vessel	Quantity of DNA (µg)	Volume of Opti-MEM 1 reduced serum medium	Volume of lipofectamine™ 2000
Per well of 8-well chamber slides	1 µg	2X 50 µl	0.5 µl
Per well of 4-well cover glass	2 µg	2X 100 µl	1 µl
6 well plate	5 µg	2X 250 µl	2.5 µl
100 mm dish	48 µg	2X 1.5 ml µl	12 µl

2.4 Analysis of secreted HBeAg

The cell culture medium was collected at 48 hours post transfection, and the HBeAg concentration was determined using the Monolisa HBe kit according to manufacturer's instructions (Bio-Rad, San Diego, CA, USA). Three independent transfection experiments were performed to test the HBeAg secreted in the culture media.

2.5 Extraction of intracellular core particle-associated HBV DNA

Intracellular core particle-associated HBV DNA was extracted using the method of Parekh (Parekh *et al*, 2003). Media were collected at 72 hours post transfection, and the cells were rinsed with PBS twice and lysed with 700 µl lysis buffer (Appendix A11). The cell lysate was centrifuged at 7300 x g for 15 min at 4 °C to pellet the nuclei. The supernatant was transferred to a new tube and supplemented with 10 mM $CaCl_2$-12 mM $MgCl_2$ (Appendix A12) , and digested with 10 U of RNase-free DNase (Roche, Mannheim, Germany) and 40 U of mung bean nuclease

(Promega, Madison, WI, USA) at 37 °C for 1 hour to degrade the transfected plasmid DNA.

A 256 µl of polyethylene glycol (PEG) solution (Appendix A13) was added to each tube and allowed to incubate at 4 °C for 1 hour before pellet the core particles by centrifugation at 7300 x g for 20 min at room temperature. The pellet was resuspended in 180 µl of resuspension solution (Appendix A14). Any remaining transfected plasmid DNA was further degraded with the addition of 5 U of RNase-free DNase, and 20 U of mung bean nuclease. The mixture was incubated for 30 min at 37 °C.

The DNase activity was stopped by the addition of 50 µl stop solution (Appendix A15). The intracellular core particle associated HBV DNA was extracted using QIAamp blood kit (Qiagen, Hilden, Germany), according to manufacturer's directions. The DNA was finally eluted in 180 µl of elution buffer.

2.6 Southern hybridization

Southern hybridization of the intracellular core particle-associated HBV DNA was carried out by electrophoresis in 1% agarose gels, denatured in the gel, neutralized and transferred to the Hybond-N nylon membrane (Amersham Bioscience, Buckinghamshire, UK) using the method of Southern (Sambrook *et al*, 1989).

DNA fragments encoding the full length HBV genome were generated from the *EcoR*I digestion of pBR325 plasmid which have a full length HBV genome insert, *adr* subtype (kindly provided by C. Bréchot, INSERM U 370, Institut Pasteur, Paris, France). *EcoR*I digested fragments were isolated by electrophoresis on 1 % agarose

gel. Fragments of correct size (3.2kb) were excised from the agarose gel, and subsequently purified using the QIAquick gel extraction kit (Qiagen, Hilden, Germany). Purified HBV fragment was used to generate ^{32}P-radiolabeled HBV probe using the Mega prime DNA labelling kit (Amersham Bioscience, Buckinghamshire, UK). The nylon membrane was hybridized with the radiolabelled probe using QuickHyb hybridization solution (Stratagene, La Jolla, CA, USA) and Mini Oven MK II (Hybaid, Waltham, MA, USA). Autoradiography was carried out at -70 °C with intensifying screens and Kodak X-Omat film (Eastman Kodak, Rochester, NY, USA) for 4 days before developing the film.

2.7 Real-time quantitative PCR amplification of HBV DNA

Real-time quantitative PCR was performed in a LightCycler, Version 2 (Roche, Mannheim, Germany) with primer and fluorescence resonance energy transfer (FRET) hybridization probe sets in the core and polymerase region of HBV genome (Ho *et al*, 2003) with modification of the probe sequences to match sequences of plasmid DNA template (pCH-9/3091).

Preparation of biological standard

HBV DNA was extracted from 200 µl of Eurohep standard serum containing 5 X 10^5 copies/ml genotype D HBV (kindly provided by Dr W.H.Gerlich, University of Giessen, Germany) using QIAamp blood kit (Qiagen, Hilden, Germany). The DNA was finally eluted in 180 µl of elution buffer.

Preparation of plasmid standard

The recombinant plasmid was purified with Qiagen Endofree Plasmid Maxi kit (Qiagen, Hilden, Germany). The concentration of the plasmid DNA was quantified using the spectrophotometer, GeneQuant (Amersham Bioscience, Buckinghamshire,

UK). Serial dilutions of the cloned plasmid DNA ranging from 5.54 x 10^2 to 5.54 x 10^8 copies of HBV DNA/ml were used for the generation of the standard curve. The PCR was repeated three times in duplicate to generate the standard curve.

Hybridization probes and primers

Forward primer (BcP1): 5'-ACCACCAAATGCCCCTAT-3'; reverse primer (BcP2): 5'-TTCTGCGACGCGGCGA-3', yielded a 130 bp PCR product. The donor fluorescent probe (HBVcD: 5'-GAGTTCTTCTTCTAGGGGACCTGC-FLUORESCEIN-3') and acceptor probe (HBVcA: 5'-LightCycler Red 640 TCGTCGTCTAACAACAGTAGTCTCCG-PHOSPHATE-3') were used as hybridization probes (TIB MOLBIOL, Berlin, Germany).

The amplification reaction mixture per capilliary (20 µl) contained 4 µl extracted HBV DNA template, 4 µl LightCycler FastStart DNA Master^{PLUS} Hybridization Probe kit (Roche, Mannheim, Germany), 1 mM each of PCR primer, 0.15 µM HBVcD (donor probe), 0.15 µM HBVcA (acceptor probe). Thermal cycling conditions were as follows: initial activation of FastStart DNA polymerase at 95 °C for 10 min followed by 40 cycles of amplification were performed at 95 °C for 5 sec, 60 °C for 15 sec and 72 °C for 20 sec. Fluorescence data were acquired at each cycle at the end of annealing step with detection channel sets at F2/F1. Biological standard was included in every single run of LightCycler PCR as an internal control. Four independent transfection experiments were performed and the HBV DNA was extracted. Each construct was tested in triplicate for each transfection. The real time quantification PCR was performed at least twice for each set of transfections.

2.8 Statistical analysis

Viral replication and HBeAg data were analysed using the one-way analysis of variance setting with the Bonferroni method for comparison between different mutations using the GraphPad InStat statistical analysis software version 3.0 (GraphPad, San Diego, CA, USA). All data were expressed as means with standard deviations. Differences were consider significant when *P*-values less than 0.05.

2.9 Analysis of the processing rate of WHV precore/core protein

2.9.1 Metabolic labelling of WHV precore/core protein and immunoprecipitation analysis

Huh7 cells were plated out in 100 mm culture dishes 24 hours before transfection with WHeAg-expression plasmids. At 48 hours post transfection, the Huh 7 cells were washed twice with cysteine, methionine-free RPMI 1640 medium. Cells were starved for 2 hours in cysteine, methionine-free medium supplemented with 2 % (v/v) dialyzed FBS, to deplete the intracellular methionine and cysteine reserves. The cells were incubated ("pulse") with Redivue™ Pro-mix, a ^{35}S *in vitro* cell labelling mix (Amersham Bioscience, Buckinghamshire, UK) at 100 μCi ^{35}S-labelled methione/cysteine per ml of medium for 3 hours. Culture medium was collected and centrifuged at 20 000 x g at 4 °C for 20 min to remove cell debris. The cells were washed twice with ice cold PBS, and lysed with ice cold lysis buffer (Appendix A16). Protease inhibitor cocktail-Complete® (Roche, Mannheim, Germany) was added to the lysis, washing buffers, and collected culture medium to prevent protein degradation. Cell lysates were centrifuged at 20 000 x g at 4 °C for 20 min to remove cell debris.

Both clarified cell lysate and culture medium were incubated with 100 µl and 200 µl of 10 % (v/v) protein A-sepharose beads (Sigma-Aldrich, St Louis, MO, USA), respectively, and incubated overnight at 4 °C on a rocking platform to reduce non-specific adsorption of irrelevant cellular proteins to the protein A-sepharose beads. The supernatant was collected after centrifugation at 20 000 x g for 20 second at 4 °C, and processed by the addition of 10 µl of rabbit polyclonal anti-WHcAg antibody (Prof T.I. Michalak, Molecular Virology and Hepatology Research, Division of Basic Medical Sciences, Memorial University of Newfoundland, Newfoundland, Canada) overnight at 4 °C on a rocking platform. The anti-WHcAg antibody was precipitated by adding 100 µl (cell lysate) or 200 µl (culture medium) of 10 % (v/v) protein A-sepharose beads (Sigma, St Louis, MO, USA) and incubated overnight at 4 °C on a rocking platform. The beads were washed twice for 20 min per wash with lysis buffer, followed by two 20 min washes with washing buffer 1 (Appendix A17). The immunoprecipiated complex was finally washed in washing buffer 2 for 20 min (Appendix A18), and centrifuged at 20 000 x g for 20 sec at 4 °C. The supernatant was removed, and the immunoprecipitated complex was resuspended in 50 µl of Laemmli loading buffer (Appendix A19).

2.9.2 Sodium dodecyl sulphate-polyacrylamide gel electrophoresis (SDS-PAGE)

SDS-PAGE gel eletrophoresis of the immunoprecipitated, pulsed precore/core protein was performed according to the method of Laemmli (Laemmli, 1970). Briefly, the protein sample was boiled for 3 min prior to electrophoresis, and resolved on a 15 % SDS-PAGE gel (Appendix A20-A23). Methyl-^{14}C labelled protein molecular weight marker (Amersham Bioscience, Buckinghamshire, UK) was loaded onto the same gel.

The polyacrylamide gel was firstly fixed in fixative solution (Appendix A24) for 30 min, and soaked in the glycerol based solution (Appendix A25) overnight to prevent gel cracking during the drying process. The gel was then immersed in *Amplify* reagent-an enhancer solution used to amplify and enhance the radioactively labelled protein signal (Amersham Bioscience, Buckinghamshire, UK) for 20 min before drying. The gel was dried, and the labelled protein visualized by fluorography, and quantified by scanning densitometry, VERSADOC^{TM} imaging system (Bio-Rad, San Diego, CA, USA).

2.10 Confocal microscopy

2.10.1 Double immunofluorescence staining

At 48 hours or 72 hours post transfection, the culture medium was removed from the 8-well LAB-TEK ® II chamber slides (Nalge Nunc International, Rochester, NY, USA) before detaching the culture slide from the plastic chamber. Culture slides were rinsed and washed in PBS, and cells were fixed in freshly prepared 4 % (v/v) paraformaldehyde in PBS (Appendix A26, A27), for 10 min at room temperature. After fixation, the cells were washed three times, for 10 min per wash in PBS, and permeabilized by incubating in 0.01 % (v/v) TX-100 in PBS (Appendix A28), for 10 min at room temperature. Cells were, washed three times, for 10 min per wash, in PBS. The cells were incubated in blocking solution, 1 % (w/v) BSA (Roche, Mannheim, Germany) prepared in PBS (Appendix A29), for 1 hour at room temperature, to block unspecific binding sites on the cells. The cells were incubated with primary antibody overnight in humidified chamber at 4 °C, and later were washed 3 times, for 10 min per wash in PBS. The cells were incubated with fluorochrome conjugated secondary antibodies and the nucleus was counterstained with, 4', 6-diamidino-2-phenylinodole, dihydrochloride (DAPI) (Molecular probe,

Eugene, OR, USA), for one hour at room temperature and protected from light. The cells were washed 4 times, for 10 min per wash in PBS at room temperature. The slides were mounted under cover slips with anti-fade mounting medium, FluorSave (Calbiochem, San Diego, CA, USA), and sealed with Entellan (Merck, Darmstadt, Germany) before viewing under confocal microscope.

Antibodies and reagents

The following primary antibodies were used in this study: monoclonal anti-protein disulphide-isomerase (PDI), 1:40 dilution (Affinity BioReagents, Golden, CO, USA); monoclonal anti-ERGIC 53, 1:1000 (Prof H Hauri, Department of Pharmacology, Biozentrum, University of Basel, Switzerland); monoclonal anti-giantin, 1:1000 (Prof H Hauri, Department of Pharmacology, Biozentrum, University of Basel, Switzerland); monoclonal anti-vimentin clone V9, 1:70 (Sigma-Aldrich, St Louis, MO, USA); monoclonal anti-pan cytokeratin, 1:70 (Sigma-Aldrich, St Louis, MO, USA); monoclonal anti-alpha (α) tubulin, 1: 1000 (Sigma-Aldrich, St Louis, MO, USA); monoclonal anti-gamma (γ) tubulin clone GTU-88, 1:1000 (Sigma-Aldrich, St Louis, MO, USA); rabbit polyclonal anti-HSP70, 1:100 (USBiological, Swampscott, MA, USA); rabbit polyclonal anti-ubiquitin, 1:100 (USBiological, Swampscott, MA, USA); rabbit polyclonal anti-human placental proteasome, 1:1000 (Prof B Dahlmann, Institute for biochemistry, Humboldt University, Berlin, Germany); monoclonal anti-HBeAg, 0.005 μg/μl (USBiological, Swampscott, MA, USA); rabbit polyclonal anti-HBcAg, 1:50 (Zymed Laboratory, San Francisco, CA, USA); rabbit polyclonal anti-WHcAg, 1:25 (Prof T.I. Michalak, Molecular Virology and Hepatology Research, Division of Basic Medical Sciences, Memorial University of Newfoundland, Newfoundland, Canada).

Secondary antibodies

AlexaFluor 488 Chicken anti rabbit IgG (H+L), 1:100 dilution; AlexaFluor 546 F(ab') $_2$ fragment of goat anti mouse IgG (H+L), 1:150; AlexaFluor 488 Donkey anti mouse IgG (H+L), 1:100; AlexaFluor 546 Goat anti rabbit IgG (H+L), 1:150 (Molecular Probe, Eugene, OR, USA).

2.10.2 Image capture and analysis

The cells were viewed using the Zeiss Axiovert 100M microscope (Carl Zeiss, Göttingen, Germany) equipped with the CARV spinning disc confocal system (BD bioscience, Sparks, MD, USA). The filters sets used were (1) fluorescein/ fluorescein isothiocyanate (FITC) for the green AlexaFluor 488 fluorochrome, (2) tetramethylrhodamine-5-isothiocyanate (TRITC) for the red AlexaFluor 546 fluorochrome and (3) 4', 6-diamidino-2-phenylinodole, dihydrochloride (DAPI) for the blue DAPI stain. Images were captured using the Hamamatsu CCD camera (Hamamatsu cooperation, Hamamatsu city, Shizuoka, Japan), and obtained using the Axiovision 2.0 software (Carl Zeiss, Göttingen, Germany) on the PC workstation. Image analysis was performed with IMAGEJ software for windows V1.34 (http://rsb.info.nih.gov/ij).

2.10.3 Imaging of HBV and WHV precore/core-eGFP fusion protein in Huh 7 cells

Huh7 cells were seeded in the Nunc chambered coverglass (Nalge Nunc International, Rochester, NY, USA) 24 hours before transfection. HBV or WHV precore/core-eGFP fusion plasmid bearing wild-type or mutant HBV precore/core sequences was transfected into the Huh7 cells using the Lipofectamine 2000 reagents with optimized protocol. Hoechst 33342 (Molecular Probe, Eugene, OR, USA) was added to the culture medium to counter stain the nucleus. Huh7 cells were incubated at 37 °C for 30 min, allowing the Hoechst stain to be taken up by the cells. The cell images were captured as described in section 2.9.2. The filters sets used were (1) fluorescein/fluorescein isothiocyanate (FITC) for the precore-eGFP fusion protein-green (2) 4,6-diamidino-2-phenylinodole, dihydrochloride (DAPI) for the Hoechst 33342 stain-blue.

CHAPTER 3

3.0 RESULTS

Transfection of Huh7 cells with various constructs was used to determine the effect of the G1862T mutation on viral replication, HBeAg expression and secretion. Southern hybridization and real time PCR were used to monitor replication following transfection with replication competent clones. Pulsed radioactive-label, immunoprecipitation, SDS-PAGE, ELISA, immunocytochemistry and confocal microscopy were used to follow HBeAg expression following transfection with HBeAg-expression construct.

3.1 Southern hybridization analysis of intracellular core particle-associated HBV DNA

Southern hybridization analysis of intracellular core particles-associated HBV DNA extracted from Huh7 cells transfected with wild-type or mutant replication competent constructs revealed the presence and characteristic pattern of HBV viral DNA replicative intermediates. These are the single stranded (SS), duplex linear (DL) and relax circular (RC) forms of DNA (Figure 3.1 A, genotype D constructs; Figure 3.1 B, genotype 'A' constructs).

A reduction of HBV replication was observed when the precore region of the genotype D was mutated to genotype 'A' context (comparing lane 1 of Figure 3.1 A and lane 1 of Figure 3.1 B). When the G1862T mutation was introduced to the genotype D construct, this mutation reduced viral replication relative to its wild-type (lane 1 versus lane 2 of Figure 3.1 A). In contrast, G1862T mutation did not reduce viral replication in genotype 'A' context (Figure 3.1 B, G1862T, genotype 'A', lane2). The silent mutation of G1888A reduced viral replication relative to

its wild-type only when introduced into the genotype D construct (Figure 3.1 A, G1888A, genotype D, lane 3), but did not reduce viral replication in genotype 'A' context (Figure 3.1 B, G1888A, genotype 'A', lane 3). When the G1862T and G1888A mutations were combined, viral replication was reduced in genotype D context (Figure 3.1 A, G1862T/G1888A, genotype D, lane 4), but the combination of G1862T with G1888A did not change viral replication in genotype 'A' context, compared to the respective wild-type constructs (Figure 3.1 B, G1862T/G1888A, genotype 'A', lane 4).

Because Southern hybridization analysis can only provide qualitative measurement of HBV replication, real time quantitative PCR, which covers a wider linear range of detection, with good reproducibility and high sensitivity, was carried out.

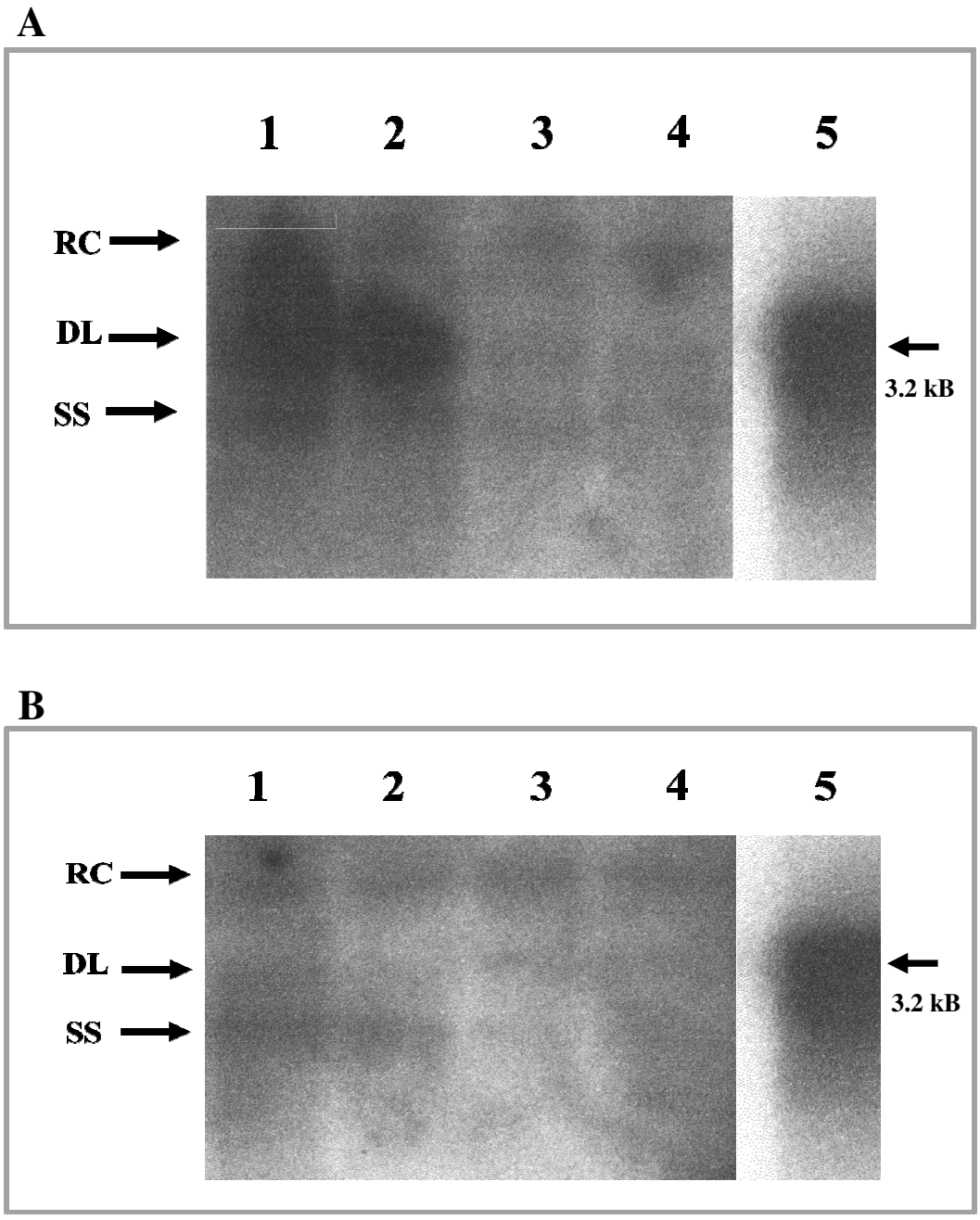

Figure 3.1 Southern hybridization analysis of intracellular core particle-associated hepatitis B virus (HBV) DNA isolated from transfected Huh7 cells. The DNA was analysed by 1 % (w/v) agarose gel electrophoresis and southern hybridized with ^{32}P labelled HBV probe. The positions of relaxed circular (RC), duplex linear (DL), and single stranded (SS) HBV DNA are indicated. **(A) genotype D constructs**: lane 1, wild-type; lane 2, G1862T; lane 3, G1888A; lane 4, G1862T/G1888A; lane 5, linear full length HBV DNA **(B) genotype 'A' constructs**: lane 1, wild-type; lane 2, G1862T; lane 3, G1888A; lane 4, G1862T/G1888A; lane 5, linear full length HBV DNA. Please note that the linear full length HBV DNA was loaded to the same agarose gel, except exposed for shorter time. High background makes differentiation of individual bands difficult.

3.2 Quantitative analysis of intracellular core particle-associated HBV DNA using real time PCR

Intracellular levels of HBV DNA in Huh7 cells transfected with wild-type or mutant HBV replication competent constructs were quantitatively measured using real time PCR. The linear dynamic range of the HBV real time PCR assay was initially determined using serial dilution of cloned plasmid DNA, with the EUROHEP genotype D included as the internal positive control. A typical amplification plot of the serial diluted plasmid DNA and EUROHEP genotype D standard is shown in Figure 3.2 A. The standard curve plotted for the linear regression analysis of these data is shown in Figure 3.2 B. Regression analysis showed a good linear correlation between PCR amplification cycles and viral loads with a correlation coefficient value of 0.996. The *y*-intercept value calculated was 41.225, and the slope of the linear regression line was - 4.079.

The G1862T mutant showed 31 % reduction of replication relative to wild-type in the genotype D construct (Figure 3.3 A, G1862T, genotype D, $P<0.05$). On the other hand, introduction of the G1862T mutations in the genotype 'A' construct did not result in a statistically significant reduction relative to the wild-type (Figure 3.3 B, G1862T, genotype 'A', $P>0.05$). Similar results were observed in cells transfected with G1888A mutant (Figure 3.3 A, G1888A, genotype D, $P<0.05$; Figure 3.3 B, G1888A, genotype 'A', $P>0.05$). The combination of G1862T and G1888A mutations further reduced replication efficiency by 51 % in genotype D construct when compared with the wild-type genotype D construct (Figure 3.3 A, G1862T/G1888A, genotype D, $P<0.001$), but did not affect viral replication in genotype 'A' construct relative to the wild-type genotype 'A' (Figure 3.3 B, G1862T/G1888A, genotype 'A', $P>0.05$). When introduced in the

genotype D construct, the G1896A mutation displayed similar HBV DNA levels to the wild-type (Figure 3.3 A, G1896A, genotype D, $P>0.05$), but a 80% reduction in viral replication was observed when the mutation was introduced into the genotype 'A' construct (Figure 3.3 B, G1896A, genotype 'A', $P<0.001$).

A

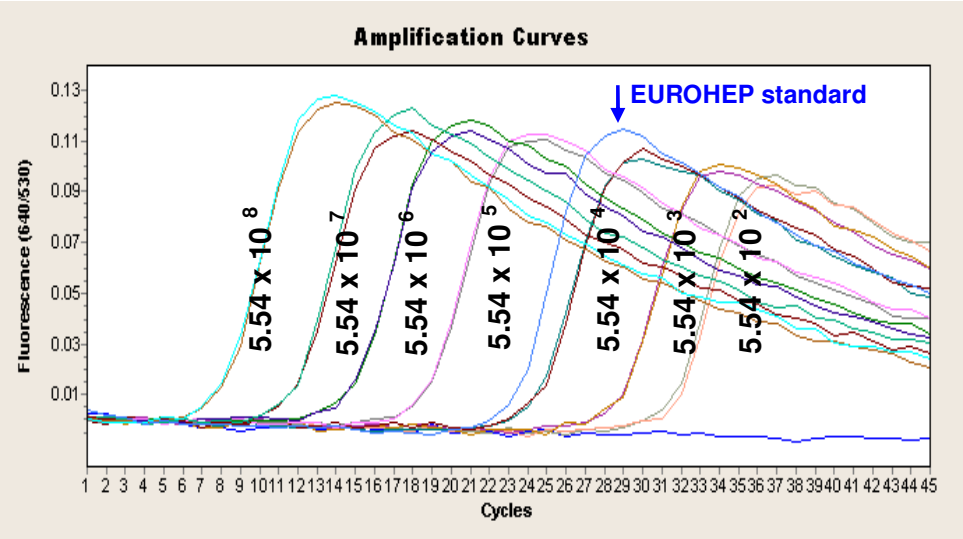

B

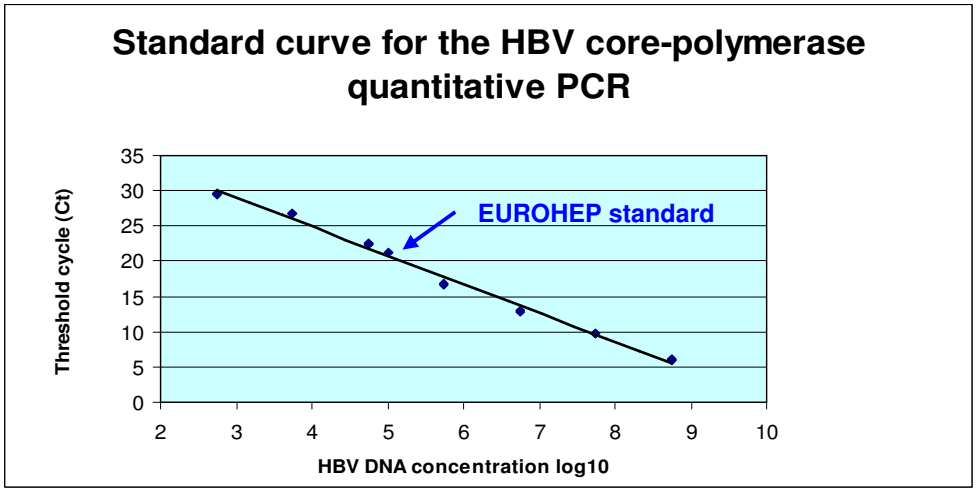

Figure 3.2 (A) Amplification plot of 10-fold serially diluted HBV plasmid DNA. Illustrated the typical sigmoidal fluorescent curves. (B) Standard curve generated for the quantification of the virus, using cloned plasmid DNA as template. Linear regression of the standard curve ranged from 10^2 to 10^8 copies of viral genome / ml. y = - 4.079 log 10 (X) + 41.225; r = - 0.996.

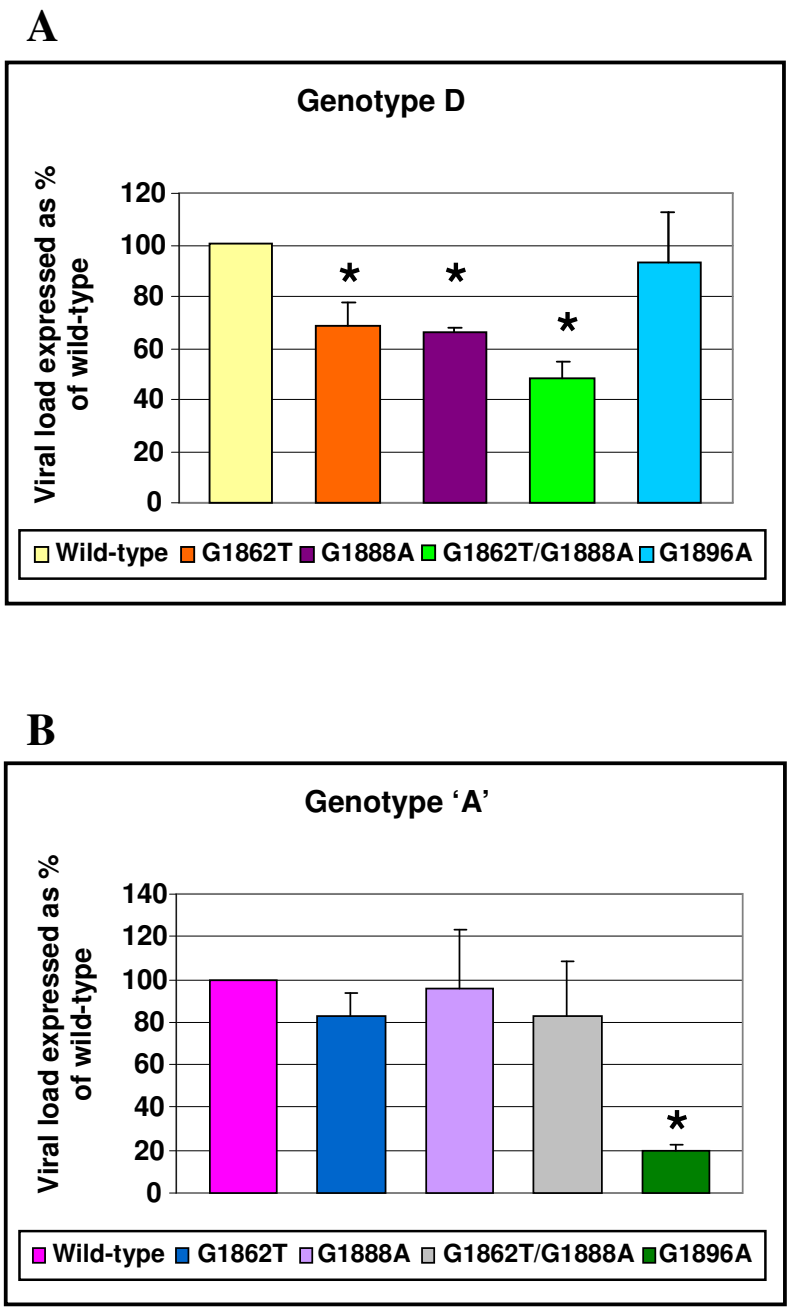

Figure 3.3 Quantification of intracellular core particle associated-hepatitis B virus (HBV) DNA. (A) genotype D constructs (B) genotype 'A' constructs. Mean values and standard deviations from three independent experiments are shown. Values are normalized to HBV copy number of the wild-type construct (100 %). Statistically significant differences compared with wild-type are indicated by an asterisk.

3.3 Effect of HBV G1862T mutation on HBeAg secretion

Secretion of HBeAg into the tissue culture medium of transfected cells was monitored using ELISA. The G1862T mutant in the HBeAg-expression genotype D constructs showed 38 % reduction in the HBeAg concentration in the supernatant relative to the wild-type (Figure 3.4 A, G1862T, genotype D, $P<0.001$). Transfection of Huh7 cells with the mutant genotype 'A' constructs resulted in a 54 % decrease in HBeAg concentration in the supernatant relative to the tranfection with wild-type construct (Figure 3.4 B, G1862T, genotype 'A', $P<0.001$). When G1888A mutation was introduced to both genotype D and 'A' constructs, the HBeAg expression levels were identical to those of wild-type (Figure 3.4 A, G1888A, genotype D, $P>0.05$; Figure 3.4 B, G1888A, genotype 'A', $P>0.05$). The degree of HBeAg reduction in the presence of G1862T alone was comparable to that when G1862T was introduced together with G1888A: 39 % for genotype D (Figure 3.4 A, G1862T/G1888A, genotype D, $P<0.001$) and 42 % for genotype 'A' (Figure 3.4 B, G1862T/G1888A, genotype 'A', $P<0.001$). As expected, the G1896A mutation completely abolished the expression of HBeAg in the supernatant when introduced in both genotype 'A' and D constructs (Figure 3.4 A, G1896A, genotype D; Figure 3.4 B, G1896A, genotype 'A').

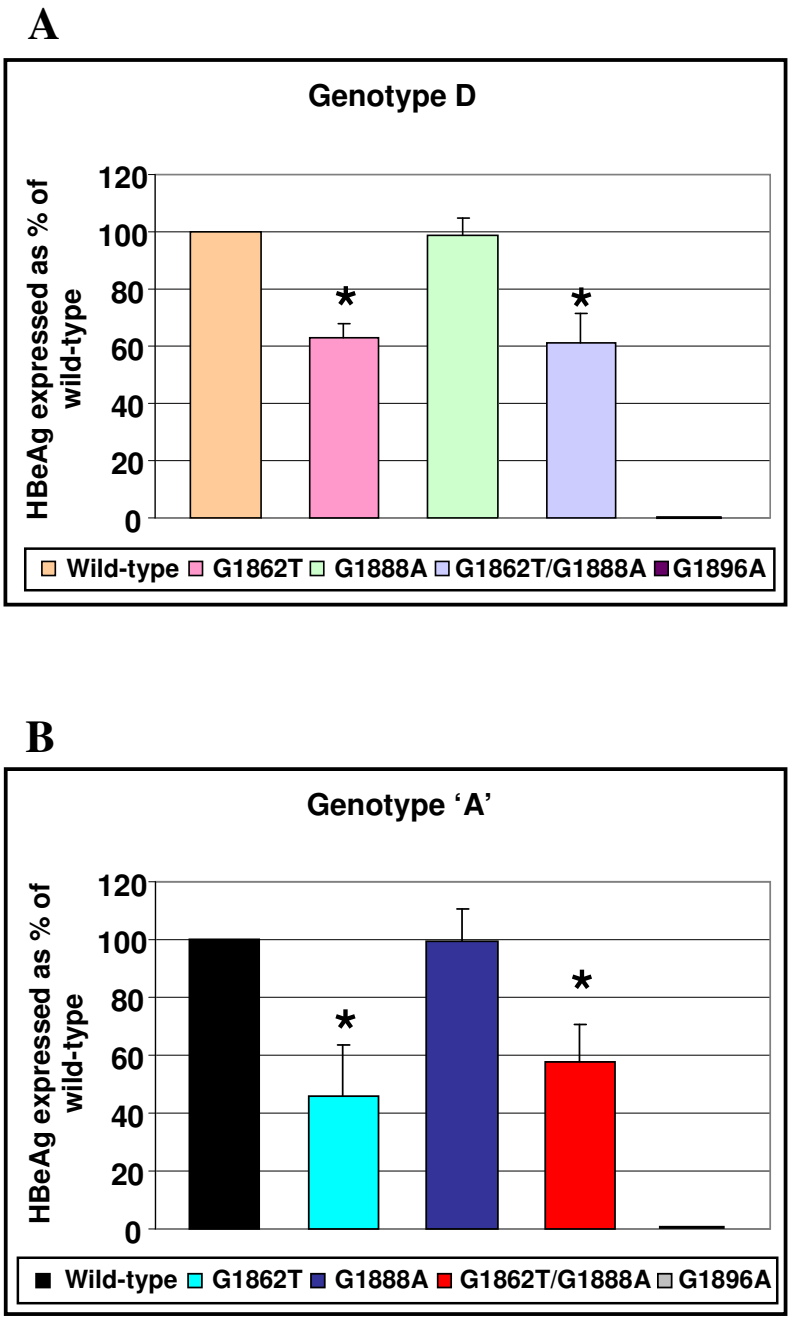

Figure 3.4 Quantification of secreted HBeAg. (A) genotype D constructs (B) genotype 'A' constructs. Mean values and standard deviations from three independent experiments are shown. Values are normalized to HBeAg of the wild-type construct (100 %). Statistically significant differences compared with wild-type are indicated by an asterisk.

3.4 Processing of wild-type versus mutant WHeAg

HBV and WHV share greater than 90 % sequence homology in the ε region. The WHV G1982T (equivalent to G1862T in HBV) occurs frequently in WHV (Li *et al*, 1996). HBV G1862T and WHV G1982T introduce phenotypic change from Val to Phe at codon 17 of the precore core precursor protein (-3 position to the signal peptidase recognition motif). The biosynthesis of wild-type WHeAg was characterized (Carlier *et al*, 1994), but not for the G1982T mutant. The processing of WHV wild-type and G1982T mutant precursor was followed using radioactive pulse labelling, immunoprecipitation and SDS-PAGE methods.

The cleavage of the amino-terminus of the WHV wild-type precursor protein after 3 hours of pulse labelling is shown in lane 4 of Figure 3.5. As measured by scanning densitometry, 23 % of the total wild-type precursor was processed into the intermediate protein ($\pm$ 27 kDa) after 3 hours of labelling. Furthermore, complete maturation of WHeAg was demonstrated by the presence of 24 kDa protein (Figure 3.5, lane 4) (Carlier *et al*, 1994). The mature wild-type WHeAg was not detected in culture medium (Figure 3.5, lane 5) because of the short duration of pulse labelling.

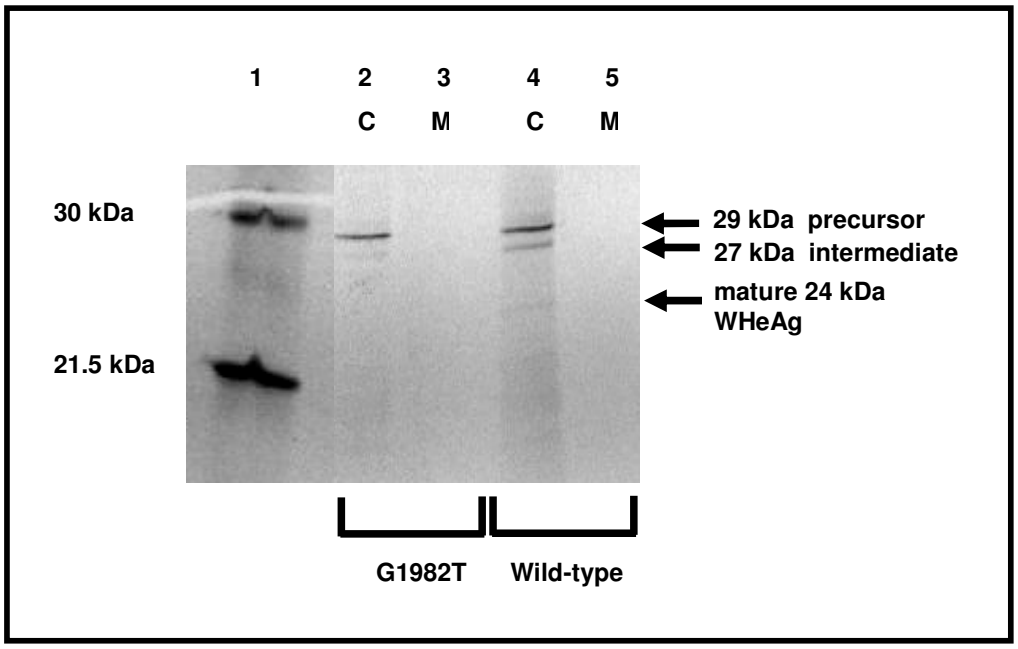

Figure 3.5 Fluorograph showed the processing of WHeAg from the precursor to intermediate form. Huh7 cells were transfected with wild-type or G1982T WHeAg expressing plasmids and pulse labelled with ^{35}S-methionine and cysteine for 3 hours. Proteins immunoprecipitated with polyclonal anti-WHcAg were resolved using 15 % polyacrylamide gel electrophoresis. C: intracellular fraction; M: extracellular culture medium. Lane 1: ^{14}C-labelled protein molecular mass marker.

On the other hand, the mutant precursor protein, which encoded Phe instead of Val at the -3 position from the signal peptide cleavage site, was processed with a lower efficiency compared to the wild-type. Only 4.8 % of the total mutant precursor was processed (Figure 3.5, lane 2). Furthermore, the 24 kDa protein was not detected in cells transfected with the mutant construct indicating the absence of complete maturation after 3 hours of pulse labelling.

3.5 Immunocytochemistry

3.5.1 Intracellular localization of wild-type and mutant precore/core protein in the early secretory organelles

Expression of wild-type and mutant HBeAg or WHeAg was followed in transfected Huh7 cells. Mock-transfected Huh7 cells in which no fluorescence was detected when stained for anti-HBeAg and cells transfected with a plasmid with the G1896A mutation, which results in the truncation of HBeAg at codon 28 (Carman *et al.*, 1989), were used as negative controls. In subgenotype A1 HBV isolates, the G1862T mutant occurs frequently together with a G1888A silent mutation (Kimbi *et al.*, 2004) (Figure 1.7). In order to preclude the possibility that G1888A could affect the phenotype of the G1862T mutant constructs in which these two mutations occurred independently or in combination were used.

The intracellular localization of the wild-type and mutant precore/core protein was investigated by confocal immunofluorescence microscopy, using antibodies targeting the precore/core protein in conjunction with antibodies against various components of the early secretory pathway. Intracellular organelle markers included the protein disulphide isomerase (PDI)-an ER resident chaperone as ER marker, ERGIC-53-a transmembrane lectin that cycles between ER, ERGIC and Golgi, as the marker for the ER-Golgi intermediate compartment (ERGIC) (Hauri *et al*, 2000), and giantin-Golgi apparatus matrix protein as marker for the Golgi apparatus (Linstedt & Hauri, 1993).

When the Huh7 cells were transfected with either genotype D or genotype 'A' wild-type HBeAg-expression constructs, the precore/core protein was evenly distributed throughout the cytoplasm, as demonstrated by the diffused reticular

and fine granular stains. Some of wild-type protein was co-localized with protein disulphide isomerase (PDI), (Figure 3.6-3.9, A-C), ERGIC-53 (Figure 3.11-3.14, A-C), and giantin (Figure 3.16-3.19, A-C), indicating that the wild-type protein is moving along the ER to the Golgi via ERGIC rapidly before being exported from the cells, suggesting the normal biogenesis of the precore/core protein. The ER marker, PDI gave a fine reticular staining pattern that extended throughout the cytoplasm (Figure 3.6-3.9, B), the ERGIC-53 label was punctuate and closer to the nucleus (Figure 3.11-3.14, B), where as the Golgi compartment labelled with anti-giantin gave a characteristic strong, juxtanuclear label (Figure 3.16-3.19, B). The G1888A mutant precore/core protein exhibited similar distribution pattern compared to those of the wild-type (Figure 3.6-3.9, G-I; Figure 3.11-3.14, G-I; Figure 3.16-3.19, G-I). The same distribution pattern was observed in cells transfected with the wild-type WHeAg-expression construct at 48hr post-transfection (Figure 3.10, A-C; Figure 3.15, A-C; Figure 3.20, A-C). There was no difference in the intensity of the staining of the markers for the different compartments of the secretory pathway.

In contrast, cells transfected with HBV G1862T (Figure 3.6-3.9, D-F), G1862T/G1888A (Figure 3.6-3.9, J-L) and WHV G1982T (Figure 3.10, D-F) mutant precore/core constructs showed, in addition to the reticular pattern, punctuate concentrations of precore/core protein that co-localized with anti-PDI, indicating the movement of mutant protein through the ER. The number of cells per counting field showing the punctuate pattern was always higher in the cultures transfected with HBV G1862T, G1862T/G1888A or WHV G1982T mutant precore/core constructs when compared to those transfected with the respective wild-type constructs. HBV G1862T (Figure 3.11-3.14, D-F), G1862T/G1888A

(Figure 3.11-3.14, J-L) or WHV G1982T (Figure 3.15, D-F) mutant precore/core protein escaped from the ER as was demonstrated by the accumulation of the proteins in the ERGIC, indicated by intense co-staining with ERGIC-53. HBV G1862T (Figure 3.16-3.19, D-F), G1862T/G1888A (Figure 3.16-3.19, J-L) and WHV G1982T (Figure 3.20, D-F) mutant precore/core proteins were co-localized with giantin to a lesser extent when compared to the wild-type. These observations demonstrated that the mutant (HBV G1862T, G1862T/G1888A and WHV G1982T) precore/core proteins are not confined to the ER but a significant proportion moves to ERGIC where they appear to accumulate and only a relatively small fraction migrate to the Golgi.

The truncated precore/core protein that results from the stop codon introduced by G1896A, localized to the nucleus (with faint staining only), and was not seen in other cellular organelles (Figure 3.6-3.9, M-O; Figure 3.11-3.14, M-O; Figure 3.16-3.19, M-O).

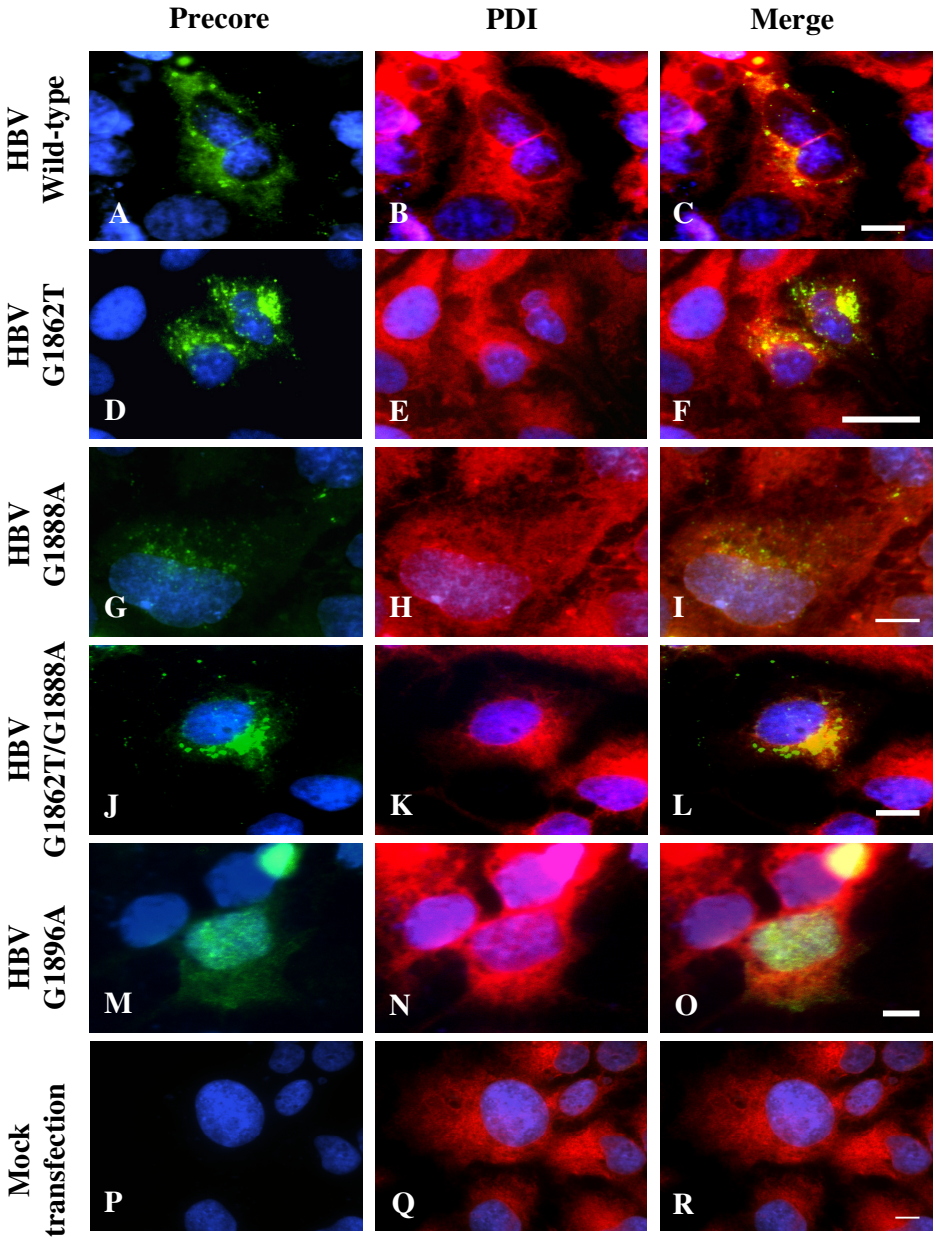

Figure 3.6 Intracellular localization of genotype D HBV precore/core protein to the ER at 48 hours post-transfection. Huh7 cells were transfected with genotype D plasmid constructs, fixed at 48 hours post-transfection, and subjected to indirect double immunofluorescence staining with antibodies against HBV precore/core protein, detected with secondary antibodies labelled with AlexaFluor 488, shown in green. The ER was detected with primary antibodies against PDI and secondary antibodies were labelled with AlexaFluor 546, shown in red. Co-localization of precore/core protein and ER can be seen by the yellow color. Nuclei were counterstained with diamidino-2-phenylindole dihydrochloride (DAPI). Scale bars, 10 μm.

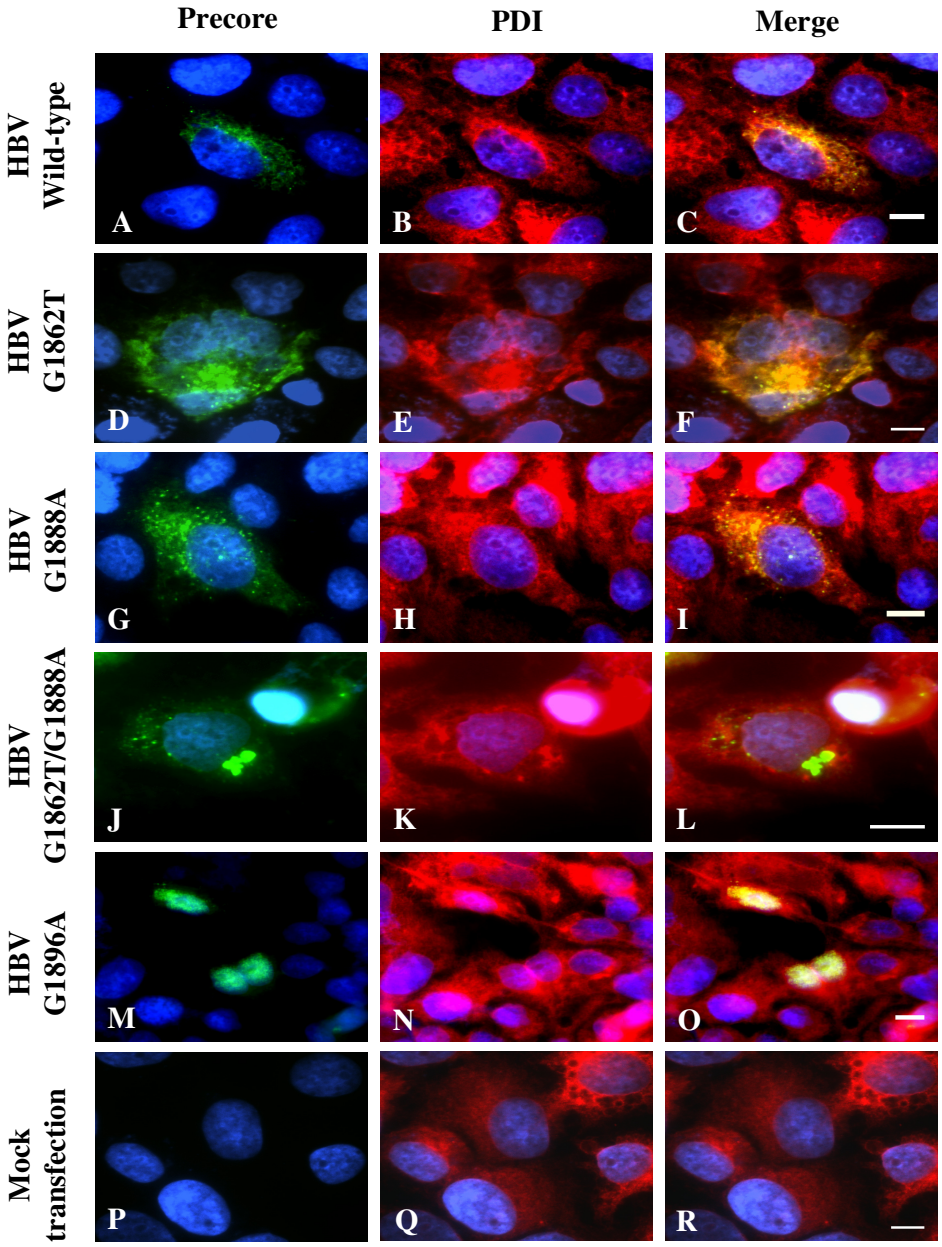

Figure 3.7 Intracellular localization of genotype D HBV precore/core protein to the ER at 72 hours post-transfection. Huh7 cells were transfected with genotype D plasmid constructs, fixed at 72 hours post-transfection, and subjected to indirect double immunofluorescence staining with antibodies against HBV precore/core protein, detected with secondary antibodies labelled with AlexaFluor 488, shown in green. The ER was detected with primary antibodies against PDI and secondary antibodies were labelled with AlexaFluor 546, shown in red. Co-localization of precore/core protein and ER can be seen by the yellow color. Nuclei were counterstained with DAPI. Scale bars, 10 μm.

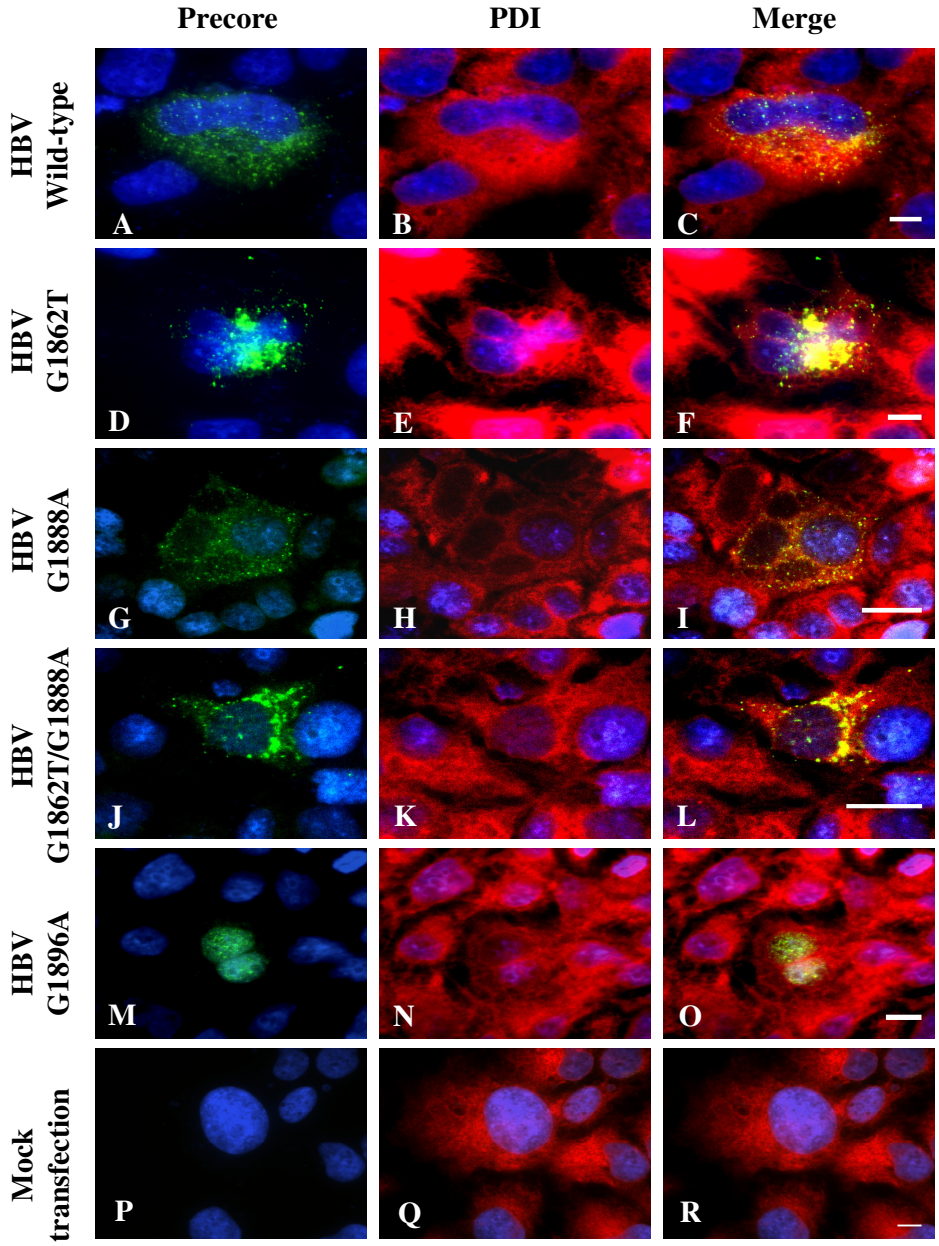

Figure 3.8 Intracellular localization of genotype 'A' HBV precore/core protein to the ER at 48 hours post-transfection. Huh7 cells were transfected with genotype 'A' plasmid constructs, fixed at 48 hours post-transfection, and subjected to indirect double immunofluorescence staining with antibodies against HBV precore/core protein, detected with secondary antibodies labelled with AlexaFluor 488, shown in green. The ER was detected with primary antibodies against PDI and secondary antibodies were labelled with AlexaFluor 546, shown in red. Co-localization of precore/core protein and ER can be seen by the yellow color. Nuclei were counterstained with DAPI. Scale bars, 10 μm.

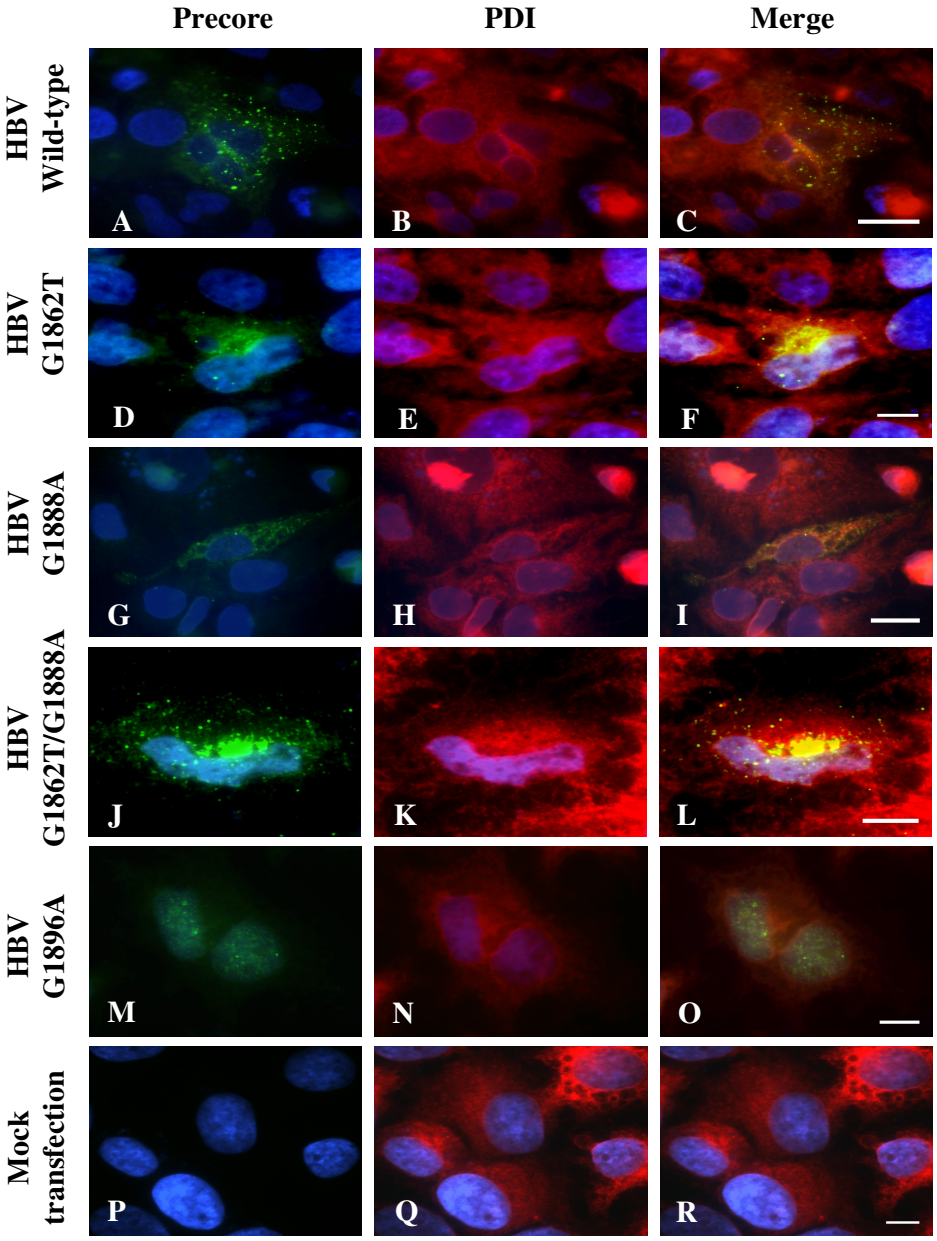

Figure 3.9 Intracellular localization of genotype 'A' HBV precore/core protein to the ER at 72 hours post-transfection. Huh7 cells were transfected with genotype 'A' plasmid constructs, fixed at 72 hours post-transfection, and subjected to indirect double immunofluorescence staining with antibodies against HBV precore/core protein, detected with secondary antibodies labelled with AlexaFluor 488, shown in green. The ER was detected with primary antibodies against PDI and secondary antibodies were labelled with AlexaFluor 546, shown in red. Co-localization of precore/core protein and ER can be seen by the yellow color. Nuclei were counterstained with DAPI. Scale bars, 10 μm.

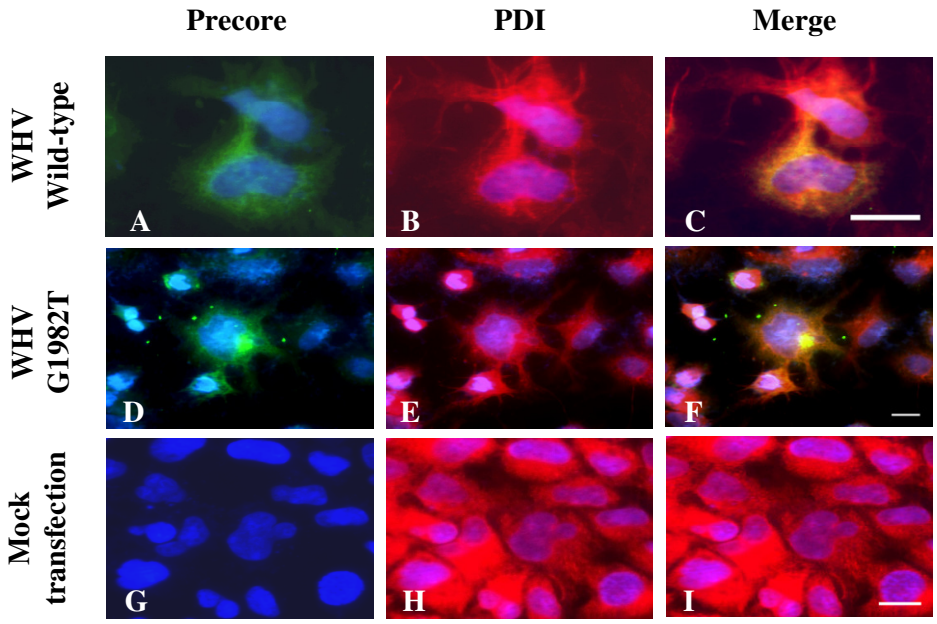

Figure 3.10 Intracellular localization of WHV precore/core protein to the ER at 48 hours post-transfection. Huh7 cells were transfected with WHV plasmid constructs, fixed at 48 hours post-transfection, and subjected to indirect double immunofluorescence staining with antibodies against WHV precore/core protein, detected with secondary antibodies labelled with AlexaFluor 488, shown in green. The ER was detected with primary antibodies against PDI and secondary antibodies were labelled with AlexaFluor 546, shown in red. Co-localization of precore/core protein and ER can be seen by the yellow color. Nuclei were counterstained with DAPI. Scale bars, 10 μm.

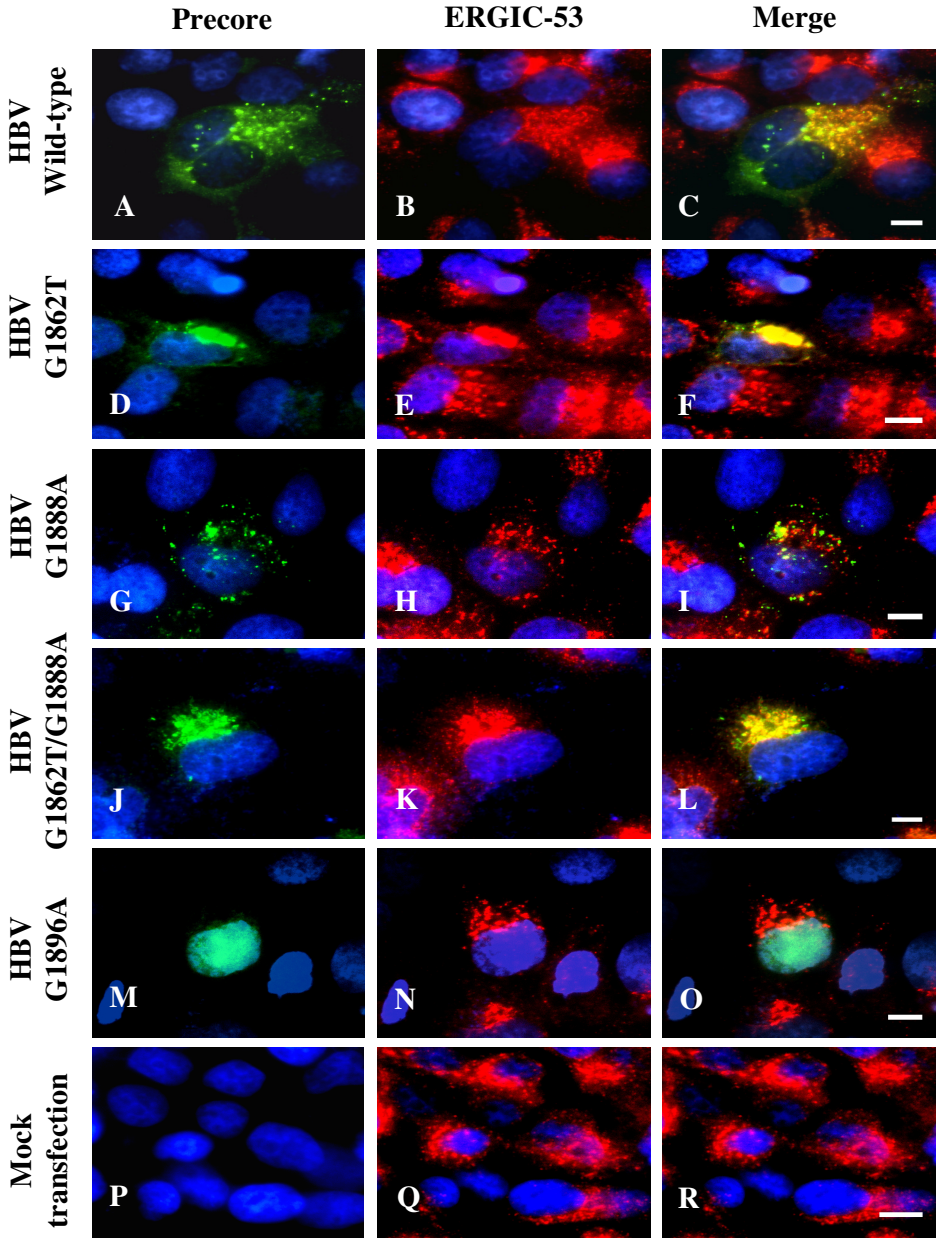

Figure 3.11 Intracellular localization of genotype D HBV precore/core protein to the ER-Golgi intermediate compartment (ERGIC) at 48 hours post-transfection. Huh7 cells were transfected with genotype D plasmid constructs, fixed at 48 hours post-transfection, and subjected to indirect double immunofluorescence staining with antibodies against HBV precore/core protein, detected with secondary antibodies labelled with AlexaFluor 488, shown in green. The ERGIC was detected with primary antibodies against ERGIC-53 and secondary antibodies were labelled with AlexaFluor 546, shown in red. Co-localization of precore/core protein and ERGIC can be seen by the yellow color. Nuclei were counterstained with DAPI. Scale bars, 10 μm.

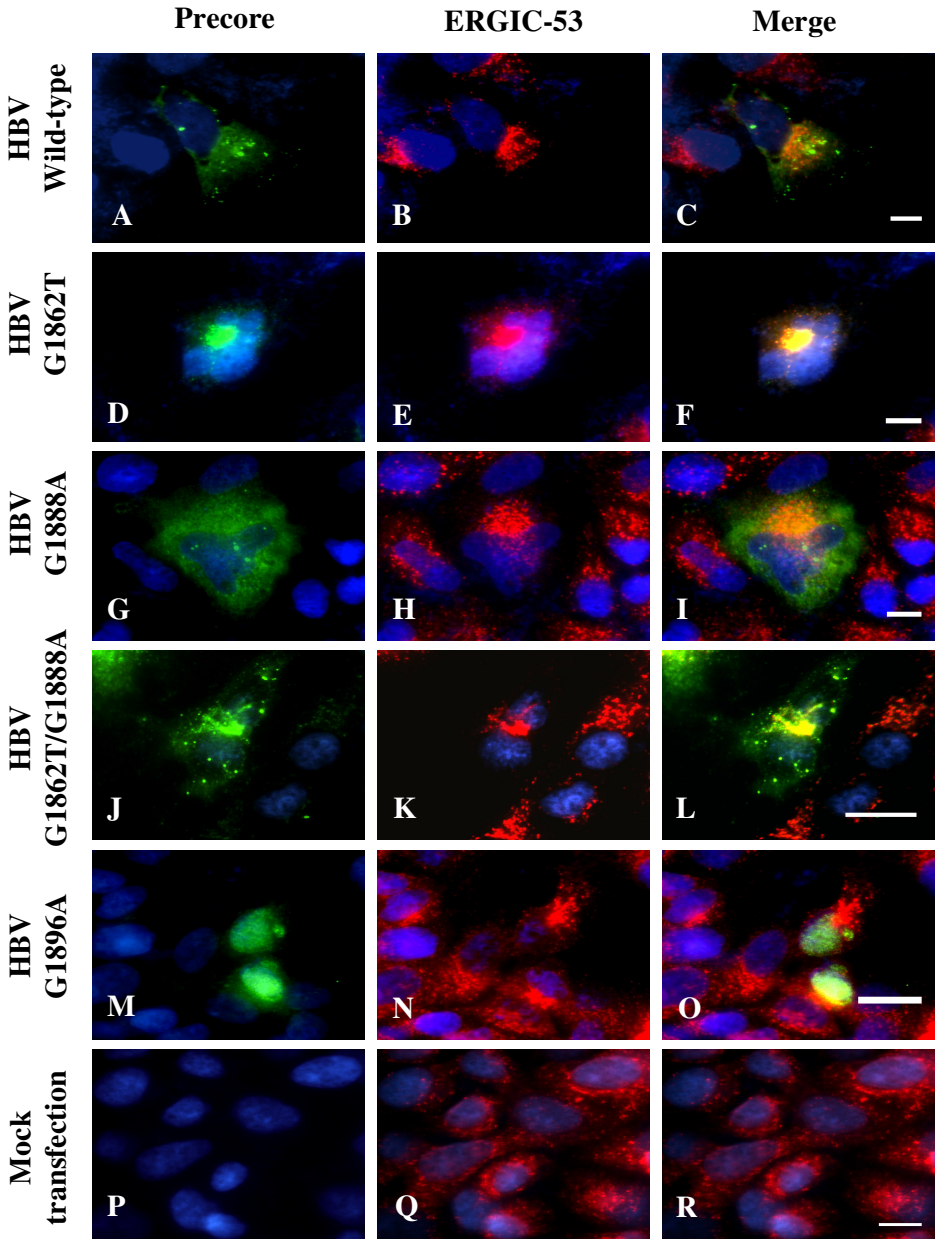

Figure 3.12 Intracellular localization of genotype D HBV precore/core protein to the ER-Golgi intermediate compartment (ERGIC) at 72 hours post-transfection. Huh7 cells were transfected with genotype D plasmid constructs, fixed at 72 hours post-transfection, and subjected to indirect double immunofluorescence staining with antibodies against HBV precore/core protein, detected with secondary antibodies labelled with AlexaFluor 488, shown in green. The ERGIC was detected with primary antibodies against ERGIC-53 and secondary antibodies were labelled with AlexaFluor 546, shown in red. Co-localization of precore/core protein and ERGIC can be seen by the yellow color. Nuclei were counterstained with DAPI. Scale bars, 10 μm.

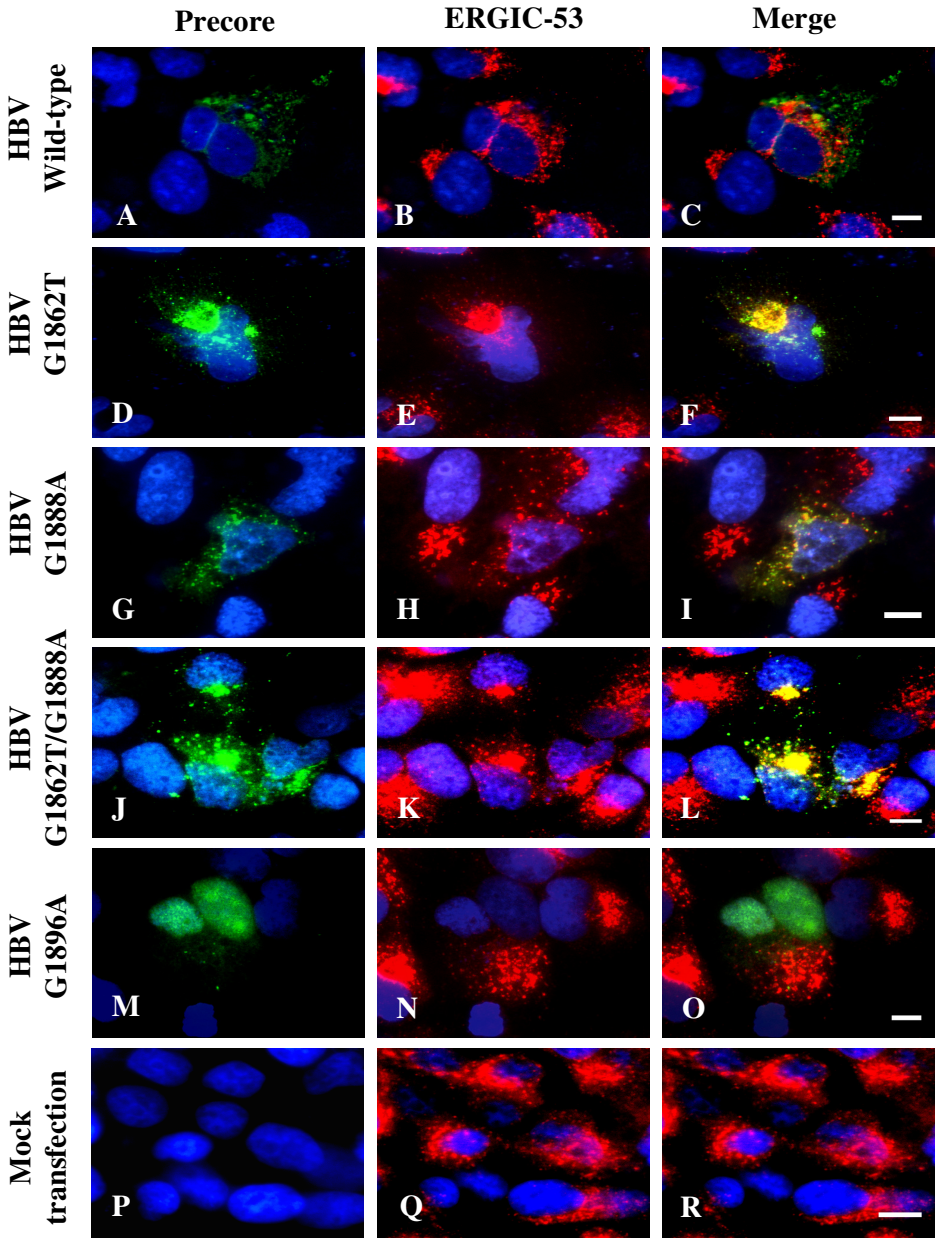

Figure 3.13 Intracellular localization of genotype 'A' HBV precore/core protein to the ER-Golgi intermediate compartment (ERGIC) at 48 hours post-transfection. Huh7 cells were transfected with genotype 'A' plasmid constructs, fixed at 48 hours post-transfection, and subjected to indirect double immunofluorescence staining with antibodies against HBV precore/core protein, detected with secondary antibodies labelled with AlexaFluor 488, shown in green. The ERGIC was detected with primary antibodies against ERGIC-53 and secondary antibodies were labelled with AlexaFluor 546, shown in red. Co-localization of precore/core protein and ERGIC can be seen by the yellow color. Nuclei were counterstained with DAPI. Scale bars, 10 μm.

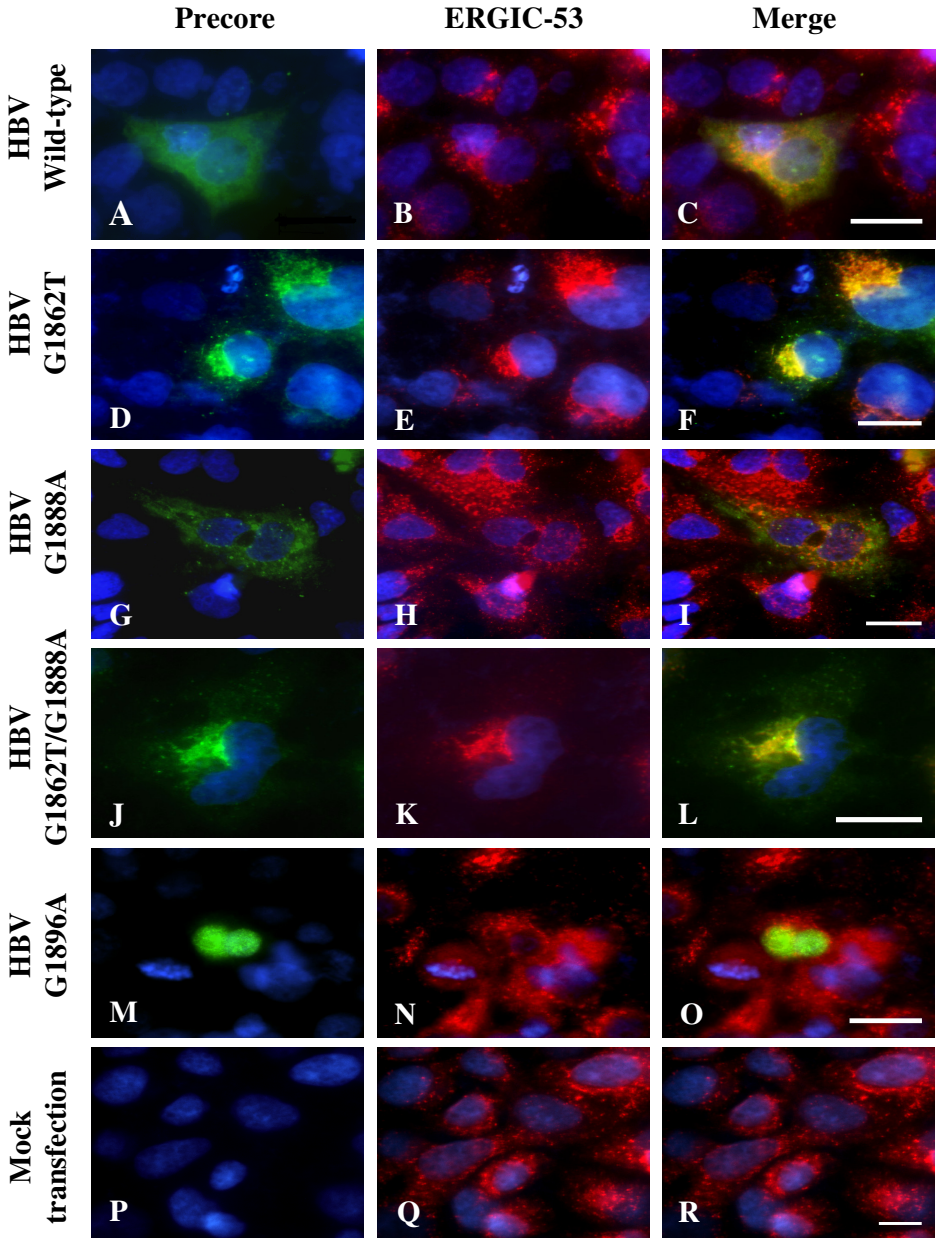

Figure 3.14 Intracellular localization of genotype 'A' HBV precore/core protein to the ER-Golgi intermediate compartment (ERGIC) at 72 hours post-transfection. Huh7 cells were transfected with genotype 'A' plasmid constructs, fixed at 72 hours post-transfection, and subjected to indirect double immunofluorescence staining with antibodies against HBV precore/core protein, detected with secondary antibodies labelled with AlexaFluor 488, shown in green. The ERGIC was detected with primary antibodies against ERGIC-53 and secondary antibodies were labelled with AlexaFluor 546, shown in red. Co-localization of precore/core protein and ERGIC can be seen by the yellow color. Nuclei were counterstained with DAPI. Scale bars, 10 μm.

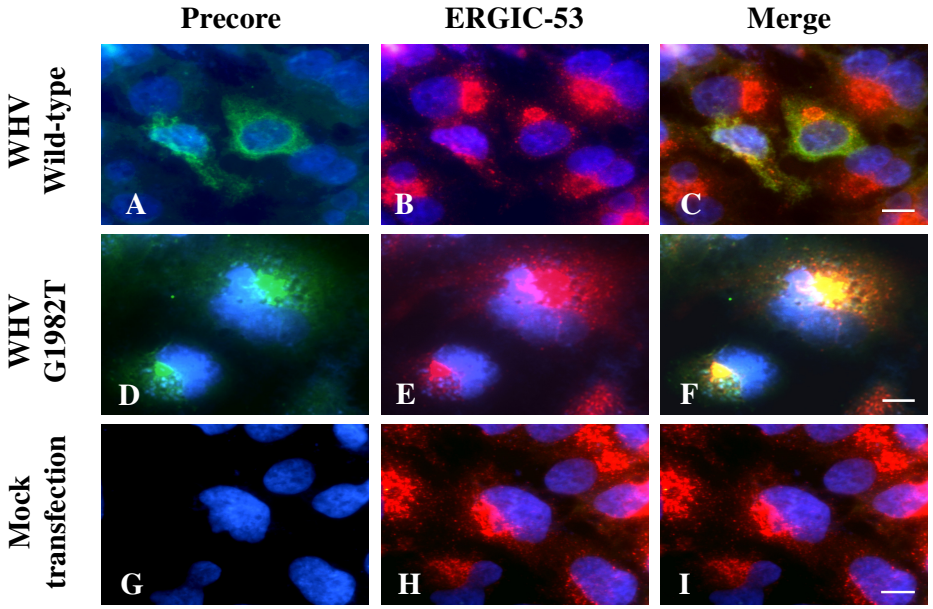

Figure 3.15 Intracellular localization of WHV precore/core protein to the ER-Golgi intermediate compartment (ERGIC) at 48 hours post-transfection. Huh7 cells were transfected with WHV plasmid constructs, fixed at 48 hours post-transfection, and subjected to indirect double immunofluorescence staining with antibodies against WHV precore/core protein, detected with secondary antibodies labelled with AlexaFluor 488, shown in green. The ERGIC was detected with primary antibodies against ERGIC-53 and secondary antibodies were labelled with AlexaFluor 546, shown in red. Co-localization of precore/core protein and ERGIC can be seen by the yellow color. Nuclei were counterstained with DAPI. Scale bars, 10 μm.

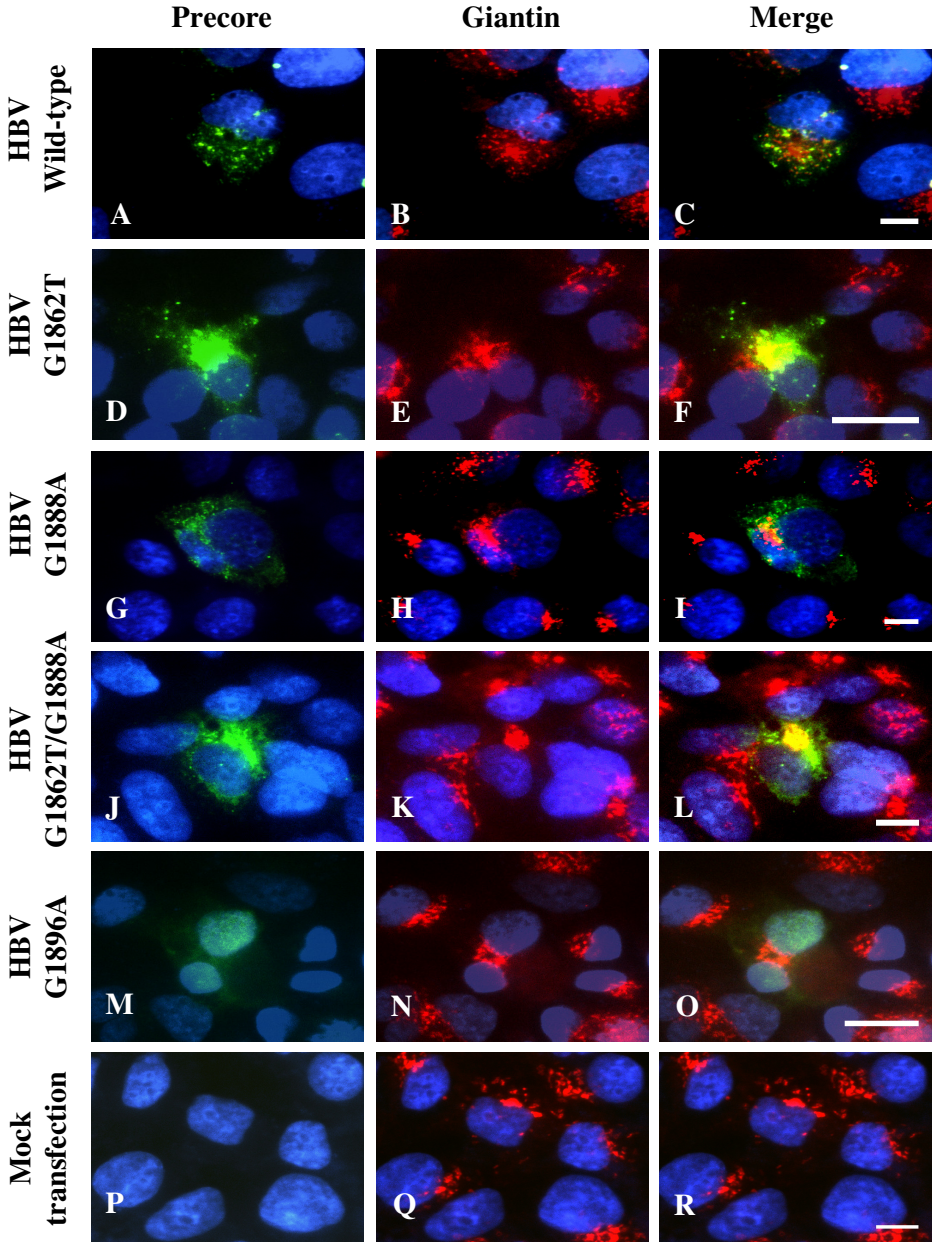

Figure 3.16 Intracellular localization of genotype D HBV precore/core protein to the Golgi at 48 hours post-transfection. Huh7 cells were transfected with genotype D plasmid constructs, fixed at 48 hours post-transfection, and subjected to indirect double immunofluorescence staining with antibodies against HBV precore/core protein, detected with secondary antibodies labelled with AlexaFluor 488, shown in green. The Golgi was detected with primary antibodies against giantin and secondary antibodies were labelled with AlexaFluor 546, shown in red. Co-localization of precore/core protein and Golgi can be seen by the yellow color. Nuclei were counterstained with DAPI. Scale bars, 10 μm.

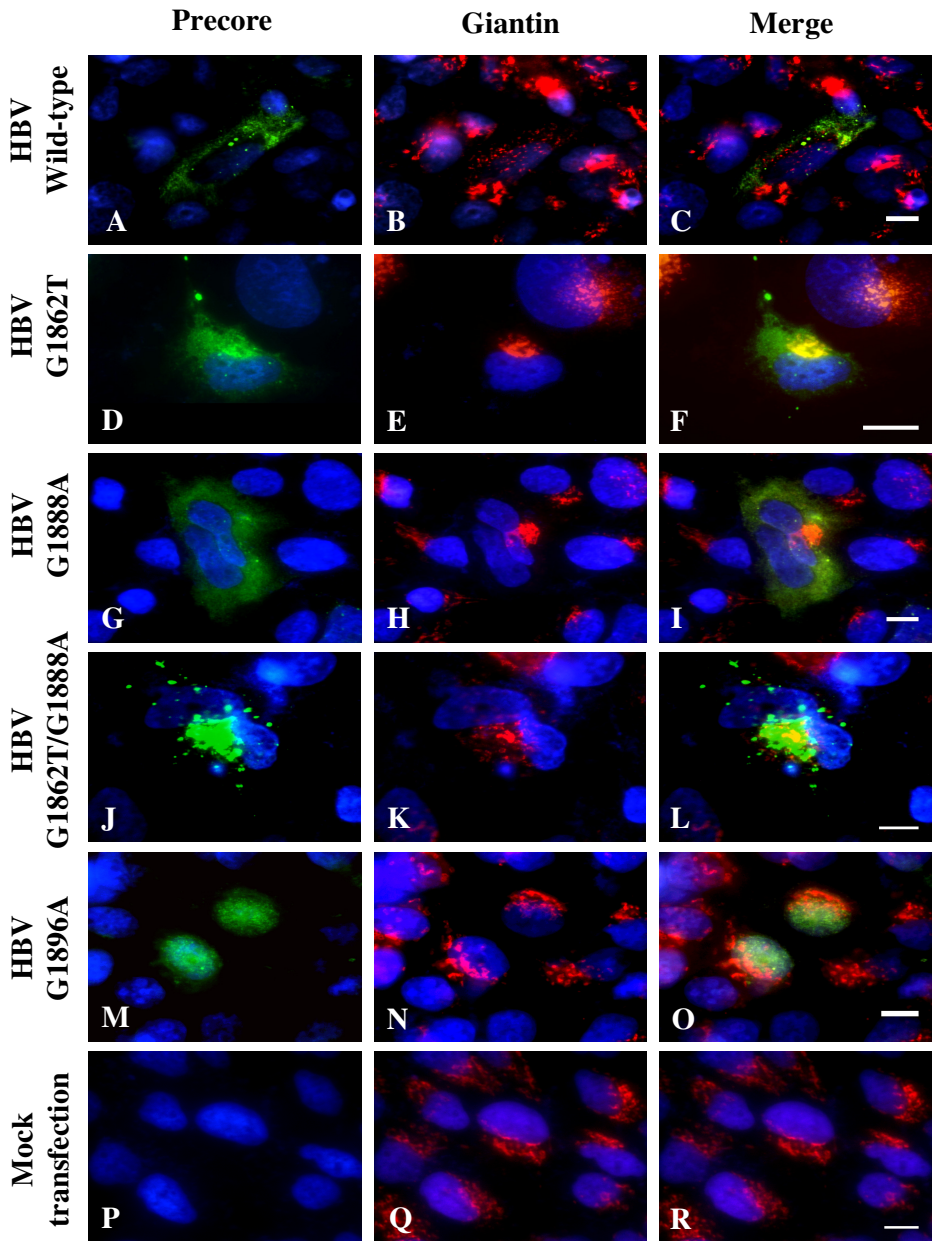

Figure 3.17 Intracellular localization of genotype D HBV precore/core protein to the Golgi at 72 hours post-transfection. Huh7 cells were transfected with genotype D plasmid constructs, fixed at 72 hours post-transfection, and subjected to indirect double immunofluorescence staining with antibodies against HBV precore/core protein, detected with secondary antibodies labelled with AlexaFluor 488, shown in green. The Golgi was detected with primary antibodies against giantin and secondary antibodies were labelled with AlexaFluor 546, shown in red. Co-localization of precore/core protein and Golgi can be seen by the yellow color. Nuclei were counterstained with DAPI. Scale bars, 10 μm.

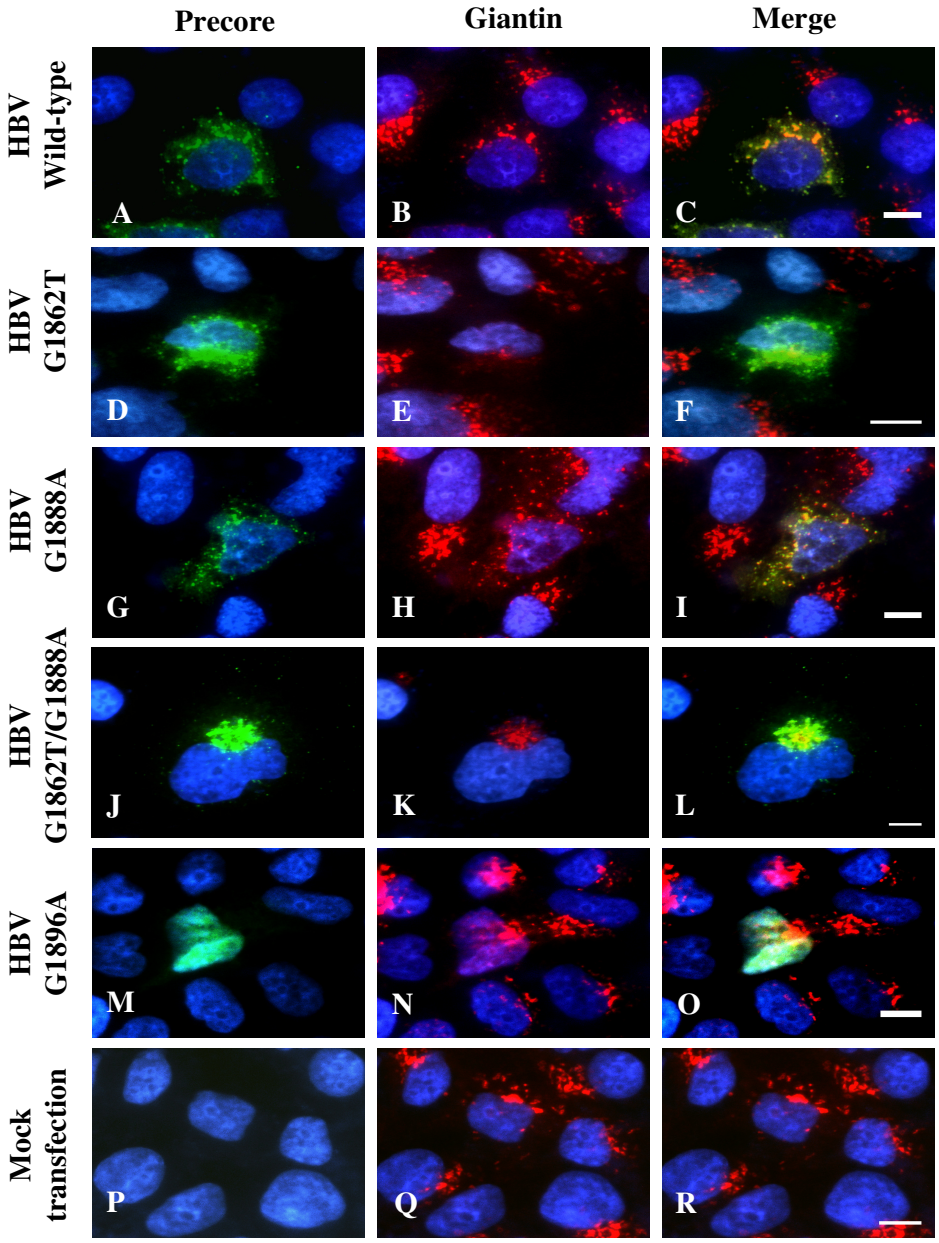

Figure 3.18 Intracellular localization of genotype 'A' HBV precore/core protein to the Golgi at 48 hours post-transfection. Huh7 cells were transfected with genotype 'A' plasmid constructs, fixed at 48 hours post-transfection and subjected to indirect double immunofluorescence staining with antibodies against HBV precore/core protein, detected with secondary antibodies labelled with AlexaFluor 488, shown in green. The Golgi was detected with primary antibodies against giantin and secondary antibodies were labelled with AlexaFluor 546, shown in red. Co-localization of precore/core protein and Golgi can be seen by the yellow color. Nuclei were counterstained with DAPI. Scale bars, 10 µm.

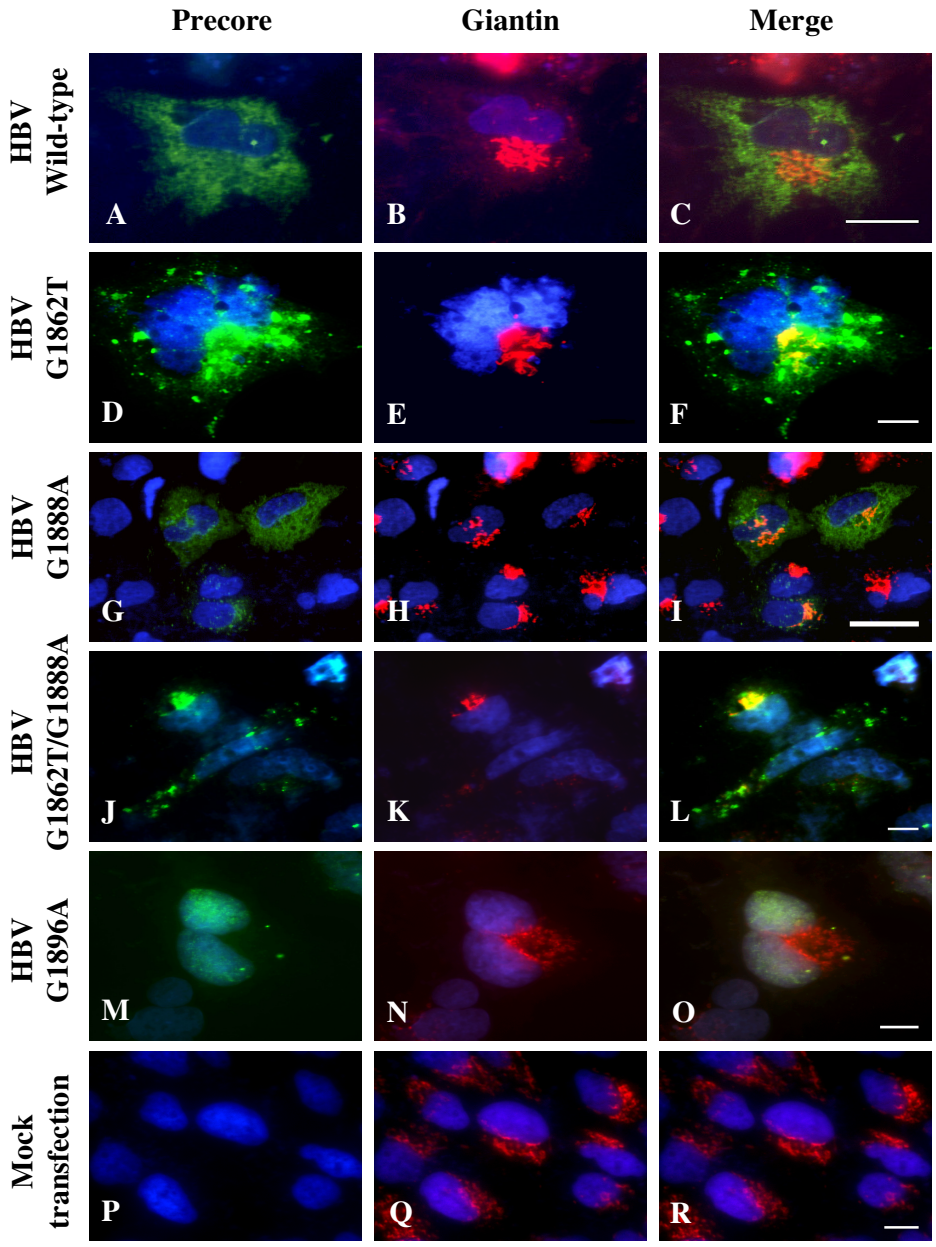

Figure 3.19 Intracellular localization of genotype 'A' HBV precore/core protein to the Golgi at 72 hours post-transfection. Huh7 cells were transfected with genotype 'A' plasmid constructs, followed by fixation at 72 hours post-transfection. The cells were subjected to indirect double immunofluorescence staining with antibodies against HBV precore/core protein, detected with secondary antibodies labelled with AlexaFluor 488, shown in green. The Golgi was detected with primary antibodies against giantin and secondary antibodies were labelled with AlexaFluor 546, shown in red. Co-localization of precore/core protein and Golgi can be seen by the yellow color. Nuclei were counterstained with DAPI. Scale bars, 10 μm.

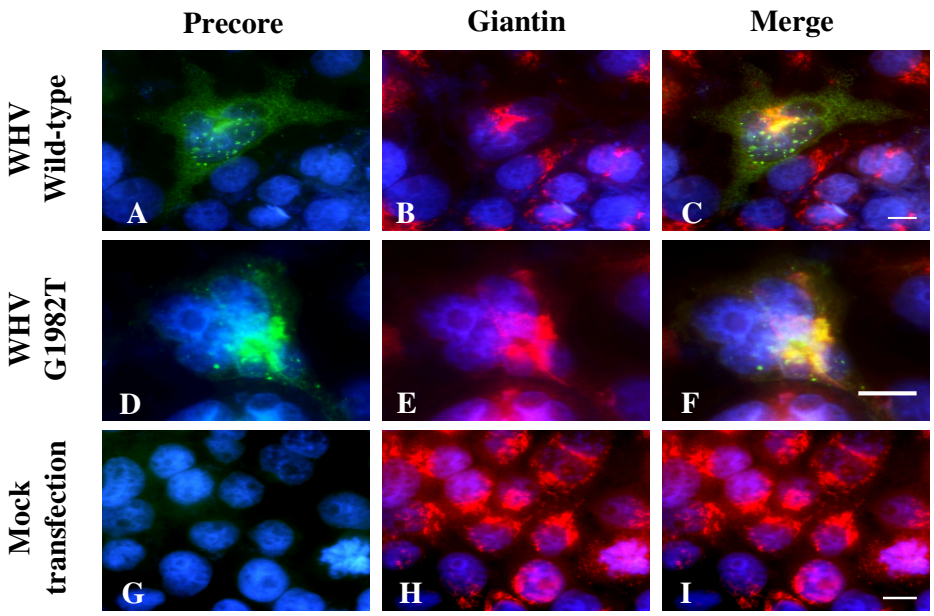

Figure 3.20 Intracellular localization of WHV precore/core protein to the Golgi at 48 hours post-transfection. Huh7 cells were transfected with WHV plasmid constructs, followed by fixation at 48 hours post-transfection. The cells were subjected to indirect double immunofluorescence staining with antibodies against WHV precore/core protein, detected with secondary antibodies labelled with AlexaFluor 488, shown in green. The Golgi was detected with primary antibodies against giantin and secondary antibodies were labelled with AlexaFluor 546, shown in red. Co-localization of precore/core protein and Golgi can be seen by the yellow color. Nuclei were counterstained with DAPI. Scale bars, 10 μm.

3.5.2 Post-ER expression of wild-type and mutant precore/core protein

Golgi apparatus is located around the MTOC (Lippincott-Schwartz, 1998). In order to confirm the mutant protein was not accumulated in the Golgi apparatus, BFA was used to disrupt the Golgi apparatus. The treatment with BFA dispersed the Golgi apparatus and re-distributed the Golgi elements to ER exit site (Figure 3.21-3.22, B, E, H, K, N and Q). Reticular type of stain pattern similar to those of ER was observed in cells transfected with HBV wild-type (Figure 3.21-3.22, A-C), G1888A mutant (Figure 3.21-3.22, G-I) or WHV wild-type (Figure 3.23, A-C) constructs. Treatment with BFA did not reduce the occurrence or disrupt the large, perinuclar structure which was staining positive for HBV G1862T (Figure 3.21-3.22, D-F) or G1862T/G1888A mutant precore/core protein (Figure 3.21-3.22, J-L). HBV G1862T or G1862T/G1888A mutant precore/core protein was not retained within the Golgi apparatus but instead appeared to be associated with another compartment, which is structurally distinct and physically close to the Golgi. The same pattern was also observed in cells transfected with WHV G1982T mutant construct at 48 hr post-transfection (Figure 3.23, D-F).

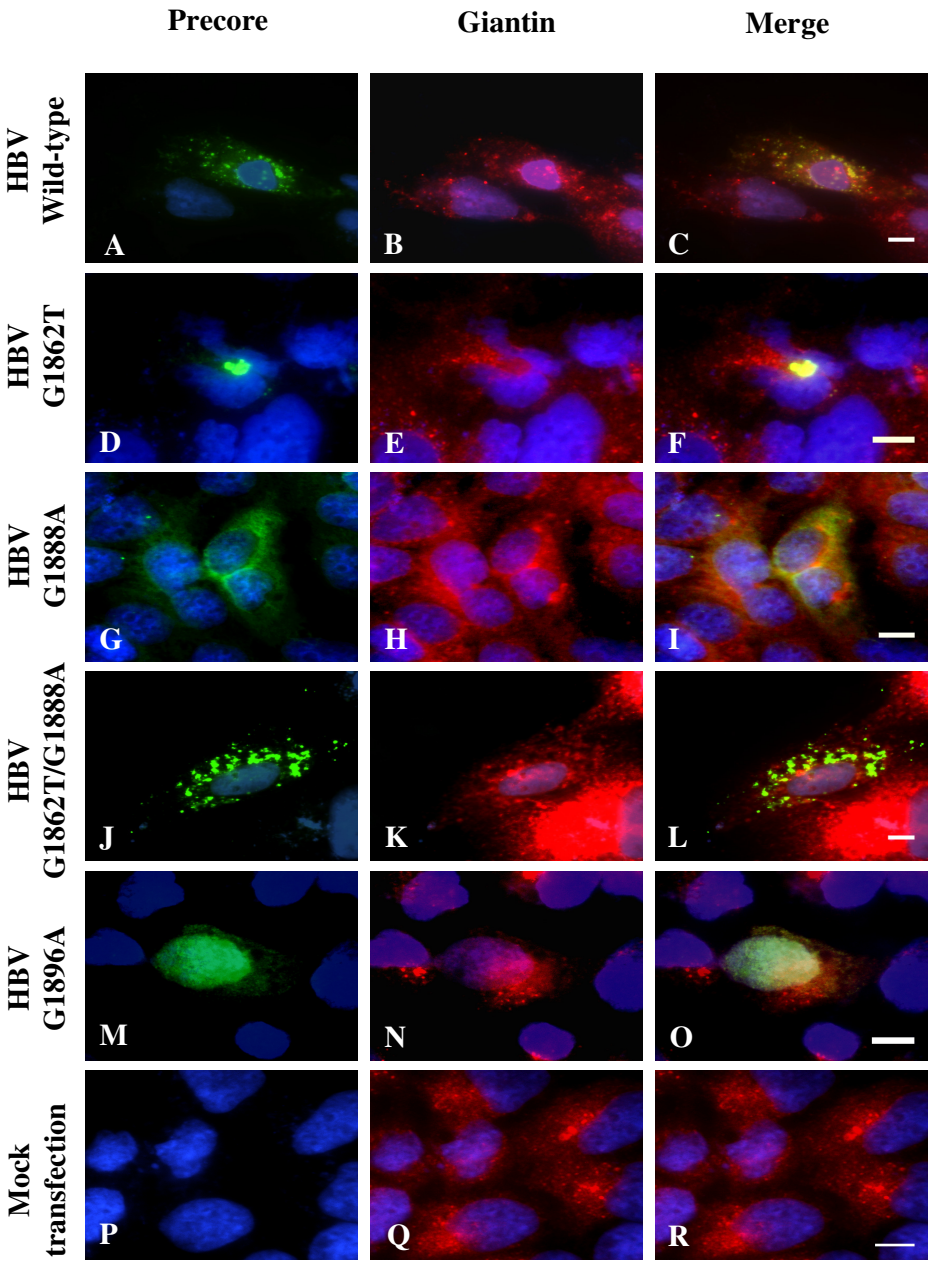

Figure 3.21 Genotype D HBV G1862T mutant precore/core protein did not accumulate in the Golgi following BFA treatment. Huh7 cells were transfected with genotype D plasmid constructs, treated with BFA prior to fixation at 72 hours post-transfection. The cells were subjected to indirect double immunofluorescence staining with antibodies against HBV precore/core protein, detected with secondary antibodies labelled with AlexaFluor 488, shown in green. The Golgi was detected with primary antibodies against giantin and secondary antibodies were labelled with AlexaFluor 546, shown in red. Co-localization of precore/core protein and Golgi can be seen by the yellow color. Nuclei were counterstained with DAPI. Scale bars, 10 μm.

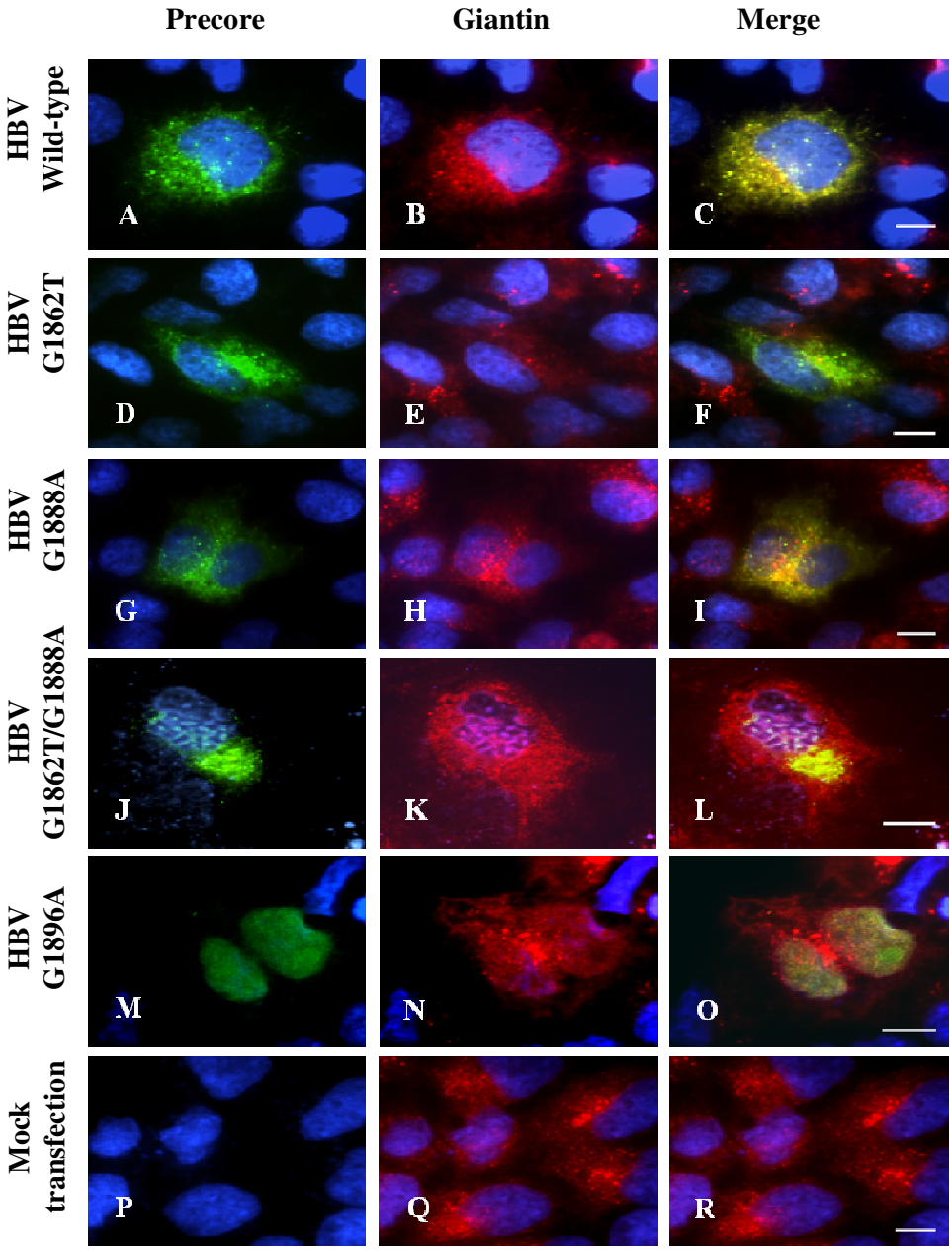

Figure 3.22 Genotype 'A' HBV G1862T mutant precore/core protein did not accumulate in the Golgi following BFA treatment. Huh7 cells were transfected with genotype 'A' plasmid constructs, treated with BFA prior to fixation at 72 hours post-transfection. The cells were subjected to indirect double immunofluorescence staining with antibodies against HBV precore/core protein, detected with secondary antibodies labelled with AlexaFluor 488, shown in green. The Golgi was detected with primary antibodies against giantin and secondary antibodies were labelled with AlexaFluor 546, shown in red. Co-localization of precore/core protein and Golgi can be seen by the yellow color. Nuclei were counterstained with DAPI. Scale bars, 10 μm.

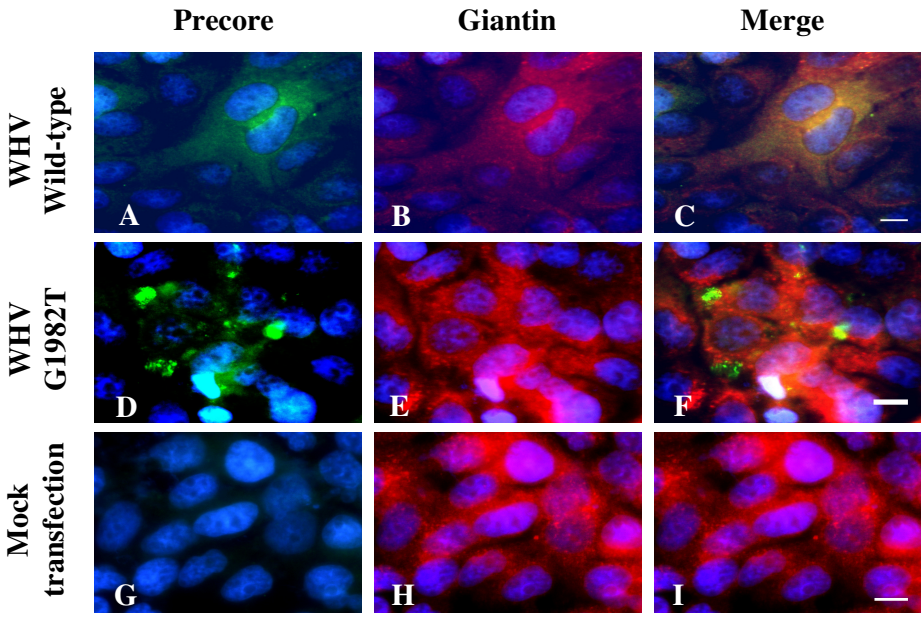

Figure 3.23 WHV G1982T mutant precore/core protein did not accumulate in the Golgi following BFA treatment. Huh7 cells were transfected with WHV plasmid constructs, treated with BFA prior to fixation at 48 hours post-transfection. The cells were subjected to indirect double immunofluorescence staining with antibodies against WHV precore/core protein, detected with secondary antibodies labelled with AlexaFluor 488, shown in green. The Golgi was detected with primary antibodies against giantin and secondary antibodies were labelled with AlexaFluor 546, shown in red. Co-localization of precore/core protein and Golgi can be seen by the yellow color. Nuclei were counterstained with DAPI. Scale bars, 10 μm.

3.5.3 Quality control of HBeAg expression by wild-type and mutant constructs

In order determine whether the quality control machinery within the cells is operative in Huh7 cells transfected with HBV mutant precore/core protein expressing constructs, the cells were stained with antibodies against precore/core protein and against Hsp70, ubiquitin and proteasomes. The distribution of HBV wild-type (Figure 3.24-3.29, A-C) and G1888A mutant precore/core protein (Figure 3.24, 3.26 and 3.28, G-I; Figure 3.25, 3.27 and 3.29, J-L) in the transfected cells were reticular and diffuse. There was no or very low association of Hsp70, ubiquitin and proteasome with wild-type or G1888A precore/core protein as none of three markers co-localized with either the wild-type (Figure 3.24-3.29, A-C) or G1888A mutant precore/core proteins (Figure 3.24, 3.26 and 3.28, G-I; Figure 3.25, 3.27 and 3.29, J-L).

Small aggregates of precore/core protein were formed throughout the cell when the cells were transfected with G1862T (Figure 3.24, 3.26 and 3.28, D; Figure 3.25, 3.27 and 3.29, G) or G1862T/ G1888A mutant constructs (Figure 3.24, 3.26 and 3.28, J; Figure 3.25, 3.27 and 3.29, M). In addition to the small aggregates, unique large perinuclar inclusions were also present in the cells transfected with HBV G1862T (Figure 3.24, 3.26 and 3.28, D-F; Figure 3.25, 3.27 and 3.29, G-I) or G1862T/G1888A mutant construct (Figure 3.24, 3.26 and 3.28, J-L; Figure 3.25, 3.27 and 3.29, M-O). Upon further examination, these large inclusions were found to strongly co-localize with the Hsp70, ubiquitin and proteasome (G1862T: Figure 3.24, 3.26 and 3.28, D-F; Figure 3.25, 3.27 and 3.29, G-I; G1862T/G1888A: Figure 3.24, 3.26 and 3.28, J-L; Figure 3.25, 3.27 and 3.29, M-

O). There was a relatively marked increased in the expression of chaperone Hsp70, ubiquitin and proteasome, found in cells transfected with HBV G1862T or G1862T/G1888A mutant construct as indicated by the solid and bright staining for the three markers (G1862T: Figure 3.24, 3.26 and 3.28, D-F; Figure 3.25, 3.27 and 3.29, G-I; G1862T/G1888A: Figure 3.24, 3.26 and 3.28, J-L; Figure 3.25, 3.27 and 3.29, M-O) when compared to those transfected with wild-type (Figure 3.24-3.29, A-C) or G1888A mutant construct (Figure 3.24, 3.26 and 3.28, G-I; Figure 3.25, 3.27 and 3.29, J-L). Cells transfected with HBV G1896A mutant construct showed the typical nuclear staining and did not co-localize with Hsp70, ubiquitin and proteasome (Figure 3.24, 3.26 and 3.28, M-O; Figure 3.25, 3.27 and 3.29, P-R).

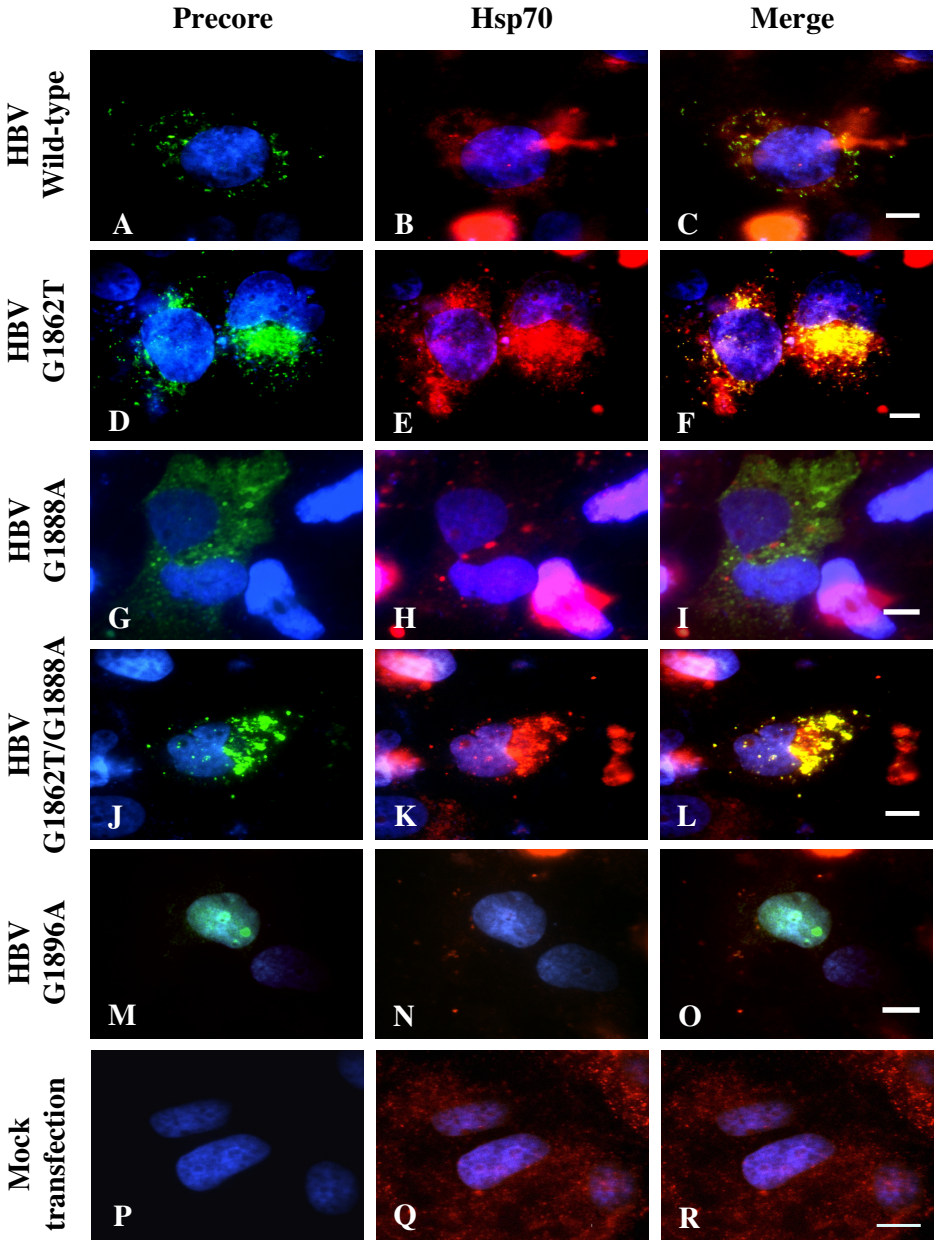

Figure 3.24 Aggresome formed by genotype D HBV G1862T mutant precore/core protein co-localized with molecular chaperone, Hsp70.
Huh7 cells were transfected with genotype D plasmid constructs followed by fixation at 72 hours post-transfection. The cells were subjected to indirect double immunofluorescence staining with antibodies against HBV precore/core protein, detected with secondary antibodies labelled with AlexaFluor 488, shown in green. The molecular chaperone was detected with primary antibodies against Hsp70 and secondary antibodies were labelled with AlexaFluor 546, shown in red. Co-localization of precore/core protein and Hsp70 can be seen by the yellow color. Nuclei were counterstained with DAPI. Scale bars, 10 μm.

Figure 3.25 Aggresome formed by genotype 'A' HBV G1862T mutant precore/core protein co-localized with molecular chaperone, Hsp70. Huh7 cells were transfected with genotype 'A' plasmid constructs followed by fixation at 72 hours post-transfection. The cells were subjected to indirect double immunofluorescence staining with antibodies against HBV precore/core protein, detected with secondary antibodies labelled with AlexaFluor 488, shown in green. The molecular chaperone was detected with primary antibodies against Hsp70 and secondary antibodies were labelled with AlexaFluor 546, shown in red. Co-localization of precore/core protein and Hsp70 can be seen by the yellow color. Nuclei were counterstained with DAPI. Scale bars, 10 μm.

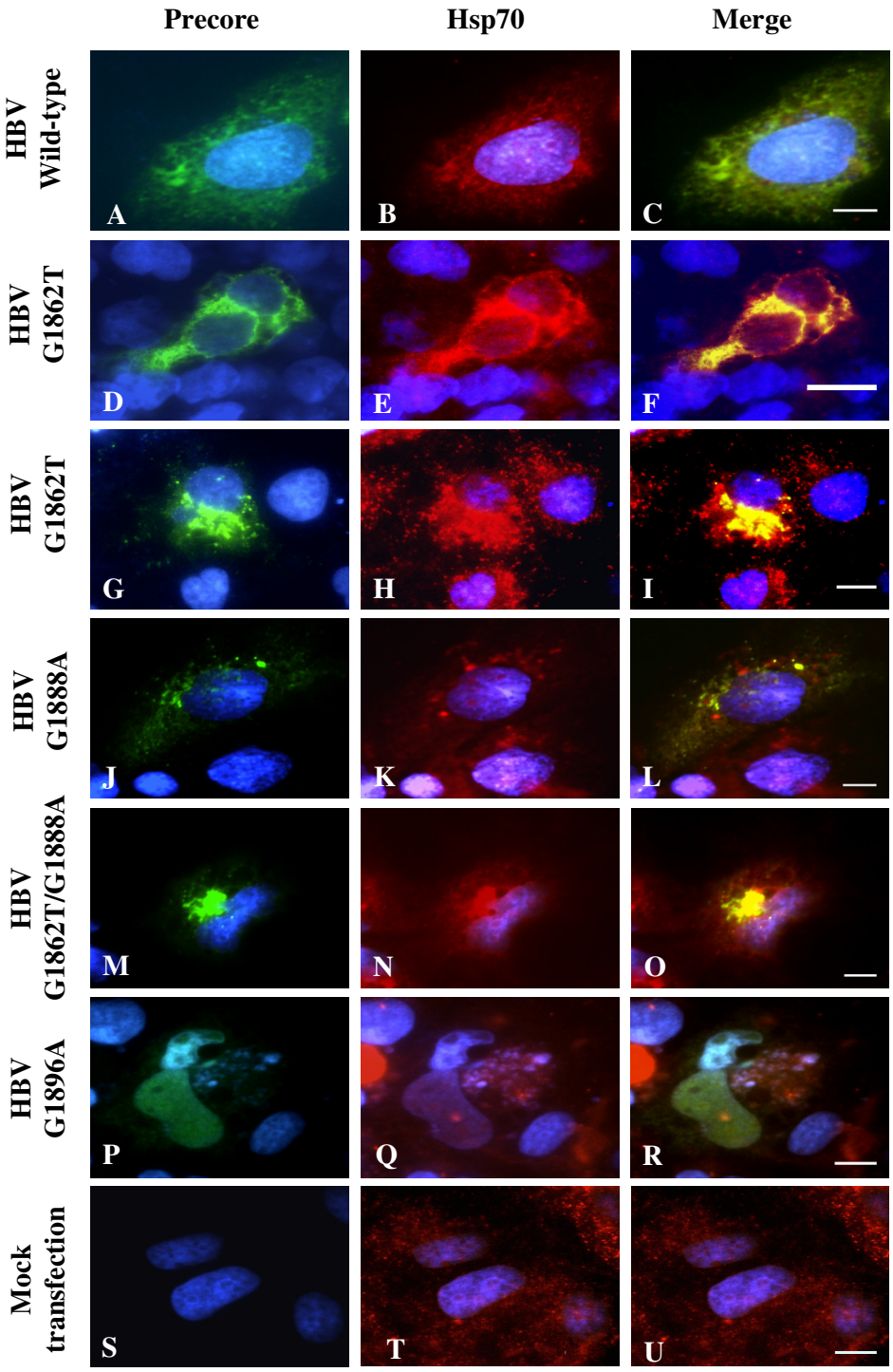
Precore
Hsp70
Merge
HBV Wild-type
HBV G1862T
HBV G1862T
HBV G1888A
HBV G1862T/G1888A
HBV G1896A
Mock transfection
A
B
C
D
E
F
G
H
I
J
K
L
M
N
O
P
Q
R
S
T
U

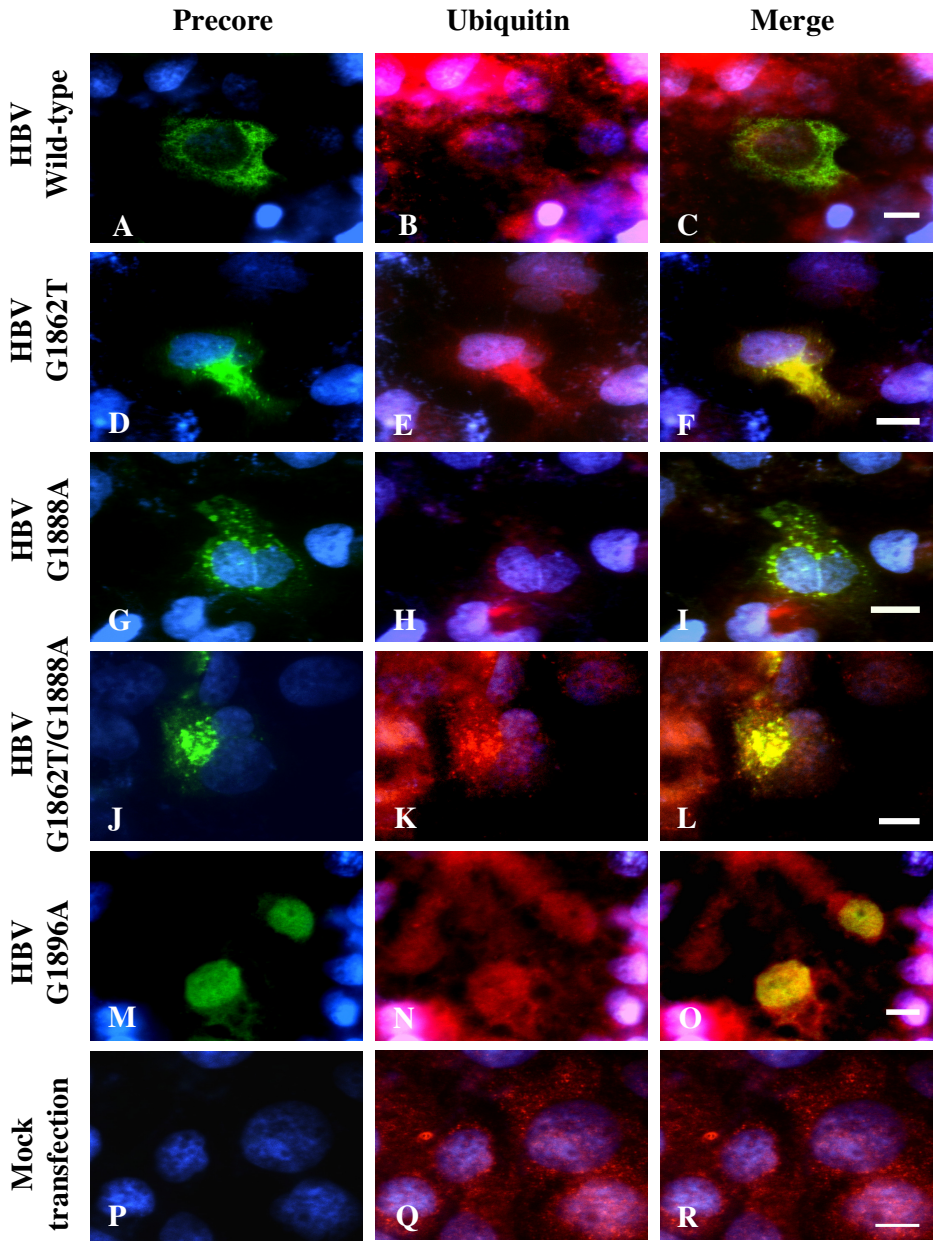

Figure 3.26 Genotype D, HBV G1862T mutant precore/core proteins was ubiquitinated and localized to the aggresome structure. Huh7 cells were transfected with genotype D plasmid constructs followed by fixation at 72 hours post-transfection. The cells were subjected to indirect double immunofluorescence staining with antibodies against HBV precore/core protein, detected with secondary antibodies labelled with AlexaFluor 488, shown in green. The ubiquitin was detected with primary antibodies against ubiquitin and secondary antibodies were labelled with AlexaFluor 546, shown in red. Co-localization of precore/core protein and ubiquitin can be seen by the yellow color. Nuclei were counterstained with DAPI. Scale bars, 10 μm.

Figure 3.27 Genotype 'A', HBV G1862T mutant precore/core protein was ubiquitnated and localized to the aggresome structure. Huh7 cells were transfected with genotype 'A' plasmid constructs followed by fixation at 72 hours post-transfection. The cells were subjected to indirect double immunofluorescence staining with antibodies against HBV precore/core protein, detected with secondary antibodies labelled with AlexaFluor 488, shown in green. The ubiquitin was detected with primary antibodies against ubiquitin and secondary antibodies were labelled with AlexaFluor 546, shown in red. Co-localization of precore/core protein and ubiquitin can be seen by the yellow color. Nuclei were counterstained with DAPI. Scale bars, 10 μm.

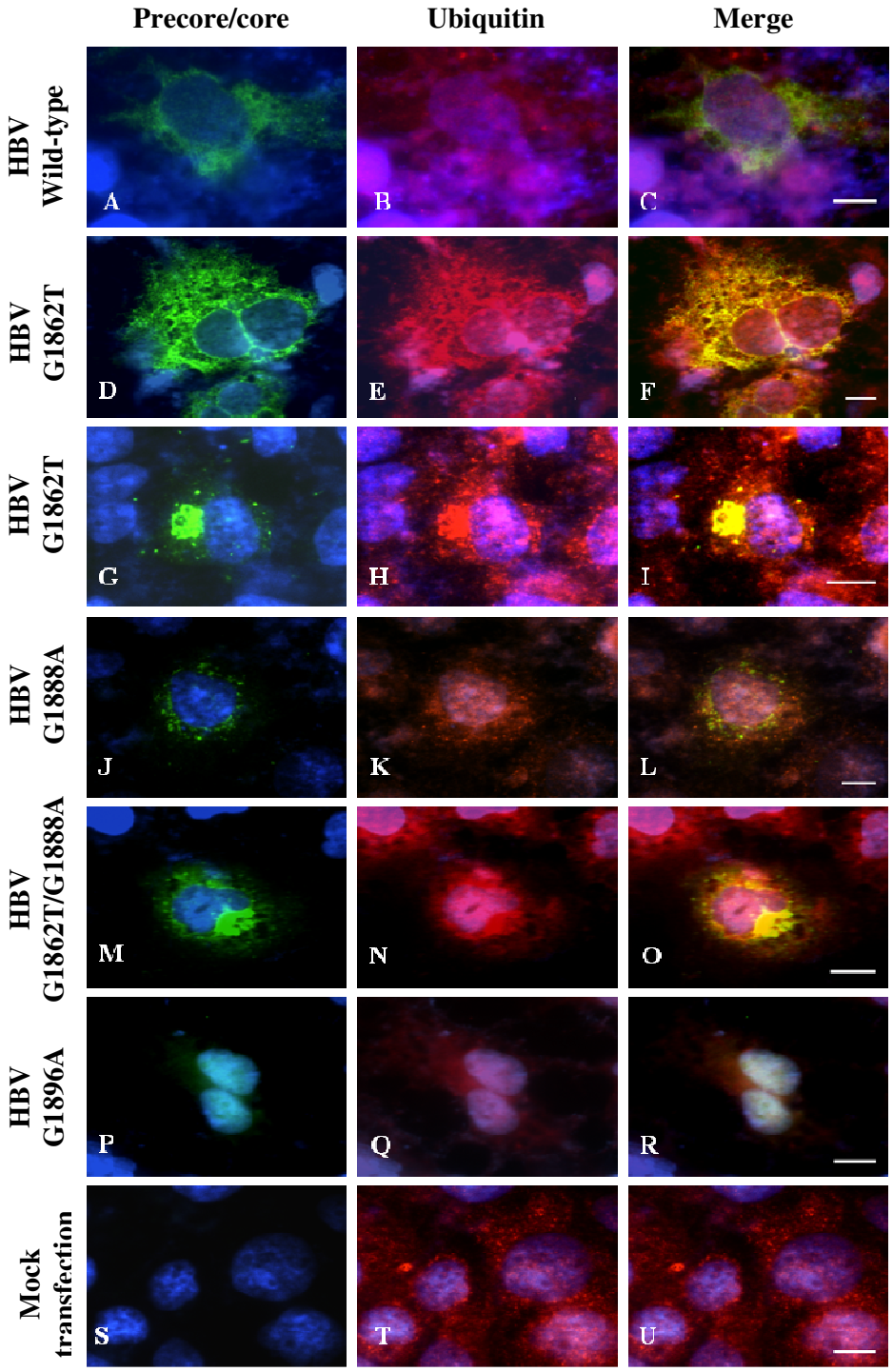
Precore/core
Ubiquitin
Merge
HBV Wild-type
HBV G1862T
HBV G1862T
HBV G1888A
HBV G1862T/G1888A
HBV G1896A
Mock transfection
A
B
C
D
E
F
G
H
I
J
K
L
M
N
O
P
Q
R
S
T
U

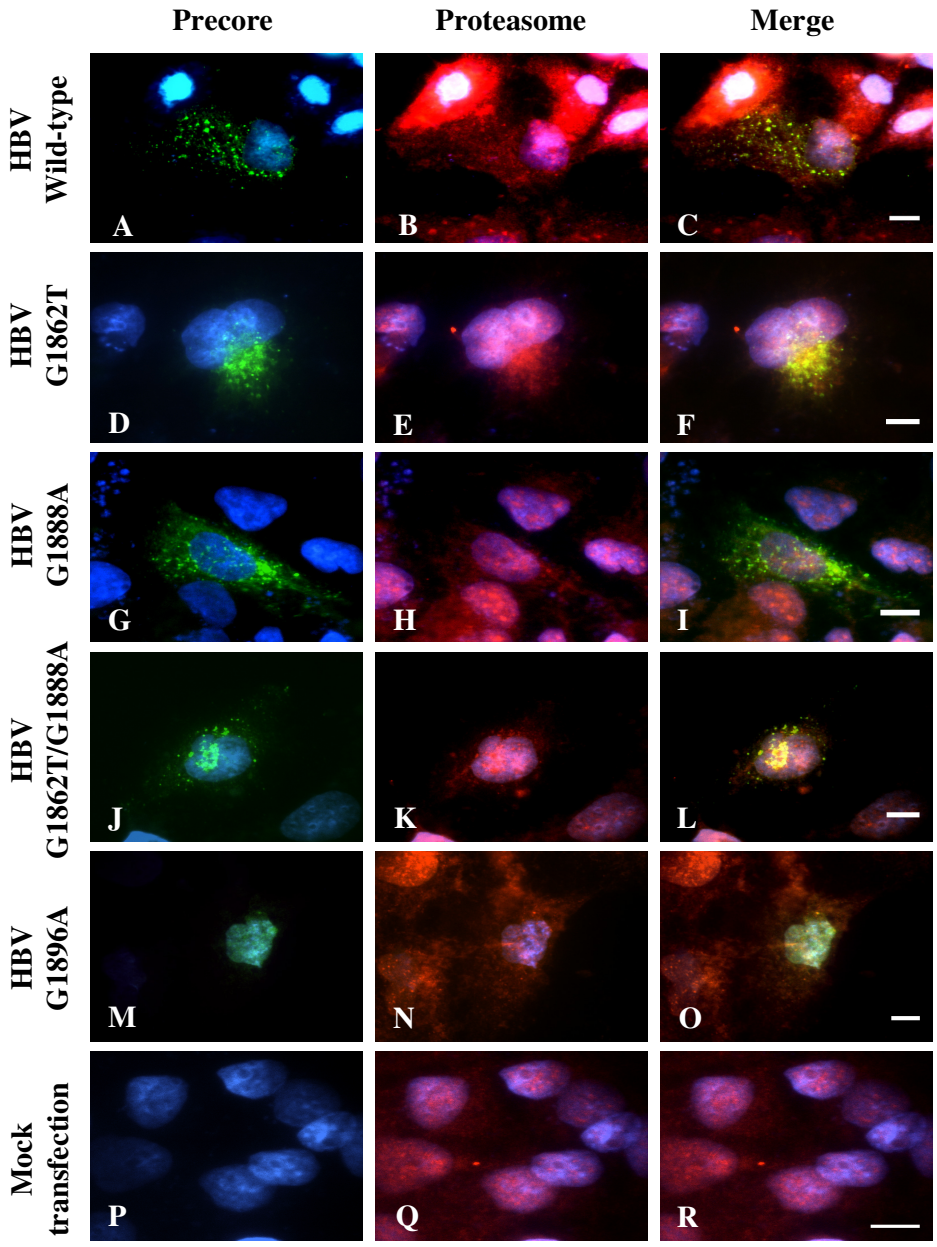

Figure 3.28 Aggresome formed by genotype D HBV G1862T mutant precore/core protein co-localized with proteasome. Huh7 cells were transfected with genotype D plasmid constructs followed by fixation at 72 hours post-transfection. The cells were subjected to indirect double immunofluorescence staining with antibodies against HBV precore/core protein, detected with secondary antibodies labelled with AlexaFluor 488, shown in green. The proteasome was detected with primary antibodies against proteasome and secondary antibodies were labelled with AlexaFluor 546, shown in red. Co-localization of precore/core protein and proteasome can be seen by the yellow color. Nuclei were counterstained with DAPI. Scale bars, 10 μm.

Figure 3.29 Aggresome formed by genotype 'A' HBV G1862T mutant precore/core protein co-localized with proteasome. Huh7 cells were transfected with genotype 'A' plasmid constructs followed by fixation at 72 hours post-transfection. The cells were subjected to indirect double immunofluorescence staining with antibodies against HBV precore/core protein, detected with secondary antibodies labelled with AlexaFluor 488, shown in green. The proteasome was detected with primary antibodies against proteasome and secondary antibodies were labelled with AlexaFluor 546, shown in red. Co-localization of precore/core protein and proteasome can be seen by the yellow color. Nuclei were counterstained with DAPI. Scale bars, 10 μm.

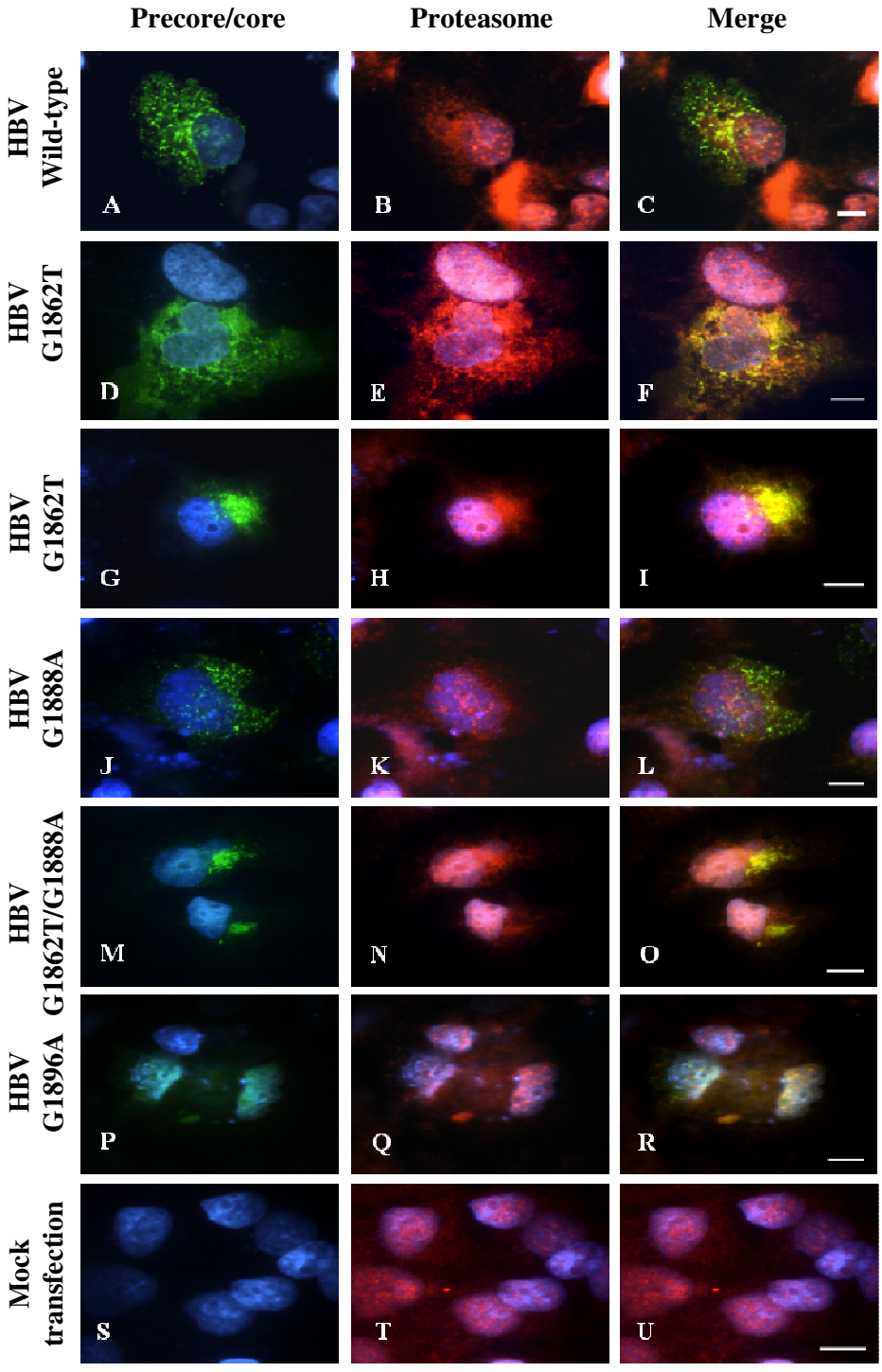
Precore/core
Proteasome
Merge
HBV Wild-type
HBV G1862T
HBV G1862T
HBV G1888A
HBV G1862T/G1888A
HBV G1896A
Mock transfection
A
B
C
D
E
F
G
H
I
J
K
L
M
N
O
P
Q
R
S
T
U

3.5.4.1 Characterization of aggregates formed following transfection with mutant constructs

The formation of aggregates was observed using immunofluorescence confocal microscopy of Huh7 cells transfected with HBV G1862T (Figure 3.24, 3.26 and 3.28, D-F; Figure 3.25, 3.27 and 3.29, G-I) or G1862T1888A mutant construct (Figure 3.24, 3.26 and 3.28, J-L; Figure 3.25, 3.27 and 3.29, M-O) but not in cells transfected with HBV wild-type (Figure 3.24-3.29, A-C) or G1888A construct (Figure 3.24, 3.26 and 3.28, G-I; Figure 3.25, 3.27 and 3.29, J-L). In addition to the wide distribution pattern seen in the cytoplasm (G1862T: Figure 3.25, 3.27 and 3.29, D-F), a more restricted staining pattern of Hsp70, ubiquitin and the proteosome was observed. As shown in Figure 3.24-3.29, Hsp70, ubiquitin and proteasome were confined to the perinuclear region in aggregates that co-localized with the mutant precore/core protein (G1862T: Figure 3.24, 3.26 and 3.28, D-F; Figure 3.25, 3.27 and 3.29, G-I; G1862T/G1888A: Figure 3.24, 3.26 and 3.28, J-L; Figure 3.25, 3.27 and 3.29, M-O) indicative of the formation of aggresomes. Between 15% and 20% of the cells transfected with mutant constructs developed inclusions or aggregates, which rarely occurred in cells transfected with the wild-type constructs.

The investigation was taken further to determine whether the inclusions formed by the HBV G1862T or G1862T G1888A mutant precore/core protein shared other features with aggresomes.

A strong co-localization between the γ-tubulin, a centrosome marker for the MTOC (Dictenberg *et al*, 1998; Wigley *et al*, 1999) and aggresomes formed by the HBV G1862T (Figure 3.30-3.33, D-F), G1862T/G1888A (Figure 3.30-3.33, J-

L) or WHV G1982T (Figure 3.34, D-F) mutant precore/core protein was observed, indicating a close physical relationship between the aggresome and centrosome. Centrioles stained as a distinct bright red spot/dot that was co-localized to the center of aggresomes formed by the HBV G1862T (Figure 3.30-3.33, D-F), G1862T/G1888A (Figure 3.30-3.33, J-L) and WHV G1982T mutant precore/core protein (Figure 3.34, D-F). In contrast cells transfected with HBV wild-type (Figure 3.30-3.33, A-C), G1888A mutant (Figure 3.30-3.33, G-I), or WHV wild-type (Figure 3.34, A-C) constructs showed typical diffused reticular pattern of precore/core protein and there was no co-localization of the γ-tubulin with the wild-type or G1888A precore proteins.

When the cells were stained with antibodies against α–tubulin, it was evident that the microtubule had the normal morphology and was not affected by the formation of aggresome in cells transfected with the HBV G1862T (Figure 3.35-3.38, D-F), G1862T/G1888A (Figure 3.35-3.38, J-L) or WHV G1982T (Figure 3.39, D-F) mutant precore/core constructs. An intact microtubule network is known to be required for the retrograde transport of misfolded proteins to the MTOC and formation of aggresomes (Johnston *et al*, 1998).

Cells expressing HBV wild-type (Figure 3.35-3.38, A-C), G1888A (Figure 3.35-3.38, G-I) or WHV wild-type (Figure 3.39, A-C) precore/core protein showed same reticular distribution pattern of precore/core protein, with the microtubules network remained intact. The microtubule network was also not affected in cells transfected with the HBV G1896A stop codon mutant construct (Figure 3.35-3.38, M-O).

The intermediate filament vimentin, was shown to be re-arranged into condensed fibers forming a ring- or cage like structure around the aggresomes in the cells transfected with HBV G1862T (Figure 3.40-3.43, D-F), G1862T/G1888A (Figure 3.40-3.43, J-L) or WHV G1982T (Figure 3.44, D-F) constructs. This rearrangement did not occur in cells transfected with HBV wild-type (Figure 3.40-3.43, A-C), G1888A (Figure 3.40-3.43, G-I), G1896A (Figure 3.40-3.43, M-O) or WHV wild-type (Figure 3.44, A-C) constructs. Furthermore, another intermediate filament protein, cytokeratin, was also found to be rearranged in a similar fashion to vimentin, forming a halo around the aggresome in cells transfected with HBV G1862T (Figure 3.45-3.48, D-F), G1862T/G1888A (Figure 3.45-3.48, J-L) or WHV G1982T (Figure 3.49, D-F) mutant constructs, but not in cells transfected with the HBV wild-type (Figure 3.45-3.48, A-C), G1888A (Figure 3.45-3.48, G-I), G1896A (Figure 3.45-3.48, M-O) or WHV wild-type (Figure 3.49, A-C) construct.

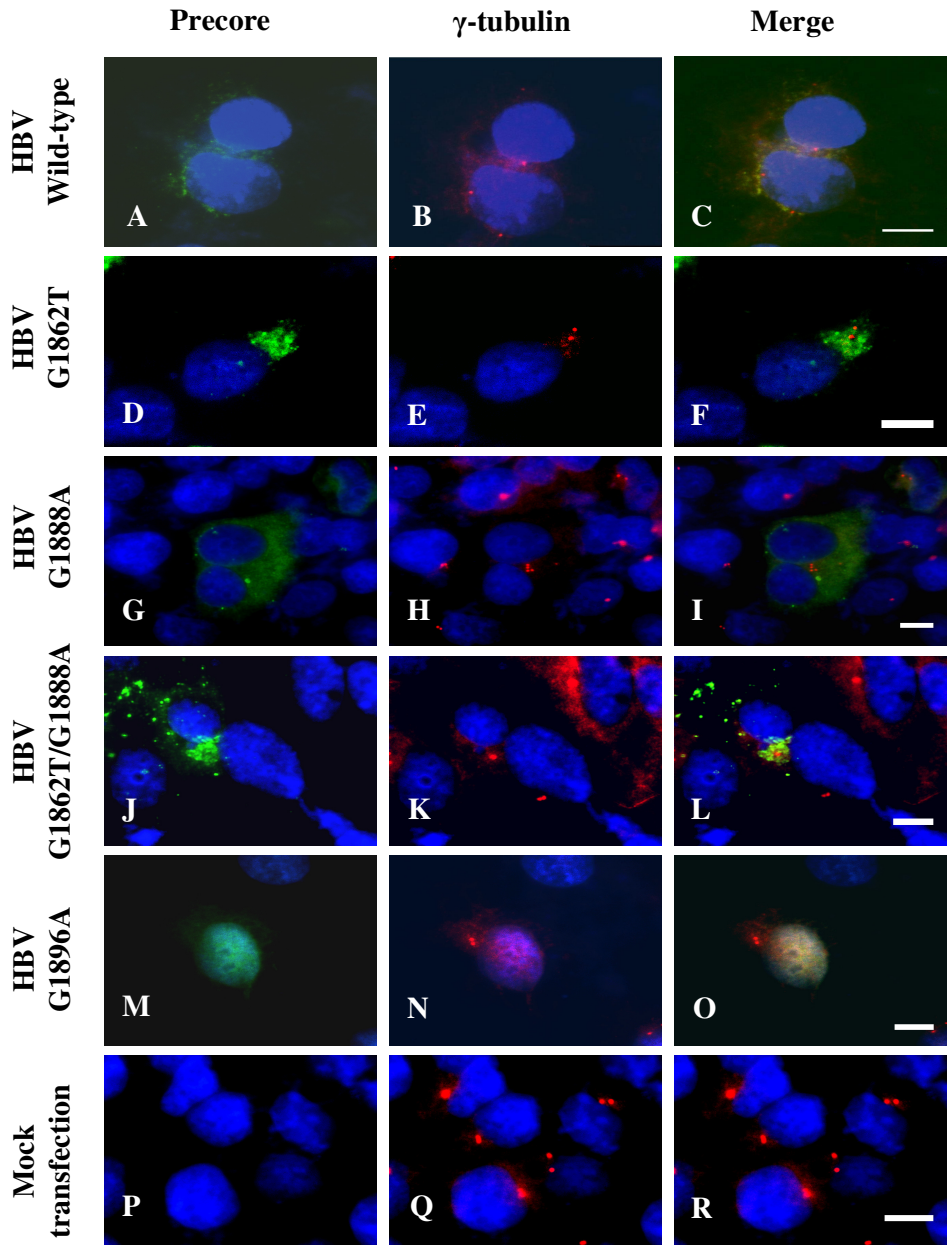

Figure 3.30 Accumulated genotype D HBV G1862T mutant precore/core protein was localized to the microtubule organization center (MTOC) at 48 hours post-transfection. Huh7 cells were transfected with genotype D plasmid constructs followed by fixation at 48 hours post-transfection. The cells were subjected to indirect double immunofluorescence staining with antibodies against HBV precore/core protein, detected with secondary antibodies labelled with AlexaFluor 488, shown in green. The MTOC was detected with primary antibodies against γ-tubulin and secondary antibodies were labelled with AlexaFluor 546, shown in red. Co-localization of precore/core protein and γ-tubulin can be seen by the yellow color. Nuclei were counterstained with DAPI. Scale bars, 10 μm.

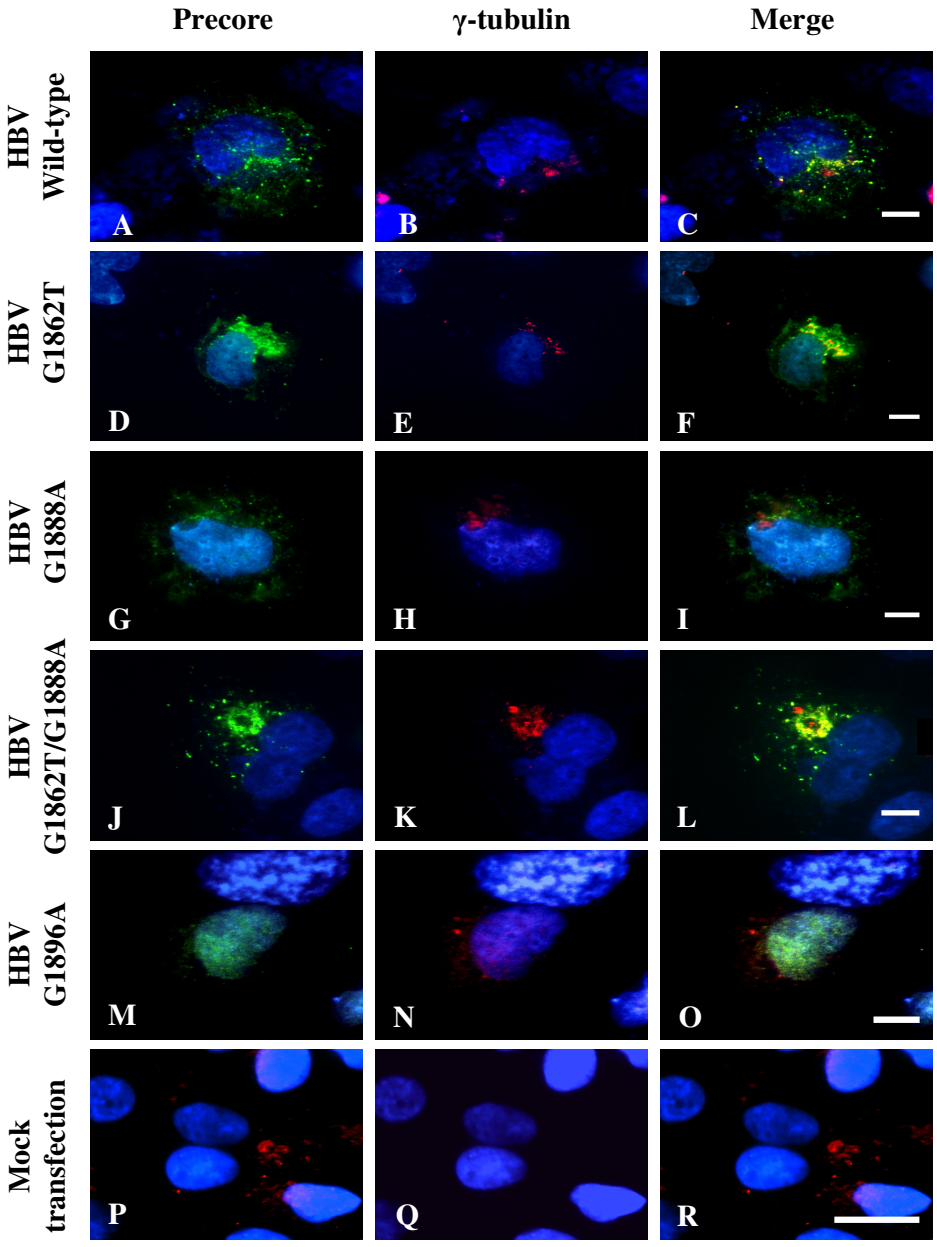

Figure 3.31 Accumulated, genotype D HBV G1862T mutant precore/core protein was localized to the microtubule organization center (MTOC) at 72 hours post-transfection. Huh7 cells were transfected with genotype D plasmid constructs followed by fixation at 72 hours post-transfection. The cells were subjected to indirect double immunofluorescence staining with antibodies against HBV precore/core protein, detected with secondary antibodies labelled with AlexaFluor 488, shown in green. The MTOC was detected with primary antibodies against γ-tubulin and secondary antibodies were labelled with AlexaFluor 546, shown in red. Co-localization of precore/core protein and γ-tubulin can be seen by the yellow color. Nuclei were counterstained with DAPI. Scale bars, 10 μm.

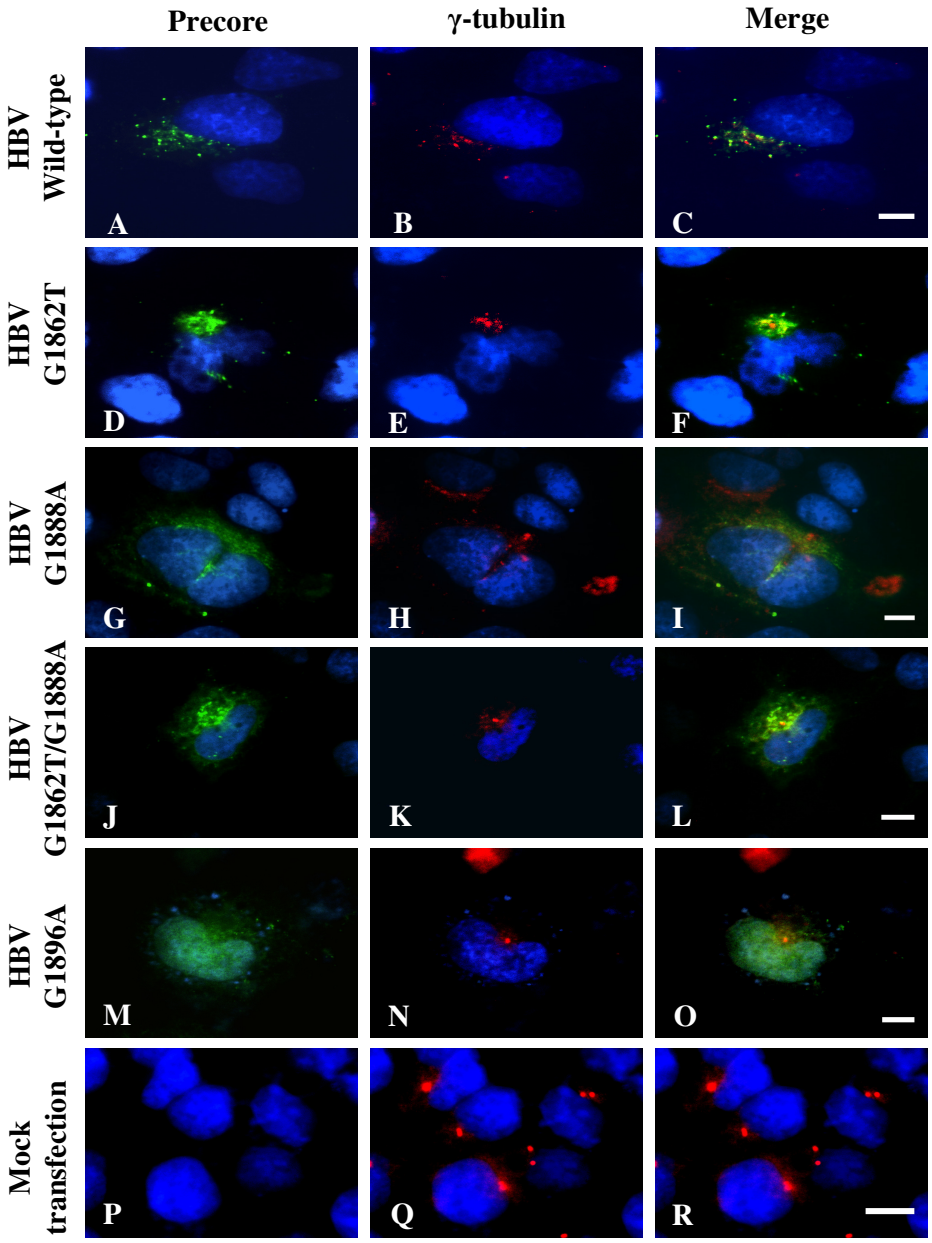

Figure 3.32 Accumulated, genotype 'A' HBV G1862T mutant precore/core protein was localized to the microtubule organization center (MTOC) at 48 hours post-transfection. Huh7 cells were transfected with genotype 'A' plasmid constructs followed by fixation at 48 hours post-transfection. The cells were subjected to indirect double immunofluorescence staining with antibodies against HBV precore/core protein, detected with secondary antibodies labelled with AlexaFluor 488, shown in green. The MTOC was detected with primary antibodies against γ-tubulin and secondary antibodies were labelled with AlexaFluor 546, shown in red. Co-localization of precore/core protein and γ-tubulin can be seen by the yellow color. Nuclei were counterstained with DAPI. Scale bars, 10 μm.

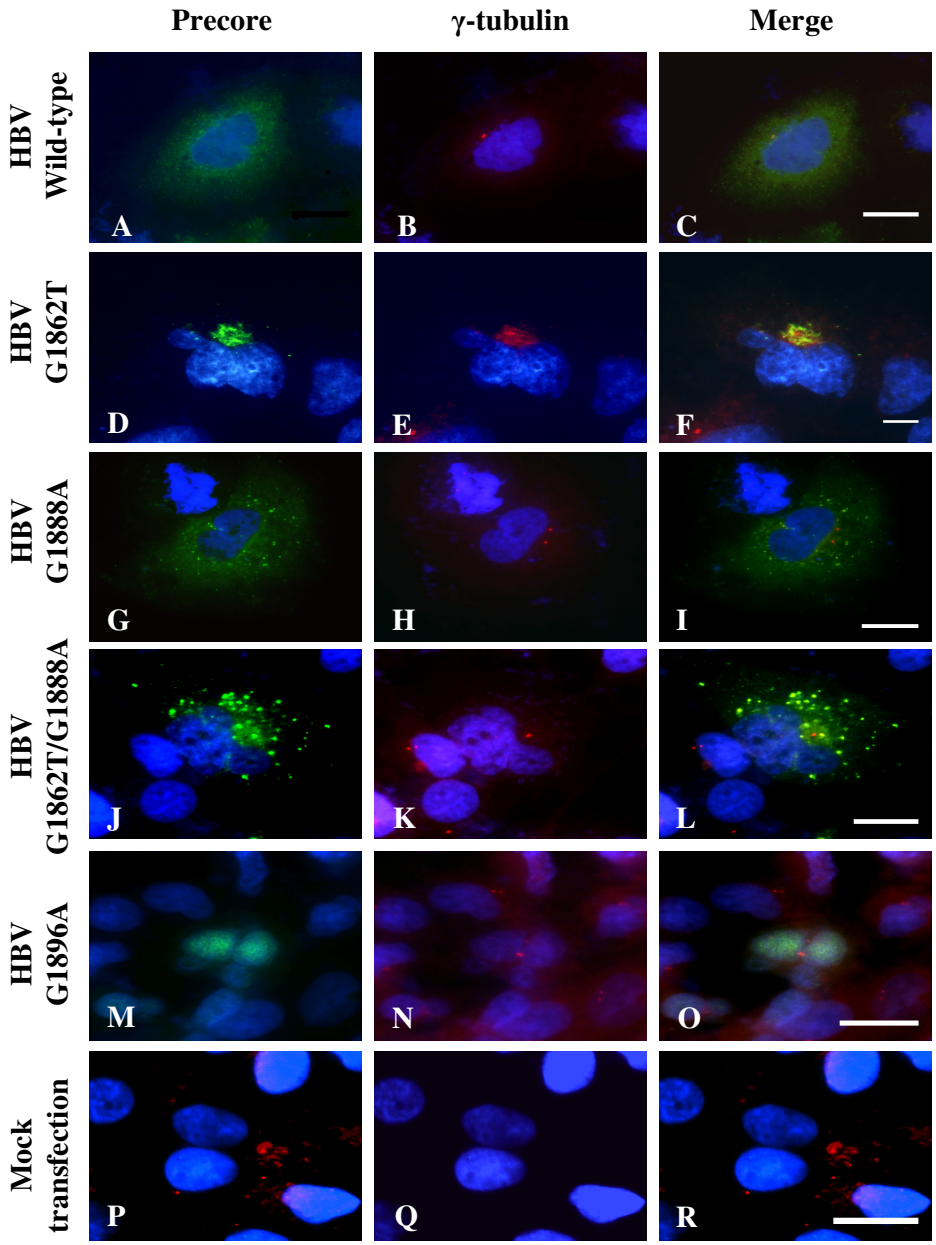

Figure 3.33 Accumulated, genotype 'A' HBV G1862T mutant precore/core protein was localized to the microtubule organization center (MTOC) at 72 hours post-transfection. Huh7 cells were transfected with genotype 'A' plasmid constructs followed by fixation at 72 hours post-transfection. The cells were subjected to indirect double immunofluorescence staining with antibodies against HBV precore/core protein, detected with secondary antibodies labelled with AlexaFluor 488, shown in green. The MTOC was detected with primary antibodies against γ-tubulin and secondary antibodies were labelled with AlexaFluor 546, shown in red. Co-localization of precore/core protein and γ-tubulin can be seen by the yellow color. Nuclei were counterstained with DAPI. Scale bars, 10 μm.

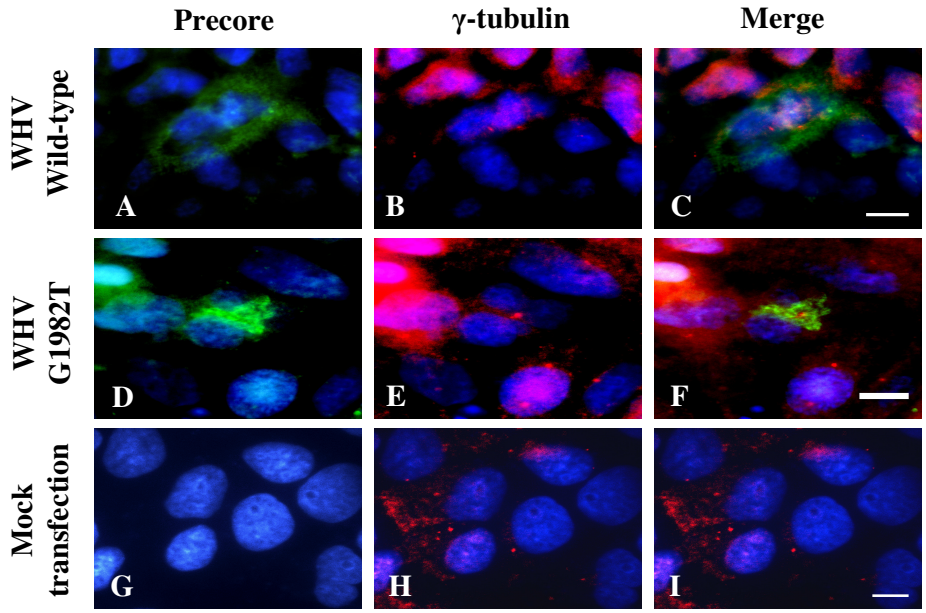

Figure 3.34 Accumulated, WHV G1982T mutant precore/core protein was localized to the microtubule organization center (MTOC) at 48 hours post-transfection. Huh7 cells were transfected with WHV precore/core plasmid constructs followed by fixation at 48 hours-post transfection. The cells were subjected to indirect double immunofluorescence staining with antibodies against WHV precore/core protein, detected with secondary antibodies labelled with AlexaFluor 488, shown in green. The MTOC was detected with primary antibodies against γ-tubulin and secondary antibodies were labelled with AlexaFluor 546, shown in red. Co-localization of precore/core protein and γ-tubulin can be seen by the yellow color. Nuclei were counterstained with DAPI. Scale bars, 10 μm.

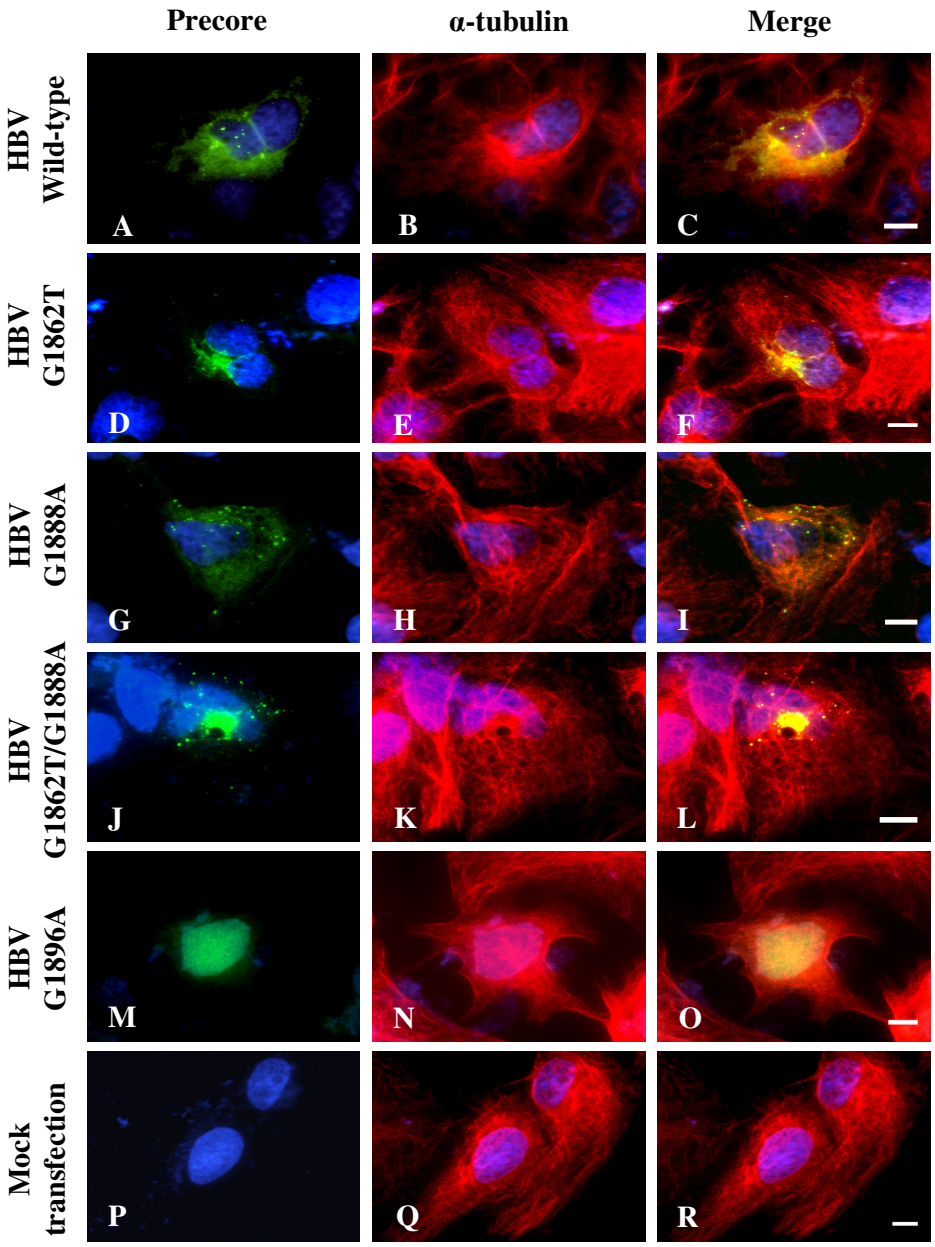

Figure 3.35 Morphology of microtubule network was not affected by the accumulation of genotype D HBV G1862T mutant precore/core protein at 48 hours post-transtection. Huh7 cells were transfected with genotype D plasmid constructs followed by fixation at 48 hours post-transfection. The cells were subjected to indirect double immunofluorescence staining with antibodies against HBV precore/core protein, detected with secondary antibodies labelled with AlexaFluor 488, shown in green. The microtubule network was detected with primary antibodies against α-tubulin and secondary antibodies were labelled with AlexaFluor 546, shown in red. Co-localization of precore/core protein and α-tubulin can be seen by the yellow color. Nuclei were counterstained with DAPI. Scale bars, 10 μm.

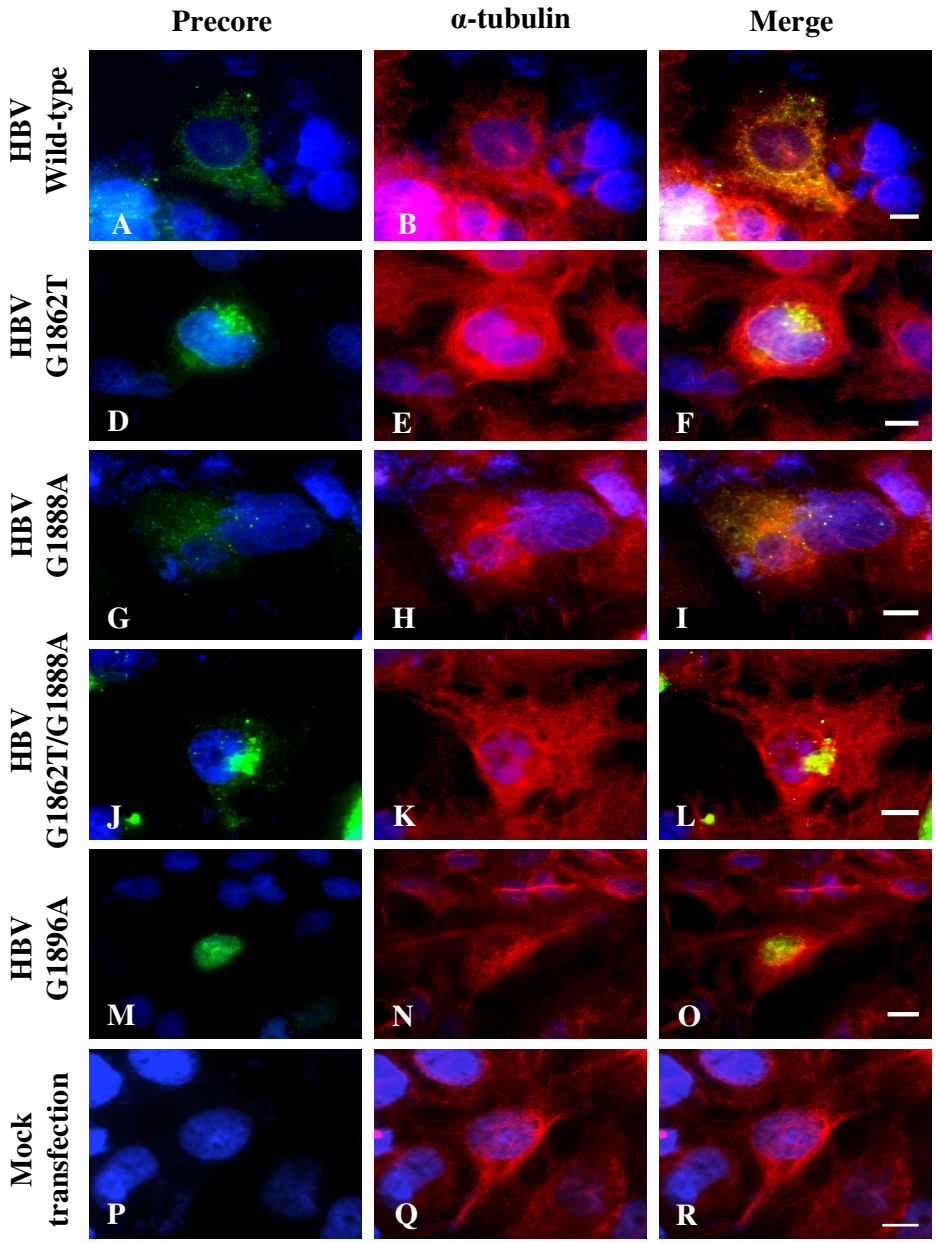

Figure 3.36 Morphology of microtubule network was not affected by the accumulation of genotype D HBV G1862T mutant precore/core protein at 72 hours post-transfection. Huh7 cells were transfected with genotype D plasmid constructs followed by fixation at 72 hours post-transfection. The cells were subjected to indirect double immunofluorescence staining with antibodies against HBV precore/core protein, detected with secondary antibodies labelled with AlexaFluor 488, shown in green. The microtubule network was detected with primary antibodies against α-tubulin and secondary antibodies were labelled with AlexaFluor 546, shown in red. Co-localization of precore/core protein and α-tubulin can be seen by the yellow color. Nuclei were counterstained with DAPI. Scale bars, 10 μm.

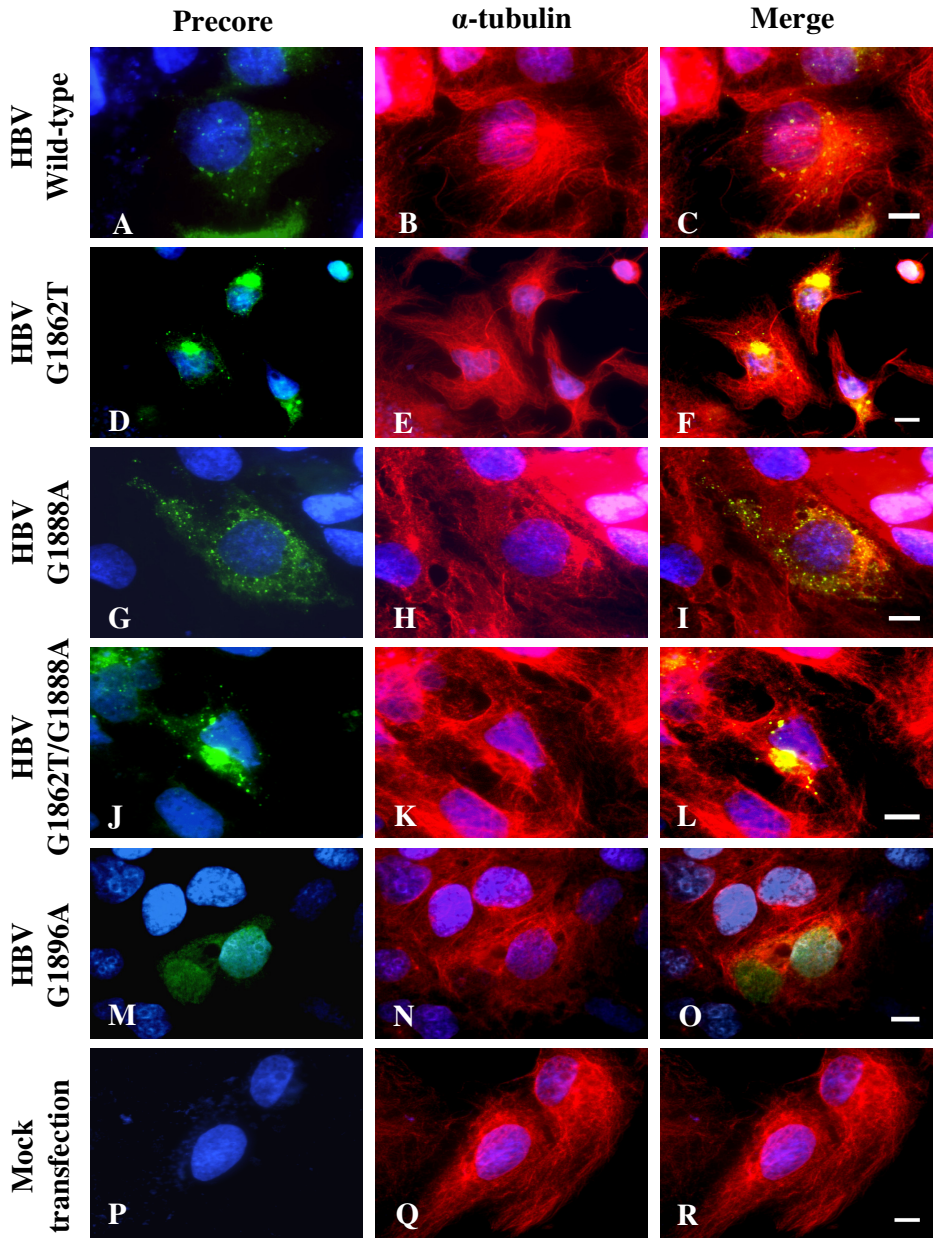

Figure 3.37 Morphology of microtubule network was not affected by the accumulation of genotype 'A' HBV G1862T mutant precore/core protein at 48 hours post-transfection. Huh7 cells were transfected with genotype 'A' plasmid constructs followed by fixation at 48 hours post-transfection. The cells were subjected to indirect double immunofluorescence staining with antibodies against HBV precore/core protein, detected with secondary antibodies labelled with AlexaFluor 488, shown in green. The microtubule network was detected with primary antibodies against α-tubulin and secondary antibodies were labelled with AlexaFluor 546, shown in red. Co-localization of precore/core protein and α-tubulin can be seen by the yellow color. Nuclei were counterstained with DAPI. Scale bars, 10 μm.

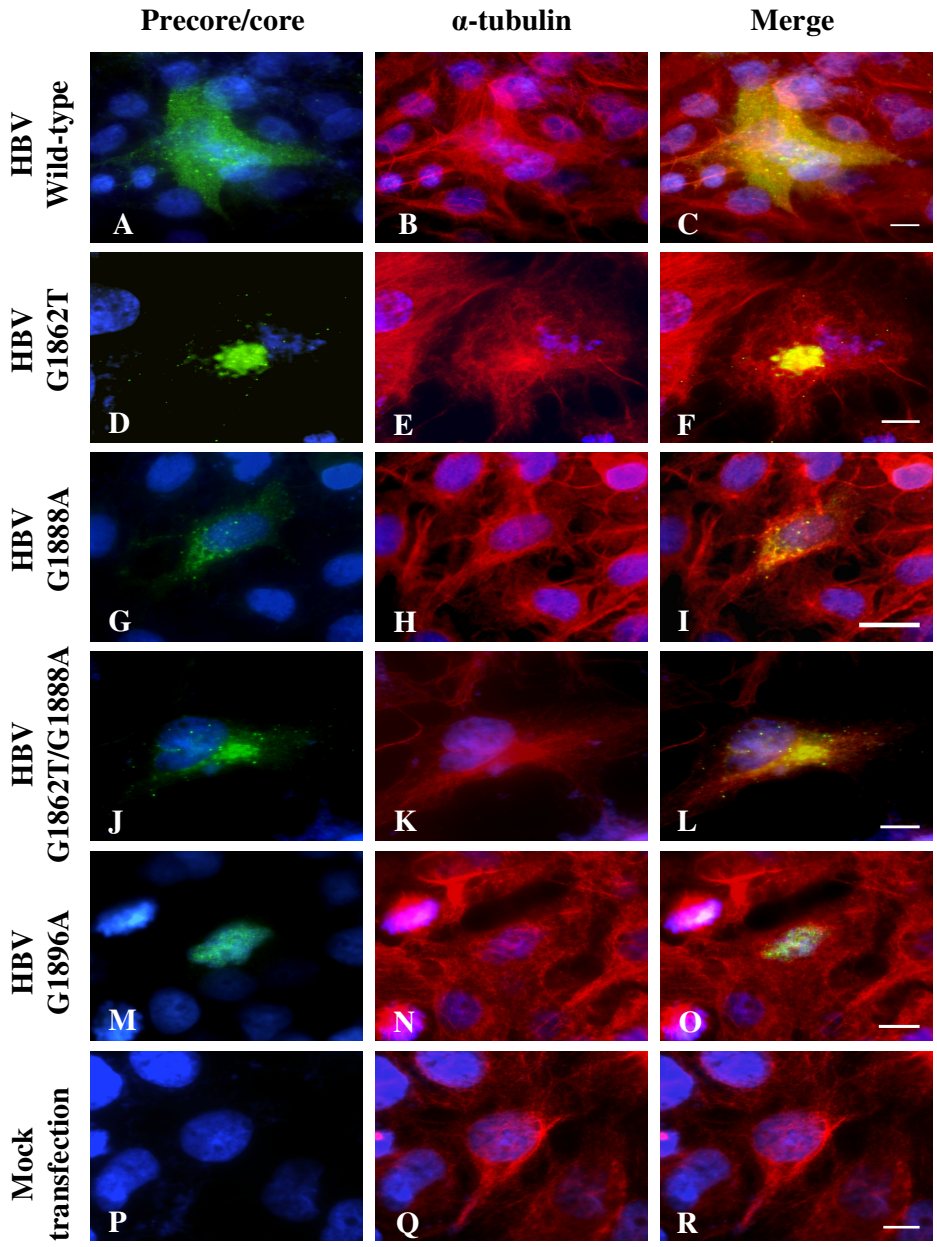

Figure 3.38 Morphology of microtubule network was not affected by the accumulation of genotype 'A' HBV G1862T mutant precore/core protein at 72 hours post-transfection. Huh7 cells were transfected with genotype 'A' plasmid constructs followed by fixation at 72 hours post-transfection. The cells were subjected to indirect double immunofluorescence staining with antibodies against HBV precore/core protein, detected with secondary antibodies labelled with AlexaFluor 488, shown in green. The microtubule network was detected with primary antibodies against α-tubulin and secondary antibodies were labelled with AlexaFluor546, shown in red. Co-localization of precore/core protein and α-tubulin can be seen by the yellow color. Nuclei were counterstained with DAPI. Scale bars, 10 μm.

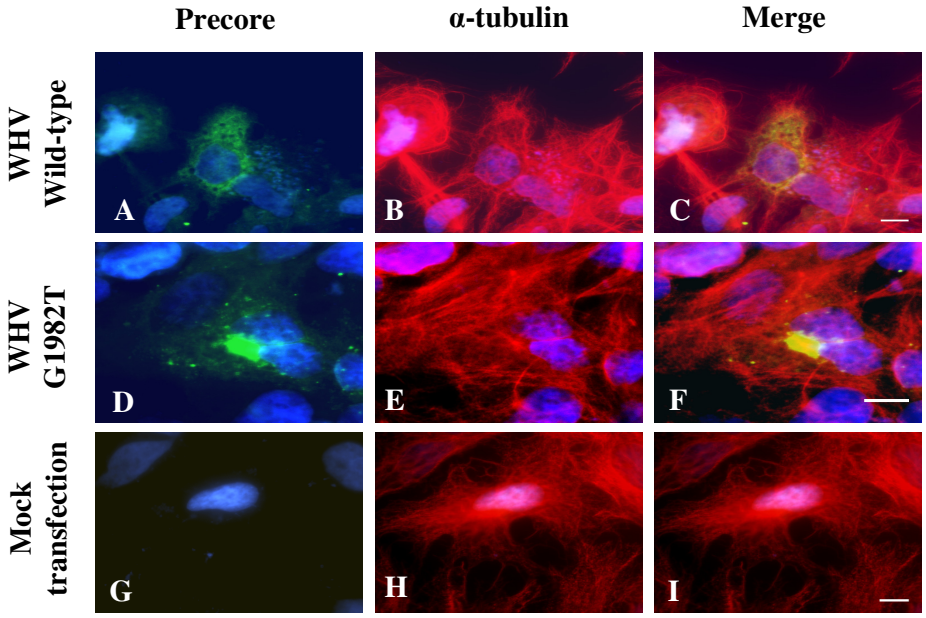

Figure 3.39 Morphology of microtubule network was not affected by the accumulation of WHV G1982T mutant precore/core protein at 48 hours post-transfection. Huh7 cells were transfected with WHV plasmid constructs followed by fixation at 48 hours post-transfection. The cells were subjected to indirect double immunofluorescence staining with antibodies against HBV precore/core protein, detected with secondary antibodies labelled with AlexaFluor 488, shown in green. The microtubule network was detected with primary antibodies against α-tubulin and secondary antibodies were labelled with AlexaFluor 546, shown in red. Co-localization of precore/core protein and α-tubulin can be seen by the yellow color. Nuclei were counterstained with DAPI. Scale bars, 10 μm.

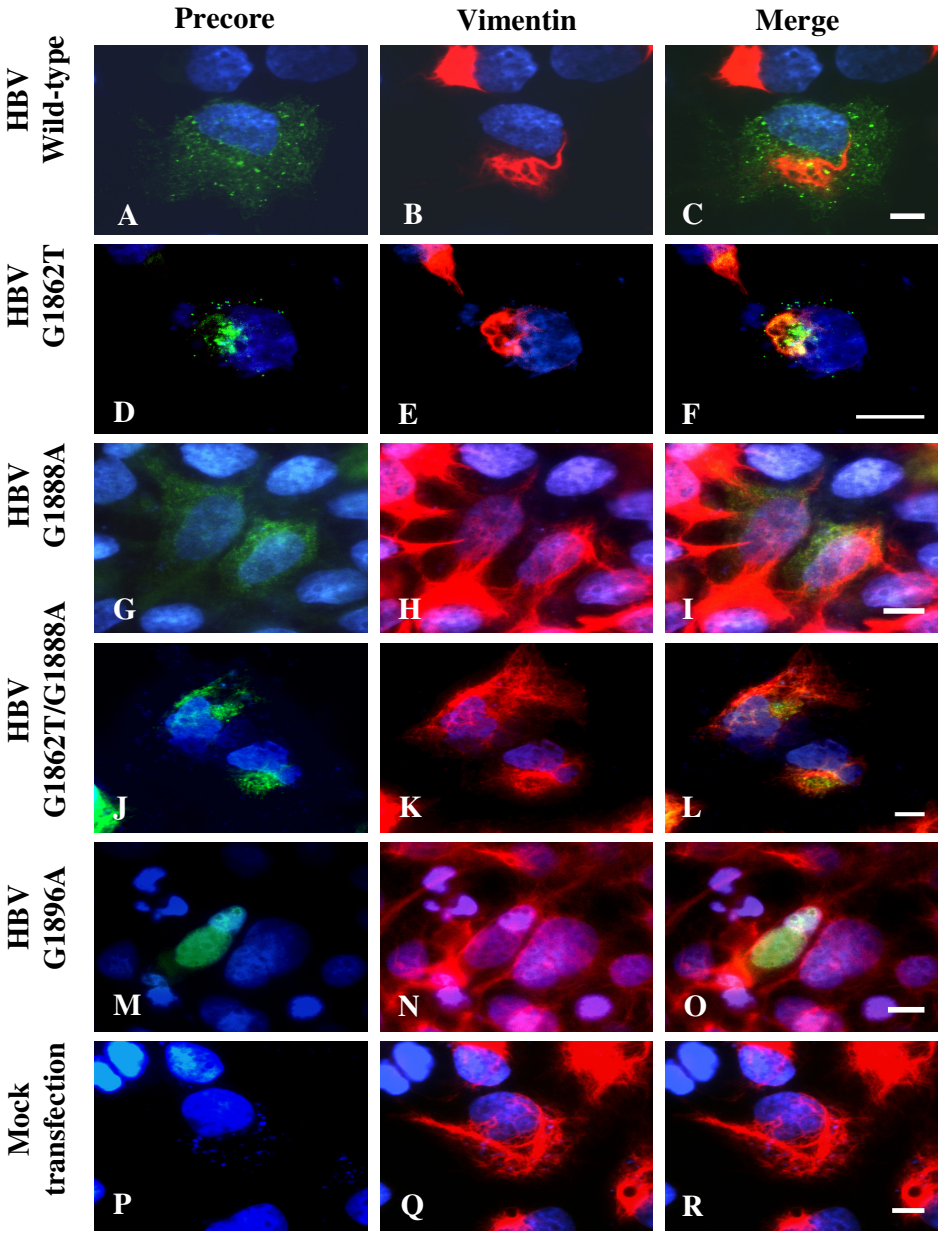

Figure 3.40 The formation of juxtanuclear aggresome by genotype D HBV G1862T precore/core protein was accompanied by a re-organization of the intermediate filament-vimentin at 48 hours post-transfection. Huh7 cells were transfected with genotype D plasmid constructs followed by fixation at 48 hours post-transfection. The cells were subjected to indirect double immunofluorescence staining with antibodies against HBV precore/core protein, detected with secondary antibodies labelled with AlexaFluor 488, shown in green. The intermediate filament was detected with primary antibodies against vimentin and secondary antibodies were labelled with AlexaFluor 546, shown in red. Co-localization of precore/core protein and vimentin can be seen by the yellow color. Nuclei were counterstained with DAPI. Scale bars, 10 μm.

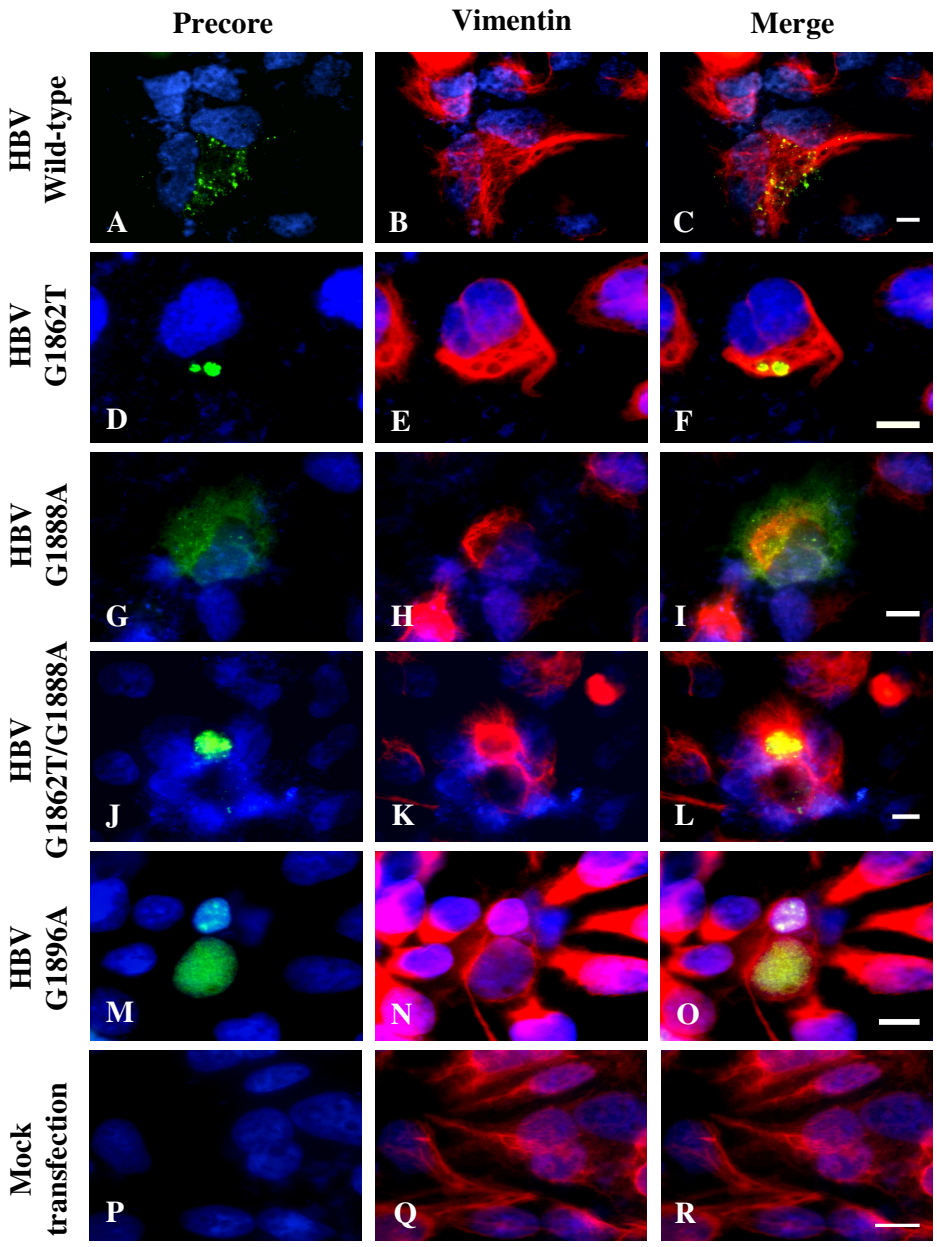

Figure 3.41 The formation of juxtanuclear aggresome by genotype D HBV G1862T precore/core protein was accompanied by a re-organization of the intermediate filament-vimentin at 72 hours post-transfection. Huh7 cells were transfected with genotype D plasmid constructs followed by fixation at 72 hours post-transfection. The cells were subjected to indirect double immunofluorescence staining with antibodies against HBV precore/core protein, detected with secondary antibodies labelled with AlexaFluor 488, shown in green. The intermediate filament was detected with primary antibodies against vimentin and secondary antibodies were labelled with AlexaFluor 546, shown in red. Co-localization of precore/core protein and vimentin can be seen by the yellow color. Nuclei were counterstained with DAPI. Scale bars, 10 μm.

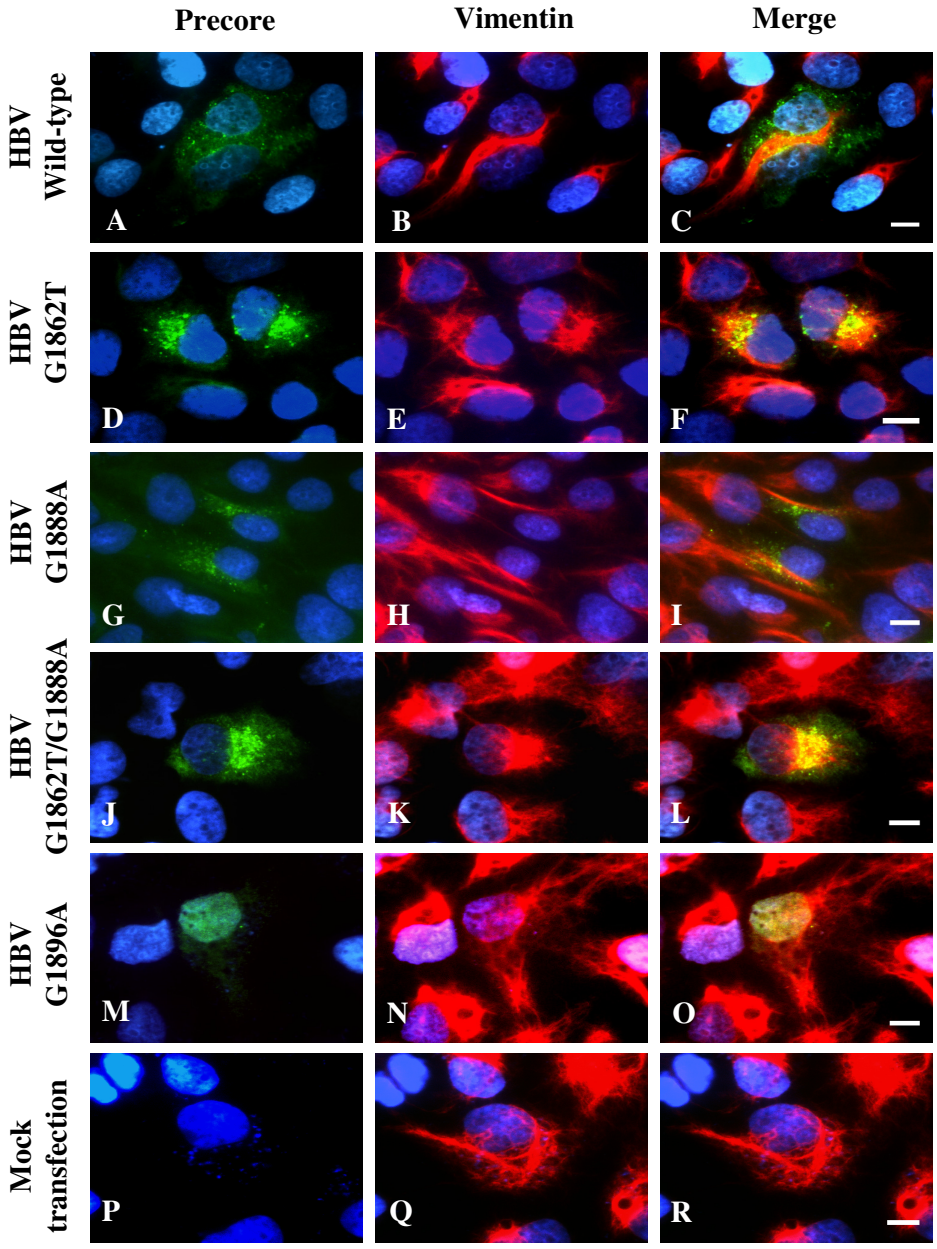

Figure 3.42 The formation of juxtanuclear aggresome by genotype 'A' HBV G1862T precore/core protein was accompanied by a re-organization of the intermediate filament-vimentin at 48 hours post-transfection. Huh7 cells were transfected with genotype 'A' plasmid constructs followed by fixation at 48 hours post-transfection. The cells were subjected to indirect double immunofluorescence staining with antibodies against HBV precore/core protein, detected with secondary antibodies labelled with AlexaFluor 488, shown in green. The intermediate filament was detected with primary antibodies against vimentin and secondary antibodies were labelled with AlexaFluor 546, shown in red. Co-localization of precore/core protein and vimentin can be seen by the yellow color. Nuclei were counterstained with DAPI. Scale bars, 10 μm.

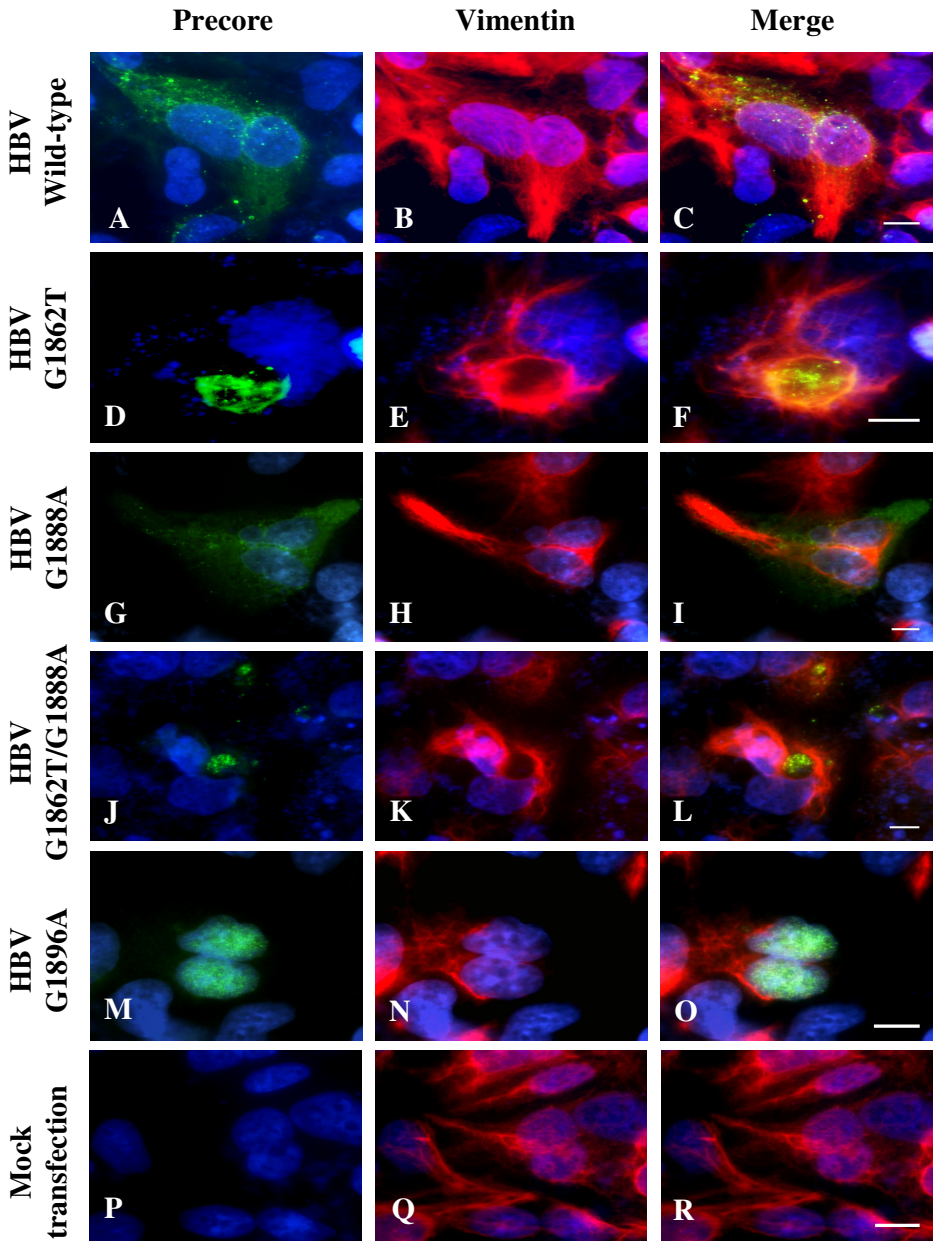

Figure 3.43 The formation of juxtanuclear aggresome by genotype 'A' HBV G1862T precore/core protein was accompanied by a re-organization of the intermediate filament-vimentin at 72 hours post-transfection. Huh7 cells were transfected with genotype 'A' plasmid constructs followed by fixation at 72 hour post-transfection. The cells were subjected to indirect double immunofluorescence staining with antibodies against HBV precore/core protein, detected with secondary antibodies labelled with AlexaFluor 488, shown in green. The intermediate filament was detected with primary antibodies against vimentin and secondary antibodies were labelled with AlexaFluor 546, shown in red. Co-localization of precore/core protein and vimentin can be seen by the yellow color. Nuclei were counterstained with DAPI. Scale bars, 10 μm.

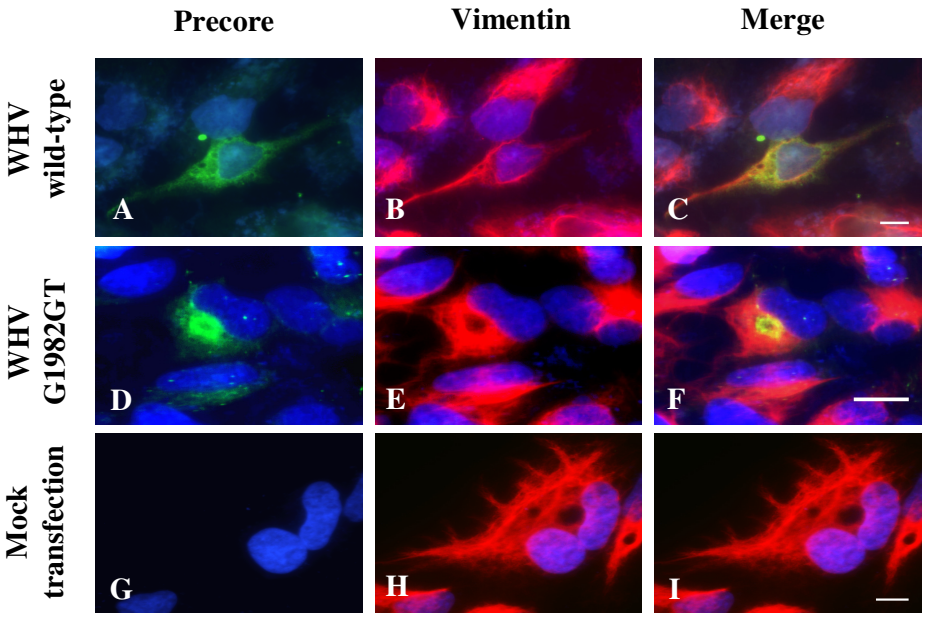

Figure 3.44 The formation of juxtanuclear aggresome by WHV G1982T precore/core protein was accompanied by a re-organization of the intermediate filament-vimentin at 48 hours post-transfection. Huh7 cells were transfected with WHV plasmid constructs followed by fixation at 48 hours post-transfection. The cells were subjected to indirect double immunofluorescence staining with antibodies against WHV precore/core protein, detected with secondary antibodies labelled with AlexaFluor 488, shown in green. The intermediate filament was detected with primary antibodies against vimentin and secondary antibodies were labelled with AlexaFluor 546, shown in red. Co-localization of precore/core protein and vimentin can be seen by the yellow color. Nuclei were counterstained with DAPI. Scale bars, 10 μm.

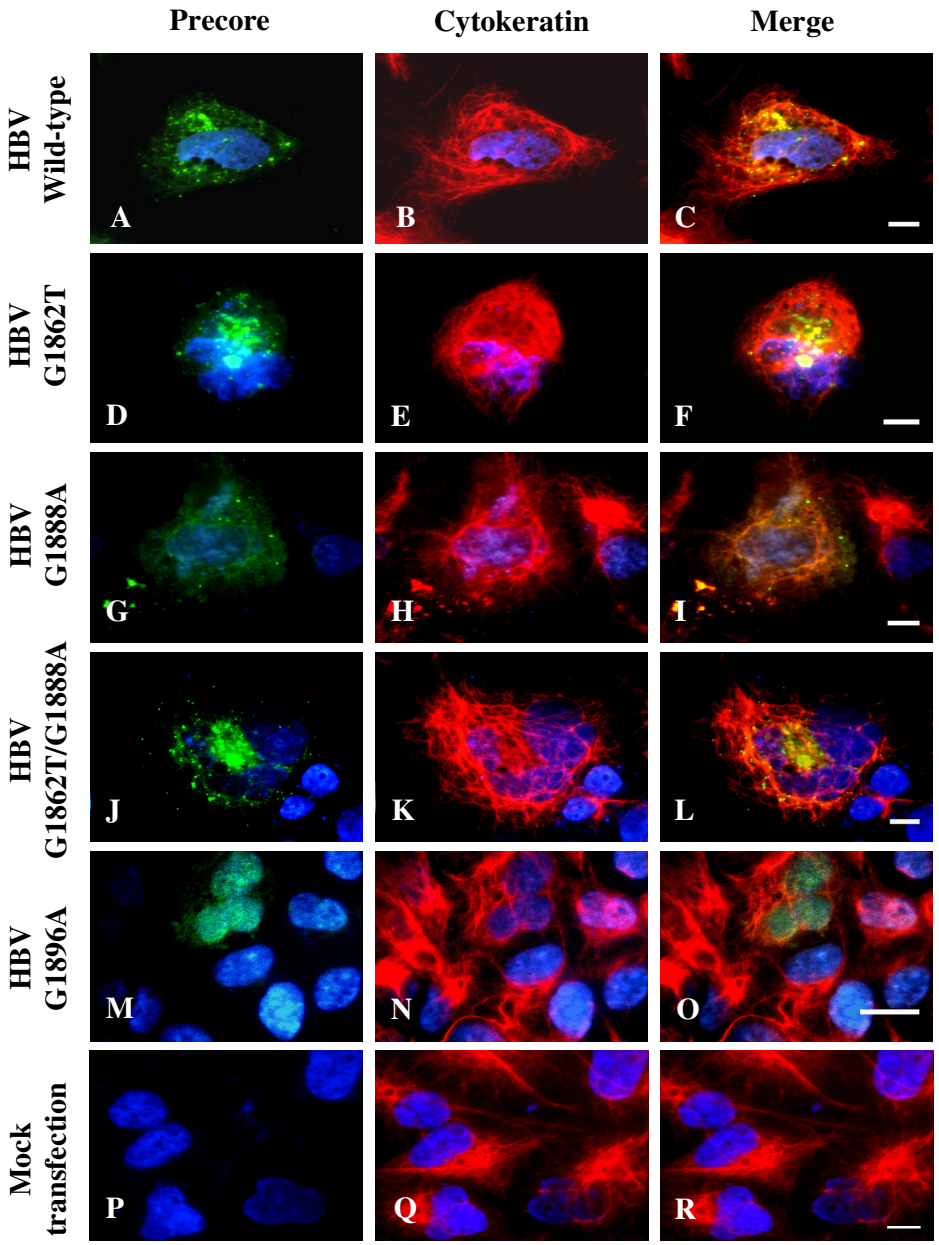

Figure 3.45 Aggresome formed by genotype D HBV G1862T precore/core protein also resulted in the rearrangement of another family of intermediate filament-cytokeratin at 48 hours post-transfection. Huh7 cells were transfected with genotype D plasmid constructs followed by fixation at 48 hours post-transfection. The cells were subjected to indirect double immunofluorescence staining with antibodies against HBV precore/core protein, detected with secondary antibodies labelled with AlexaFluor 488, shown in green. The intermediate filament was detected with primary antibodies against pan cytokeratin and secondary antibodies were labelled with AlexaFluor 546, shown in red. Co-localization of precore/core protein and cytokeratin can be seen by the yellow color. Nuclei were counterstained with DAPI. Scale bars, 10 μm.

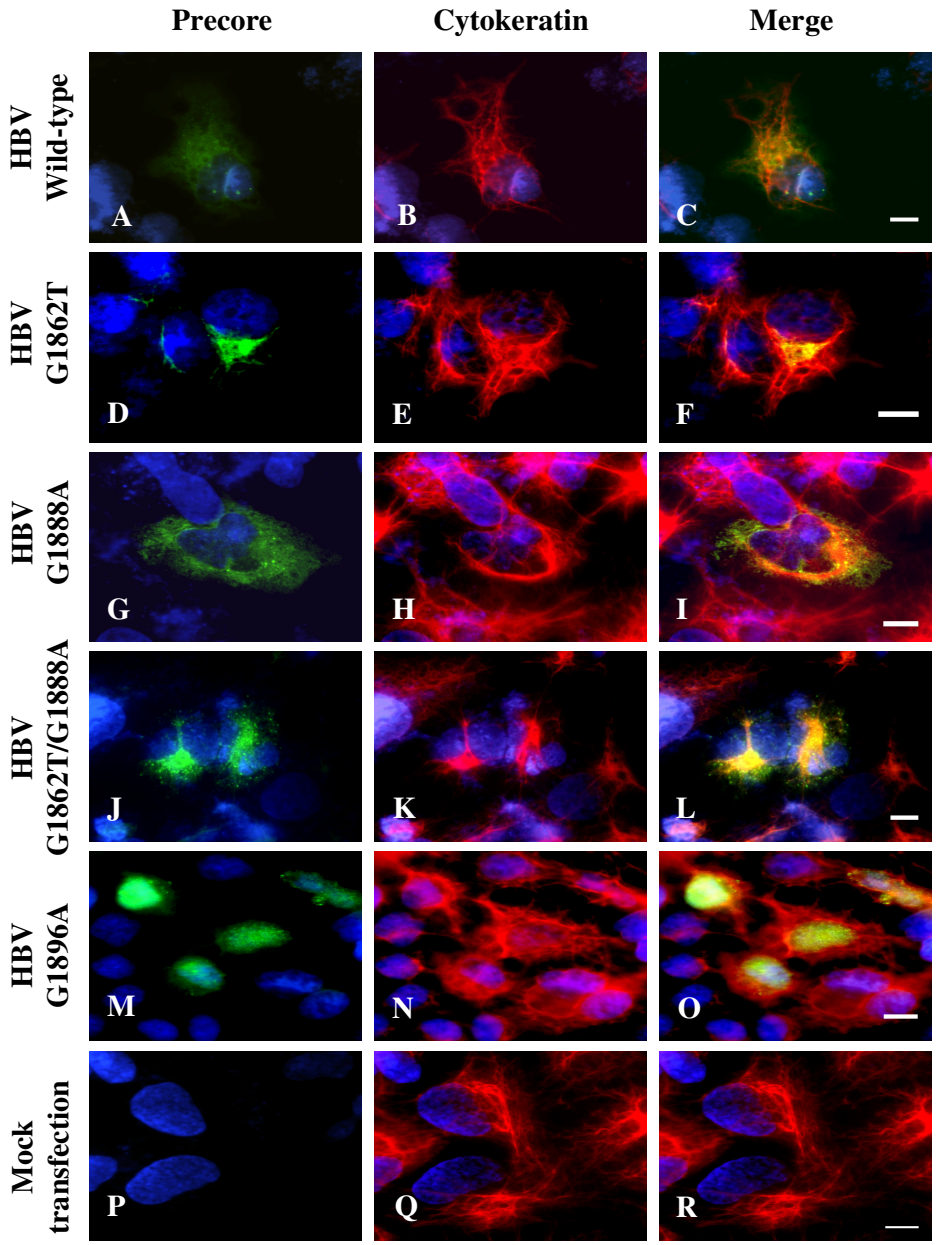

Figure 3.46 Aggresome formed by genotype D HBV G1862T precore/core protein also resulted in the rearrangement of another family of intermediate filament-cytokeratin at 72 hous post-transfeciton. Huh7 cells were transfected with genotype D plasmid constructs followed by fixation at 72 hours post-transfection. The cells were subjected to indirect double immunofluorescence staining with antibodies against HBV precore/core protein, detected with secondary antibodies labelled with AlexaFluor 488, shown in green. The intermediate filament was detected with primary antibodies against pan cytokeratin and secondary antibodies were labelled with AlexaFluor 546, shown in red. Co-localization of precore/core protein and cytokeratin can be seen by the yellow color. Nuclei were counterstained with DAPI. Scale bars, 10 μm.

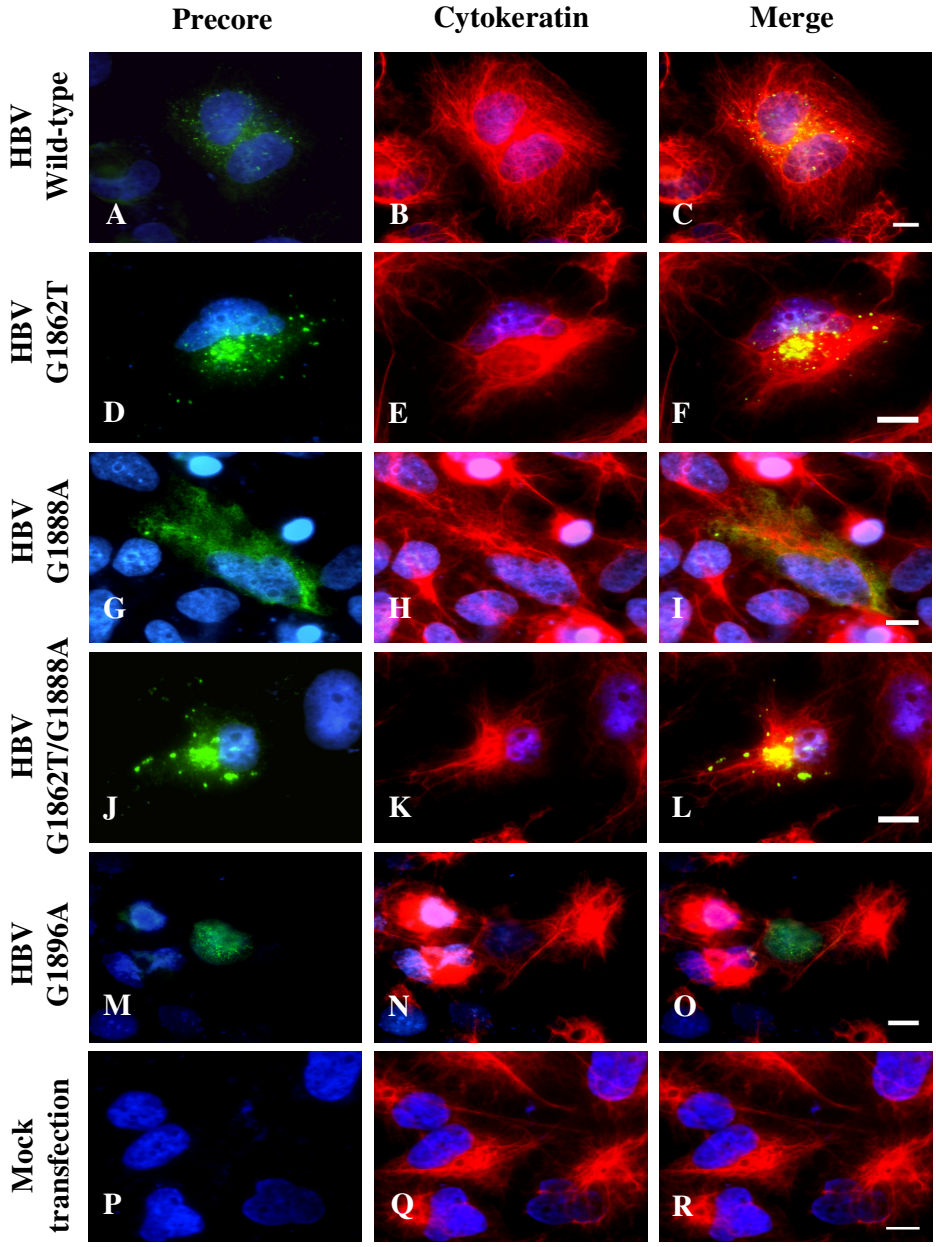

Figure 3.47 Aggresome formed by genotype 'A' HBV G1862T precore/core protein also resulted in the rearrangement of another family of intermediate filament-cytokeratin at 48 hours post-transfection. Huh7 cells were transfected with genotype 'A' plasmid constructs followed by fixation at 48 hours post-transfection. The cells were subjected to indirect double immunofluorescence staining with antibodies against HBV precore/core protein, detected with secondary antibodies labelled with AlexaFluor 488, shown in green. The intermediate filament was detected with primary antibodies against pan cytokeratin and secondary antibodies were labelled with AlexaFluor 546, shown in red. Co-localization of precore/core protein and cytokeratin can be seen by the yellow color. Nuclei were counterstained with DAPI. Scale bars, 10 μm.

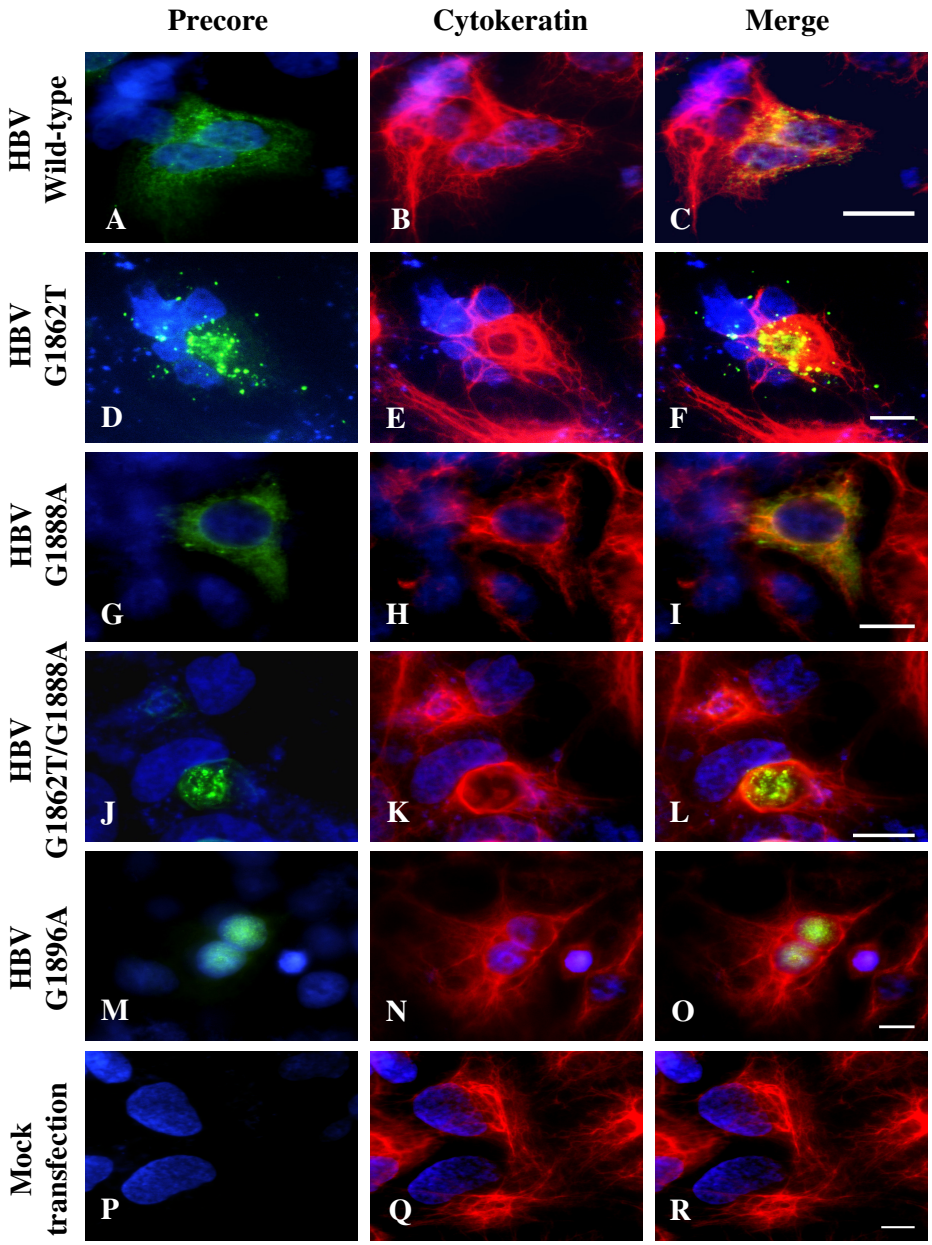

Figure 3.48 Aggresome formed by genotype 'A' HBV G1862T precore/core protein also resulted in the rearrangement of another family of intermediate filament-cytokeratin at 72 hours post-transfection. Huh7 cells were transfected with genotype 'A' plasmid constructs followed by fixation at 72 hours post-transfection. The cells were subjected to indirect double immunofluorescence staining with antibodies against HBV precore/core protein, detected with secondary antibodies labelled with AlexaFluor 488, shown in green. The intermediate filament was detected with primary antibodies against pan cytokeratin and secondary antibodies were labelled with AlexaFluor 546, shown in red. Co-localization of precore/core protein and cytokeratin can be seen by the yellow color. Nuclei were counterstained with DAPI. Scale bars, 10 μm.

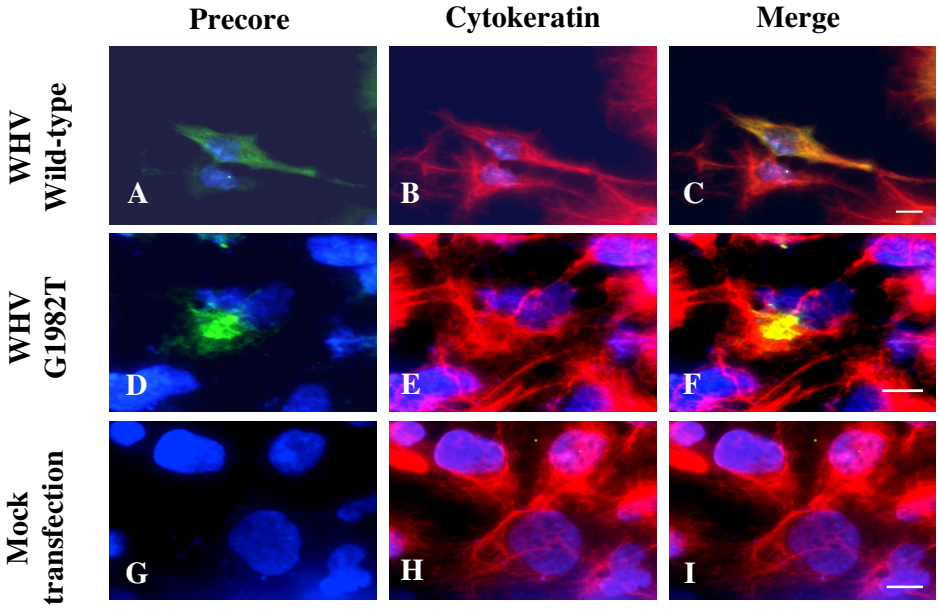

Figure 3.49 Aggresome formed by WHV G1982T precore/core protein also resulted in the rearrangement of another family of intermediate filament-cytokeratin at 48 hours post-transfection. Huh7 cells were transfected with WHV plasmid constructs followed by fixation at 48 hours post-transfection. The cells were subjected to indirect double immunofluorescence staining with antibodies against WHV precore/core protein, detected with secondary antibodies labelled with AlexaFluor 488, shown in green. The intermediate filament was detected with primary antibodies against pan cytokeratin and secondary antibodies were labelled with AlexaFluor 546, shown in red. Co-localization of precore/core protein and cytokeratin can be seen by the yellow color. Nuclei were counterstained with DAPI. Scale bars, 10 μm.

3.5.4.2 Effect of proteasome inhibitor on the aggresome formation

To evaluate the effect of cellular stress on aggresome formation in cells expressing the wild-type or mutant precore/core mutants, transfected cells were incubated with the proteasome inhibitor, MG132. When cells transfected with wild-type constructs were treated with MG132, there was a relatively small increase in the expression of precore/core protein when compared to untreated cells. The increase was more pronounced when the cells were transfected with HBV G1862T (Figure 3.50-3.55, D-F) or G1862T/G1888A (Figure 3.50-3.55, J-L) constructs. There was in addition an increase in the size and fluorescent intensity of the aggresomes formed in the cells treated with MG132. Concomitantly, the expression of Hsp70, ubiquitin and proteasome, which co-localize with aggresomes, was also increased when Huh 7 cells transfected with HBV G1862T (Figure 3.50-3.55, D-F) or G1862T/G1888A (Figure 3.50-3.55, J-L) constructs, were treated with MG132. A single, large, juxtanuclear aggresome impinged on the nuclear envelope causing its distortion. Reniform nuclei were observed in the cells transfected with HBV G1862T precore/core constructs at 72 hr post-transfection following MG132 treatment (Figure 3.50-3.55, D-F), G1862T/G1888A (Figure 3.50-3.55, J-L). The distortion of the nuclear envelope has been shown to be a unique feature of cells bearing single, large aggresomes (Johnston, 1998).

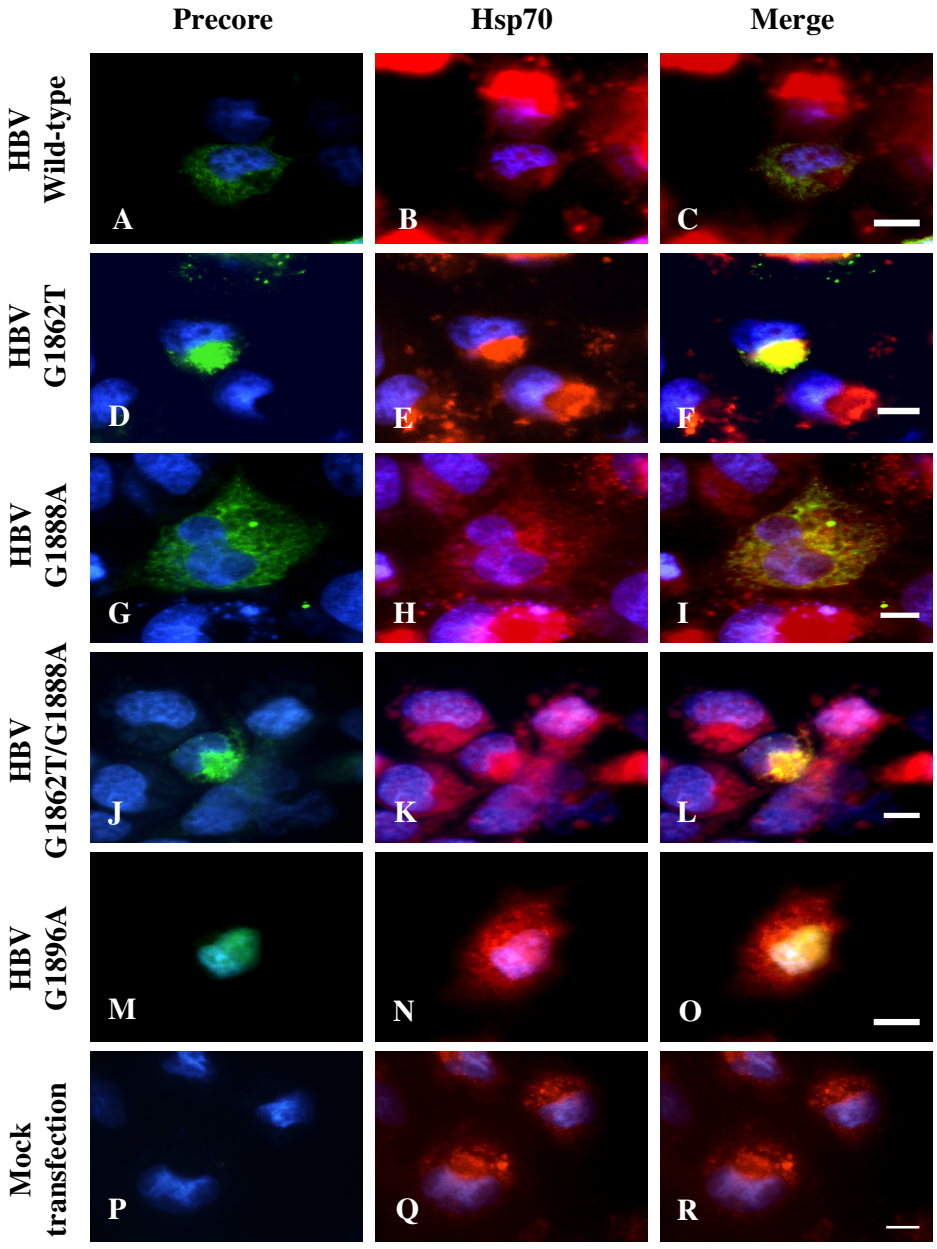

Figure 3.50 Proteasomal inhibition promotes aggresome formation by the genotype D HBV G1862T mutant precore/core protein. Genotype D HBV G1862T precore/core protein co-localized with Hsp70. Huh7 cells were transfected with genotype D plasmid constructs, treated with MG132, a proteasome inhibitor. The cells were fixed at 72 hours post-transfection, and were subjected to indirect double immunofluorescence staining with antibodies against HBV precore/core protein, detected with secondary antibodies labelled with AlexaFluor 488, shown in green. The molecular chaperone was detected with primary antibodies against Hsp70 and secondary antibodies were labelled with AlexaFluor 546, shown in red. Co-localization of precore/core protein and Hsp70 can be seen by the yellow color. Nuclei were counterstained with DAPI. Scale bars, 10 μm.

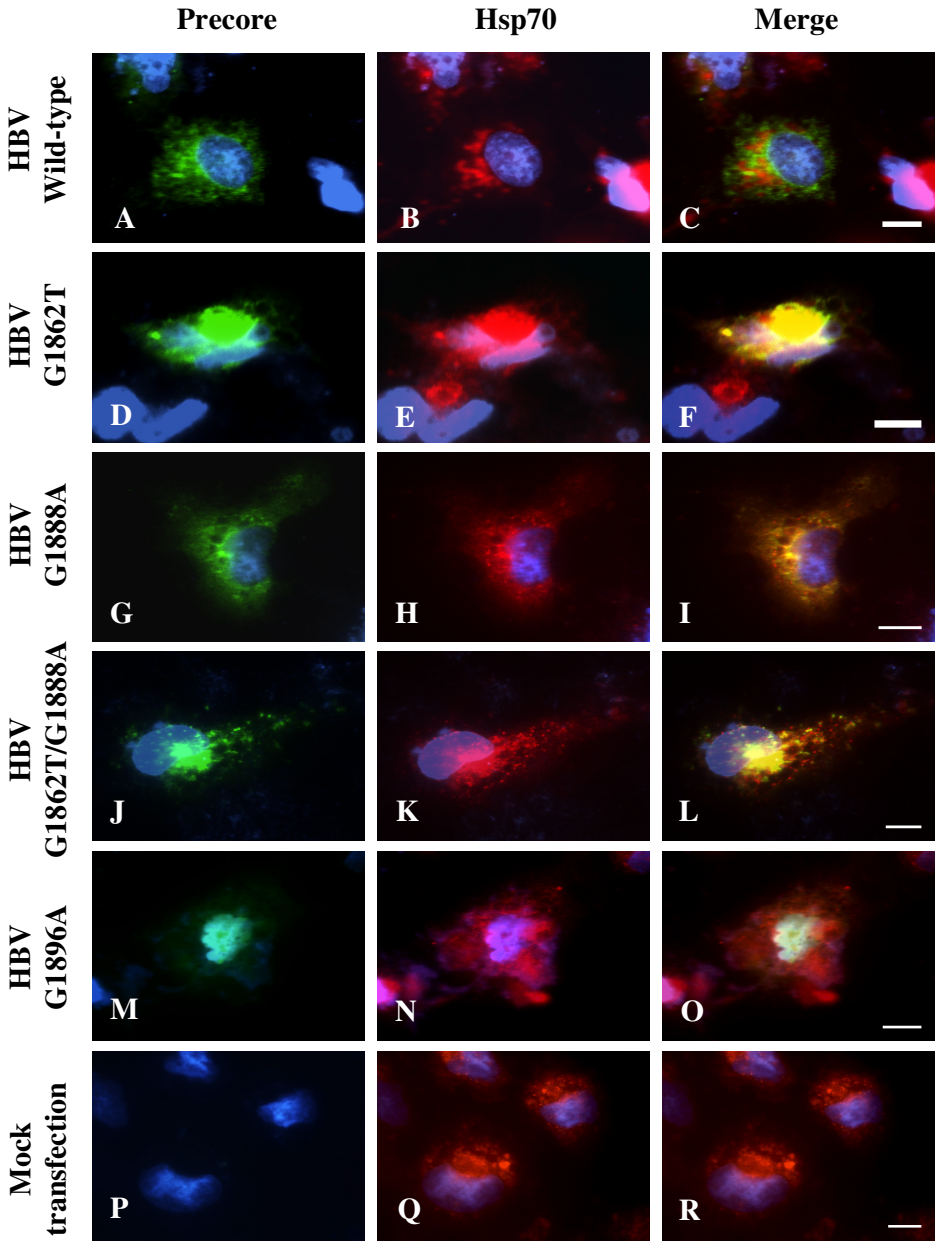

Figure 3.51 Proteasomal inhibition promotes aggresome formation by the genotype 'A' HBV G1862T mutant precore/core protein. Genotype 'A' HBV G1862T precore/core protein co-localized with Hsp70. Huh7 cells were transfected with genotype 'A' plasmid constructs, and treated with MG132, a proteasome inhibitor. The cells were fixed at 72 hours post-transfection, and were subjected to indirect double immunofluorescence staining with antibodies against HBV precore/core protein, detected with secondary antibodies labelled with AlexaFluor 488, shown in green. The molecular chaperone was detected with primary antibodies against Hsp70 and secondary antibodies were labelled with AlexaFluor 546, shown in red. Co-localization of precore/core protein and Hsp70 can be seen by the yellow color. Nuclei were counterstained with DAPI. Scale bars, 10 μm.

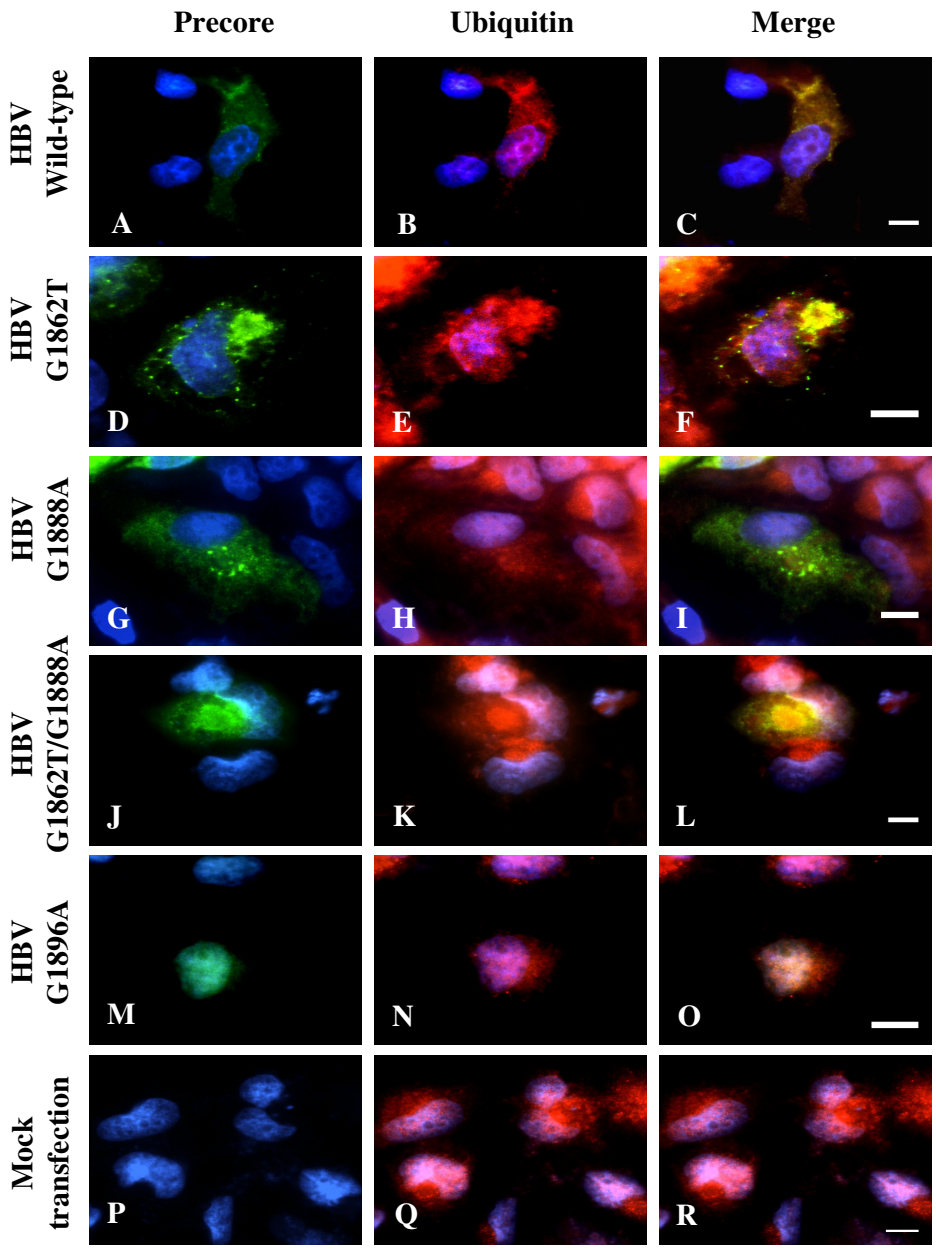

Figure 3.52 Proteasomal inhibition promotes aggresome formation by the genotype D HBV G1862T mutant precore/core protein. Genotype D HBV G1862T precore/core protein co-localized with ubiquitin. Huh7 cells were transfected with genotype D plasmid constructs, and treated with MG132, a proteasome inhibitor. The cells were fixed at 72 hours post-transfection, and were subjected to indirect double immunofluorescence staining with antibodies against HBV precore/core protein, detected with secondary antibodies labelled with AlexaFluor 488, shown in green. The ubiquitin was detected with primary antibodies against ubiquitin and secondary antibodies were labelled with AlexaFluor 546, shown in red. Co-localization of precore/core protein and ubiquitin can be seen by the yellow color. Nuclei were counterstained with DAPI. Scale bars, 10 μm.

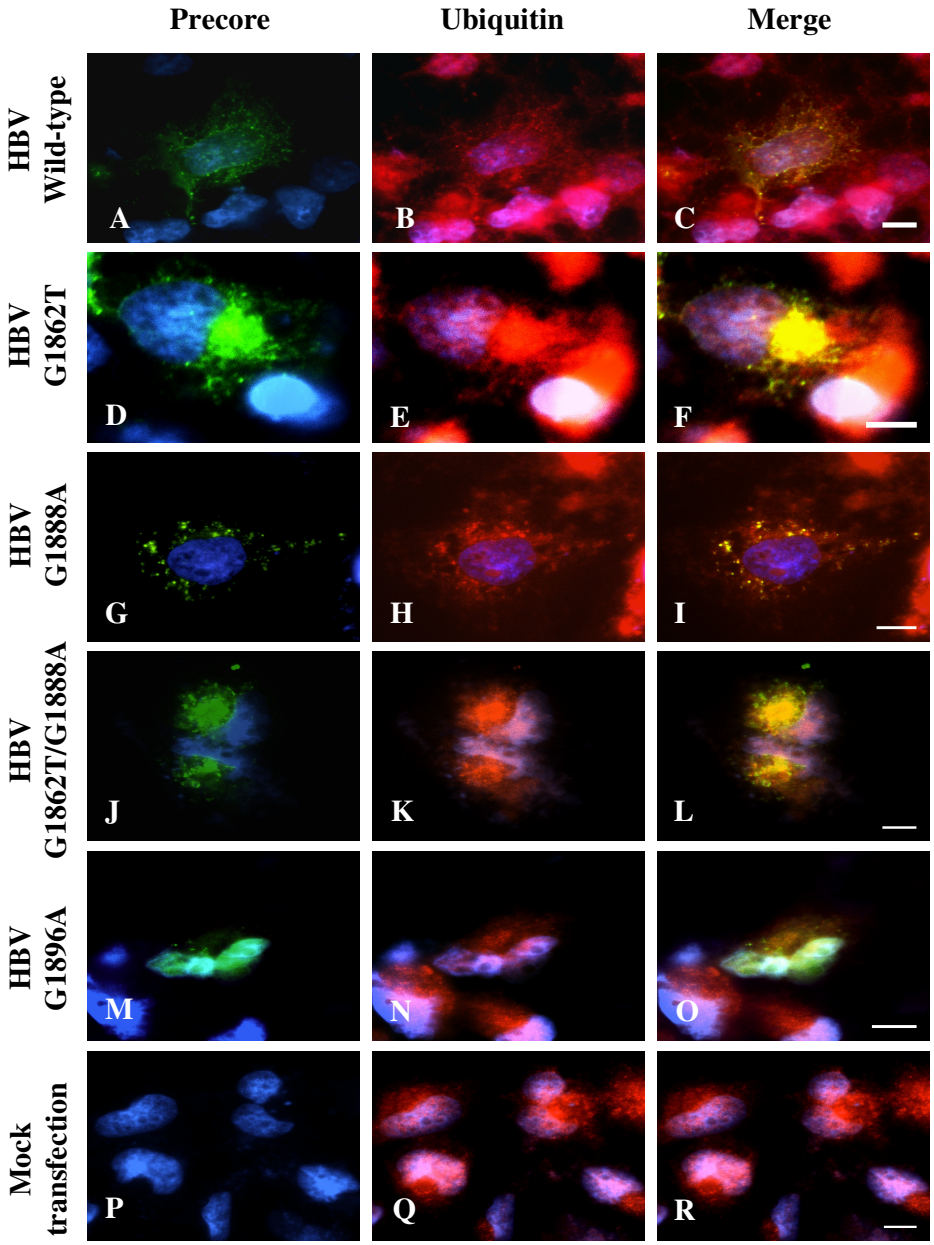

Figure 3.53 Proteasomal inhibition promotes aggresome formation by the genotype 'A' HBV G1862T mutant precore/core protein. Genotype 'A' HBV G1862T precore/core protein co-localized with ubiquitin. Huh7 cells were transfected with genotype 'A' plasmid constructs, treated with MG132, a proteasome inhibitor. The cells were fixed at 72 hours post-transfection, and were subjected to indirect double immunofluorescence staining with antibodies against HBV precore/core protein, detected with secondary antibodies labelled with AlexaFluor 488, shown in green. The ubiquitin was detected with primary antibodies against ubiquitin and secondary antibodies were labelled with AlexaFluor 546, shown in red. Co-localization of precore/core protein and ubiquitin can be seen by the yellow color. Nuclei were counterstained with DAPI. Scale bars, 10 μm.

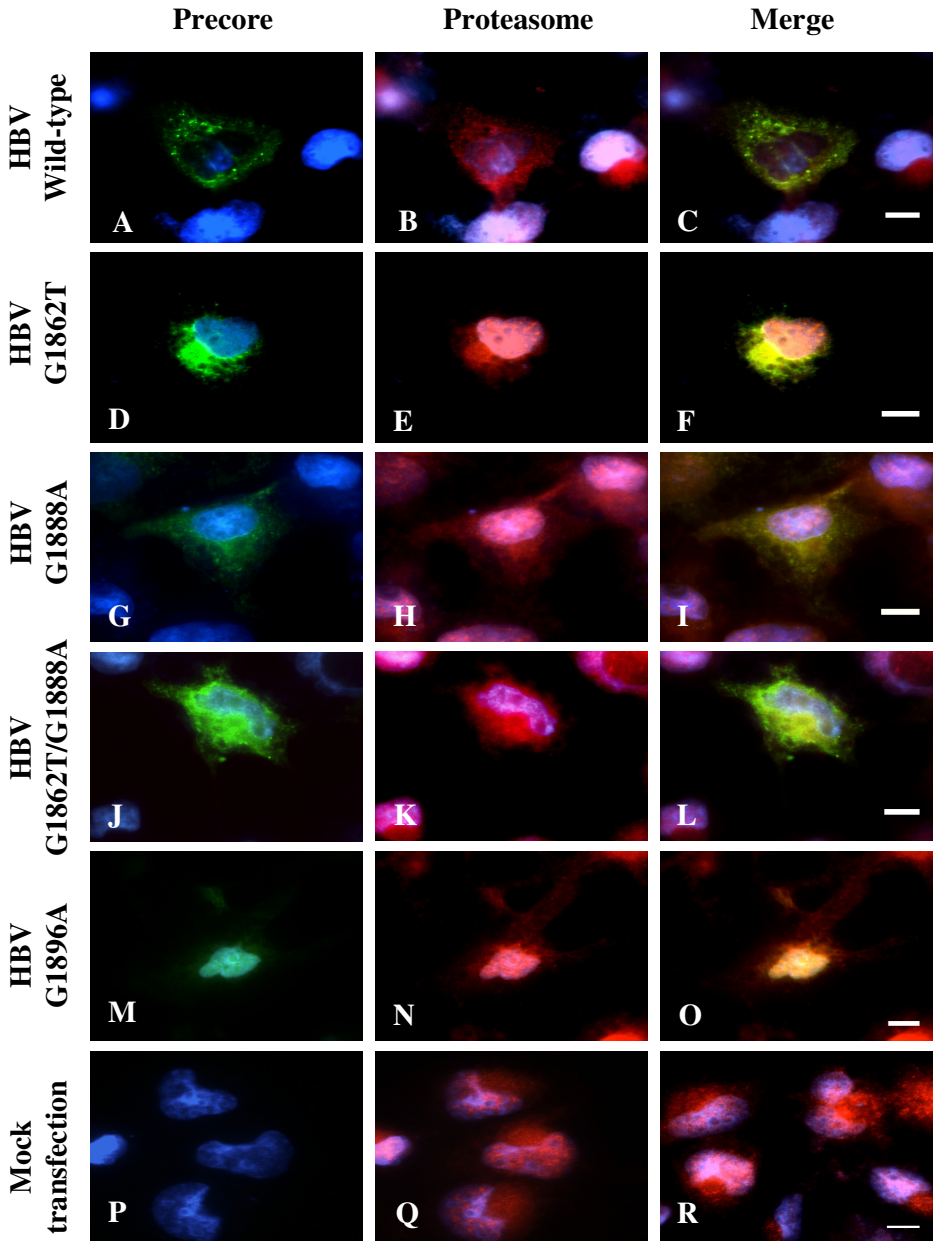

Figure 3.54 Proteasomal inhibition promotes aggresome formation by the genotype D HBV G1862T mutant precore/core protein. Genotype D HBV G1862T precore/core protein co-localized with proteasome. Huh7 cells were transfected with genotype D plasmid constructs, treated with MG132, a proteasome inhibitor. The cells were fixed at 72 hours post-transfection, and were subjected to indirect double immunofluorescence staining with antibodies against HBV precore/core protein, detected with secondary antibodies labelled with AlexaFluor 488, shown in green. The proteasome was detected with primary antibodies against proteasome and secondary antibodies were labelled with AlexaFluor 546, shown in red. Co-localization of precore/core protein and proteasome can be seen by the yellow color. Nuclei were counterstained with DAPI. Scale bars, 10 μm.

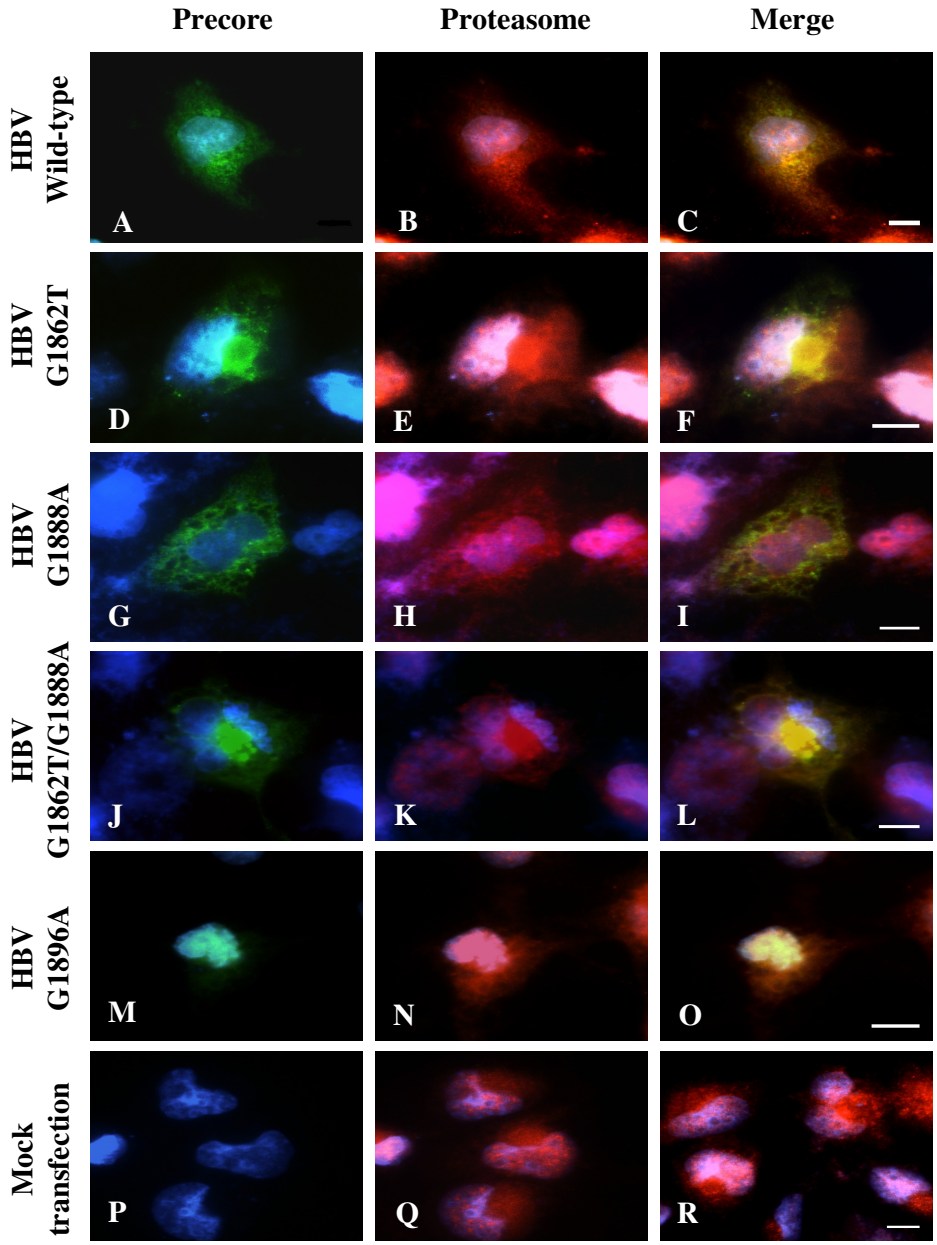

Figure 3.55 Proteasomal inhibition promotes aggresome formation by the genotype 'A' HBV G1862T mutant precore/core protein. Genotype 'A' HBV G1862T precore/core protein co-localized with proteasome. Huh7 cells were transfected with genotype 'A' plasmid constructs, treated with MG132, a proteasome inhibitor. The cells were fixed at 72 hours post-transfection, and were subjected to indirect double immunofluorescence staining with antibodies against HBV precore/core protein, detected with secondary antibodies labelled with AlexaFluor 488, shown in green. The proteasome was detected with primary antibodies against proteasome and secondary antibodies were labelled with AlexaFluor 546, shown in red. Co-localization of precore/core protein and proteasome can be seen by the yellow color. Nuclei were counterstained with DAPI. Scale bars, 10 μm.

3.5.4.3 Dynamics of aggresomes formation: a precore/core protein-eGFP fusion protein study

In order to monitor the dynamic movement of HBV or WHV precore/core protein in the secretory pathway, the HBV and WHV precore/core protein-eGFP fusion protein expression vectors were designed and generated. These expression vectors had a flexible poly-linker between the upstream precore/core gene and the downstream eGFP gene. These constructs were used to transfect Huh7 cells and the expression of eGFP fusion protein in live cells was followed using confocal microscopy.

Huh7 cells expressing HBV wild-type (Figure 3.56-3.57, A and C), G1888A (Figure 3.56-3.57, I and K) or WHV wild-type (Figure 3.58, A and C) precore/core-eGFP fusion protein showed a faint, reticular pattern of eGFP distribution throughout the cytoplasm of the cells with small green fluorescent specks found only occasionally both at 48 hr and 72 hr post-transfection. In contrast, green fluorescent signals in the perinuclear region of the cells were observed in Huh7 cells expressing HBV G1862T (Figure 3.56-3.57, E and G), G1862T/G1888A (Figure 3.56-3.57, M and O) or WHV G1982T (Figure 3.58, E and G) precore/core-fusion proteins. These fluorescent signals were similar in appearance to aggresomes. There was no significant difference in the expression of the wild-type proteins when the cells transfected with HBV wild-type (Figure 3.56-3.57, B and D), G1888A (Figure 3.56-3.57, J and L), or WHV wild-type (Figure 3.58, B and D) constructs were treated with MG132. There was no difference in the pattern and distribution of green fluorescence. In contrast, when Huh7 cells transfected with HBV G1862T (Figure 3.56-3.57, F and H), G1862T/G1888A (Figure 3.56-3.57, N and P) or WHV G1982T (Figure 3.58, F

and H) precore/core-eGFP construst were treated with MG132, the aggresomes developed earlier and were even larger, more compact and with brighter fluorescence intensity compared to those in cells not treated with MG132. Moreover, the size of aggresomes increased with time between 48 hr and 72 hr post-transfection (HBV G1862T: Figure 3.56-3.57, F and H; HBV G1862T/G1888A: Figure 3.56-3.57, N and P; WHV G1982T: Figure 3.58, F and H).

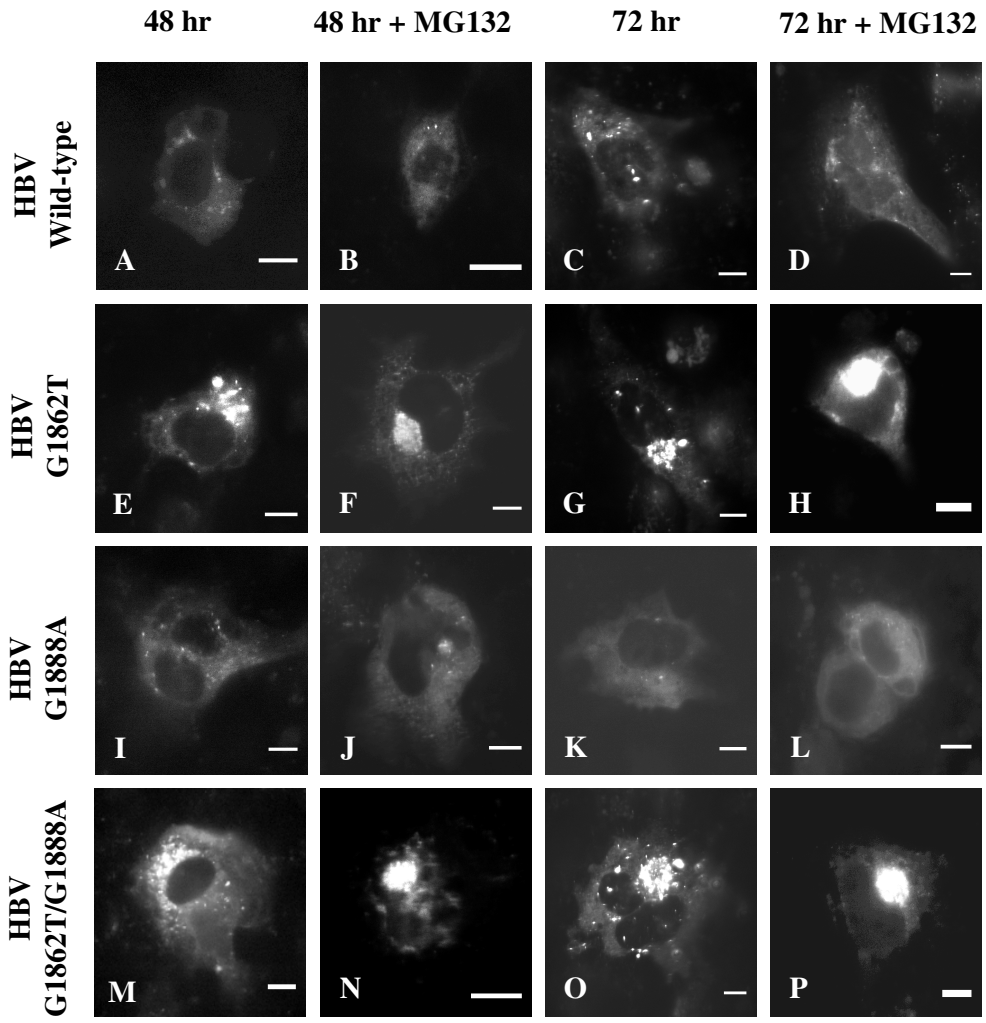

Figure 3.56 Expression of genotype 'A' HBV precore/core-eGFP fusion protein in Huh7 cells. Green fluorescent signals in the perinuclear region of the cells were observed in Huh7 cells expressing HBV G1862T and G1862T/G1888A precore/core-fusion proteins. Huh7 cells were transfected with genotype 'A' HBV precore/core-eGFP fusion constructs, and treated with proteasome inhibitor, MG132. The cells were not fixed. Confocal images were taken either at 48 hours or 72 hours post-transfection. Scale bars, 10 μm.

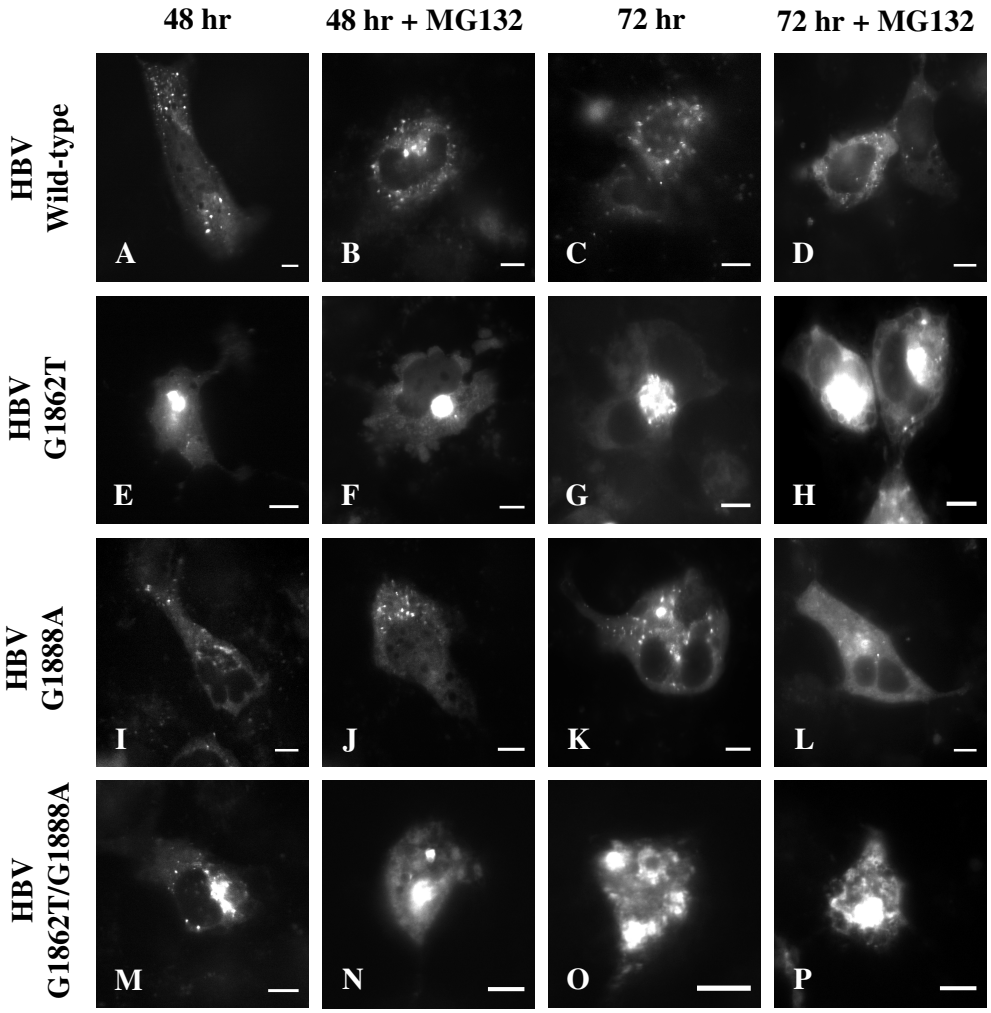

Figure 3.57 Expression of genotype D HBV precore/core-eGFP fusion protein in Huh7 cells. Green fluorescent signals in the perinuclear region of the cells were observed in Huh7 cells expressing HBV G1862T and G1862T/G1888A precore/core-fusion proteins. Huh7 cells were transfected with genotype D HBV precore/core-eGFP fusion constructs, and treated with proteasome inhibitor, MG132. The cells were not fixed. Confocal images were taken either at 48 hours or 72 hours post-transfection. Scale bars, 10 μm.

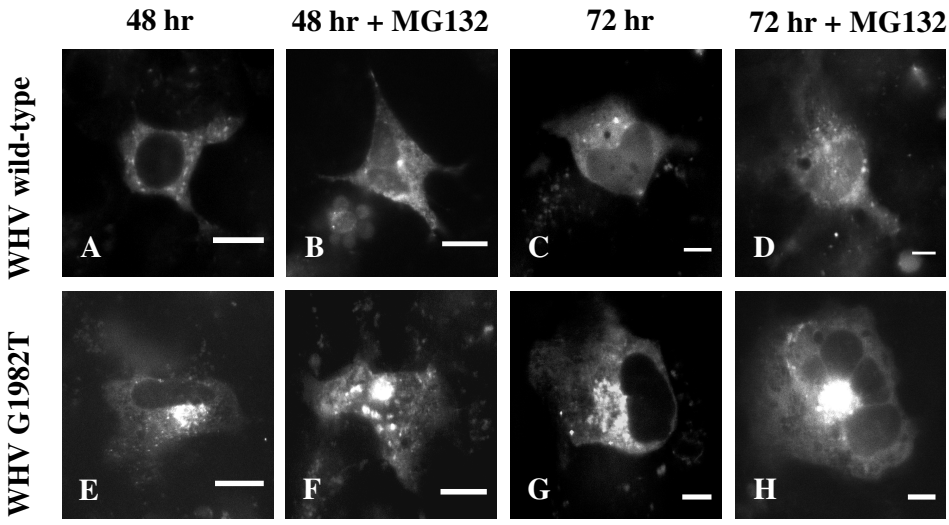

Figure 3.58 Expression of WHV precore/core-eGFP fusion protein in Huh7 cells. Green fluorescent signals in the perinuclear region of the cells were observed in Huh7 cells expressing WHV G1982T precore/core-fusion proteins. Huh7 cells were transfected WHV precore/core-eGFP fusion constructs, and treated with proteasome inhibitor, MG132. The cells were not fixed. Confocal images were taken either at 48 hours or 72 hours post-transfection. Scale bars, 10 μm.

CHAPTER 4

4.0 DISCUSSION

The G1862T mutation is a distinctive characteristic of subgenotype A1 of HBV, which is the most prevalent subgenotype circulating in South Africa (Kramvis *et al*, 1997; Kramvis *et al*, 1998; Sugauchi *et al*, 2004a; Kramvis *et al*, 2008). The objective of this study was to functionally characterize this mutation in tissue culture cells. The G1862T mutation could conceivably have two functional consequences. First, because G1862T occurs within the bulge of ε (Fallows & Goff, 1995), which plays a pivotal role in the initiation of reverse transcription of pgRNA (Knaus & Nassal, 1993; Pollack & Ganem, 1993), this mutation could interfere with HBV replication. Secondly, because the precore/core open reading frame on the precore mRNA, which encodes for the precursor of HBeAg, overlaps the region that codes for ε on the pgRNA, the G1862T missense mutation (Val to Phe) could interfere with the signal peptide cleavage and affect HBeAg expression. Both possibilities were investigated in this study by measuring HBV DNA levels using a replication competent plasmid and HBeAg expression using a HBeAg-expression plasmid.

This study was initiated several years ago, when advanced molecular techniques for full length HBV genome amplification had not been developed, and subgenotype A1 had not been recognized and characterized. Moreover, the high frequency of G1862T in subgenotype A1 had not been established. Thus pCH-9/3091-wt, a terminally redundant, 1.3 X unit over-length, replication competent genotype D HBV genome was used as template to generate mutant constructs (Nassal, 1992). In the pCH-9/3091-wt plasmid, the transcription of HBV pgRNA is controlled by the CMV IE promoter whereas recently developed cloning

techniques allow transcription of HBV pgRNA to be controlled by the native HBV promoter. The pCH-9/3091-wt plasmid was designed to support the transcription of pgRNA but not precore mRNA. Therefore, the precore/core gene was PCR amplified and cloned into the pCR3.1 plasmid, where the transcription of precore mRNA was controlled by the CMV promoter and this latter plasmid was used to monitor HBeAg expression *in vitro*.

Effect of mutation on HBV replication

Using real time PCR to quantify HBV DNA loads, the HBV DNA levels were significantly reduced when the G1862T mutation was introduced into a genotype D replication competent construct (pCH-9/3091) but not when introduced into the genotype 'A' construct (Figure 3.3). This is in agreement with the reported impairment of HBV replication by the G1862T mutation in genotype D (Guarnieri *et al*, 2006), and subgenotype B2 (Inoue *et al*, 2009). A virus with a high replication rate will eventually lead to the rapid cell lysis and host death, and hence result in a reduced probability of stable host-to-host transmission. On the other extreme, a virus with a low replication rate will result in increased viral clearance and reduced host-to-host transmission. In order for a virus to survive, it requires an optimal and steady rate of viral replication (Sallie, 2005). This could explain why the G1862T mutation occurs more frequently in genotype A (Kramvis *et al*, 2008) than any other genotypes (Hou *et al*, 2002; Kramvis *et al*, 2008).

The G1862T mutation is situated immediately after the UUC sequence (Figure 1.7) (nt 1863-1865) that is used as template by the reverse transcriptase to synthesise the DNA primer for the minus strand DNA (Nassal & Rieger, 1996).

This short oligo primer is then transferred to the complementary acceptor site at DR1 that is close to the 3' end of the pgRNA, where the extension of the minus strand DNA continues and is completed to form the minus strand DNA (Nassal & Schaller, 1996). The study of Rieger and Nassal showed that nt 1864 and 1865 are sufficient for the DNA primer to transfer to the DR1 position (Rieger & Nassal, 1995), and therefore nucleotide variations at position 1862 would not be expected to affect primer synthesis or reverse transcription. The stability of the secondary structure of ε is important in maintaining optimal reverse transcription (Kramvis & Kew, 1998) and therefore the possibility exists that the introduction of G1862T resulted in the destabilization of ε. However, computation of minimum free energy (ΔG) using *mfold* (http://mfold.bioinfo.rpi.edu/cgi-bin/rna-form1.cgi) showed no significant change in the ΔG when the mutation was introduced into either genotype A or genotype D sequences (Mathews *et al*, 1999; Zuker, 2003). On the other hand, the introduction of G1896A in the genotype A sequence leads to ~20% reduction in ΔG, a significant reduction. Therefore, reduced HBV DNA replication using pCH-9/3091 plasmid constructs cannot be attributed to either interference with reverse transcription or destabilization of ε.

A comparable level of reduction in the HBV DNA level was also observed when G1888A mutation was introduced into genotype D construct but not into genotype 'A' construct (Figure 3.3). The G1888A mutation formed a stable Watson-Crick base pair with 1871T stabilizing the structure of ε in the genotype 'A' construct. G1888A mutation could possibly contribute to the destabilization of the ε in the genotype D context, thereby affecting reverse transcription (Rodriguez-Frias *et al*, 1995) and subsequently reducing viral replication. When the G1862T and G1888A mutations were combined in the genotype D context, the combination of

the two mutations further reduced viral replication when compared to G1862T or G1888A mutations individually. In contrast to the genotype D context, the combination of the G1862T and G1888A mutations did not affect viral replication in the genotype 'A' context (Figure 3.3). The G1862T and G1888A mutations individually or in combination may possibly have evolutionary advantage in the genotype 'A' context because G1862T and G1888A mutations are frequently associated with subgenotype A1. Kramvis *et al* suggested that both mutations may have co-evolved (Kramvis *et al*, 2008).

As expected and previously demonstrated (Tong *et al*, 1992; Li *et al*, 1993; Lok *et al*, 1994; Yuan *et al*, 1995), the G1896A mutation did not affect viral replication in the genotype D context, where the structure of ε was stabilized by the Watson-Crick base pair of nucleotide 1858T with 1896A (Kramvis *et al*, 1997). On the other hand, when the G1896A mutation was introduced into the genotype 'A' context, the stable Watson-Crick base pair formed by nucleotide 1858C with 1896G was disrupted. The formation of wobble base pair by 1858C and 1896A destabilized the structure of ε, compromising viral replication (Li *et al*, 1993; Rodriguez-Frias *et al*, 1995). The classical G1896A stop codon mutation was commonly associated with genotype D, but not with genotypes A, C and E (Kramvis *et al*, 2008). This mutation is rarely found in genotype A (Li *et al*, 1993), and this was later confirmed by the study of Kramvis *et al*, in which the frequency of G1896A mutation in the different genotypes was statistically analysed (Kramvis *et al*, 2008). In the present study, a statistically significantly decrease in viral replication was observed when G1896A mutant was introduced into genotype 'A', confirming the findings of Li *et al* (Li *et al*, 1993). The introduction of the G1896A mutation in genotype 'A' context would certainly

compromise the maintenance of a constant viral replication rate and therefore the virus would evolutionarily be eliminated.

Expression of HBeAg/WHeAg in Huh 7 cells

HBeAg/WHeAg-expression constructs were used to follow the secretion and expression of both wild-type and mutant HBeAg/WHeAg. The wild-type HBV and WHV precore/core proteins localized to the sites of the secretory pathway necessary for the expression of HBeAg and WHeAg (Lippincott-Schwartz *et al*, 2000; Lippincott-Schwartz, 2001; Rutishauser & Spiess, 2002; Ellgaard L, 2004), namely the ER (Figure 3.6-3.10), ERGIC (Figure 3.11-3.15) and the Golgi (Figure 3.16-3.20). This distribution of wild-type protein was not disturbed by the treatment of the cells with proteasome inhibitor, MG132 (Figure 3.50-3.55). These observations demonstrated that the wild-type protein was post-translationally modified correctly, HBeAg/WHeAg was formed and proceeded through the secretory pathway normally. It was either expressed on the cell surface or secreted from the cell.

On the other hand, when cells were transfected with the mutant constructs, there was a reduction of HBeAg expression in the supernatant, relative to the wild-type (38% for genotype D and 54% for genotype 'A') (Figure 3.4). This is in agreement with the study of Hou and colleagues that showed reduced HBeAg expression when the G1862T mutation was present in a genotype B HBeAg-expressing construct (Hou *et al*, 2002). However, this was not found to be the case when this mutation was introduced into genotype D and subgenotype B2 constructs in more recent studies in which HBeAg expression was not significantly affected by the introduction of the mutation (Guarnieri *et al*, 2006;

Inoue *et al*, 2009). These discrepancies between results could be explained by the fact that HBeAg-expression constructs were used in the present study and that of Hou *et al* (Hou *et al*, 2002) whereas replication competent plasmids were used by Guarnieri *et al* and Inoue *et al* (Guarnieri *et al*, 2006; Inoue *et al*, 2009). Moreover, the plasmids were derived from templates belonging to different genotypes/subgenotypes.

Accumulation of mutant precore/core protein in the ER and ERGIC

The precursor protein produced by the G1862T mutant did not transfer to the ERGIC and beyond and therefore accumulated in the ER, indicating that it failed to meet the ER quality control requirements. Retention of mutant proteins in the ER can be found in the mutant α-1-antitrypsin (Sifers *et al*, 1988; Lomas & Parfrey, 2004), thyroglobulin (Kim & Arvan, 1998; Kim *et al*, 2000), mutant low density lipoprotein receptor (Pathak *et al*, 1988), mutant collagen alpha 1 chain (Bogaert *et al*, 1992), mutant proinsulin (Wang *et al*, 1999), G145R variant of HBsAg (Kalinina *et al*, 2001), L215Q mutant of HBsAg (Araujo *et al*, 2008) and overexpressed wild-type LHBs protein (Xu *et al*, 1997).

Despite the retention in the ER compartment, a proportion of the precore/core protein reached the ERGIC and *cis*-Golgi compartments (Figure 3.6-3.20). Quality control requirements in respect to correct protein folding and assembly must be met in these two compartments. Most incorrectly, incompletely folded or misfolded proteins detected at this point are retrogradely transported back to the ER by the COP I vesicles, for further refolding (Hammond & Helenius, 1994; Caldwell *et al*, 2001; Taxis *et al*, 2002; Trombetta & Parodi, 2003; Romisch,

2005). This sequence of events explains the demonstration of the precursor protein found in compartments beyond the ER.

Similar results have been described for misfolded vesicular stomatitis virus (VSV) G protein (Hammond & Helenius, 1994). When the amount of misfolded VSV G protein increased in the ER, some of the protein started to move to ERGIC and the Golgi. The extent of escape from ER correlates more closely with the expression level of G protein than with time after infection. It was postulated that the appearance of G protein in ERGIC and the Golgi occurs by some type of saturation phenomenon in ER (Hammond & Helenius, 1994). Misfolded proteins are able to escape ER quality control check point, be transported beyond ER, recycle between ER and Golgi. This seems to be the case in misfolded VSV G protein (Hammond & Helenius, 1994) and unassembled MHC class I molecules (Hsu *et al*, 1991). The retention of the misfolded precore/core protein in the ER and ERGIC agrees with the model proposed by Hammond and Helenius (Hammond & Helenius, 1994) and occurs for mutant ΔF508 cystic fibrosis transmembrane regulator (CFTR) (Gilbert *et al*, 1998), presenilin-1 (Johnston *et al*, 1998), mutant proinsulin in the Akita diabetes model (Zuber *et al*, 2004; Fan *et al*, 2007) and mutant vasopressin receptor in nephrogenic diabetes insipidus (Hermosilla *et al*, 2004; Oueslati *et al*, 2007). Moreover, accumulation in Golgi has been described for the mutant L77R HBsAg (Chua *et al*, 2005).

Further evidence that the mutant proteins were misfolded was the increased expression of chaperones, such as Hsp70 (Figure 3.24-3.25), involved in protein folding, translocation and degradation (Hartl, 1996; Hartl & Hayer-Hartl, 2002; De Los Rios *et al*, 2006). This finding was to be expected because misfolded

proteins but not wild-type proteins usually have their hydrophobic domains exposed, promoting chaperone binding (Heath *et al*, 2001).

If chaperone binding does not result in correct folding and assembly of the proteins, the accumulated proteins will be targeted by the unfolded protein response (UPR) and endoplasmic reticulum associated degradation (ERAD) pathways co-operatively (Travers *et al*, 2000; Hampton, 2002; Kostova & Wolf, 2003; Meusser *et al*, 2005). The defective protein is first unfolded, then retrotranslocated and exported from the ER through the Sec61 translocon to the cytosol (Pilon *et al*, 1997; Tsai *et al*, 2002) where it is polyubiquitinated and then transferred to the 26S proteasome complex for degradation (Hampton, 2002; Kostova & Wolf, 2003). The 26S proteasome complex is responsible for the majority of non-lysosomal protein degradation in eukaryotic cells (Hochstrasser, 1996).

Increased levels of both ubiquitin (Figure 3.26-3.27) and proteasomes (Figure 3.28-3.29) were also detected in the cells infected with mutant constructs, but not in cells infected with the wild-type constructs. The misfolded precore/core proteins were found to have accumulated along the microtubules in the cytosol, where they formed mini-aggregates (Figure 3.35-3.39). This is further evidence that the mutant protein was not correctly folded because *in vitro* studies have shown that misfolded proteins are prone to aggregation (Ellgaard *et al*, 1999). Moreover, protein aggregation has been shown to impair and inhibit the ubiquitin-proteasome system (Sitte *et al*, 2000; Bence *et al*, 2001; Bennett *et al*, 2005). Furthermore, the accumulation of ubiquitinated protein conjugates can lead to cell cycle arrest and cell death (Bence *et al*, 2001).

Over time, cells become overloaded with the accumulation of misfolded protein in the ER. The ER homeostasis is disturbed, and ER transmembrane sensors detect the onset of ER stress and trigger the ER stress response (Rutkowski & Kaufman, 2004; Schroder & Kaufman, 2005). The mammalian ER stress response results in the inhibition of protein synthesis, the up-regulation of genes responsible for the expression of chaperones and ERAD components,esponsible for protein degradation, and the activation of apoptosis (Groenendyk & Michalak, 2005; Rutkowski & Kaufman, 2007; Yoshida, 2007). When the ER stress is prolonged or becomes chronic, UPR and ERAD pathways fail to clear the accumulated misfolded proteins. If ER homeostasis cannot be restored or returned to its normal status, the cells undergo programmed cellular death, that is, apoptosis (Soldatenkov & Dritschilo, 1997; Ellgaard & Helenius, 2003; Lai *et al*, 2007).

The precore signal sequence has been shown to play an important role not only in the secretion of HBeAg but also in determining its structural and aggregational properties (Schlicht & Wasenauer, 1991; Wasenauer *et al*, 1992). Therefore, it is possible that the aggregation is caused by the interference of the mutation with post-translational modification of the precursor molecule.

From this observation, it can be intimated, as previously predicted by Kramvis *et al* (Kramvis *et al*, 1998) and Valliammai *et al* (Valliammai *et al*, 1995), and shown for *Escherichia coli* alkaline phosphatase (Karamyshev *et al*, 1998) and *Escherichia coli* maltose-binding protein (Fikes *et al*, 1990), that the -3,-1 rule (von Heijne, 1983; von Heijne, 1984) holds true for the post-translational modification of the HBeAg precursor.

Using metabolic labelling, it was demonstrated in this study that the presence of G1982T mutation in WHV construct impaired the maturation of the WHeAg precursor relative to the wild-type (Figure 3.5). This impaired processing of WHeAg precursor is comparable to the impairment caused by the HBV G1862T mutation (Hou *et al*, 2002). Karamyshev *et al* proposed two possible mechanisms for the impairment of mutant precursor processing (Karamyshev *et al*, 1998): (1) the translocation of precursor protein across ER membrane is blocked, therefore the precursor is not accessible to the signal peptidase; (2) direct inhibition of the signal peptide cleavage as a result of the protein structural change caused by the introduction of the Phe, with its aromatic ring. The Phe expressed as result of the G1862T in HBV (or G1982T in WHV) mutation, is a "forbidden" amino acid at position -3 to the signal peptide cleavage site. According to the -3, -1 rule, the acceptable cleavage domains conform to the following: (1) the residue at position -1 from the cleavage site must be small and neutral (Ala, Cys, Gly, Ser, Thr, or Gln); (2) The residue at position -3 must not have aromatic (His, Phe, Tyr, and Trp), charged (Asp, Glu, Lys, and Arg), or large polar side chains (Asn and Gln); (3) Pro residue is prohibited in the region between -3 and +1 position (Perlman & Halvorson, 1983; von Heijne, 1983; von Heijne, 1984). Such structural regularity at the -3, -1 position is considered to be necessary for signal peptidase recognition. In the study of Karamyshev *et al*, the *Escherichia coli* alkaline phosphatase was used to test the -3, -1 rule, it was found that the efficient signal peptidase cleavage requires highly specific amino acids at -1 position, whereas the requirement of the amino acids at -3 position are less stringent (Karamyshev *et al*, 1998). In the bacterial signal peptidase structural model, the substrate specificity at -1 position is more stringent as a result of a much smaller binding pocket for the amino acid side chain at -1 position (Karla *et al*, 2005). In

contrast, more relaxed substrate specificity at -3 position was observed (Karla *et al*, 2005). The binding pocket for the amino acid side chain at -3 position was found to be bigger and broader. Therefore, the binding pocket can be able to accommodate (accept) amino acids with larger aliphatic side chains (Paetzel *et al*, 1998; Ekici *et al*, 2007).

There are large differences in the molecular volume between Val (140 $Å^3$) and Phe (189.9 $Å^3$) (Zamyatnin, 1972), as well as in the accessible surface area between Val (155 $Å^2$) and Phe (210 $Å^2$) (Chothia, 1976). When the Val is replaced by Phe, the bulky aromatic side chain of Phe would introduce a molecular volume constraint, which would affect the packing within its immediate surrounding environment. Secondly, it also creates a steric constraint with the change of side chain conformational entropy. Both factors will restrict the conformation, thereby interfering with and hindering the proper positioning and docking of precore/core protein (substrate) to the binding pocket of signal peptidase, and subsequently affecting signal peptide cleavage at the amino end of the precore/core protein.

The Val side chain is relatively non-reactive, and is rarely directly involved in protein function, but it can play a role in substrate recognition (Betts & Russell, 2003). Generally, it is regarded as not ideal to substitute Val with Phe. As Phe is an aromatic, hydrophobic amino acid, and is usually substituted with other amino acids of the same type. It is noteworthy that Phe is never found -1 or -3 position in the SWISS-PROT data set of signal peptides (Bendtsen *et al*, 2004). The experimental introduction of Phe at the -3 position of the signal peptidase recognition motif of the *Escherichia coli* alkaline phosphatase (Karamyshev *et al*,

1998) and *Escherichia coli* maltose-binding protein (Fikes *et al*, 1990) completely abolished signal peptide processing.

Substitution of the amino acid at -3 position of signal peptide with amino acids other than Phe can also result in the impairment of precursor protein processing. Coagulation factor $X_{Santo\ Domingo}$ is a mutant form of human coagulation factor X in which a point mutation results in the substitution of Gly to Arg at the critical -3 position of the signal peptide (Watzke *et al*, 1991). Patients bearing this mutation exhibit a severe bleeding diathesis associated with less than 1 % coagulation factor X enzymatic activity and less than 5% circulating coagulation factor X protein. In a later study, it was found that this mutation did not interfere with targeting and translocation to the RER, rather it is the cleavage of factor X by signal peptidase that is markedly impaired (Racchi *et al*, 1993).

Aggresome formation by mutant precore/core proteins

Signal peptides influence the timing and efficiency of signal peptide cleavage (Rutkowski *et al*, 2003). Impaired signal peptide cleavage can create protein folding constraints (Stevens & Argon, 1999), which can result in the aggregation of the protein in the cytoplasm as was observed in the present study.

Mini-aggregates increased in size over time and were transported, presumably by the protein dynein, along microtubules to the MTOC in the region of the centrosome, which co-localizes with γ-tubulin in a perinuclear position (Hartl, 1996; Johnston *et al*, 1998; Kopito & Sitia, 2000; Harada *et al*, 2001). Using antibodies against α-tubulin, an intact microtubule network was shown to be associated with the retrograde transport of the smaller aggregates along the

microtubules and their deposition at the MTOC (Figure 3.30-3.34 for γ-tubulin, and Figure 3.35-3.39 for α-tubulin) (Kopito & Sitia, 2000; Garcia-Mata *et al*, 2002). At this site, indigestible aggregates were spontaneously sequestered into aggresomes (Johnston *et al*, 1998; Kopito & Sitia, 2000; Garcia-Mata *et al*, 2002) even in the absence of proteasome inhibitor. In agreement with Johnson *et al* (Johnston *et al*, 1998), this data shows that the aggregation of the mutant precursor of HBeAg occurred when the expression of the misfolded protein exceeded the degradation capacity of the proteasome, and the accumulation of mutant HBV proteins was greatly enhanced when proteasome activity was inhibited (Figure 3.50-3.55). The fact that aggresomes did not form in cells transfected with wild-type constructs indicates that the accumulation of the mutant protein is as a result of its defective expression rather than the ubiquitin-proteasome machinery not functioning in Huh7 cells (Gu *et al*, 2003).

The aggregates of the unprocessed HBeAg precursor demonstrated the hallmarks of aggresomes. They were ubiquitin-rich aggregates in the region of the MTOC (Figure 3.30-3.34 for γ-tubulin, and Figure 3.26-3.27 for ubiquitin) (Harada *et al*, 2001; Heath *et al*, 2001; Waelter *et al*, 2001; Garcia-Mata RG *et al*, 2002; Saliba *et al*, 2002) that recruited Hsp70 and proteasomes (Figure 3.24-3.25 for Hsp70, Figure 3.28-3.29 for proteasomes) (Johnston *et al*, 1998; Wigley *et al*, 1999; Garcia-Mata *et al*, 2002) and were surrounded by a vimentin sheath (Figure 3.40-3.44) (Johnston *et al*, 1998; Harada *et al*, 2001; Garcia-Mata *et al*, 2002; Saliba *et al*, 2002). Although before aggregating, some of the misfolded protein did reach the Golgi apparatus, aggresome formation did not require an intact Golgi apparatus, because these structures were undisturbed by BFA treatment that has been shown to cause disassembly (Fujiwara *et al*, 1988) and protein redistribution

(Doms *et al*, 1989) of the Golgi to the ER (Figure 3.21-3.23). This is consistent with similar findings for other proteins and other cellular systems (Johnston *et al*, 1998).

Thus, in agreement with a previously published study (Garcia-Mata *et al*, 1999), the current study shows that aggresome formation is not dependent on the presence of the proteosome inhibitor-MG132, and that aggresomes occur spontaneously in cells transiently transfected with mutant HBV constructs. Protein misfolding was necessary for aggresome formation, which did not occur to any extent in cells transfected with the wild-type constructs even in the presence of the proteasome inhibitor. The formation of aggresomes demonstrates that the precore/core protein encoded for by the G1862T mutant in HBV (G1982T in WHV) results in misfolding of the protein because misfolded proteins have been shown to be involved in aggresome formation (Garcia-Mata *et al*, 1999).

Aggresome formation has been proposed to be a generalized cellular response induced when the proteolytic degradation capabilities of the proteasome are surpassed by the production of incorrectly folded proteins (Johnston *et al*, 1998; Kopito & Sitia, 2000). It is a cellular cyto-protective mechanism in which the potentially toxic misfolded protein is transported to and disposed of in a centralized region (enclosure) (Johnston *et al*, 1998). This process decreases the intracellular levels of misfolded protein, enhances and facilitates their degradation, thereby increasing cell survival (Taylor *et al*, 2003; Arrasate *et al*, 2004; Tanaka *et al*, 2004a). These observations are consistent with the model proposed by Johnston *et al* (Johnston *et al*, 1998) and this model can therefore be used to describe the formation of aggressomes by mutant HBeAg precursor in the

case of both HBV and WHV in cells transfected with HBeAg-expression plasmids.

Viral infection and aggresomes

Although cytoplasmic inclusions have long been recognized as markers of viral infection, they have only more recently been shown to be aggresomes or aggresome-like structures. There has been a spurt of publications that describe the formation of aggresomes at various stages of the life cycle of a number of viruses. Moreover, the ability of aggresomes to concentrate proteins and attract chaperones, may make them suitable viral assembly sites (Heath *et al*, 2001; Wileman, 2006; Netherton *et al*, 2007). African swine fever virus (Heath *et al*, 2001), vaccinia virus (Ploubidou *et al*, 2000), Epstein-Barr virus (EBV) (Laszlo *et al*, 1991), overexpressed and misfolded Sin Nombre virus G1 protein (Spiropoulou *et al*, 2003), rabies virus (Lahaye *et al*, 2009), adenovirus type 5 E4 or F3 (Araujo *et al*, 2005) and E1B-55K (Liu *et al*, 2005) proteins have been shown to assemble spontaneously in the absence of proteasome inhibitors in sites that resemble aggresomes. In the case of herpes simplex virus 2, virus assembly occurs in aggresome-like structures that recruit chaperones, but unlike aggresomes do not require an intact microtubule network and are not characterized by a vimentin cage (Nozawa *et al*, 2004). In an attempt to evade class I MHC antigen presentation (Ploegh, 1998), EBV-encoded nuclear antigen 1 (EBNA1) has been shown to impair proteolysis by the ubiquitin-proteasome system (Levitskaya *et al*, 1997; Ploegh, 1998). Antigen processing and presentation are synchronized with dendritic cell maturation, by the storage of ubiquitinated influenza virus nucleoprotein in dendritic cell aggresome-like induced structures (Herter *et al*, 2005). Moreover, in earlier publications, parts of the aggresome pathway have

been reported to be activated during the assembly of several viruses. A vimentin cage has been shown to form around African swine fever virus (Heath *et al*, 2001), human immunodeficiency virus (Karczewski & Strebel, 1996), Theiler's virus (Nedellec *et al*, 1998), reovirus inclusions (Sharpe *et al*, 1982; Parker *et al*, 2002), vaccinia virus (Ferreira *et al*, 1994) and iridovirus assembly sites (Murti & Goorha, 1983). The present study is the first demonstration of aggresome formation as a result of the accumulation of hepadnaviral proteins.

ER stress, aggresome formation and liver disease progression

Hepatocytes have a well-developed ER structure that is crucial for the efficient and rapid synthesis of secretory proteins. ER stress response has been shown to induce mitochondrial dysfunction, up-regulate the synthesis of triglycerides and cholesterol, promote oxidative stress, initiate inflammatory response, and apoptosis (Ji, 2008; Zhang & Kaufman, 2008). All of these events play a role in the pathogenesis of liver disorders including genetic disorders of fibrinogen, fumaryl acetoacetate hydrolase, and α-1-antitrypsin, iron absorptions, saturated fat and cholesterol, heavy metals, lipopolysaccharide, reactive oxygen species and hyperhomocysteinemia, as well as acquired diseases caused by hepatitis B and C virus–induced viral hepatitis, drugs, alcohol, and scurvy (Kaplowitz *et al*, 2007; Ji, 2008). ER stress is involved in different liver-related disorders ranging from elevated alanine aminotransferase levels, fatty liver, keratin inclusions, inflammation, apoptosis, hepatitis, cirrhosis, liver failure and hepatocellular carcinoma (Arai *et al*, 2006; Ji & Kaplowitz, 2006; Wang *et al*, 2006; Ji, 2008) .

The retention of HBV mutant precore protein in the ER observed in this study can possibly be a contributing factor to HBV-related hepatocarcinogenesis. Two

types of LHBs produced by the pre-S1 and pre-S2 deletion mutants are retained in the ER, causing ER stress, inducing signal transactivators to activate different signaling pathways which may lead to hepatocarcinogensis (Wang *et al*, 2006). Pre-S deletion mutants can upregulate cyclooxygenase-2 (Hung *et al*, 2004), and cyclin A to induce cell cycle progression and nodular proliferation in hepatocytes of transgenic mice (Wang *et al*, 2005). Moreover, the overexpression of cytoplasmic cyclin A may be initiated by ER stress, and may contribute to the increased multi-nucleation and DNA aneuploidy observed in the transgenic mice liver expressing defective pre-S proteins (Wang *et al*, 2005). ER stress triggered by pre-S deletion mutants induces oxidative stress, which leads to oxidative DNA damage of HBV-infected hepatocytes (Hsieh *et al*, 2004). Oxidative DNA damage may result in genomic instability, mutation of hepatocytes, and eventually progress to HCC (Wang *et al*, 2006). HBV pre-S mutants play a role in the model of ER stress associated viral-related hepatocarcinogenesis (Wang *et al*, 2006).

The aggresomes formed in cells transfected with G1862T mutant construct resembled Mallory-Denk bodies, aggresomes found in primary hepatocytes (Riley *et al*, 2002). In 1911, F.B. Mallory first described cytoplasmic hyaline inclusions in hepatocytes of alcoholic hepatitis patient, and this type of inclusion was initially called Mallory body (Mallory, 1911). In 1975, H. Denk and colleagues described the first animal model of Mallory body, renamed Mallory-Denk body (Zatloukal *et al*, 2007). Mallory-Denk bodies can be found in variable sizes (Mallory, 1911); small inclusions are associated with intermediate filament throughout cytoplasm and the large inclusions are located within the perinuclear region of hepatocytes (Denk *et al*, 2000; Ku *et al*, 2007; Zatloukal *et al*, 2007; Strnad *et al*, 2008). The major components of the Mallory-Denk bodies are

keratin 8/18, ubiquitin and sequestosome 1/p62-a stress inducible adapter protein that has high affinity for polyubiquitinated proteins (Stumptner *et al*, 2007; Strnad *et al*, 2008). Hsp70, Hsp90, subunits of 20S and 26S proteasome are the minor constituents of the Mallory-Denk bodies (Riley *et al*, 2002; Riley *et al*, 2003). Re-arrangement of cytokeratin that is related to the formation of Mallory-Denk bodies in hepatocytes was also observed in cells transfected with the G1862T mutant construct (Figure 3.45-3.49). Mallory bodies have been shown to form in diseased liver, ranging from childhood cirrhosis, alcoholic hepatitis, alcoholic cirrhosis, Wilson's disease, primary biliary cirrhosis, nonalcoholic cirrhosis and hepatocellular carcinoma (Jensen & Gluud, 1994). Aggresome formation in liver cells has been implicated in hereditary liver diseases including α-1-antitrypsin deficiency (Propst *et al*, 1994; Rudnick *et al*, 2004) and hereditary tyrosinemia type 1 (Kvittingen, 1986), which can develop into hepatocellular carcinoma.

The G1862T mutation is characteristic of subgenotype A1 of HBV. In this study, it was shown that the introduction of this mutation into genotype A precore context plasmid lead to the accumulation of the precursor of HBeAg in the ERGIC. This is as a result of Phe substitution at -3 position interfering with signal peptide cleavage and preventing maturation of the precursor into HBeAg. Furthermore, the accumulation of the HBeAg was shown to lead to the formation of aggresomes.

From the available data, the consequences and implications of aggresome formation by mutant HBeAg and WHeAg precursor molecules with respect to liver disease progression are difficult to predict. In three studies (Kimbi *et al*, 2004; Sugauchi *et al*, 2004a; Tanaka *et al*, 2004b) in which the patients/carriers

were infected with subgenotype A1, the G1862T mutation was found in 35 patients with liver disease and 14 asymptomatic carriers (ASCs), whereas the wild-type sequence was detected in only 9 patients with liver disease and 20 ASCs ($P<0.001$). In the study of Hou *et al*, the G1862T mutation was detected in 13.7 % of Chinese patients with genotype B HBV induced fulminant hepatitis compared with 2.5 % chronic carriers of the virus (the prevalence of the mutation in uncomplicated acute hepatitis B was not studied), and it was concluded that the variant may be a contributing factor in fulminant hepatitis (Hou *et al*, 2002; Inoue *et al*, 2009). However, these analyses were not in the case control format with respect to the presence or absence of G1862T and thus it is difficult to reach any firm conclusions. Moreover, in the one study that showed subgenotype A1 to be more hepatocarcinogenic than other genotypes and subgenotypes, the presence of G1862T was not determined (Kew *et al*, 2005). Therefore prospective, longitudinal studies to follow the development of liver disease in relation to the G1862T mutant are necessary together with further transfection studies with subgenotype A1 replication competent constructs with authentic promoters.

APPENDICES

APPENDIX A SOLUTIONS AND REAGENTS

A1. *Luria-Bertini broth agar plates with ampicillin*

15 g agar (Pronadisa, Madrid)

10 g Tryptone (Pronadisa, Madrid)

5 g yeast extract (Pronadisa, Madrid)

10 g NaCl

Make up to 1 litre with distilled water and autoclave. Cool to 55 ^{o}C, followed by the addition of 1 ml of ampicillin (50mg/ml). Pour into 60mm petri dishes and store at 4 ^{o}C.

A2. *Luria-Bertini broth (LB) (1 litre)*

10 g Tryptone (Pronadisa, Madrid)

5g yeast extract (Pronadisa, Madrid)

10 g NaCl

Make up to 1 litre with distilled water and autoclave.

A3. *Ampicillin (50 mg/ml)*

1 g ampicillin (Roche, Germany)

Make up to a final volume of 20 ml with distilled water. Sterilize by filtration using 0.22 µm filter (Sartorius, Germany). Solution is stored in 1 ml aliquots at -20^{o}C.

A4. *1% Agarose*

1 g agarose

10 ml 10x TBE

Make up to 100 ml with distilled water

A5. *10 X gel loading dye*

50 % (v/v) glycerol

0.25 % (w/v) bromophenol blue

0.25 % xylene cyanol

0.1 M ETDA pH8

Make up to volume with distilled water.

A6. *10x Tris Boric Acid EDTA Buffer (TBE)*

2.5 litres of 10x TBE

270 g Tris base (Roche, Germany)

127.5 g Boric acid (Sigma-Aldrich, USA)

18.6 g of EDTA (Saarchem, SA)

Make up to 2.5 litres with distilled water and autoclave.

A7. *Luria-Bertini broth agar plates with kanamycin*

15 g agar (Pronadisa, Madrid)

10 g Tryptone (Pronadisa, Madrid)

5 g yeast extract (Pronadisa, Madrid)

10 g NaCl

Make up to 1 litre with distilled water and autoclave. Cool to 55 ^{o}C and add 1 ml of kanamycin (50mg/ml). Pour into 60mm petri dishes and store at 4 ^{o}C.

A8. *kanaymycin (50 mg/ml)*

1 g kanamycin (Roche, Germany)

Make up to a final volume of 20 ml with distilled water. Sterilize by filtration using 0.22 µm filter (Sartorius, Germany). The solution is stored in 1 ml aliquots at -20 ^{o}C.

A9. *ISE-RPMI 1640 medium*

10.4 g Powdered Roswell Park Memorial Institute (RPMI) 1640 + L-Glutamine (Gibco-BRL, UK)

1.19 g Hepes (Roche, Germany)

2 g $NaHCO_3$ (Saarchem, SA)

Dissolve in 1 litre of distilled water. Add the following filter sterilized supplements:

1 ml Na_2SeO_3 (3 x 10^{-5} M)

1 ml $FeSO_4.7H_2O$ (1 x 10^{-4} M)

1 ml of solution 3: $(NH_4)_6MO_7O_2.4H_2O$ (3 x 10^{-6} M)/ $MnCl_2.4H_2O$ (3 x 10^{-7} M)/ NH_4VO_3 (1 x 10^{-5} M)

100 µl Linoleic/Oleic acid BSA complex (3 x 10^{-5} M)

1 ml Ethanolamine (3 x 10^{-2} M)

The ISE-RPMI1640 medium was prepared from RPMI-1640 powder, with L-Glutamine (51800-035) (Gibco, Scotland, UK), buffering salts, trace elements, fatty acids supplements. The pH was adjusted to 7.12, sterilized by filtration using the 0.22 µm filter (Sartorius, Germany). The medium was stored at 4^{o}C for a maximum period of one month.

Stock solution for the supplements:

All supplement stock solutions were sterilized by membrane filtration using 0.22 filters and stored at -20 ^{o}C

Na_2SeO_3 (3 x 10^{-5} M)

Dissolved 518.7 mg of Na_2SeO_3 (Sigma-Aldrich, USA) in 100 ml distilled water and dilute at 1/1000.

$FeSO_4.7H_2O$ (1 x 10^{-4} M)

Dissolve 278 mg $FeSO_4.7H_2O$ (Sigma-Aldrich, USA) in 100 ml distilled water, add one drop of concentrated HCL, and then dilute at 1/100.

$(NH_4)_6MO_7O_2.4H_2O$ (3 x 10^{-6} M)

Dissolve 37.1mg $(NH_4)_6MO_7O_2.4H_2O$ (Sigma-Aldrich, USA) in 100 ml of distilled water, dissolve 59.4 mg of $MnCl_2.4H_2O$ (Sigma-Aldrich, USA) in 100 ml of distilled water and dilute to 1/100, dissolve 11.7 mg NH_4VO_3 (Sigma-Aldrich, USA) in 100 ml of distilled water. Combine the three solutions together.

Linoleic/Oleic acid BSA complex (3 x 10^{-5} M)

Dissolve 302 µg linoleic acid and 10 mg linoleic acid-water soluable (Sigma-Aldrich, USA), 305.8 µg oleic acid and 9.38 mg oleic acid soluable (Sigma-Aldrich, USA) in 36 ml of distilled water.

Ethanolamine (3 x 10^{-2} M)

Dissolve 183.2 mg ethanolamine (Sigma-Aldrich, USA) in 100 ml of

distilled water.

A10. *0.01 % (w/v) ethylene diamine tetra-acetic acid di-sodium salt (EDTA) / PBS*

0.5 g ethylene diamine tetra-acetic acid di-sodium salt (EDTA) (Saarchem, SA)

Make up to 50 ml with PBS to prepare the 1 % (w/v) stock solution. Prepare the final 0.01 % (w/v) solution from the 1 % stock solution with PBS.

A11. *Cell lysis buffer*

10 mM HEPES (pH 7.5)

100 mM NaCl

1 mM EDTA

1% (v/v) NP-40

The lysis buffer was prepared and filter sterilized.

A12. *10 mM $CaCl_2$-12 mM $MgCl_2$*

100 mM $CaCl_2$

120 mM $MgCl_2$

Prepare the 10 X concentration stock of both $CaCl_2$ and 120 mM $MgCl_2$ with cell lysis buffer (A11). The solution was prepared and autoclaved. Add 1/10 volume to the supernatant.

A13. *PEG solution*

1.2 M NaCl

60 mM EDTA

30% (w/v) sucrose

26% (w/v) PEG 8000

The solution was prepared and autoclaved.

A14. *Resuspension solution for enzyme digestion*

10 mM Tris (pH 7.5)

6 mM $MgCl_2$

8 mM $CaCl_2$

A15. *Stop solution for enzyme activity*

50 mM EDTA

10 mM Tris –HCl buffer, pH 7.5

A16. *Lysis solution for pulse chased cells*

50 mM Tris-HCl, pH 7.5

150 mM NaCl

1 % (v/v) Nonidet P40

0.5 % (w/v) sodium dexoycholate

Protease inhibitor cocktail-Complete® (Roche, Germany) was added just before experiments.

A17. *Washing buffer 1*

50 mM Tris-HCl, pH 7.5

500 mM NaCl

0.1 % (v/v) Nonident P40

0.05 % (w/v) sodium deoxycholate

Protease inhibitor cocktail-Complete® was added just before experiments.

A18. *Washing buffer 2*

10 mM Tris-HCl, pH 7.5

0.1 % (v/v) Nonident P40

0.05 % (w/v) sodium deoxycholate

Protease inhibitor cocktail-Complete® was added just before experiments.

A19. *loading buffer*

50 ml 1M Tris pH 6.8

30 g SDS

1 g bromophenol blue

100ml glycerol

Make up to 250 ml with distilled water , and add 100 µl of 2M

dithiothreitol (DTT) to 400 ml.

A20. *30% acrylamide solution*

30 g acrylamide (Sigma, Germany)

0.8 g bisacrylamide (Promega, USA)

Make up to 100 ml with distilled water.

A21. *15% Protein gel mix*

96 ml water

100 ml 1.5M Tris pH 8.8

2 ml 20% (w/v) SDS

For 1 gel use 4.9 ml of this plus

5 ml of 30% acrylamide (Sigma, Germany)

0.1 ml of 10% APS (Ammonium persulphate, Promega, USA)

4 µl of TEMED (Promega, USA)

A22. *Stacking gel mix*

139.75ml distilled water

63 ml 0.5M Tris pH 6.8

1.25 ml 20% SDS

For 1 gel use 2.04 ml of this plus

415 µl of 30% acrylamide (Sigma, Germany)

25 µl of 10% APS (Ammonium persulphate, Promega, USA)

2.5 µl of TEMED (Promega, USA)

A23. *Protein running buffer 10x*

75 g Tris base

470 g Glycine

25 g SDS

Make up to 2.5 litres with distilled water.

A24. *SDS-PAGE fixative solution*

10 % (v/v) acetic acid

40 % (v/v) methanol

Make up to volume with distilled water.

A25. *Acetic acid, methanol and glycerol solution*

7 % (v/v) acetic acid,

7 % (v/v) methanol

10 % (v/v) glycerol

Make up to volume with distilled water.

A26. *4 % (w/v) Paraformaldehyde, fixative solution*

4 g paraformaldehyde (Saarchem, SA)

100 ml of PBS

Dissolve 4 g of paraformaldehyde with 100 ml of boiling PBS (A28). Add 1 M sodium hydroxide solution drop by drop to adjust the pH to 7.4.

A27. *Phosphate buffered saline (PBS)*

0.2 g KCl

8 g NaCl

0.2 g KH2PO4

1.15 g Na2H2PO4

Dissolve, make up volume to 1 *l* and adjust pH to 7.4.

A28. *0.01 % (v/v) Trixton X-100 solution*

1 ml Trixton X-100 (Roche, Mannheim, Germany) } 1 % (v/v) stock solution

99 ml PBS

0.01 % Trixton X-100 solution is diluted from the 1 % stock solution with PBS.

A29. *Blocking solution, 1 % (w/v) BSA*

1g BSA (Roche, Mannheim, Germany)

Make up to 100 ml with PBS.

APPENDIX B HUMAN ETHIC CLEARANCE CERTIFICATE

UNIVERSITY OF THE WITWATERSRAND, JOHANNESBURG
Division of the Deputy Registrar (Research)

HUMAN RESEARCH ETHICS COMMITTEE (MEDICAL)
R14/49 Miss Chien-Yu Chen

CLEARANCE CERTIFICATE	**M10225**
PROJECT	Effect of the 1862 Mutation on the Replication of the Hepatitis B Virus
INVESTIGATORS	Miss Chien-Yu Chen.
DEPARTMENT	Internal Medicine
DATE CONSIDERED	26/02/2010
DECISION OF THE COMMITTEE*	Approved unconditionally

Unless otherwise specified this ethical clearance is valid for 5 years and may be renewed upon application.

DATE 26/02/2010 **CHAIRPERSON** .....
(Professor PE Cleaton-Jones)

*Guidelines for written 'informed consent' attached where applicable
cc: Supervisor : Prof A Kramvis

DECLARATION OF INVESTIGATOR(S)

To be completed in duplicate and **ONE COPY** returned to the Secretary at Room 10004, 10th Floor, Senate House, University.
I/We fully understand the conditions under which I am/we are authorized to carry out the abovementioned research and I/we guarantee to ensure compliance with these conditions. Should any departure to be contemplated from the research procedure as approved I/we undertake to resubmit the protocol to the Committee. **I agree to a completion of a yearly progress report.**

PLEASE QUOTE THE PROTOCOL NUMBER IN ALL ENQUIRIES...

REFERENCES

Abraham TM, Loeb DD (2006) Base pairing between the 5' half of epsilon and a cis-acting sequence, phi, makes a contribution to the synthesis of minus-strand DNA for human hepatitis B virus. *J Virol* 80(9)**:** 4380-4387

Abraham TM, Loeb DD (2007) The topology of hepatitis B virus pregenomic RNA promotes its replication. *J Virol* 81(21)**:** 11577-11584

Ahn SH, Kramvis A, Kawai S, Spangenberg HC, Li J, Kimbi G, Kew M, Wands J, Tong S (2003) Sequence variation upstream of precore translation initiation codon reduces hepatitis B virus e antigen production. *Gastroenterology* 125(5)**:** 1370-1378

Ahn YO (1996) Strategy for vaccination against hepatitis B in areas with high endemicity: focus on Korea. *Gut* 38 Suppl 2**:** S63-66

Alberti A, Diana S, Scullard GH, Eddleston WF, Williams R (1978) Full and empty Dane particles in chronic hepatitis B virus infection: relation to hepatitis B e antigen and presence of liver damage. *Gastroenterology* 75(5)**:** 869-874

Appenzeller-Herzog C, Hauri HP (2006) The ER-Golgi intermediate compartment (ERGIC): in search of its identity and function. *J Cell Sci* 119(Pt 11)**:** 2173-2183

Appenzeller C, Andersson H, Kappeler F, Hauri HP (1999) The lectin ERGIC-53 is a cargo transport receptor for glycoproteins. *Nat Cell Biol* 1(6)**:** 330-334

Arai M, Kondoh N, Imazeki N, Hada A, Hatsuse K, Kimura F, Matsubara O, Mori K, Wakatsuki T, Yamamoto M (2006) Transformation-associated gene regulation by ATF6alpha during hepatocarcinogenesis. *FEBS Lett* 580(1)**:** 184-190

Araujo FD, Stracker TH, Carson CT, Lee DV, Weitzman MD (2005) Adenovirus type 5 E4orf3 protein targets the Mre11 complex to cytoplasmic aggresomes. *J Virol* 79(17)**:** 11382-11391

Araujo NM, Vianna CO, Soares CC, Gomes SA (2008) A unique amino acid substitution, L215Q, in the hepatitis B virus small envelope protein of a genotype F isolate that inhibits secretion of hepatitis B virus subviral particles. *Intervirology* 51(2)**:** 81-86

Arauz-Ruiz P, Norder H, Robertson BH, Magnius LO (2002) Genotype H: a new Amerindian genotype of hepatitis B virus revealed in Central America. *J Gen Virol* 83(Pt 8)**:** 2059-2073

Arauz-Ruiz P, Norder H, Visona KA, Magnius LO (1997) Genotype F prevails in HBV infected patients of hispanic origin in Central America and may carry the precore stop mutant. *J Med Virol* 51(4)**:** 305-312

Arbuthnot P, Capovilla A, Kew M (2000) Putative role of hepatitis B virus X protein in hepatocarcinogenesis: effects on apoptosis, DNA repair, mitogen-activated protein kinase and JAK/STAT pathways. *J Gastroenterol Hepatol* 15(4)**:** 357-368

Arrasate M, Mitra S, Schweitzer ES, Segal MR, Finkbeiner S (2004) Inclusion body formation reduces levels of mutant huntingtin and the risk of neuronal death. *Nature* 431(7010)**:** 805-810

Arvan P, Zhao X, Ramos-Castaneda J, Chang A (2002) Secretory pathway quality control operating in Golgi, plasmalemmal, and endosomal systems. *Traffic* 3(11)**:** 771-780

Banerjee A, Kurbanov F, Datta S, Chandra PK, Tanaka Y, Mizokami M, Chakravarty R (2006) Phylogenetic relatedness and genetic diversity of hepatitis B virus isolates in Eastern India. *J Med Virol* 78(9)**:** 1164-1174

Bang G, Kim KH, Guarnieri M, Zoulim F, Kawai S, Li J, Wands J, Tong S (2005) Effect of mutating the two cysteines required for HBe antigenicity on hepatitis B virus DNA replication and virion secretion. *Virology* 332(1)**:** 216-224

Bannykh SI, Rowe T, Balch WE (1996) The organization of endoplasmic reticulum export complexes. *J Cell Biol* 135(1)**:** 19-35

Baptista M, Kramvis A, Kew MC (1999) High prevalence of 1762(T) 1764(A) mutations in the basic core promoter of hepatitis B virus isolated from black Africans with hepatocellular carcinoma compared with asymptomatic carriers. *Hepatology* 29(3)**:** 946-953

Bartenschlager R, Junker-Niepmann M, Schaller H (1990) The P gene product of hepatitis B virus is required as a structural component for genomic RNA encapsidation. *J Virol* 64(11)**:** 5324-5332

Bartenschlager R, Schaller H (1992) Hepadnaviral assembly is initiated by polymerase binding to the encapsidation signal in the viral RNA genome. *Embo J* 11(9)**:** 3413-3420

Beasley RP (1988) Hepatitis B virus. The major etiology of hepatocellular carcinoma. *Cancer* 61(10)**:** 1942-1956

Beck J, Nassal M (1997) Sequence- and structure-specific determinants in the interaction between the RNA encapsidation signal and reverse transcriptase of avian hepatitis B viruses. *J Virol* 71(7)**:** 4971-4980

Beck J, Nassal M (2007) Hepatitis B virus replication. *World J Gastroenterol* 13(1)**:** 48-64

Bence NF, Sampat RM, Kopito RR (2001) Impairment of the ubiquitin-proteasome system by protein aggregation. *Science* 292(5521)**:** 1552-1555

Bendtsen JD, Nielsen H, von Heijne G, Brunak S (2004) Improved prediction of signal peptides: SignalP 3.0. *J Mol Biol* 340(4)**:** 783-795

Bennett EJ, Bence NF, Jayakumar R, Kopito RR (2005) Global impairment of the ubiquitin-proteasome system by nuclear or cytoplasmic protein aggregates precedes inclusion body formation. *Mol Cell* 17(3)**:** 351-365

Beterams G, Bottcher B, Nassal M (2000) Packaging of up to 240 subunits of a 17 kDa nuclease into the interior of recombinant hepatitis B virus capsids. *FEBS Lett* 481(2)**:** 169-176

Betts MJ, Russell RB (2003) Amino acid properties and consequences of subsitutions. *Bioinformatics for Geneticists Barnes,MR and Gray, IC eds Wiley*

Birnbaum F, Nassal M (1990) Hepatitis B virus nucleocapsid assembly: primary structure requirements in the core protein. *J Virol* 64(7)**:** 3319-3330

Blanchet M, Sureau C (2007) Infectivity determinants of the hepatitis B virus pre-S domain are confined to the N-terminal 75 amino acid residues. *J Virol* 81(11)**:** 5841-5849

Blobel G, Dobberstein B (1975) Transfer of proteins across membranes. I. Presence of proteolytically processed and unprocessed nascent immunoglobulin light chains on membrane-bound ribosomes of murine myeloma. *J Cell Biol* 67(3)**:** 835-851

Blumberg BS, and H. J. Alter. (1967) A "new" antigen in leukemic serum. *JAMA* 191**:** 541-546

Bogaert R, Tiller GE, Weis MA, Gruber HE, Rimoin DL, Cohn DH, Eyre DR (1992) An amino acid substitution (Gly853-->Glu) in the collagen alpha 1(II) chain produces hypochondrogenesis. *J Biol Chem* 267(31)**:** 22522-22526

Bosch FX, Ribes J, Cleries R, Diaz M (2005) Epidemiology of hepatocellular carcinoma. *Clin Liver Dis* 9(2)**:** 191-211, v

Bowyer SM, van Staden L, Kew MC, Sim JG (1997) A unique segment of the hepatitis B virus group A genotype identified in isolates from South Africa. *J Gen Virol* 78 (Pt 7)**:** 1719-1729

Brodsky JL, McCracken AA (1999) ER protein quality control and proteasome-mediated protein degradation. *Semin Cell Dev Biol* 10(5)**:** 507-513

Brown (1999) *Genomes*: Oxford: Bios Scientific Publishers.

Bruss V (2004) Envelopment of the hepatitis B virus nucleocapsid. *Virus Res* 106(2)**:** 199-209

Bruss V (2007) Hepatitis B virus morphogenesis. *World J Gastroenterol* 13(1)**:** 65-73

Bruss V, Ganem D (1991) The role of envelope proteins in hepatitis B virus assembly. *Proc Natl Acad Sci U S A* 88(3)**:** 1059-1063

Bruss V, Gerlich WH (1988) Formation of transmembraneous hepatitis B e-antigen by cotranslational in vitro processing of the viral precore protein. *Virology* 163(2)**:** 268-275

Bruss V, Hagelstein J, Gerhardt E, Galle PR (1996) Myristylation of the large surface protein is required for hepatitis B virus in vitro infectivity. *Virology* 218(2)**:** 396-399

Buckwold VE, Xu Z, Chen M, Yen TS, Ou JH (1996) Effects of a naturally occurring mutation in the hepatitis B virus basal core promoter on precore gene expression and viral replication. *J Virol* 70(9)**:** 5845-5851

Burnett RJ, Francois G, Kew MC, Leroux-Roels G, Meheus A, Hoosen AA, Mphahlele MJ (2005) Hepatitis B virus and human immunodeficiency virus co-infection in sub-Saharan Africa: a call for further investigation. *Liver Int* 25(2)**:** 201-213

Caldwell SR, Hill KJ, Cooper AA (2001) Degradation of endoplasmic reticulum (ER) quality control substrates requires transport between the ER and Golgi. *J Biol Chem* 276(26)**:** 23296-23303

Carlier D, Jean-Jean O, Rossignol JM (1994) Characterization and biosynthesis of the woodchuck hepatitis virus e antigen. *J Gen Virol* 75 (Pt 1)**:** 171-175

Carman WF, Jacyna MR, Hadziyannis S, Karayiannis P, McGarvey MJ, Makris A, Thomas HC (1989) Mutation preventing formation of hepatitis B e antigen in patients with chronic hepatitis B infection. *Lancet* 2(8663)**:** 588-591

Cattaneo R, Will H, Hernandez N, Schaller H (1983) Signals regulating hepatitis B surface antigen transcription. *Nature* 305(5932)**:** 336-338

Cattaneo R, Will H, Schaller H (1984) Hepatitis B virus transcription in the infected liver. *Embo J* 3(9)**:** 2191-2196

Cavinta L, Sun J, May A, Yin J, von Meltzer M, Radtke M, Barzaga NG, Cao G, Schaefer S (2009) A new isolate of hepatitis B virus from the Philippines possibly representing a new subgenotype C6. *J Med Virol* 81(6)**:** 983-987

Ceres P, Zlotnick A (2002) Weak protein-protein interactions are sufficient to drive assembly of hepatitis B virus capsids. *Biochemistry* 41(39)**:** 11525-11531

Chandra PK, Biswas A, Datta S, Banerjee A, Panigrahi R, Chakrabarti S, De BK, Chakravarty R (2009) Subgenotypes of hepatitis B virus genotype D (D1, D2, D3 and D5) in India: differential pattern of mutations, liver injury and occult HBV infection. *J Viral Hepat* 16(10)**:** 749-756

Chang C, Enders G, Sprengel R, Peters N, Varmus HE, Ganem D (1987) Expression of the precore region of an avian hepatitis B virus is not required for viral replication. *J Virol* 61(10)**:** 3322-3325

Chang LJ, Ganem D, Varmus HE (1990a) Mechanism of translation of the hepadnaviral polymerase (P) gene. *Proc Natl Acad Sci U S A* 87(13)**:** 5158-5162

Chang LJ, Hirsch RC, Ganem D, Varmus HE (1990b) Effects of insertional and point mutations on the functions of the duck hepatitis B virus polymerase. *J Virol* 64(11)**:** 5553-5558

Chen HS, Kaneko S, Girones R, Anderson RW, Hornbuckle WE, Tennant BC, Cote PJ, Gerin JL, Purcell RH, Miller RH (1993) The woodchuck hepatitis virus X gene is important for establishment of virus infection in woodchucks. *J Virol* 67(3)**:** 1218-1226

Chen HS, Kew MC, Hornbuckle WE, Tennant BC, Cote PJ, Gerin JL, Purcell RH, Miller RH (1992) The precore gene of the woodchuck hepatitis virus genome is not essential for viral replication in the natural host. *J Virol* 66(9)**:** 5682-5684

Chen M, Sallberg M, Hughes J, Jones J, Guidotti LG, Chisari FV, Billaud JN, Milich DR (2005) Immune tolerance split between hepatitis B virus precore and core proteins. *J Virol* 79(5)**:** 3016-3027

Chen MT, Billaud JN, Sallberg M, Guidotti LG, Chisari FV, Jones J, Hughes J, Milich DR (2004) A function of the hepatitis B virus precore protein is to regulate the immune response to the core antigen. *Proc Natl Acad Sci U S A* 101(41)**:** 14913-14918

Chen YC, Delbrook K, Dealwis C, Mimms L, Mushahwar IK, Mandecki W (1996) Discontinuous epitopes of hepatitis B surface antigen derived from a filamentous phage peptide library. *Proc Natl Acad Sci U S A* 93(5)**:** 1997-2001

Chiaramonte M, Stroffolini T, Ngatchu T, Rapicetta M, Lantum D, Kaptue L, Chionne P, Conti S, Sarrecchia B, Naccarato R (1991) Hepatitis B virus infection in Cameroon: a seroepidemiological survey in city school children. *J Med Virol* 33(2)**:** 95-99

Chothia C (1976) The nature of the accessible and buried surfaces in proteins. *J Mol Biol* 105(1)**:** 1-12

Chouteau P, Le Seyec J, Cannie I, Nassal M, Guguen-Guillouzo C, Gripon P (2001) A short N-proximal region in the large envelope protein harbors a determinant that contributes to the species specificity of human hepatitis B virus. *J Virol* 75(23)**:** 11565-11572

Chua PK, Wang RY, Lin MH, Masuda T, Suk FM, Shih C (2005) Reduced secretion of virions and hepatitis B virus (HBV) surface antigen of a naturally occurring HBV variant correlates with the accumulation of the small S envelope protein in the endoplasmic reticulum and Golgi apparatus. *J Virol* 79(21)**:** 13483-13496

Chuang WL, Chang WY, Lu SN, Su WP, Lin ZY, Chen SC, Hsieh MY, Wang LY, You SL, Chen CJ (1992) The role of hepatitis B and C viruses in

hepatocellular carcinoma in a hepatitis B endemic area. A case-control study. *Cancer* 69(8)**:** 2052-2054

Colgrove R, Simon G, Ganem D (1989) Transcriptional activation of homologous and heterologous genes by the hepatitis B virus X gene product in cells permissive for viral replication. *J Virol* 63(9)**:** 4019-4026

Conway JF, Cheng N, Zlotnick A, Wingfield PT, Stahl SJ, Steven AC (1997) Visualization of a 4-helix bundle in the hepatitis B virus capsid by cryo-electron microscopy. *Nature* 386(6620)**:** 91-94

Cooper MS, Cornell-Bell AH, Chernjavsky A, Dani JW, Smith SJ (1990) Tubulovesicular processes emerge from trans-Golgi cisternae, extend along microtubules, and interlink adjacent trans-golgi elements into a reticulum. *Cell* 61(1)**:** 135-145

Crowther RA, Kiselev NA, Bottcher B, Berriman JA, Borisova GP, Ose V, Pumpens P (1994) Three-dimensional structure of hepatitis B virus core particles determined by electron cryomicroscopy. *Cell* 77(6)**:** 943-950

Csala M, Banhegyi G, Benedetti A (2006) Endoplasmic reticulum: a metabolic compartment. *FEBS Lett* 580(9)**:** 2160-2165

Dane DS, Cameron CH, Briggs M (1970) Virus-like particles in serum of patients with Australia-antigen-associated hepatitis. *Lancet* 1(7649)**:** 695-698

Dayel MJ, Hom EF, Verkman AS (1999) Diffusion of green fluorescent protein in the aqueous-phase lumen of endoplasmic reticulum. *Biophys J* 76(5)**:** 2843-2851

de Bruin WC, Hertogs K, Leenders WP, Depla E, Yap SH (1995) Hepatitis B virus: specific binding and internalization of small HBsAg by human hepatocytes. *J Gen Virol* 76 (Pt 4)**:** 1047-1050

De Los Rios P, Ben-Zvi A, Slutsky O, Azem A, Goloubinoff P (2006) Hsp70 chaperones accelerate protein translocation and the unfolding of stable protein aggregates by entropic pulling. *Proc Natl Acad Sci U S A* 103(16)**:** 6166-6171

De Meyer S, Gong ZJ, Suwandhi W, van Pelt J, Soumillion A, Yap SH (1997) Organ and species specificity of hepatitis B virus (HBV) infection: a review of literature with a special reference to preferential attachment of HBV to human hepatocytes. *J Viral Hepat* 4(3)**:** 145-153

Delius H, Gough NM, Cameron CH, Murray K (1983) Structure of the hepatitis B virus genome. *J Virol* 47(2)**:** 337-343

Denk H, Stumptner C, Zatloukal K (2000) Mallory bodies revisited. *J Hepatol* 32(4)**:** 689-702

Devesa M, Loureiro CL, Rivas Y, Monsalve F, Cardona N, Duarte MC, Poblete F, Gutierrez MF, Botto C, Pujol FH (2008) Subgenotype diversity of hepatitis B virus American genotype F in Amerindians from Venezuela and the general population of Colombia. *J Med Virol* 80(1)**:** 20-26

Devesa M, Pujol FH (2007) Hepatitis B virus genetic diversity in Latin America. *Virus Res* 127(2)**:** 177-184

Dictenberg JB, Zimmerman W, Sparks CA, Young A, Vidair C, Zheng Y, Carrington W, Fay FS, Doxsey SJ (1998) Pericentrin and gamma-tubulin form a protein complex and are organized into a novel lattice at the centrosome. *J Cell Biol* 141(1)**:** 163-174

Dierstein R, Wickner W (1986) Requirements for substrate recognition by bacterial leader peptidase. *Embo J* 5(2)**:** 427-431

Doms R, Russ G, Yewdell J (1989) Brefeldin A redistributes resident and itinerant Golgi proteins to the endoplasmic reticulum. *J Cell Biol* 109(1)**:** 61-72

Doudna JA, Batey RT (2004) Structural insights into the signal recognition particle. *Annu Rev Biochem* 73**:** 539-557

Dusheiko GM, Bowyer SM, Sjogren MH, Ritchie MJ, Santos AP, Kew MC (1985) Replication of hepatitis B virus in adult carriers in an endemic area. *J Infect Dis* 152(3)**:** 566-571

Dusheiko GM, Brink BA, Conradie JD, Marimuthu T, Sher R (1989a) Regional prevalence of hepatitis B, delta, and human immunodeficiency virus infection in southern Africa: a large population survey. *Am J Epidemiol* 129(1)**:** 138-145

Dusheiko GM, Conradie JD, Brink BA, Marimuthu T, Sher R (1989b) Differences in the regional prevalence of chronic hepatitis B in southern Africa--implications for vaccination. *S Afr Med J* 75(10)**:** 473-478

Eckhardt SG, Milich DR, McLachlan A (1991) Hepatitis B virus core antigen has two nuclear localization sequences in the arginine-rich carboxyl terminus. *J Virol* 65(2)**:** 575-582

Egea PF, Stroud RM, Walter P (2005) Targeting proteins to membranes: structure of the signal recognition particle. *Curr Opin Struct Biol* 15(2)**:** 213-220

Ekici OD, Karla A, Paetzel M, Lively MO, Pei D, Dalbey RE (2007) Altered -3 substrate specificity of Escherichia coli signal peptidase 1 mutants as revealed by screening a combinatorial peptide library. *J Biol Chem* 282(1)**:** 417-425

Ellgaard L HA (2004) Quality control in the endoplasmic reticulum. *Nat Rev Mol Cell Biol* 4**:** 181 - 191

Ellgaard L, Helenius A (2003) Quality control in the endoplasmic reticulum. *Nat Rev Mol Cell Biol* 4(3)**:** 181-191

Ellgaard L, Molinari M, Helenius A (1999) Setting the standards: quality control in the secretory pathway. *Science* 286(5446)**:** 1882-1888

Fallows DA, Goff SP (1995) Mutations in the epsilon sequences of human hepatitis B virus affect both RNA encapsidation and reverse transcription. *J Virol* 69(5)**:** 3067-3073

Fan JY, Roth J, Zuber C (2007) Expression of mutant Ins2C96Y results in enhanced tubule formation causing enlargement of pre-Golgi intermediates of CHO cells. *Histochem Cell Biol* 128(2)**:** 161-173

Feitelson MA (1994) Biology of hepatitis B virus variants. *Lab Invest* 71(3)**:** 324-349

Fernholz D, Galle PR, Stemler M, Brunetto M, Bonino F, Will H (1993) Infectious hepatitis B virus variant defective in pre-S2 protein expression in a chronic carrier. *Virology* 194(1)**:** 137-148

Ferreira LR, Moussatche N, Moura Neto V (1994) Rearrangement of intermediate filament network of BHK-21 cells infected with vaccinia virus. *Arch Virol* 138(3-4)**:** 273-285

Fields HA, Hollinger FB, Desmyter J, Melnick JL, Dreesman GR (1977) Biochemical and biophysical properties of hepatitis B core particles derived from Dane particles and infected hepatocytes. *Intervirology* 8(6)**:** 336-350

Fikes JD, Barkocy-Gallagher GA, Klapper DG, Bassford PJ, Jr. (1990) Maturation of Escherichia coli maltose-binding protein by signal peptidase I in

vivo. Sequence requirements for efficient processing and demonstration of an alternate cleavage site. *J Biol Chem* 265(6)**:** 3417-3423

Francois G, Kew M, Van Damme P, Mphahlele MJ, Meheus A (2001) Mutant hepatitis B viruses: a matter of academic interest only or a problem with far-reaching implications? *Vaccine* 19(28-29)**:** 3799-3815

Freed EO (2004) HIV-1 and the host cell: an intimate association. *Trends Microbiol* 12(4)**:** 170-177

Friguet B, Stadtman ER, Szweda LI (1994) Modification of glucose-6-phosphate dehydrogenase by 4-hydroxy-2-nonenal. Formation of cross-linked protein that inhibits the multicatalytic protease. *J Biol Chem* 269(34)**:** 21639-21643

Fujiwara T, Oda K, Yokota S, Takatsuki A, Ikehara Y (1988) Brefeldin A causes disassembly of the Golgi complex and accumulation of secretory proteins in the endoplasmic reticulum. *J Biol Chem* 263(34)**:** 18545-18552

Galibert F, Chen TN, Mandart E (1982) Nucleotide sequence of a cloned woodchuck hepatitis virus genome: comparison with the hepatitis B virus sequence. *J Virol* 41(1)**:** 51-65

Galibert F, Mandart E, Fitoussi F, Tiollais P, Charnay P (1979) Nucleotide sequence of the hepatitis B virus genome (subtype ayw) cloned in E. coli. *Nature* 281(5733)**:** 646-650

Ganem D, Prince AM (2004) Hepatitis B virus infection--natural history and clinical consequences. *N Engl J Med* 350(11)**:** 1118-1129

Ganem D, Varmus HE (1987) The molecular biology of the hepatitis B viruses. *Annu Rev Biochem* 56**:** 651-693

Garcia-Mata R, Bebok Z, Sorscher EJ, Sztul ES (1999) Characterization and dynamics of aggresome formation by a cytosolic GFP-chimera. *J Cell Biol* 146(6)**:** 1239-1254

Garcia-Mata R, Gao YS, Sztul E (2002) Hassles with taking out the garbage: aggravating aggresomes. *Traffic* 3(6)**:** 388-396

Garcia-Mata RG, Gao YS, E S (2002) Hassles with taking out the garbage: Aggravating aggresomes. *Traffic* 3**:** 388 - 396

Garcia PD, Ou JH, Rutter WJ, Walter P (1988) Targeting of the hepatitis B virus precore protein to the endoplasmic reticulum membrane: after signal peptide cleavage translocation can be aborted and the product released into the cytoplasm. *J Cell Biol* 106(4)**:** 1093-1104

Gerber MA, Thung SN (1985) Molecular and cellular pathology of hepatitis B. *Lab Invest* 52(6)**:** 572-590

Gerin JL, Cote PJ, Korba BE, Tennant BC (1989) Hepadnavirus-induced liver cancer in woodchucks. *Cancer Detect Prev* 14(2)**:** 227-229

Gerin JL, Ford EC, Purcell RH (1975) Biochemical characterization of Australia antigen. Evidence for defective particles of hepatitis B virus. *Am J Pathol* 81(3)**:** 651-668

Gerlich WH, Lu X, Heermann KH (1993) Studies on the attachment and penetration of hepatitis B virus. *J Hepatol* 17 Suppl 3**:** S10-14

Gerlich WH, Robinson WS (1980) Hepatitis B virus contains protein attached to the 5' terminus of its complete DNA strand. *Cell* 21(3)**:** 801-809

Gil-Torregrosa BC, Raul Castano A, Del Val M (1998) Major histocompatibility complex class I viral antigen processing in the secretory pathway defined by the trans-Golgi network protease furin. *J Exp Med* 188(6)**:** 1105-1116

Gilbert A, Jadot M, Leontieva E, Wattiaux-De Coninck S, Wattiaux R (1998) Delta F508 CFTR localizes in the endoplasmic reticulum-Golgi intermediate compartment in cystic fibrosis cells. *Exp Cell Res* 242(1)**:** 144-152

Gillece P, Luz JM, Lennarz WJ, de La Cruz FJ, Romisch K (1999) Export of a cysteine-free misfolded secretory protein from the endoplasmic reticulum for degradation requires interaction with protein disulfide isomerase. *J Cell Biol* 147(7)**:** 1443-1456

Gilmore R, Blobel G, Walter P (1982) Protein translocation across the endoplasmic reticulum. I. Detection in the microsomal membrane of a receptor for the signal recognition particle. *J Cell Biol* 95(2 Pt 1)**:** 463-469

Gorelick FS, Shugrue C (2001) Exiting the endoplasmic reticulum. *Mol Cell Endocrinol* 177(1-2)**:** 13-18

Grandjacques C, Pradat P, Stuyver L, Chevallier M, Chevallier P, Pichoud C, Maisonnas M, Trepo C, Zoulim F (2000) Rapid detection of genotypes and mutations in the pre-core promoter and the pre-core region of hepatitis B virus genome: correlation with viral persistence and disease severity. *J Hepatol* 33(3)**:** 430-439

Gripon P, Le Seyec J, Rumin S, Guguen-Guillouzo C (1995) Myristylation of the hepatitis B virus large surface protein is essential for viral infectivity. *Virology* 213(2)**:** 292-299

Groenendyk J, Michalak M (2005) Endoplasmic reticulum quality control and apoptosis. *Acta Biochim Pol* 52(2)**:** 381-395

Grune T, Jung T, Merker K, Davies KJ (2004) Decreased proteolysis caused by protein aggregates, inclusion bodies, plaques, lipofuscin, ceroid, and 'aggresomes' during oxidative stress, aging, and disease. *Int J Biochem Cell Biol* 36(12)**:** 2519-2530

Grune T, Reinheckel T, Davies KJ (1997) Degradation of oxidized proteins in mammalian cells. *Faseb J* 11(7)**:** 526-534

Gu WJ, Corti O, Araujo F, Hampe C, Jacquier S, Lucking CB, Abbas N, Duyckaerts C, Rooney T, Pradier L, Ruberg M, Brice A (2003) The C289G and C418R missense mutations cause rapid sequestration of human Parkin into insoluble aggregates. *Neurobiol Dis* 14(3)**:** 357-364

Guarnieri M, Kim KH, Bang G, Li J, Zhou Y, Tang X, Wands J, Tong S (2006) Point mutations upstream of hepatitis B virus core gene affect DNA replication at the step of core protein expression. *J Virol* 80(2)**:** 587-595

Guidotti LG, Matzke B, Pasquinelli C, Shoenberger JM, Rogler CE, Chisari FV (1996) The hepatitis B virus (HBV) precore protein inhibits HBV replication in transgenic mice. *J Virol* 70(10)**:** 7056-7061

Gunther S (2006) Genetic variation in HBV infection: genotypes and mutants. *J Clin Virol* 36 Suppl 1**:** S3-S11

Guo H, Jiang D, Zhou T, Cuconati A, Block TM, Guo JT (2007) Characterization of the intracellular deproteinized relaxed circular DNA of hepatitis B virus: an intermediate of covalently closed circular DNA formation. *J Virol* 81(22)**:** 12472-12484

Halic M, Beckmann R (2005) The signal recognition particle and its interactions during protein targeting. *Curr Opin Struct Biol* 15(1)**:** 116-125

Hammond AT, Glick BS (2000) Dynamics of transitional endoplasmic reticulum sites in vertebrate cells. *Mol Biol Cell* 11(9)**:** 3013-3030

Hammond C, Helenius A (1994) Quality control in the secretory pathway: retention of a misfolded viral membrane glycoprotein involves cycling between the ER, intermediate compartment, and Golgi apparatus. *J Cell Biol* 126(1)**:** 41-52

Hampton RY (2002) ER-associated degradation in protein quality control and cellular regulation. *Curr Opin Cell Biol* 14(4)**:** 476-482

Hannoun C, Soderstrom A, Norkrans G, Lindh M (2005) Phylogeny of African complete genomes reveals a West African genotype A subtype of hepatitis B virus and relatedness between Somali and Asian A1 sequences. *J Gen Virol* 86(Pt 8)**:** 2163-2167

Hantz O, Allaudeen HS, Ooka T, De Clercq E, Trepo C (1984) Inhibition of human and woodchuck hepatitis virus DNA polymerase by the triphosphates of acyclovir, 1-(2'-deoxy-2'-fluoro-beta-D-arabinofuranosyl)-5-iodocytosine and E-5-(2-bromovinyl)-2'-deoxyuridine. *Antiviral Res* 4(4)**:** 187-199

Harada M, Sakisaka S, Terada K, Kimura R, Kawaguchi T, Koga H, Kim M, Taniguchi E, Hanada S, Suganuma T, Furuta K, Sugiyama T, Sata M (2001) A mutation of the Wilson disease protein, ATP7B, is degraded in the proteasomes and forms protein aggregates. *Gastroenterology* 120(4)**:** 967-974

Hardie DR, Williamson C (1997) Analysis of the preS1 gene of hepatitis B virus (HBV) to define epidemiologically linked and un-linked infections in South Africa. *Arch Virol* 142(9)**:** 1829-1841

Hartl FU (1996) Molecular chaperones in cellular protein folding. *Nature* 381(6583)**:** 571-579

Hartl FU, Hayer-Hartl M (2002) Molecular chaperones in the cytosol: from nascent chain to folded protein. *Science* 295(5561)**:** 1852-1858

Hauri HP, Kappeler F, Andersson H, Appenzeller C (2000) ERGIC-53 and traffic in the secretory pathway. *J Cell Sci* 113 (Pt 4)**:** 587-596

Havens W (1946) Period of infectivity of patients with experimentally induced infectious hepatitis. *J Exp Med* 83**:** 251-258

Heath CM, Windsor M, Wileman T (2001) Aggresomes resemble sites specialized for virus assembly. *J Cell Biol* 153(3)**:** 449-455

Heermann KH, Goldmann U, Schwartz W, Seyffarth T, Baumgarten H, Gerlich WH (1984) Large surface proteins of hepatitis B virus containing the pre-s sequence. *J Virol* 52(2)**:** 396-402

Heermann KH, Kruse F, Seifer M, Gerlich WH (1987) Immunogenicity of the gene S and Pre-S domains in hepatitis B virions and HBsAg filaments. *Intervirology* 28(1)**:** 14-25

Hermosilla R, Oueslati M, Donalies U, Schonenberger E, Krause E, Oksche A, Rosenthal W, Schulein R (2004) Disease-causing V(2) vasopressin receptors are retained in different compartments of the early secretory pathway. *Traffic* 5(12)**:** 993-1005

Herter S, Osterloh P, Hilf N, Rechtsteiner G, Hohfeld J, Rammensee HG, Schild H (2005) Dendritic cell aggresome-like-induced structure formation and delayed antigen presentation coincide in influenza virus-infected dendritic cells. *J Immunol* 175(2)**:** 891-898

Hirsch RC, Lavine JE, Chang LJ, Varmus HE, Ganem D (1990) Polymerase gene products of hepatitis B viruses are required for genomic RNA packaging as wel as for reverse transcription. *Nature* 344(6266)**:** 552-555

Ho SK, Yam WC, Leung ET, Wong LP, Leung JK, Lai KN, Chan TM (2003) Rapid quantification of hepatitis B virus DNA by real-time PCR using fluorescent hybridization probes. *J Med Microbiol* 52(Pt 5)**:** 397-402

Hochstrasser M (1996) Ubiquitin-dependent protein degradation. *Annu Rev Genet* 30**:** 405-439

Hoofnagle JH, Dusheiko GM, Seeff LB, Jones EA, Waggoner JG, Bales ZB (1981) Seroconversion from hepatitis B e antigen to antibody in chronic type B hepatitis. *Ann Intern Med* 94(6)**:** 744-748

Hou J, Lin Y, Waters J, Wang Z, Min J, Liao H, Jiang J, Chen J, Luo K, Karayiannis P (2002) Detection and significance of a G1862T variant of hepatitis B virus in Chinese patients with fulminant hepatitis. *J Gen Virol* 83(Pt 9)**:** 2291-2298

Hruska JF, Clayton DA, Rubenstein JL, Robinson WS (1977) Structure of hepatitis B Dane particle DNA before and after the Dane particle DNA polymerase reaction. *J Virol* 21(2)**:** 666-672

Hsieh YH, Su IJ, Wang HC, Chang WW, Lei HY, Lai MD, Chang WT, Huang W (2004) Pre-S mutant surface antigens in chronic hepatitis B virus infection induce oxidative stress and DNA damage. *Carcinogenesis* 25(10)**:** 2023-2032

Hsu VW, Yuan LC, Nuchtern JG, Lippincott-Schwartz J, Hammerling GJ, Klausner RD (1991) A recycling pathway between the endoplasmic reticulum and the Golgi apparatus for retention of unassembled MHC class I molecules. *Nature* 352(6334)**:** 441-444

Hsu YS, Chien RN, Yeh CT, Sheen IS, Chiou HY, Chu CM, Liaw YF (2002) Long-term outcome after spontaneous HBeAg seroconversion in patients with chronic hepatitis B. *Hepatology* 35(6)**:** 1522-1527

Hu J, Flores D, Toft D, Wang X, Nguyen D (2004) Requirement of heat shock protein 90 for human hepatitis B virus reverse transcriptase function. *J Virol* 78(23)**:** 13122-13131

Hu J, Toft DO, Seeger C (1997) Hepadnavirus assembly and reverse transcription require a multi-component chaperone complex which is incorporated into nucleocapsids. *Embo J* 16(1)**:** 59-68

Hubschen JM, Andernach IE, Muller CP (2008) Hepatitis B virus genotype E variability in Africa. *J Clin Virol* 43(4)**:** 376-380

Hung JH, Su IJ, Lei HY, Wang HC, Lin WC, Chang WT, Huang W, Chang WC, Chang YS, Chen CC, Lai MD (2004) Endoplasmic reticulum stress stimulates the expression of cyclooxygenase-2 through activation of NF-kappaB and pp38 mitogen-activated protein kinase. *J Biol Chem* 279(45)**:** 46384-46392

Huovila AP, Eder AM, Fuller SD (1992) Hepatitis B surface antigen assembles in a post-ER, pre-Golgi compartment. *J Cell Biol* 118(6)**:** 1305-1320

Hurtley SM, Bole DG, Hoover-Litty H, Helenius A, Copeland CS (1989) Interactions of misfolded influenza virus hemagglutinin with binding protein (BiP). *J Cell Biol* 108(6)**:** 2117-2126

Huy TT, Abe K (2004) Molecular epidemiology of hepatitis B and C virus infections in Asia. *Pediatr Int* 46(2)**:** 223-230

Huy TT, Ushijima H, Sata T, Abe K (2006) Genomic characterization of HBV genotype F in Bolivia: genotype F subgenotypes correlate with geographic distribution and T(1858) variant. *Arch Virol* 151(3)**:** 589-597

Hwang WL, Su TS (1998) Translational regulation of hepatitis B virus polymerase gene by termination-reinitiation of an upstream minicistron in a length-dependent manner. *J Gen Virol* 79 (Pt 9)**:** 2181-2189

Imai M, Nomura M, Gotanda T, Sano T, Tachibana K, Miyamoto H, Takahashi K, Toyama S, Miyakawa Y, Mayumi M (1982) Demonstration of two distinct antigenic determinants on hepatitis B e antigen by monoclonal antibodies. *J Immunol* 128(1)**:** 69-72

Inoue J, Ueno Y, Nagasaki F, Wakui Y, Kondo Y, Fukushima K, Niitsuma H, Shimosegawa T (2009) Enhanced intracellular retention of a hepatitis B virus strain associated with fulminant hepatitis. *Virology* 395(2)**:** 202-209

Ito K, Kim KH, Lok AS, Tong S (2009) Characterization of genotype-specific carboxyl-terminal cleavage sites of hepatitis B virus e antigen precursor and identification of furin as the candidate enzyme. *J Virol* 83(8)**:** 3507-3517

Jammeh S, Tavner F, Watson R, Thomas HC, Karayiannis P (2008) Effect of basal core promoter and pre-core mutations on hepatitis B virus replication. *J Gen Virol* 89(Pt 4)**:** 901-909

Jarosch E, Geiss-Friedlander R, Meusser B, Walter J, Sommer T (2002) Protein dislocation from the endoplasmic reticulum--pulling out the suspect. *Traffic* 3(8)**:** 530-536

Jensen K, Gluud C (1994) The Mallory body: morphological, clinical and experimental studies (Part 1 of a literature survey). *Hepatology* 20(4 Pt 1)**:** 1061-1077

Ji C (2008) Dissection of endoplasmic reticulum stress signaling in alcoholic and non-alcoholic liver injury. *J Gastroenterol Hepatol* 23 Suppl 1**:** S16-24

Ji C, Kaplowitz N (2006) ER stress: can the liver cope? *J Hepatol* 45(2)**:** 321-333

Johnston JA, Ward CL, Kopito RR (1998) Aggresomes: a cellular response to misfolded proteins. *J Cell Biol* 143(7)**:** 1883-1898

Junker-Niepmann M, Bartenschlager R, Schaller H (1990) A short cis-acting sequence is required for hepatitis B virus pregenome encapsidation and sufficient for packaging of foreign RNA. *Embo J* 9(10)**:** 3389-3396

Junker M, Galle P, Schaller H (1987) Expression and replication of the hepatitis B virus genome under foreign promoter control. *Nucleic Acids Res* 15(24)**:** 10117-10132

Kalinina T, Riu A, Fischer L, Will H, Sterneck M (2001) A dominant hepatitis B virus population defective in virus secretion because of several S-gene mutations from a patient with fulminant hepatitis. *Hepatology* 34(2)**:** 385-394

Kann M, Schmitz A, Rabe B (2007) Intracellular transport of hepatitis B virus. *World J Gastroenterol* 13(1)**:** 39-47

Kaplowitz N, Than TA, Shinohara M, Ji C (2007) Endoplasmic reticulum stress and liver injury. *Semin Liver Dis* 27(4)**:** 367-377

Karamyshev AL, Karamysheva ZN, Kajava AV, Ksenzenko VN, Nesmeyanova MA (1998) Processing of Escherichia coli alkaline phosphatase: role of the primary structure of the signal peptide cleavage region. *J Mol Biol* 277(4)**:** 859-870

Karczewski MK, Strebel K (1996) Cytoskeleton association and virion incorporation of the human immunodeficiency virus type 1 Vif protein. *J Virol* 70(1)**:** 494-507

Karla A, Lively MO, Paetzel M, Dalbey R (2005) The identification of residues that control signal peptidase cleavage fidelity and substrate specificity. *J Biol Chem* 280(8)**:** 6731-6741

Kato H, Orito E, Gish RG, Sugauchi F, Suzuki S, Ueda R, Miyakawa Y, Mizokami M (2002) Characteristics of hepatitis B virus isolates of genotype G and their phylogenetic differences from the other six genotypes (A through F). *J Virol* 76(12)**:** 6131-6137

Keenan RJ, Freymann DM, Stroud RM, Walter P (2001) The signal recognition particle. *Annu Rev Biochem* 70**:** 755-775

Kenney JM, von Bonsdorff CH, Nassal M, Fuller SD (1995) Evolutionary conservation in the hepatitis B virus core structure: comparison of human and duck cores. *Structure* 3(10)**:** 1009-1019

Kew MC (1996) Progress towards the comprehensive control of hepatitis B in Africa: a view from South Africa. *Gut* 38 Suppl 2**:** S31-36

Kew MC, Kramvis A, Yu MC, Arakawa K, Hodkinson J (2005) Increased hepatocarcinogenic potential of hepatitis B virus genotype A in Bantu-speaking sub-saharan Africans. *J Med Virol* 75(4)**:** 513-521

Kew MC, MacKay ME, Mindel A, Joffe BI, Kusman B, MacNab GM, Seftel HC (1976) Prevalence of hepatitis B surface antigen and antibody in white and black patients with diabetes mellitus. *J Clin Microbiol* 4(6)**:** 467-469

Kidd-Ljunggren K, Ekdahl K, Oberg M, Kurathong S, Lolekha S (1995) Hepatitis B virus strains in Thailand: genomic variants in chronic carriers. *J Med Virol* 47(4)**:** 454-461

Kiire CF (1996) The epidemiology and prophylaxis of hepatitis B in sub-Saharan Africa: a view from tropical and subtropical Africa. *Gut* 38 Suppl 2**:** S5-12

Kim PS, Arvan P (1998) Endocrinopathies in the family of endoplasmic reticulum (ER) storage diseases: disorders of protein trafficking and the role of ER molecular chaperones. *Endocr Rev* 19(2)**:** 173-202

Kim PS, Ding M, Menon S, Jung CG, Cheng JM, Miyamoto T, Li B, Furudate S, Agui T (2000) A missense mutation G2320R in the thyroglobulin gene causes non-goitrous congenital primary hypothyroidism in the WIC-rdw rat. *Mol Endocrinol* 14(12)**:** 1944-1953

Kimbi GC, Kramvis A, Kew MC (2004) Distinctive sequence characteristics of subgenotype A1 isolates of hepatitis B virus from South Africa. *J Gen Virol* 85(Pt 5)**:** 1211-1220

Kimura T, Ohno N, Terada N, Rokuhara A, Matsumoto A, Yagi S, Tanaka E, Kiyosawa K, Ohno S, Maki N (2005) Hepatitis B virus DNA-negative dane particles lack core protein but contain a 22-kDa precore protein without C-terminal arginine-rich domain. *J Biol Chem* 280(23)**:** 21713-21719

Kisselev AF, Kaganovich D, Goldberg AL (2002) Binding of hydrophobic peptides to several non-catalytic sites promotes peptide hydrolysis by all active sites of 20 S proteasomes. Evidence for peptide-induced channel opening in the alpha-rings. *J Biol Chem* 277(25)**:** 22260-22270

Klumperman J, Schweizer A, Clausen H, Tang BL, Hong W, Oorschot V, Hauri HP (1998) The recycling pathway of protein ERGIC-53 and dynamics of the ER-Golgi intermediate compartment. *J Cell Sci* 111 (Pt 22)**:** 3411-3425

Knaus T, Nassal M (1993) The encapsidation signal on the hepatitis B virus RNA pregenome forms a stem-loop structure that is critical for its function. *Nucleic Acids Res* 21(17)**:** 3967-3975

Koch HG, Moser M, Muller M (2003) Signal recognition particle-dependent protein targeting, universal to all kingdoms of life. *Rev Physiol Biochem Pharmacol* 146**:** 55-94

Koch J, Tampe R (2006) The macromolecular peptide-loading complex in MHC class I-dependent antigen presentation. *Cell Mol Life Sci* 63(6)**:** 653-662

Kodama K, Ogasawara N, Yoshikawa H, Murakami S (1985) Nucleotide sequence of a cloned woodchuck hepatitis virus genome: evolutional relationship between hepadnaviruses. *J Virol* 56(3)**:** 978-986

Kopito RR (2000) Aggresomes, inclusion bodies and protein aggregation. *Trends Cell Biol* 10(12)**:** 524-530

Kopito RR, Sitia R (2000) Aggresomes and Russell bodies. Symptoms of cellular indigestion? *EMBO Rep* 1(3)**:** 225-231

Kostova Z, Wolf DH (2003) For whom the bell tolls: protein quality control of the endoplasmic reticulum and the ubiquitin-proteasome connection. *Embo J* 22(10)**:** 2309-2317

Kozak M (1987) At least six nucleotides preceding the AUG initiator codon enhance translation in mammalian cells. *J Mol Biol* 196(4)**:** 947-950

Kozak M (1999) Initiation of translation in prokaryotes and eukaryotes. *Gene* 234(2)**:** 187-208

Kramvis A, Arakawa K, Yu MC, Nogueira R, Stram DO, Kew MC (2008) Relationship of serological subtype, basic core promoter and precore mutations to genotypes/subgenotypes of hepatitis B virus. *J Med Virol* 80(1)**:** 27-46

Kramvis A, Bukofzer S, Kew MC, Song E (1997) Nucleic acid sequence analysis of the precore region of hepatitis B virus from sera of southern African black adult carriers of the virus. *Hepatology* 25(1)**:** 235-240

Kramvis A, Kew M, Francois G (2005) Hepatitis B virus genotypes. *Vaccine* 23(19)**:** 2409-2423

Kramvis A, Kew MC (1998) Structure and function of the encapsidation signal of hepadnaviridae. *J Viral Hepat* 5(6)**:** 357-367

Kramvis A, Kew MC (2007a) Epidemiology of hepatitis B virus in Africa, its genotypes and clinical associations of genotypes. *Hepatol Res* 37(s1)**:** S9-S19

Kramvis A, Kew MC (2007b) Molecular characterization of subgenotype A1 (subgroup Aa) of hepatitis B virus. *Hepatol Res* 37(s1)**:** S27-32

Kramvis A, Kew MC, Bukofzer S (1998) Hepatitis B virus precore mutants in serum and liver of Southern African Blacks with hepatocellular carcinoma. *J Hepatol* 28(1)**:** 132-141

Kramvis A, Weitzmann L, Owiredu WK, Kew MC (2002) Analysis of the complete genome of subgroup A' hepatitis B virus isolates from South Africa. *J Gen Virol* 83(Pt 4)**:** 835-839

Krugman SGJ, Hammond J. (1967) Infectious hepatitis: evidence for two distinctive clinical, epidemiological, and immunological types of infection. *JAMA* 200**:** 365-373

Ku NO, Strnad P, Zhong BH, Tao GZ, Omary MB (2007) Keratins let liver live: Mutations predispose to liver disease and crosslinking generates Mallory-Denk bodies. *Hepatology* 46(5)**:** 1639-1649

Kurbanov F, Tanaka Y, Fujiwara K, Sugauchi F, Mbanya D, Zekeng L, Ndembi N, Ngansop C, Kaptue L, Miura T, Ido E, Hayami M, Ichimura H, Mizokami M (2005) A new subtype (subgenotype) Ac (A3) of hepatitis B virus and recombination between genotypes A and E in Cameroon. *J Gen Virol* 86(Pt 7)**:** 2047-2056

Kurosaki M, Enomoto N, Asahina Y, Sakuma I, Ikeda T, Tozuka S, Izumi N, Marumo F, Sato C (1996) Mutations in the core promoter region of hepatitis B virus in patients with chronic hepatitis B. *J Med Virol* 49(2)**:** 115-123

Kvittingen EA (1986) Hereditary tyrosinemia type I--an overview. *Scand J Clin Lab Invest Suppl* 184**:** 27-34

Laemmli UK (1970) Cleavage of structural proteins during the assembly of the head of bacteriophage T4. *Nature* 227(5259)**:** 680-685

Lahaye X, Vidy A, Pomier C, Obiang L, Harper F, Gaudin Y, Blondel D (2009) Functional characterization of Negri bodies (NBs) in rabies virus-infected cells: Evidence that NBs are sites of viral transcription and replication. *J Virol* 83(16)**:** 7948-7958

Lai E, Teodoro T, Volchuk A (2007) Endoplasmic reticulum stress: signaling the unfolded protein response. *Physiology (Bethesda)* 22**:** 193-201

Landers TA, Greenberg HB, Robinson WS (1977) Structure of hepatitis B Dane particle DNA and nature of the endogenous DNA polymerase reaction. *J Virol* 23(2)**:** 368-376

Lanford RE, Notvall L, Lee H, Beames B (1997) Transcomplementation of nucleotide priming and reverse transcription between independently expressed TP and RT domains of the hepatitis B virus reverse transcriptase. *J Virol* 71(4)**:** 2996-3004

Laszlo L, Tuckwell J, Self T, Lowe J, Landon M, Smith S, Hawthorne JN, Mayer RJ (1991) The latent membrane protein-1 in Epstein-Barr virus-transformed lymphoblastoid cells is found with ubiquitin-protein conjugates and heat-shock protein 70 in lysosomes oriented around the microtubule organizing centre. *J Pathol* 164(3)**:** 203-214

Lavanchy D (2004) Hepatitis B virus epidemiology, disease burden, treatment, and current and emerging prevention and control measures. *J Viral Hepat* 11(2)**:** 97-107

Lavanchy D (2005) Worldwide epidemiology of HBV infection, disease burden, and vaccine prevention. *J Clin Virol* 34 Suppl 1**:** S1-3

Le Seyec J, Chouteau P, Cannie I, Guguen-Guillouzo C, Gripon P (1999) Infection process of the hepatitis B virus depends on the presence of a defined sequence in the pre-S1 domain. *J Virol* 73(3)**:** 2052-2057

Lee J, Shin MK, Lee HJ, Yoon G, Ryu WS (2004) Three novel cis-acting elements required for efficient plus-strand DNA synthesis of the hepatitis B virus genome. *J Virol* 78(14)**:** 7455-7464

Lepere C, Regeard M, Le Seyec J, Gripon P (2007) The translocation motif of hepatitis B virus envelope proteins is dispensable for infectivity. *J Virol* 81(14)**:** 7816-7818

Levitskaya J, Sharipo A, Leonchiks A, Ciechanover A, Masucci MG (1997) Inhibition of ubiquitin/proteasome-dependent protein degradation by the Gly-Ala repeat domain of the Epstein-Barr virus nuclear antigen 1. *Proc Natl Acad Sci U S A* 94(23)**:** 12616-12621

Li DH, Newbold JE, Cullen JM (1996) Natural populations of woodchuck hepatitis virus contain variant precore and core sequences including a premature stop codon in the epsilon motif. *Virology* 220(1)**:** 256-262

Li JS, Tong SP, Wen YM, Vitvitski L, Zhang Q, Trepo C (1993) Hepatitis B virus genotype A rarely circulates as an HBe-minus mutant: possible contribution of a single nucleotide in the precore region. *J Virol* 67(9)**:** 5402-5410

Liang TJ (2009) Hepatitis B: the virus and disease. *Hepatology* 49(5 Suppl)**:** S13-21

Liaw YF (2009) HBeAg seroconversion as an important end point in the treatment of chronic hepatitis B. *Hepatol Int*

Liaw YF, Tai DI, Chu CM, Chen TJ (1988) The development of cirrhosis in patients with chronic type B hepatitis: a prospective study. *Hepatology* 8(3)**:** 493-496

Lien JM, Aldrich CE, Mason WS (1986) Evidence that a capped oligoribonucleotide is the primer for duck hepatitis B virus plus-strand DNA synthesis. *J Virol* 57(1)**:** 229-236

Lien JM, Petcu DJ, Aldrich CE, Mason WS (1987) Initiation and termination of duck hepatitis B virus DNA synthesis during virus maturation. *J Virol* 61(12)**:** 3832-3840

Lin SM, Yu ML, Lee CM, Chien RN, Sheen IS, Chu CM, Liaw YF (2007) Interferon therapy in HBeAg positive chronic hepatitis reduces progression to cirrhosis and hepatocellular carcinoma. *J Hepatol* 46(1)**:** 45-52

Lindh M (1997) HBV precore mutants and response to interferon. *Hepatology* 25(6)**:** 1547-1548

Lindh M, Andersson AS, Gusdal A (1997) Genotypes, nt 1858 variants, and geographic origin of hepatitis B virus--large-scale analysis using a new genotyping method. *J Infect Dis* 175(6)**:** 1285-1293

Linstedt AD, Hauri HP (1993) Giantin, a novel conserved Golgi membrane protein containing a cytoplasmic domain of at least 350 kDa. *Mol Biol Cell* 4(7)**:** 679-693

Lippincott-Schwartz J (1998) Cytoskeletal proteins and Golgi dynamics. *Curr Opin Cell Biol* 10(1)**:** 52-59

Lippincott-Schwartz J (2001) The secretory membrane system studied in real-time. Robert Feulgen Prize Lecture, 2001. *Histochem Cell Biol* 116(2)**:** 97-107

Lippincott-Schwartz J, Roberts TH, Hirschberg K (2000) Secretory protein trafficking and organelle dynamics in living cells. *Annu Rev Cell Dev Biol* 16**:** 557-589

Liu Y, Shevchenko A, Berk AJ (2005) Adenovirus exploits the cellular aggresome response to accelerate inactivation of the MRN complex. *J Virol* 79(22)**:** 14004-14016

Locarnini S, McMillan J, Bartholomeusz A (2003) The hepatitis B virus and common mutants. *Semin Liver Dis* 23(1)**:** 5-20

Loeb DD, Hirsch RC, Ganem D (1991) Sequence-independent RNA cleavages generate the primers for plus strand DNA synthesis in hepatitis B viruses: implications for other reverse transcribing elements. *Embo J* 10(11)**:** 3533-3540

Lok AS, Akarca U, Greene S (1994) Mutations in the pre-core region of hepatitis B virus serve to enhance the stability of the secondary structure of the pre-genome encapsidation signal. *Proc Natl Acad Sci U S A* 91(9)**:** 4077-4081

Lomas DA, Parfrey H (2004) Alpha1-antitrypsin deficiency. 4: Molecular pathophysiology. *Thorax* 59(6)**:** 529-535

Lu X, Block T (2004) Study of the early steps of the Hepatitis B Virus life cycle. *Int J Med Sci* 1(1)**:** 21-33

Lu X, Block TM, Gerlich WH (1996) Protease-induced infectivity of hepatitis B virus for a human hepatoblastoma cell line. *J Virol* 70(4)**:** 2277-2285

Lu X, Hazboun T, Block T (2001) Limited proteolysis induces woodchuck hepatitis virus infectivity for human HepG2 cells. *Virus Res* 73(1)**:** 27-40

Lu X, Mehta A, Dadmarz M, Dwek R, Blumberg BS, Block TM (1997) Aberrant trafficking of hepatitis B virus glycoproteins in cells in which N-glycan processing is inhibited. *Proc Natl Acad Sci U S A* 94(6)**:** 2380-2385

Lu X, Mehta A, Dwek R, Butters T, Block T (1995) Evidence that N-linked glycosylation is necessary for hepatitis B virus secretion. *Virology* 213(2)**:** 660-665

Luini A, Mironov AA, Polishchuk EV, Polishchuk RS (2008) Morphogenesis of post-Golgi transport carriers. *Histochem Cell Biol* 129(2)**:** 153-161

Luirink J, Sinning I (2004) SRP-mediated protein targeting: structure and function revisited. *Biochim Biophys Acta* 1694(1-3)**:** 17-35

Lurman A (1855) Eine icterus Epidemic. *Berlin Klin* Wochenschr(22)**:** 20-23

Lusida MI, Nugrahaputra VE, Soetjipto, Handajani R, Nagano-Fujii M, Sasayama M, Utsumi T, Hotta H (2008) Novel subgenotypes of hepatitis B virus genotypes C and D in Papua, Indonesia. *J Clin Microbiol* 46(7)**:** 2160-2166

MacCallum FO, and D. J. Bauer. (1947) Homologous serum hepatitis. *Lancet* 2**:** 691-692

Maddrey WC (2001) Hepatitis B--an important public health issue. *Clin Lab* 47(1-2)**:** 51-55

Magnius LO, Espmark A (1972a) A new antigen complex co-occurring with Australia antigen. *Acta Pathol Microbiol Scand B Microbiol Immunol* 80(2)**:** 335-337

Magnius LO, Espmark JA (1972b) New specificities in Australia antigen positive sera distinct from the Le Bouvier determinants. *J Immunol* 109(5)**:** 1017-1021

Mahoney FJ (1999) Update on diagnosis, management, and prevention of hepatitis B virus infection. *Clin Microbiol Rev* 12(2)**:** 351-366

Makuwa M, Souquiere S, Telfer P, Apetrei C, Vray M, Bedjabaga I, Mouinga-Ondeme A, Onanga R, Marx PA, Kazanji M, Roques P, Simon F (2006) Identification of hepatitis B virus subgenotype A3 in rural Gabon. *J Med Virol* 78(9)**:** 1175-1184

Mallory F (1911) Cirrhosis of the liver. Five different types of lesions from which it may arise. *Bul Johns Hopkins Hosp* 22**:** 69–75

Malpiece Y, Michel ML, Carloni G, Revel M, Tiollais P, Weissenbach J (1983) The gene S promoter of hepatitis B virus confers constitutive gene expression. *Nucleic Acids Res* 11(13)**:** 4645-4654

Marquardt T, Hebert DN, Helenius A (1993) Post-translational folding of influenza hemagglutinin in isolated endoplasmic reticulum-derived microsomes. *J Biol Chem* 268(26)**:** 19618-19625

Martoglio B, Dobberstein B (1998) Signal sequences: more than just greasy peptides. *Trends Cell Biol* 8(10)**:** 410-415

Mast EE, Alter MJ (1993) Epidemology of viral hepatitis: an overview. *Semin in Virol***:** 273-283

Mathews DH, Sabina J, Zuker M, Turner DH (1999) Expanded sequence dependence of thermodynamic parameters improves prediction of RNA secondary structure. *J Mol Biol* 288(5)**:** 911-940

Mayer MP, Bukau B (2005) Hsp70 chaperones: cellular functions and molecular mechanism. *Cell Mol Life Sci* 62(6)**:** 670-684

McClellan AJ, Tam S, Kaganovich D, Frydman J (2005) Protein quality control: chaperones culling corrupt conformations. *Nat Cell Biol* 7(8)**:** 736-741

McCracken AA, Brodsky JL (2000) A molecular portrait of the response to unfolded proteins. *Genome Biol* 1(2)**:** REVIEWS1013

McGlynn KA, London WT (2005) Epidemiology and natural history of hepatocellular carcinoma. *Best Pract Res Clin Gastroenterol* 19(1)**:** 3-23

McLachlan A, Milich DR, Raney AK, Riggs MG, Hughes JL, Sorge J, Chisari FV (1987) Expression of hepatitis B virus surface and core antigens: influences of pre-S and precore sequences. *J Virol* 61(3)**:** 683-692

Menne S, Cote PJ (2007) The woodchuck as an animal model for pathogenesis and therapy of chronic hepatitis B virus infection. *World J Gastroenterol* 13(1)**:** 104-124

Messageot F, Salhi S, Eon P, Rossignol JM (2003) Proteolytic processing of the hepatitis B virus e antigen precursor. Cleavage at two furin consensus sequences. *J Biol Chem* 278(2)**:** 891-895

Meusser B, Hirsch C, Jarosch E, Sommer T (2005) ERAD: the long road to destruction. *Nat Cell Biol* 7(8)**:** 766-772

Meyer DI, Krause E, Dobberstein B (1982) Secretory protein translocation across membranes-the role of the "docking protein'. *Nature* 297(5868)**:** 647-650

Mezzacasa A, Helenius A (2002) The transitional ER defines a boundary for quality control in the secretion of tsO45 VSV glycoprotein. *Traffic* 3(11)**:** 833-849

Milich DR (1988) T- and B-cell recognition of hepatitis B viral antigens. *Immunol Today* 9(12)**:** 380-386

Milich DR (1997) Influence of T-helper cell subsets and crossregulation in hepatitis B virus infection. *J Viral Hepat* 4 Suppl 2**:** 48-59

Milich DR, Chen MK, Hughes JL, Jones JE (1998) The secreted hepatitis B precore antigen can modulate the immune response to the nucleocapsid: a mechanism for persistence. *J Immunol* 160(4)**:** 2013-2021

Miller RH, Kaneko S, Chung CT, Girones R, Purcell RH (1989) Compact organization of the hepatitis B virus genome. *Hepatology* 9(2)**:** 322-327

Minami Y, Weissman AM, Samelson LE, Klausner RD (1987) Building a multichain receptor: synthesis, degradation, and assembly of the T-cell antigen receptor. *Proc Natl Acad Sci U S A* 84(9)**:** 2688-2692

Miyakawa Y, Mizokami M (2003) Classifying hepatitis B virus genotypes. *Intervirology* 46(6)**:** 329-338

Molloy SS, Anderson ED, Jean F, Thomas G (1999) Bi-cycling the furin pathway: from TGN localization to pathogen activation and embryogenesis. *Trends Cell Biol* 9(1)**:** 28-35

Moriyama K (1997) Reduced antigen production by hepatitis B virus harbouring nucleotide deletions in the overlapping X gene and precore-core promoter. *J Gen Virol* 78 (Pt 6)**:** 1479-1486

Moriyama K, Okamoto H, Tsuda F, Mayumi M (1996) Reduced precore transcription and enhanced core-pregenome transcription of hepatitis B virus DNA after replacement of the precore-core promoter with sequences associated with e antigen-seronegative persistent infections. *Virology* 226(2)**:** 269-280

Mulyanto, Depamede SN, Surayah K, Tsuda F, Ichiyama K, Takahashi M, Okamoto H (2009) A nationwide molecular epidemiological study on hepatitis B virus in Indonesia: identification of two novel subgenotypes, B8 and C7. *Arch Virol* 154(7)**:** 1047-1059

Murti KG, Goorha R (1983) Interaction of frog virus-3 with the cytoskeleton. I. Altered organization of microtubules, intermediate filaments, and microfilaments. *J Cell Biol* 96(5)**:** 1248-1257

Mushahwar IK, Overby LR (1981) An enzyme immunoassay for hepatitis B e-antigen and antibody. *J Virol Methods* 3(2)**:** 89-97

Mwangi J, Nganga Z, Songok E, Kinyua J, Lagat N, Muriuki J, Lihana R, Khamadi S, Osman S, Lwembe R, Kiptoo M, Mwau M, Chirchir R, Mpoke S, Nyamongo J, Okoth F, Yamada R, Kageyama S, Ichimura H (2008) Molecular genetic diversity of hepatitis B virus in Kenya. *Intervirology* 51(6)**:** 417-421

Nagasaka A, Hige S, Marutani M, Tsunematsu I, Saito M, Yamamoto Y, Konishi S, Asaka M (1998) Prevalence of mutations in core promoter/precore region in Japanese patients with chronic hepatitis B virus infection. *Dig Dis Sci* 43(11)**:** 2473-2478

Nagasaki F, Niitsuma H, Cervantes JG, Chiba M, Hong S, Ojima T, Ueno Y, Bondoc E, Kobayashi K, Ishii M, Shimosegawa T (2006) Analysis of the entire

nucleotide sequence of hepatitis B virus genotype B in the Philippines reveals a new subgenotype of genotype B. *J Gen Virol* 87(Pt 5)**:** 1175-1180

Nakabayashi H, Taketa K, Miyano K, Yamane T, Sato J (1982) Growth of human hepatoma cells lines with differentiated functions in chemically defined medium. *Cancer Res* 42(9)**:** 3858-3863

Nakano T, Lu L, Hu X, Mizokami M, Orito E, Shapiro C, Hadler S, Robertson B (2001) Characterization of hepatitis B virus genotypes among Yucpa Indians in Venezuela. *J Gen Virol* 82(Pt 2)**:** 359-365

Nassal M (1992) The arginine-rich domain of the hepatitis B virus core protein is required for pregenome encapsidation and productive viral positive-strand DNA synthesis but not for virus assembly. *J Virol* 66(7)**:** 4107-4116

Nassal M (2008) Hepatitis B viruses: reverse transcription a different way. *Virus Res* 134(1-2)**:** 235-249

Nassal M, Junker-Niepmann M, Schaller H (1990) Translational inactivation of RNA function: discrimination against a subset of genomic transcripts during HBV nucleocapsid assembly. *Cell* 63(6)**:** 1357-1363

Nassal M, Rieger A (1993) An intramolecular disulfide bridge between Cys-7 and Cys61 determines the structure of the secretory core gene product (e antigen) of hepatitis B virus. *J Virol* 67(7)**:** 4307-4315

Nassal M, Rieger A (1996) A bulged region of the hepatitis B virus RNA encapsidation signal contains the replication origin for discontinuous first-strand DNA synthesis. *J Virol* 70(5)**:** 2764-2773

Nassal M, Rieger A, Steinau O (1992) Topological analysis of the hepatitis B virus core particle by cysteine-cysteine cross-linking. *J Mol Biol* 225(4)**:** 1013-1025

Nassal M, Schaller H (1996) Hepatitis B virus replication--an update. *J Viral Hepat* 3(5)**:** 217-226

Nedellec P, Vicart P, Laurent-Winter C, Martinat C, Prevost MC, Brahic M (1998) Interaction of Theiler's virus with intermediate filaments of infected cells. *J Virol* 72(12)**:** 9553-9560

Neefe JR, S. S. Gellis, and J. Stokes (1946) serum hepatitis and infectious (epidemic) hepatitis: studies in volunteers bearing on immunological and other characteristics of etiologic agents. *Am J Med* 1**:** 3-22

Netherton C, Moffat K, Brooks E, Wileman T (2007) A guide to viral inclusions, membrane rearrangements, factories, and viroplasm produced during virus replication. *Adv Virus Res* 70**:** 101-182

Neurath AR, Adamowicz P, Kent SB, Riottot MM, Strick N, Parker K, Offensperger W, Petit MA, Wahl S, Budkowska A, et al. (1986a) Characterization

of monoclonal antibodies specific for the pre-S2 region of the hepatitis B virus envelope protein. *Mol Immunol* 23(9)**:** 991-997

Neurath AR, Kent SB, Strick N, Parker K (1986b) Identification and chemical synthesis of a host cell receptor binding site on hepatitis B virus. *Cell* 46(3)**:** 429-436

Nguyen VT, Law MG, Dore GJ (2009) Hepatitis B-related hepatocellular carcinoma: epidemiological characteristics and disease burden. *J Viral Hepat* 16(7)**:** 453-463

Nicchitta CV, Lerner RS, Stephens SB, Dodd RD, Pyhtila B (2005) Pathways for compartmentalizing protein synthesis in eukaryotic cells: the template-partitioning model. *Biochem Cell Biol* 83(6)**:** 687-695

Nomura T, Lin Y, Dorjsuren D, Ohno S, Yamashita T, Murakami S (1999) Human hepatitis B virus X protein is detectable in nuclei of transfected cells, and is active for transactivation. *Biochim Biophys Acta* 1453(3)**:** 330-340

Norder H, Arauz-Ruiz P, Blitz L, Pujol FH, Echevarria JM, Magnius LO (2003) The T(1858) variant predisposing to the precore stop mutation correlates with one of two major genotype F hepatitis B virus clades. *J Gen Virol* 84(Pt 8)**:** 2083-2087

Norder H, Courouce AM, Coursaget P, Echevarria JM, Lee SD, Mushahwar IK, Robertson BH, Locarnini S, Magnius LO (2004) Genetic diversity of hepatitis B

virus strains derived worldwide: genotypes, subgenotypes, and HBsAg subtypes. *Intervirology* 47(6)**:** 289-309

Norder H, Courouce AM, Magnius LO (1992a) Molecular basis of hepatitis B virus serotype variations within the four major subtypes. *J Gen Virol* 73 (Pt 12)**:** 3141-3145

Norder H, Courouce AM, Magnius LO (1994) Complete genomes, phylogenetic relatedness, and structural proteins of six strains of the hepatitis B virus, four of which represent two new genotypes. *Virology* 198(2)**:** 489-503

Norder H, Hammas B, Lee SD, Bile K, Courouce AM, Mushahwar IK, Magnius LO (1993) Genetic relatedness of hepatitis B viral strains of diverse geographical origin and natural variations in the primary structure of the surface antigen. *J Gen Virol* 74 (Pt 7)**:** 1341-1348

Norder H, Hammas B, Lofdahl S, Courouce AM, Magnius LO (1992b) Comparison of the amino acid sequences of nine different serotypes of hepatitis B surface antigen and genomic classification of the corresponding hepatitis B virus strains. *J Gen Virol* 73 (Pt 5)**:** 1201-1208

Nozawa N, Yamauchi Y, Ohtsuka K, Kawaguchi Y, Nishiyama Y (2004) Formation of aggresome-like structures in herpes simplex virus type 2-infected cells and a potential role in virus assembly. *Exp Cell Res* 299(2)**:** 486-497

Nurainy N, Muljono DH, Sudoyo H, Marzuki S (2008) Genetic study of hepatitis B virus in Indonesia reveals a new subgenotype of genotype B in east Nusa Tenggara. *Arch Virol* 153(6)**:** 1057-1065

Odemuyiwa SO, Mulders MN, Oyedele OI, Ola SO, Odaibo GN, Olaleye DO, Muller CP (2001) Phylogenetic analysis of new hepatitis B virus isolates from Nigeria supports endemicity of genotype E in West Africa. *J Med Virol* 65(3)**:** 463-469

Oess S, Hildt E (2000) Novel cell permeable motif derived from the PreS2-domain of hepatitis-B virus surface antigens. *Gene Ther* 7(9)**:** 750-758

Okamoto H, Tsuda F, Akahane Y, Sugai Y, Yoshiba M, Moriyama K, Tanaka T, Miyakawa Y, Mayumi M (1994) Hepatitis B virus with mutations in the core promoter for an e antigen-negative phenotype in carriers with antibody to e antigen. *J Virol* 68(12)**:** 8102-8110

Okamoto H, Tsuda F, Sakugawa H, Sastrosoewignjo RI, Imai M, Miyakawa Y, Mayumi M (1988) Typing hepatitis B virus by homology in nucleotide sequence: comparison of surface antigen subtypes. *J Gen Virol* 69 (Pt 10)**:** 2575-2583

Olinger CM, Venard V, Njayou M, Oyefolu AO, Maiga I, Kemp AJ, Omilabu SA, le Faou A, Muller CP (2006) Phylogenetic analysis of the precore/core gene of hepatitis B virus genotypes E and A in West Africa: new subtypes, mixed infections and recombinations. *J Gen Virol* 87(Pt 5)**:** 1163-1173

Ou JH, Bao H, Shih C, Tahara SM (1990) Preferred translation of human hepatitis B virus polymerase from core protein- but not from precore protein-specific transcript. *J Virol* 64(9)**:** 4578-4581

Ou JH, Laub O, Rutter WJ (1986) Hepatitis B virus gene function: the precore region targets the core antigen to cellular membranes and causes the secretion of the e antigen. *Proc Natl Acad Sci U S A* 83(6)**:** 1578-1582

Oueslati M, Hermosilla R, Schonenberger E, Oorschot V, Beyermann M, Wiesner B, Schmidt A, Klumperman J, Rosenthal W, Schulein R (2007) Rescue of a nephrogenic diabetes insipidus-causing vasopressin V2 receptor mutant by cell-penetrating peptides. *J Biol Chem* 282(28)**:** 20676-20685

Owiredu WK, Kramvis A, Kew MC (2001) Molecular analysis of hepatitis B virus genomes isolated from black African patients with fulminant hepatitis B. *J Med Virol* 65(3)**:** 485-492

Paetzel M, Dalbey RE, Strynadka NC (1998) Crystal structure of a bacterial signal peptidase in complex with a beta-lactam inhibitor. *Nature* 396(6707)**:** 186-190

Paran N, Geiger B, Shaul Y (2001) HBV infection of cell culture: evidence for multivalent and cooperative attachment. *Embo J* 20(16)**:** 4443-4453

Parekh S, Zoulim F, Ahn SH, Tsai A, Li J, Kawai S, Khan N, Trepo C, Wands J, Tong S (2003) Genome replication, virion secretion, and e antigen expression of

naturally occurring hepatitis B virus core promoter mutants. *J Virol* 77(12)**:** 6601-6612

Parker JS, Broering TJ, Kim J, Higgins DE, Nibert ML (2002) Reovirus core protein mu2 determines the filamentous morphology of viral inclusion bodies by interacting with and stabilizing microtubules. *J Virol* 76(9)**:** 4483-4496

Pasek M, Goto T, Gilbert W, Zink B, Schaller H, MacKay P, Leadbetter G, Murray K (1979) Hepatitis B virus genes and their expression in E. coli. *Nature* 282(5739)**:** 575-579

Pathak RK, Merkle RK, Cummings RD, Goldstein JL, Brown MS, Anderson RG (1988) Immunocytochemical localization of mutant low density lipoprotein receptors that fail to reach the Golgi complex. *J Cell Biol* 106(6)**:** 1831-1841

Patzer EJ, Nakamura GR, Simonsen CC, Levinson AD, Brands R (1986) Intracellular assembly and packaging of hepatitis B surface antigen particles occur in the endoplasmic reticulum. *J Virol* 58(3)**:** 884-892

Perlman D, Halvorson HO (1983) A putative signal peptidase recognition site and sequence in eukaryotic and prokaryotic signal peptides. *J Mol Biol* 167(2)**:** 391-409

Pilon M, Schekman R, Romisch K (1997) Sec61p mediates export of a misfolded secretory protein from the endoplasmic reticulum to the cytosol for degradation. *Embo J* 16(15)**:** 4540-4548

Ploegh HL (1998) Viral strategies of immune evasion. *Science* 280(5361)**:** 248-253

Ploubidou A, Moreau V, Ashman K, Reckmann I, Gonzalez C, Way M (2000) Vaccinia virus infection disrupts microtubule organization and centrosome function. *Embo J* 19(15)**:** 3932-3944

Poch O, Sauvaget I, Delarue M, Tordo N (1989) Identification of four conserved motifs among the RNA-dependent polymerase encoding elements. *Embo J* 8(12)**:** 3867-3874

Pollack JR, Ganem D (1993) An RNA stem-loop structure directs hepatitis B virus genomic RNA encapsidation. *J Virol* 67(6)**:** 3254-3263

Pollack JR, Ganem D (1994) Site-specific RNA binding by a hepatitis B virus reverse transcriptase initiates two distinct reactions: RNA packaging and DNA synthesis. *J Virol* 68(9)**:** 5579-5587

Pontisso P, Ruvoletto MG, Gerlich WH, Heermann KH, Bardini R, Alberti A (1989) Identification of an attachment site for human liver plasma membranes on hepatitis B virus particles. *Virology* 173(2)**:** 522-530

Popper H, Roth L, Purcell RH, Tennant BC, Gerin JL (1987) Hepatocarcinogenicity of the woodchuck hepatitis virus. *Proc Natl Acad Sci U S A* 84(3)**:** 866-870

Pourkarim MR, Lemey P, Amini-Bavil-Olyaee S, Maes P, Van Ranst M (2009) Novel hepatitis B virus subgenotype A6 in African-Belgian patients. *J Clin Virol*

Preisler-Adams S, Schlayer HJ, Peters T, Hettler F, Gerok W, Rasenack J (1993) Sequence analysis of hepatitis B virus DNA in immunologically negative infection. *Arch Virol* 133(3-4)**:** 385-396

Prince AM (1968) An antigen detected in the blood of patients during the incubation of serum hepatitis. *Proc Natl Acad Sci USA* 60**:** 814-821

Propst T, Propst A, Dietze O, Judmaier G, Braunsteiner H, Vogel W (1994) Prevalence of hepatocellular carcinoma in alpha-1-antitrypsin deficiency. *J Hepatol* 21(6)**:** 1006-1011

Racchi M, Watzke HH, High KA, Lively MO (1993) Human coagulation factor X deficiency caused by a mutant signal peptide that blocks cleavage by signal peptidase but not targeting and translocation to the endoplasmic reticulum. *J Biol Chem* 268(8)**:** 5735-5740

Radziwill G, Tucker W, Schaller H (1990) Mutational analysis of the hepatitis B virus P gene product: domain structure and RNase H activity. *J Virol* 64(2)**:** 613-620

Rall LB, Standring DN, Laub O, Rutter WJ (1983) Transcription of hepatitis B virus by RNA polymerase II. *Mol Cell Biol* 3(10)**:** 1766-1773

Remacle AG, Shiryaev SA, Oh ES, Cieplak P, Srinivasan A, Wei G, Liddington RC, Ratnikov BI, Parent A, Desjardins R, Day R, Smith JW, Lebl M, Strongin AY (2008) Substrate cleavage analysis of furin and related proprotein convertases. A comparative study. *J Biol Chem* 283(30)**:** 20897-20906

Revill P, Yuen L, Walsh R, Perrault M, Locarnini S, Kramvis A (2010) Bioinformatic analysis of the hepadnavirus e-antigen and its precursor identifies remarkable sequence conservation in all orthohepadnaviruses. *J Med Virol* 82(1)**:** 104-115

Rieger A, Nassal M (1995) Distinct requirements for primary sequence in the 5'- and 3'-part of a bulge in the hepatitis B virus RNA encapsidation signal revealed by a combined in vivo selection/in vitro amplification system. *Nucleic Acids Res* 23(19)**:** 3909-3915

Rieger A, Nassal M (1996) Specific hepatitis B virus minus-strand DNA synthesis requires only the 5' encapsidation signal and the 3'-proximal direct repeat DR1. *J Virol* 70(1)**:** 585-589

Riley NE, Li J, McPhaul LW, Bardag-Gorce F, Lue YH, French SW (2003) Heat shock proteins are present in mallory bodies (cytokeratin aggresomes) in human liver biopsy specimens. *Exp Mol Pathol* 74(2)**:** 168-172

Riley NE, Li J, Worrall S, Rothnagel JA, Swagell C, van Leeuwen FW, French SW (2002) The Mallory body as an aggresome: in vitro studies. *Exp Mol Pathol* 72(1)**:** 17-23

Rodriguez-Frias F, Buti M, Jardi R, Cotrina M, Viladomiu L, Esteban R, Guardia J (1995) Hepatitis B virus infection: precore mutants and its relation to viral genotypes and core mutations. *Hepatology* 22(6)**:** 1641-1647

Romisch K (2005) Endoplasmic reticulum-associated degradation. *Annu Rev Cell Dev Biol* 21**:** 435-456

Roseman AM, Berriman JA, Wynne SA, Butler PJ, Crowther RA (2005) A structural model for maturation of the hepatitis B virus core. *Proc Natl Acad Sci U S A* 102(44)**:** 15821-15826

Rudnick DA, Liao Y, An JK, Muglia LJ, Perlmutter DH, Teckman JH (2004) Analyses of hepatocellular proliferation in a mouse model of alpha-1-antitrypsin deficiency. *Hepatology* 39(4)**:** 1048-1055

Ruiz-Opazo N, Chakraborty PR, Shafritz DA (1982a) Characterization of viral genomes in the liver and serum of chimpanzee long-term hepatitis B virus carriers: a possible role for supercoiled HBV-DNA in persistent HBV infection. *J Cell Biochem* 19(3)**:** 281-292

Ruiz-Opazo N, Chakraborty PR, Shafritz DA (1982b) Evidence for supercoiled hepatitis B virus DNA in chimpanzee liver and serum Dane particles: possible implications in persistent HBV infection. *Cell* 29(1)**:** 129-136

Rutishauser J, Spiess M (2002) Endoplasmic reticulum storage diseases. *Swiss Med Wkly* 132(17-18)**:** 211-222

Rutkowski DT, Kaufman RJ (2004) A trip to the ER: coping with stress. *Trends Cell Biol* 14(1)**:** 20-28

Rutkowski DT, Kaufman RJ (2007) That which does not kill me makes me stronger: adapting to chronic ER stress. *Trends Biochem Sci* 32(10)**:** 469-476

Rutkowski DT, Ott CM, Polansky JR, Lingappa VR (2003) Signal sequences initiate the pathway of maturation in the endoplasmic reticulum lumen. *J Biol Chem* 278(32)**:** 30365-30372

Sakamoto T, Tanaka Y, Orito E, Co J, Clavio J, Sugauchi F, Ito K, Ozasa A, Quino A, Ueda R, Sollano J, Mizokami M (2006) Novel subtypes (subgenotypes) of hepatitis B virus genotypes B and C among chronic liver disease patients in the Philippines. *J Gen Virol* 87(Pt 7)**:** 1873-1882

Sakamoto T, Tanaka Y, Simonetti. J., Osiowy C, Borresen M, Koch A, Kurbanov F, Sugiyama M, Minuk G, McMahon B, Joh T, Mizokami M (2007) Classification of hepatitis B virus genotype B into 2 major types based on

characterization of a novel subgenotype in Arctic indigenous populations. *J Infect Dis* 196(10)**:** 1487-1492

Sakamoto Y, Yamada G, Mizuno M, Nishihara T, Kinoyama S, Kobayashi T, Takahashi T, Nagashima H (1983) Full and empty particles of hepatitis B virus in hepatocytes from patients with HBsAg-positive chronic active hepatitis. *Lab Invest* 48(6)**:** 678-682

Saliba RS, Munro PM, Luthert PJ, Cheetham ME (2002) The cellular fate of mutant rhodopsin: quality control, degradation and aggresome formation. *J Cell Sci* 115(Pt 14)**:** 2907-2918

Sallie R (2005) Replicative homeostasis: a fundamental mechanism mediating selective viral replication and escape mutation. *Virol J* 2**:** 10

Sambrook J, Fritsch EF, Maniatis T (1989) Molecular Cloning: A Laboratory Manual. N. Ford, C. Nolan, and M. Ferguson (ed.), Molecular cloning, 2nd ed. Cold Spring Harbor Laboratory Press, Cold Spring Harbor, N.Y. .

Saraste J, Kuismanen E (1992) Pathways of protein sorting and membrane traffic between the rough endoplasmic reticulum and the Golgi complex. *Semin Cell Biol* 3(5)**:** 343-355

Sayeed A, Ng DT (2005) Search and destroy: ER quality control and ER-associated protein degradation. *Crit Rev Biochem Mol Biol* 40(2)**:** 75-91

Scaglioni PP, Melegari M, Wands JR (1997a) Biologic properties of hepatitis B viral genomes with mutations in the precore promoter and precore open reading frame. *Virology* 233(2)**:** 374-381

Scaglioni PP, Melegari M, Wands JR (1997b) Posttranscriptional regulation of hepatitis B virus replication by the precore protein. *J Virol* 71(1)**:** 345-353

Schaaf SG, Beck J, Nassal M (1999) A small 2'-OH- and base-dependent recognition element downstream of the initiation site in the RNA encapsidation signal is essential for hepatitis B virus replication initiation. *J Biol Chem* 274(53)**:** 37787-37794

Schaefer S (2007) Hepatitis B virus taxonomy and hepatitis B virus genotypes. *World J Gastroenterol* 13(1)**:** 14-21

Schaller H, Fischer M (1991) Transcriptional control of hepadnavirus gene expression. *Curr Top Microbiol Immunol* 168**:** 21-39

Schlicht HJ, Radziwill G, Schaller H (1989) Synthesis and encapsidation of duck hepatitis B virus reverse transcriptase do not require formation of core-polymerase fusion proteins. *Cell* 56(1)**:** 85-92

Schlicht HJ, Salfeld J, Schaller H (1987) The duck hepatitis B virus pre-C region encodes a signal sequence which is essential for synthesis and secretion of processed core proteins but not for virus formation. *J Virol* 61(12)**:** 3701-3709

Schlicht HJ, Wasenauer G (1991) The quaternary structure, antigenicity, and aggregational behavior of the secretory core protein of human hepatitis B virus are determined by its signal sequence. *J Virol* 65(12)**:** 6817-6825

Schmoranzer J, Goulian M, Axelrod D, Simon SM (2000) Imaging constitutive exocytosis with total internal reflection fluorescence microscopy. *J Cell Biol* 149(1)**:** 23-32

Schodel F, Peterson D, Milich D (1996) Hepatitis B virus core and e antigen: immune recognition and use as a vaccine carrier moiety. *Intervirology* 39(1-2)**:** 104-110

Schroder M, Kaufman RJ (2005) The mammalian unfolded protein response. *Annu Rev Biochem* 74**:** 739-789

Schweizer A, Matter K, Ketcham CM, Hauri HP (1991) The isolated ER-Golgi intermediate compartment exhibits properties that are different from ER and cis-Golgi. *J Cell Biol* 113(1)**:** 45-54

Seeger C, Ganem D, Varmus HE (1986) Biochemical and genetic evidence for the hepatitis B virus replication strategy. *Science* 232(4749)**:** 477-484

Seeger C, Mason WS (2000) Hepatitis B virus biology. *Microbiol Mol Biol Rev* 64(1)**:** 51-68

Selabe SG, Song E, Burnett RJ, Mphahlele MJ (2009) Frequent detection of hepatitis B virus variants associated with lamivudine resistance in treated South African patients infected chronically with different HBV genotypes. *J Med Virol* 81(6)**:** 996-1001

Sen N, Cao F, Tavis JE (2004) Translation of duck hepatitis B virus reverse transcriptase by ribosomal shunting. *J Virol* 78(21)**:** 11751-11757

Sharpe AH, Chen LB, Fields BN (1982) The interaction of mammalian reoviruses with the cytoskeleton of monkey kidney CV-1 cells. *Virology* 120(2)**:** 399-411

Shen LM, Lee JI, Cheng SY, Jutte H, Kuhn A, Dalbey RE (1991) Use of site-directed mutagenesis to define the limits of sequence variation tolerated for processing of the M13 procoat protein by the Escherichia coli leader peptidase. *Biochemistry* 30(51)**:** 11775-11781

Shepard CW, Simard EP, Finelli L, Fiore AE, Bell BP (2006) Hepatitis B virus infection: epidemiology and vaccination. *Epidemiol Rev* 28**:** 112-125

Shin MK, Lee J, Ryu WS (2004) A novel cis-acting element facilitates minus-strand DNA synthesis during reverse transcription of the hepatitis B virus genome. *J Virol* 78(12)**:** 6252-6262

Siddiqui A, Jameel S, Mapoles J (1986) Transcriptional control elements of hepatitis B surface antigen gene. *Proc Natl Acad Sci U S A* 83(3)**:** 566-570

Siddiqui A, Jameel S, Mapoles J (1987) Expression of the hepatitis B virus X gene in mammalian cells. *Proc Natl Acad Sci U S A* 84(8)**:** 2513-2517

Sifers RN, Brashears-Macatee S, Kidd VJ, Muensch H, Woo SL (1988) A frameshift mutation results in a truncated alpha 1-antitrypsin that is retained within the rough endoplasmic reticulum. *J Biol Chem* 263(15)**:** 7330-7335

Sirma H, Giannini C, Poussin K, Paterlini P, Kremsdorf D, Brechot C (1999) Hepatitis B virus X mutants, present in hepatocellular carcinoma tissue abrogate both the antiproliferative and transactivation effects of HBx. *Oncogene* 18(34)**:** 4848-4859

Sitia R, Braakman I (2003) Quality control in the endoplasmic reticulum protein factory. *Nature* 426(6968)**:** 891-894

Sitte N, Huber M, Grune T, Ladhoff A, Doecke WD, Von Zglinicki T, Davies KJ (2000) Proteasome inhibition by lipofuscin/ceroid during postmitotic aging of fibroblasts. *Faseb J* 14(11)**:** 1490-1498

Soldatenkov VA, Dritschilo A (1997) Apoptosis of Ewing's sarcoma cells is accompanied by accumulation of ubiquitinated proteins. *Cancer Res* 57(18)**:** 3881-3885

Sommer T, Wolf DH (1997) Endoplasmic reticulum degradation: reverse protein flow of no return. *Faseb J* 11(14)**:** 1227-1233

Song E, Dusheiko GM, Bowyer S, Kew MC (1984) Hepatitis B virus replication in southern Africa blacks with HBsAg-positive hepatocellular carcinoma. *Hepatology* 4(4)**:** 608-610

Spandau DF, Lee CH (1988) trans-activation of viral enhancers by the hepatitis B virus X protein. *J Virol* 62(2)**:** 427-434

Speed MA, Wang DI, King J (1996) Specific aggregation of partially folded polypeptide chains: the molecular basis of inclusion body composition. *Nat Biotechnol* 14(10)**:** 1283-1287

Spiro RG (2002) Protein glycosylation: nature, distribution, enzymatic formation, and disease implications of glycopeptide bonds. *Glycobiology* 12(4)**:** 43R-56R

Spiropoulou CF, Goldsmith CS, Shoemaker TR, Peters CJ, Compans RW (2003) Sin Nombre virus glycoprotein trafficking. *Virology* 308(1)**:** 48-63

Standring DN, Ou JH, Masiarz FR, Rutter WJ (1988) A signal peptide encoded within the precore region of hepatitis B virus directs the secretion of a heterogeneous population of e antigens in Xenopus oocytes. *Proc Natl Acad Sci U S A* 85(22)**:** 8405-8409

Standring DN, Rutter WJ, Varmus HE, Ganem D (1984) Transcription of the hepatitis B surface antigen gene in cultured murine cells initiates within the presurface region. *J Virol* 50(2)**:** 563-571

Stannard LM, Hodgkiss M (1979) Morphological irregularities in Dane particle cores. *J Gen Virol* 45(2)**:** 509-514

Staprans S, Loeb DD, Ganem D (1991) Mutations affecting hepadnavirus plus-strand DNA synthesis dissociate primer cleavage from translocation and reveal the origin of linear viral DNA. *J Virol* 65(3)**:** 1255-1262

Stephens DJ, Lin-Marq N, Pagano A, Pepperkok R, Paccaud JP (2000) COPI-coated ER-to-Golgi transport complexes segregate from COPII in close proximity to ER exit sites. *J Cell Sci* 113 (Pt 12)**:** 2177-2185

Sterneck M, Kalinina T, Otto S, Gunther S, Fischer L, Burdelski M, Greten H, Broelsch CE, Will H (1998) Neonatal fulminant hepatitis B: structural and functional analysis of complete hepatitis B virus genomes from mother and infant. *J Infect Dis* 177(5)**:** 1378-1381

Stevens CE, Beasley RP, Tsui J, Lee WC (1975) Vertical transmission of hepatitis B antigen in Taiwan. *N Engl J Med* 292(15)**:** 771-774

Stevens CE, Szmuness W, Goodman AI, Weseley SA, Fotino M (1980) Hepatitis B vaccine: immune responses in haemodialysis patients. *Lancet* 2(8206)**:** 1211-1213

Stevens FJ, Argon Y (1999) Protein folding in the ER. *Semin Cell Dev Biol* 10(5)**:** 443-454

Stoeckl L, Funk A, Kopitzki A, Brandenburg B, Oess S, Will H, Sirma H, Hildt E (2006) Identification of a structural motif crucial for infectivity of hepatitis B viruses. *Proc Natl Acad Sci U S A* 103(17)**:** 6730-6734

Strnad P, Zatloukal K, Stumptner C, Kulaksiz H, Denk H (2008) Mallory-Denk-bodies: lessons from keratin-containing hepatic inclusion bodies. *Biochim Biophys Acta* 1782(12)**:** 764-774

Stumptner C, Fuchsbichler A, Zatloukal K, Denk H (2007) In vitro production of Mallory bodies and intracellular hyaline bodies: the central role of sequestosome 1/p62. *Hepatology* 46(3)**:** 851-860

Stuyver L, De Gendt S, Van Geyt C, Zoulim F, Fried M, Schinazi RF, Rossau R (2000) A new genotype of hepatitis B virus: complete genome and phylogenetic relatedness. *J Gen Virol* 81(Pt 1)**:** 67-74

Stuyver LJ, Locarnini SA, Lok A, Richman DD, Carman WF, Dienstag JL, Schinazi RF (2001) Nomenclature for antiviral-resistant human hepatitis B virus mutations in the polymerase region. *Hepatology* 33(3)**:** 751-757

Su H, Yee JK (1992) Regulation of hepatitis B virus gene expression by its two enhancers. *Proc Natl Acad Sci U S A* 89(7)**:** 2708-2712

Su Q, Schroder CH, Hofmann WJ, Otto G, Pichlmayr R, Bannasch P (1998) Expression of hepatitis B virus X protein in HBV-infected human livers and hepatocellular carcinomas. *Hepatology* 27(4)**:** 1109-1120

Sugauchi F, Kumada H, Acharya SA, Shrestha SM, Gamutan MT, Khan M, Gish RG, Tanaka Y, Kato T, Orito E, Ueda R, Miyakawa Y, Mizokami M (2004a) Epidemiological and sequence differences between two subtypes (Ae and Aa) of hepatitis B virus genotype A. *J Gen Virol* 85(Pt 4)**:** 811-820

Sugauchi F, Kumada H, Sakugawa H, Komatsu M, Niitsuma H, Watanabe H, Akahane Y, Tokita H, Kato T, Tanaka Y, Orito E, Ueda R, Miyakawa Y, Mizokami M (2004b) Two subtypes of genotype B (Ba and Bj) of hepatitis B virus in Japan. *Clin Infect Dis* 38(9)**:** 1222-1228

Sugauchi F, Mizokami M, Orito E, Ohno T, Kato H, Suzuki S, Kimura Y, Ueda R, Butterworth LA, Cooksley WG (2001) A novel variant genotype C of hepatitis B virus identified in isolates from Australian Aborigines: complete genome sequence and phylogenetic relatedness. *J Gen Virol* 82(Pt 4)**:** 883-892

Summers J, Mason WS (1982) Replication of the genome of a hepatitis B--like virus by reverse transcription of an RNA intermediate. *Cell* 29(2)**:** 403-415

Summers J, O'Connell A, Millman I (1975) Genome of hepatitis B virus: restriction enzyme cleavage and structure of DNA extracted from Dane particles. *Proc Natl Acad Sci U S A* 72(11)**:** 4597-4601

Tai AW, Chuang JZ, Bode C, Wolfrum U, Sung CH (1999) Rhodopsin's carboxy-terminal cytoplasmic tail acts as a membrane receptor for cytoplasmic dynein by binding to the dynein light chain Tctex-1. *Cell* 97(7)**:** 877-887

Takahashi K, Aoyama K, Ohno N, Iwata K, Akahane Y, Baba K, Yoshizawa H, Mishiro S (1995) The precore/core promoter mutant (T1762A1764) of hepatitis B virus: clinical significance and an easy method for detection. *J Gen Virol* 76 (Pt 12)**:** 3159-3164

Takahashi K, Machida A, Funatsu G, Nomura M, Usuda S, Aoyagi S, Tachibana K, Miyamoto H, Imai M, Nakamura T, Miyakawa Y, Mayumi M (1983) Immunochemical structure of hepatitis B e antigen in the serum. *J Immunol* 130(6)**:** 2903-2907

Takahashi T, Kaga K, Akahane Y, Yamashita T, Miyakawa Y, Mayumi M (1980) Isolation of Dane particles containing a DNA strand by metrizamide density gradient. *J Med Microbiol* 13(1)**:** 163-166

Tanaka M, Kim YM, Lee G, Junn E, Iwatsubo T, Mouradian MM (2004a) Aggresomes formed by alpha-synuclein and synphilin-1 are cytoprotective. *J Biol Chem* 279(6)**:** 4625-4631

Tanaka Y, Hasegawa I, Kato T, Orito E, Hirashima N, Acharya SK, Gish RG, Kramvis A, Kew MC, Yoshihara N, Shrestha SM, Khan M, Miyakawa Y, Mizokami M (2004b) A case-control study for differences among hepatitis B virus infections of genotypes A (subtypes Aa and Ae) and D. *Hepatology* 40(3)**:** 747-755

Tang H, McLachlan A (2002) A pregenomic RNA sequence adjacent to DR1 and complementary to epsilon influences hepatitis B virus replication efficiency. *Virology* 303(1)**:** 199-210

Tatematsu K, Tanaka Y, Kurbanov F, Sugauchi F, Mano S, Maeshiro T, Nakayoshi T, Wakuta M, Miyakawa Y, Mizokami M (2009) A genetic variant of hepatitis B virus divergent from known human and ape genotypes isolated from a Japanese patient and provisionally assigned to new genotype J. *J Virol* 83(20)**:** 10538-10547

Tavis JE, Perri S, Ganem D (1994) Hepadnavirus reverse transcription initiates within the stem-loop of the RNA packaging signal and employs a novel strand transfer. *J Virol* 68(6)**:** 3536-3543

Taxis C, Vogel F, Wolf DH (2002) ER-golgi traffic is a prerequisite for efficient ER degradation. *Mol Biol Cell* 13(6)**:** 1806-1818

Taylor JP, Tanaka F, Robitschek J, Sandoval CM, Taye A, Markovic-Plese S, Fischbeck KH (2003) Aggresomes protect cells by enhancing the degradation of toxic polyglutamine-containing protein. *Hum Mol Genet* 12(7)**:** 749-757

Terradillos O, Billet O, Renard CA, Levy R, Molina T, Briand P, Buendia MA (1997) The hepatitis B virus X gene potentiates c-myc-induced liver oncogenesis in transgenic mice. *Oncogene* 14(4)**:** 395-404

Terradillos O, Pollicino T, Lecoeur H, Tripodi M, Gougeon ML, Tiollais P, Buendia MA (1998) p53-independent apoptotic effects of the hepatitis B virus HBx protein in vivo and in vitro. *Oncogene* 17(16)**:** 2115-2123

Theamboonlers A, Jantaradsamee P, Kaew-In N, Tangkijvanich P, Hirsch P, Poovorawan Y (1999) The predominant genotypes of hepatitis B virus in Thailand. *Ann Trop Med Parasitol* 93(7)**:** 737-743

Thomas HC, Jacyna M, Waters J, Main J (1988) Virus-host interaction in chronic hepatitis B virus infection. *Semin Liver Dis* 8(4)**:** 342-349

Thompson AJ, Nguyen T, Iser D, Ayres A, Jackson K, Littlejohn M, Slavin J, Bowden S, Gane EJ, Abbott W, Lau GK, Lewin SR, Visvanathan K, Desmond PV, Locarnini SA. (2010) Serum hepatitis B surface antigen and hepatitis B e antigen titers: disease phase influences correlation with viral load and intrahepatic hepatitis B virus markers. *Hepatology* 51(6): 1933-44.

Thrower JS, Hoffman L, Rechsteiner M, Pickart CM (2000) Recognition of the polyubiquitin proteolytic signal. *Embo J* 19(1)**:** 94-102

Tiollais P, Pourcel C, Dejean A (1985) The hepatitis B virus. *Nature* 317(6037)**:** 489-495

Tong S (2007) Impact of viral genotypes and naturally occurring mutations on biological properties of hepatitis B virus. *Hepatol Res* 37(s1)**:** S3-8

Tong S, Kim KH, Chante C, Wands J, Li J (2005) Hepatitis B Virus e Antigen Variants. *Int J Med Sci* 2(1)**:** 2-7

Tong SP, Li JS, Vitvitski L, Trepo C (1990) Active hepatitis B virus replication in the presence of anti-HBe is associated with viral variants containing an inactive pre-C region. *Virology* 176(2)**:** 596-603

Tong SP, Li JS, Vitvitski L, Trepo C (1992) Replication capacities of natural and artificial precore stop codon mutants of hepatitis B virus: relevance of pregenome encapsidation signal. *Virology* 191(1)**:** 237-245

Toomre D, Steyer JA, Keller P, Almers W, Simons K (2000) Fusion of constitutive membrane traffic with the cell surface observed by evanescent wave microscopy. *J Cell Biol* 149(1)**:** 33-40

Tran TT, Trinh TN, Abe K (2008) New complex recombinant genotype of hepatitis B virus identified in Vietnam. *J Virol* 82(11)**:** 5657-5663

Travers KJ, Patil CK, Wodicka L, Lockhart DJ, Weissman JS, Walter P (2000) Functional and genomic analyses reveal an essential coordination between the unfolded protein response and ER-associated degradation. *Cell* 101(3)**:** 249-258

Treinin M, Laub O (1987) Identification of a promoter element located upstream from the hepatitis B virus X gene. *Mol Cell Biol* 7(1)**:** 545-548

Trepo CG, Robert D, Motin J, Trepo D, Sepetjian M, Prince AM (1976) Hepatitis B antigen (HBSAg) and/or antibodies (anti-HBS and anti-HBC) in fulminant hepatitis: pathogenic and prognostic significance. *Gut* 17(1)**:** 10-13

Trombetta ES, Parodi AJ (2003) Quality control and protein folding in the secretory pathway. *Annu Rev Cell Dev Biol* 19**:** 649-676

Tsai B, Ye Y, Rapoport TA (2002) Retro-translocation of proteins from the endoplasmic reticulum into the cytosol. *Nat Rev Mol Cell Biol* 3(4)**:** 246-255

Tuttleman JS, Pourcel C, Summers J (1986) Formation of the pool of covalently closed circular viral DNA in hepadnavirus-infected cells. *Cell* 47(3)**:** 451-460

Ueda K, Tsurimoto T, Matsubara K (1991) Three envelope proteins of hepatitis B virus: large S, middle S, and major S proteins needed for the formation of Dane particles. *J Virol* 65(7)**:** 3521-3529

Valliammai T, Thyagarajan SP, Zuckerman AJ, Harrison TJ (1995) Precore and core mutations in HBV from individuals in India with chronic infection. *J Med Virol* 45(3)**:** 321-325

van Zonneveld M, Honkoop P, Hansen BE, Niesters HG, Darwish Murad S, de Man RA, Schalm SW, Janssen HL (2004) Long-term follow-up of alpha-interferon treatment of patients with chronic hepatitis B. *Hepatology* 39(3)**:** 804-810

Vieth S, Manegold C, Drosten C, Nippraschk T, Gunther S (2002) Sequence and phylogenetic analysis of hepatitis B virus genotype G isolated in Germany. *Virus Genes* 24(2)**:** 153-156

Visvanathan K, Skinner NA, Thompson AJ, Riordan SM, Sozzi V, Edwards R, Rodgers S, Kurtovic J, Chang J, Lewin S, Desmond P, Locarnini S (2007) Regulation of Toll-like receptor-2 expression in chronic hepatitis B by the precore protein. *Hepatology* 45(1)**:** 102-110

Voeltz GK, Rolls MM, Rapoport TA (2002) Structural organization of the endoplasmic reticulum. *EMBO Rep* 3(10)**:** 944-950

von Heijne G (1983) Patterns of amino acids near signal-sequence cleavage sites. *Eur J Biochem* 133(1)**:** 17-21

von Heijne G (1984) How signal sequences maintain cleavage specificity. *J Mol Biol* 173(2)**:** 243-251

von Heijne G (1985) Signal sequences. The limits of variation. *J Mol Biol* 184(1)**:** 99-105

von Heijne G (1986) Towards a comparative anatomy of N-terminal topogenic protein sequences. *J Mol Biol* 189(1)**:** 239-242

von Heijne G (1990) The signal peptide. *J Membr Biol* 115(3)**:** 195-201

Waelter S, Boeddrich A, Lurz R, Scherzinger E, Lueder G, Lehrach H, Wanker EE (2001) Accumulation of mutant huntingtin fragments in aggresome-like inclusion bodies as a result of insufficient protein degradation. *Mol Biol Cell* 12(5)**:** 1393-1407

Walter P, Gilmore R, Blobel G (1984) Protein translocation across the endoplasmic reticulum. *Cell* 38(1)**:** 5-8

Walter P, Ibrahimi I, Blobel G (1981) Translocation of proteins across the endoplasmic reticulum. I. Signal recognition protein (SRP) binds to in-vitro-assembled polysomes synthesizing secretory protein. *J Cell Biol* 91(2 Pt 1)**:** 545-550

Walter P, Johnson AE (1994) Signal sequence recognition and protein targeting to the endoplasmic reticulum membrane. *Annu Rev Cell Biol* 10**:** 87-119

Wang GH, Seeger C (1992) The reverse transcriptase of hepatitis B virus acts as a protein primer for viral DNA synthesis. *Cell* 71(4)**:** 663-670

Wang GH, Seeger C (1993) Novel mechanism for reverse transcription in hepatitis B viruses. *J Virol* 67(11)**:** 6507-6512

Wang GH, Zoulim F, Leber EH, Kitson J, Seeger C (1994) Role of RNA in enzymatic activity of the reverse transcriptase of hepatitis B viruses. *J Virol* 68(12)**:** 8437-8442

Wang HC, Chang WT, Chang WW, Wu HC, Huang W, Lei HY, Lai MD, Fausto N, Su IJ (2005) Hepatitis B virus pre-S2 mutant upregulates cyclin A expression and induces nodular proliferation of hepatocytes. *Hepatology* 41(4)**:** 761-770

Wang HC, Huang W, Lai MD, Su IJ (2006) Hepatitis B virus pre-S mutants, endoplasmic reticulum stress and hepatocarcinogenesis. *Cancer Sci* 97(8)**:** 683-688

Wang J, Lee AS, Ou JH (1991) Proteolytic conversion of hepatitis B virus e antigen precursor to end product occurs in a postendoplasmic reticulum compartment. *J Virol* 65(9)**:** 5080-5083

Wang J, Takeuchi T, Tanaka S, Kubo SK, Kayo T, Lu D, Takata K, Koizumi A, Izumi T (1999) A mutation in the insulin 2 gene induces diabetes with severe pancreatic beta-cell dysfunction in the Mody mouse. *J Clin Invest* 103(1)**:** 27-37

Wang X, Qian X, Guo HC, Hu J (2003) Heat shock protein 90-independent activation of truncated hepadnavirus reverse transcriptase. *J Virol* 77(8)**:** 4471-4480

Wasenauer G, Kock J, Schlicht HJ (1992) A cysteine and a hydrophobic sequence in the noncleaved portion of the pre-C leader peptide determine the biophysical properties of the secretory core protein (HBe protein) of human hepatitis B virus. *J Virol* 66(9)**:** 5338-5346

Watson ME (1984) Compilation of published signal sequences. *Nucleic Acids Res* 12(13)**:** 5145-5164

Watzke HH, Wallmark A, Hamaguchi N, Giardina P, Stafford DW, High KA (1991) Factor XSanto Domingo. Evidence that the severe clinical phenotype arises from a mutation blocking secretion. *J Clin Invest* 88(5)**:** 1685-1689

Weber M, Bronsema V, Bartos H, Bosserhoff A, Bartenschlager R, Schaller H (1994) Hepadnavirus P protein utilizes a tyrosine residue in the TP domain to prime reverse transcription. *J Virol* 68(5)**:** 2994-2999

Weiser B, Ganem D, Seeger C, Varmus HE (1983) Closed circular viral DNA and asymmetrical heterogeneous forms in livers from animals infected with ground squirrel hepatitis virus. *J Virol* 48(1)**:** 1-9

Weiss RA (2002) Virulence and pathogenesis. *Trends Microbiol* 10(7)**:** 314-317

Westland C, Delaney Wt, Yang H, Chen SS, Marcellin P, Hadziyannis S, Gish R, Fry J, Brosgart C, Gibbs C, Miller M, Xiong S (2003) Hepatitis B virus genotypes and virologic response in 694 patients in phase III studies of adefovir dipivoxil1. *Gastroenterology* 125(1)**:** 107-116

Wetzel R (1994) Mutations and off-pathway aggregation of proteins. *Trends Biotechnol* 12(5)**:** 193-198

WHO (2008) Hepatitis B. Fact Sheets No.204. *http://wwwwhoint/mediacentre/factsheets/fs204/en/*

Wickner S, Maurizi MR, Gottesman S (1999) Posttranslational quality control: folding, refolding, and degrading proteins. *Science* 286(5446)**:** 1888-1893

Wigley WC, Fabunmi RP, Lee MG, Marino CR, Muallem S, DeMartino GN, Thomas PJ (1999) Dynamic association of proteasomal machinery with the centrosome. *J Cell Biol* 145(3)**:** 481-490

Wileman T (2006) Aggresomes and autophagy generate sites for virus replication. *Science* 312(5775)**:** 875-878

Will H, Reiser W, Weimer T, Pfaff E, Buscher M, Sprengel R, Cattaneo R, Schaller H (1987) Replication strategy of human hepatitis B virus. *J Virol* 61(3)**:** 904-911

Wolf DH, Hilt W (2004) The proteasome: a proteolytic nanomachine of cell regulation and waste disposal. *Biochim Biophys Acta* 1695(1-3)**:** 19-31

Xu Z, Jensen G, Yen TS (1997) Activation of hepatitis B virus S promoter by the viral large surface protein via induction of stress in the endoplasmic reticulum. *J Virol* 71(10)**:** 7387-7392

Yaginuma K, Koike K (1989) Identification of a promoter region for 3.6-kilobase mRNA of hepatitis B virus and specific cellular binding protein. *J Virol* 63(7)**:** 2914-2920

Yamada G, Takahashi T, Mizuno M, Sakamoto Y, Kaga K, Kobayashi T, Nagashima H (1980) Immunoelectron microscopic observation of hepatitis B surface antigen on the surface of liver cells from patients with hepatitis B virus infection. *Acta Med Okayama* 34(3)**:** 175-187

Yeh CT, Liaw YF, Ou JH (1990) The arginine-rich domain of hepatitis B virus precore and core proteins contains a signal for nuclear transport. *J Virol* 64(12)**:** 6141-6147

Yoshida H (2007) ER stress and diseases. *Febs J* 274(3)**:** 630-658

Yu M, Summers J (1991) A domain of the hepadnavirus capsid protein is specifically required for DNA maturation and virus assembly. *J Virol* 65(5)**:** 2511-2517

Yuan TT, Faruqi A, Shih JW, Shih C (1995) The mechanism of natural occurrence of two closely linked HBV precore predominant mutations. *Virology* 211(1)**:** 144-156

Yuh CH, Ting LP (1990) The genome of hepatitis B virus contains a second enhancer: cooperation of two elements within this enhancer is required for its function. *J Virol* 64(9)**:** 4281-4287

Zamyatnin AA (1972) Protein volume in solution. *Prog Biophys Mol Biol* 24**:** 107-123

Zatloukal K, French SW, Stumptner C, Strnad P, Harada M, Toivola DM, Cadrin M, Omary MB (2007) From Mallory to Mallory-Denk bodies: what, how and why? *Exp Cell Res* 313(10)**:** 2033-2049

Zhang K, Kaufman RJ (2006) The unfolded protein response: a stress signaling pathway critical for health and disease. *Neurology* 66(2 Suppl 1)**:** S102-109

Zhang K, Kaufman RJ (2008) From endoplasmic-reticulum stress to the inflammatory response. *Nature* 454(7203)**:** 455-462

Zheng J, Schodel F, Peterson DL (1992) The structure of hepadnaviral core antigens. Identification of free thiols and determination of the disulfide bonding pattern. *J Biol Chem* 267(13)**:** 9422-9429

Zheng YW, Riegler J, Wu J, Yen TS (1994) Novel short transcripts of hepatitis B virus X gene derived from intragenic promoter. *J Biol Chem* 269(36)**:** 22593-22598

Zhou S, Standring DN (1992) Hepatitis B virus capsid particles are assembled from core-protein dimer precursors. *Proc Natl Acad Sci U S A* 89(21)**:** 10046-10050

Zoulim F, Saputelli J, Seeger C (1994) Woodchuck hepatitis virus X protein is required for viral infection in vivo. *J Virol* 68(3)**:** 2026-2030

Zoulim F, Seeger C (1994) Reverse transcription in hepatitis B viruses is primed by a tyrosine residue of the polymerase. *J Virol* 68(1)**:** 6-13

Zuber C, Fan JY, Guhl B, Roth J (2004) Misfolded proinsulin accumulates in expanded pre-Golgi intermediates and endoplasmic reticulum subdomains in pancreatic beta cells of Akita mice. *Faseb J* 18(7)**:** 917-919

Zuker M (2003) Mfold web server for nucleic acid folding and hybridization prediction. *Nucleic Acids Res* 31(13)**:** 3406-3415